universität wien

DISSERTATION

Titel der Dissertation

„Novel Molecular Tools for Microbial Ecology: Development and Application to Decipher Trophic Structures of Nitrifying Communities“

Band 1 von 1

Verfasser

Jan Dolinšek

angestrebter akademischer Grad

Doktor der Naturwissenschaften (Dr.rer.nat.)

Wien, 2014

Studienkennzahl lt. Studienblatt:	A 091 444
Dissertationsgebiet lt. Studienblatt:	Ökologie
Betreuer:	Prof. Dr. Michael Wagner

Contents

Chapter I

Introduction and Outline

Introduction

Symbiosis and bacterial predation

The German botanist and mycologist Anton de Bary defined symbiosis as a cohabitation of dissimilar organisms. Although the term is often used to describe associations in which both partners receive benefits (mutualism), de Bary´s definition of symbiosis does not exclude neutral (commensalism) or antagonistic (parasitism and predation) relationships. Cooperation typically provides competitive advantages over non-symbiotic organisms for both partners (individual benefits can be in the form of mobility, energy source accessibility, protection, expanded metabolic potential etc.), and allows occupation of niches otherwise unavailable to any of the partners alone. On the other side of the symbiosis spectrum are parasitism and predation. Parasitism is defined as interaction in which one species gains advantage (increased fitness) on expense of its partner (decreased fitness). While cohabitation can be prolonged in parasitism, predation is normally short-lived and results in the demise of one partner. A number of described interactions among bacteria and their hosts provide advantage to only one partner (some Wolbachia) or the costs and benefits of interaction are difficult to explain (1). Boundaries between parasitism, commensalism, and mutualism can be blurred or shift over time due to changed environmental circumstances (2, 3).

Microbe-microbe interactions have attracted much less attention than microbe-eukaryote symbioses. Partly due to technical limitations, which are only recently being alleviated by new technologies and methods (4). Metabolically coupled syntrophic associations are likely the best studied mutualistic interactions between two microbes. Prominent examples are anaerobic methane oxidation (5, 6), anaerobic (often methanogenic) communities degrading fatty acids, alcohols and some other hydrocarbons (7, 8), and the more recently described electron transfer between two species growing as co-culture, either direct (9) or through conductive minerals (10). Although all microbial partners have not been determined yet, bacteria acting as electric wires can transfer electric current over centimeter distances in marine sediments and thus couple spatially separated oxidation and reduction reactions (11, 12). Although not a strict microbe-microbe association, the symbiosis between an uncultured nitrogen-fixing cyanobacterium (UCYN-A) and unicellular algae could also be regarded this type of mutualism (13).

Likely being an ancient trait, several types of parasitic (predatory) symbioses can be found in the microbial world (14, 15). Among representatives are bacteria that actively degrade living bacteria and use released nutrients to support their own growth and metabolism. These predatory/parasitic bacteria are physiologically and phylogenetically diverse and are found in several phyla. Similarly diverse are their predatory strategies, ranging from cooperative or "wolfpack" predation to the invasion of the periplasmic space of their prey and division by septation (Figure 1). The best studied predatory bacteria are *Myxococcus xanthus*, several members of the *Bdellovibrio* and *Bacteriovorax* genera (all *Deltaproteobacteria*), and *Micavibrio aeruginosavorus* (*Alphaproteobacteria*) (14, 16, 17).

The best characterized predatory bacterium, *Bdellovibro bacterivorus*, was described more than 50 years ago (17-20). While older work was focusing mostly on physiology and electron-microscopy based experiments, the recent *Bdellovibrio*-research renaissance has seen the use of many modern genomic and post-genomic technologies (17, 21-29). The predatory life-cycle of *Bdellovibrio bacteriovorous* starts with a highly motile free-swimming phase, where *Bdellovibrio* senses and actively swims toward its prey. After encountering potential prey, a short termed recognition phase follows, which results in the invasion of preys periplasmic space or in the detachment of *Bdellovibrio*. Once in the periplasm, *Bdellovibrio* establishes a metabolic connection with its prey via several transporters and membrane proteins, and at the same time releases its arsenal of macromolecule-degrading proteins. At this stage, the predator grows into a long filament and finally divides by septation, producing an even or odd number of progeny (illustrated in Figure 1B). Typically, the consumption of one *E. coli* cell results in four to six attack-phase *Bdellovibrios* that, after maturation, escape from the prey's outer membrane and begin a new predatory cycle (17, 30, 31). Genomic studies pointed out a number of proteins involved in motility and a remarkable orchestra of catabolizing enzymes (nucleases, proteases and lipases) supported by an amount of transport proteins. A recent transcriptome study revealed more about regulation of the molecular machinery that finally leads to successful predation (29). Although considered as obligate predators, mutants of *Bdellovibrio bacteriovorous* (they occur with the frequency of approx. 1/10^7 bacteria) can grow axenically in complex medium, pointing on a thin line between predatory and saprophytic lifestyles.

Another obligate predatory bacterium that has been well studied is *Micavibrio aeruginosavorous*. When isolated in the early 1980ies, it was affiliated to the *Bdellovibrio*

genus based on morphological and activity studies (32-34). *Micavibrio aeruginosavorous* came back into the spotlight only in 2006, when a research group led by Edouard Jurkevitch performed a survey of predatory bacteria in soil samples to find that a proportion of isolated predatory bacteria were not *Bdellovibrio*-related *Deltaproteobacteria*, but rather clustered phylogenetically together with *Micavibrio aeroginosavorous* ARL-13. The following phylogenetic analysis showed that *Micavibrio* species form a deep branching lineage within the *Alphaproteobacteria* (35). Much like *Bdellovibrio exovorus* JSS^{T}, isolated *Micavibro* EPB did not invade periplasmic space of their prey, but remained attached to the outer membrane, dividing by binary fission (35, 36) (Figure 1C).

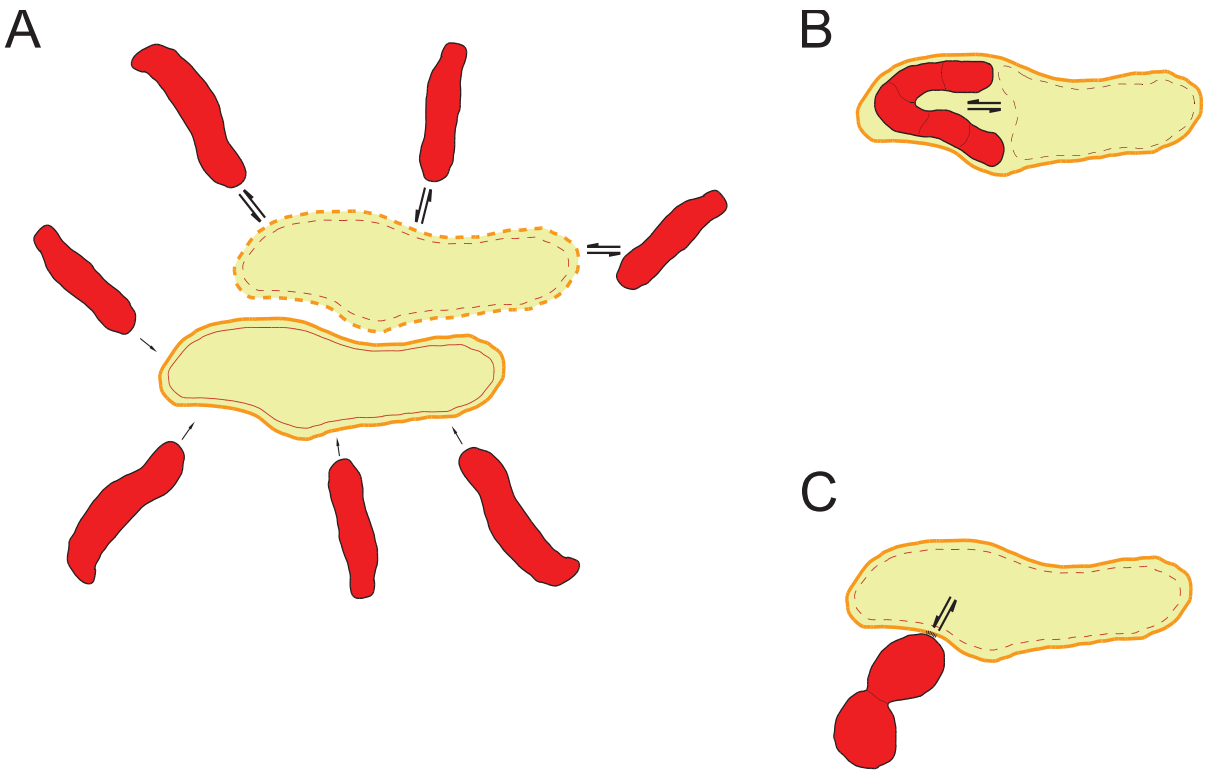

Figure 1: Three known modes of bacterial predation. (A) Bacteria "attack" as a wolfpack, release digestive enzymes and take up nutrients released from the prey cells. Typically, this strategy is used by facultative predatory bacteria. On the other hand, obligatory predators employ either (B) invasion of the periplasmic space, where they digest prey cell, grow and finally divide by septation or (C) epibiotic predation. Epibiotic predators attach to their prey via a junction through which they secrete digestive enzymes and take up released biomolecules. Adapted from Jurkevitch (2007).

In the macroscale world, predation significantly contributes to the population control of lower trophic levels. Predation and grazing are known to increase the diversity of lower trophic levels, and thereby functional redundancy and ecosystem resilience (37). In contrast to the

macroscale biomes, where predation and its consequences are well documented, little is known about the ecological impact of bacterial predators in natural or engineered environments. Most of studies aiming at enumerating predatory bacteria in the environment were based on counting plaques resulting from consumption and concomitant lysis of soft agar-embedded prey bacteria. As authors often pointed out, such approaches suffer from a narrow prey specificity of predators and a limited prey cultivation capacity of investigators (34, 38, 39). Albeit difficult-to-culture bacteria represent the majority of microbial biomass and biotic diversity, little is known on the potential predation that they may face. Only recently, molecular methods were utilized to measure environmental abundances and address niche diversification of predatory bacteria (34, 40, 41). Furthermore, the comparison of 11 genomes of known predatory bacteria with a selection of 19 genomes of non-predatory bacteria pointed out the dependence of predatory bacteria on adhesion-assisting proteins, proteases, and on the import of riboflavin and several amino acids. Another distinguishing feature of predatory lifestyle seems to be isoprenoid synthesis pathway. The presence of (at least part of) the mevalonate pathway is one of the characteristics of a predatory or intracellular lifestyle (28). The authors suggest that with the help of rapidly growing data on bacterial (meta)genomes, such analyses will identify hitherto undetected predatory bacteria and in turn assist the quantification of bacterial predation in various environments (28).

Recognizably predatory, but nevertheless cryptic is the symbiosis between the hyperthermophilic, lithoautotrophic crenarchaeon *Ignicoccus hospitalis* and *Nanoarchaeum equitans*, the first described member of the phylum *Nanoarchaeota* (42-44). Being studied in the "pre-molecular" era, there are some examples of predatory bacteria that were not characterized in detail. They differ from already described predators not only by morphology, but also by invasion and division modes (45, 46). Regrettably, there are no molecular data from those studies that would allow researchers to utilize modern tools to locate them in the environment and study them in greater detail.

Nitrifying microbial communities

Nitrogen is the major component of the Earth's atmosphere and one of the key elements constituting its biosphere. The transformations between nitrogen forms are almost exclusively

the domain of microbes (summarized in Figure 2). The bulk of biological nitrogen turnover (fixation and assimilation) aims to provide cells with a nitrogen form that may be readily incorporated into biomass, mainly into nucleic and amino acids. A large pool of nitrogen, the relatively inert nitrogen gas (N_2) that constitutes 78% of the atmosphere (47), is unavailable to most organisms, and those that can tap this resource must invest a considerable amount of energy to do so (16 ATP molecules are necessary to reduce one N_2 molecule into two NH_3). A phlyogenetically diverse guild of microorganisms named diazotrophs ultimately provides the rest of living organisms with nitrogen in its "reactive" state (47, 48), and only in the last one and a half centuries, humans have significantly contributed to N-cycle by Haber-Bosch process (industrial N-fixation) and fossil fuel combustion (47, 49). Reduced nitrogen forms may also be used to fuel microbial growth; as electron donor in the stepwise oxidation to nitrate during nitrification (50-52). Closing the loop, denitrification describes the successive processes in which oxidized nitrogen forms serve as terminal electron acceptor in environments devoid of oxygen, and are finally reduced to nitrogen gas (50). Additionally, several members of the *Planctomycetes* phylum can exploit the anaerobic ammonia oxidation (ANAMMOX), an energy-gaining process where ammonium is the electron donor and nitrite the electron acceptor (53, 54).

The aerobic nitrification consists of two reactions, the oxidation of ammonia to nitrite (N oxidation state -3 to +3) and the oxidation of nitrite to nitrate (N oxidation state +3 to +5). The following reactions show the stoichiometry of the processes (adapted from 52):

$$2H^+ + NH_3 + 2e^- + O_2 \rightarrow NH_2OH + H_2O \qquad \text{(eq. 1)}$$

$$NH_2OH + H_2O \rightarrow HNO_2 + 4H^+ + 4e^- \qquad \text{(eq. 2)}$$

$$NO_2^- + H_2O \rightarrow NO_3^- + 2H^+ + 2e^- \qquad \text{(eq. 3)}$$

The reduction potential from the first oxidation step (combined equations 1 and 2) is harnessed by two distinct groups of chemolitoautotrophic microorganisms, namely ammonia-oxidising bacteria (AOB) and ammonia-oxidising archaea (AOA) (50, 52, 55-59). Nitrite produced by AOB and AOA can be further oxidized to nitrate by chemolithoautotrophic nitrite-oxidising bacteria (NOB). Known AOA fall within the recently proposed archeal phylum *Thaumarchaeota* (60, 61). All AOB described so far are *Proteobacteria*, from the

classes *Beta*- (genera *Nitrosomonas* and *Nitrosospira*) and *Gammaproteobacteria* (genus *Nitrosococcus*). Both AOA and AOB may be found in a variety of natural and artificial environments. To a big surprise of the scientific community, recently discovered AOA (62-64) were found to be the driving force behind nitrification in a majority of natural habitats (oceans, sediments, and soils), and isolated strains seem to be adapted to a broader range of environmental conditions than AOB isolates (for a review see 58, 65). Less phylogenetically coherent are NOB. Their representatives belong to the phyla *Nitrospirae* (*Nitrospira*), *Chloroflexi* (*Nitrolancea*), and the classes *Alpha*- (*Nitrobacter*), *Beta*- (*Nitrotoga*), and *Gammaproteobacteria* (*Nitrococcus*) (66, 67). Finally, recent calculations based on a concatenated protein sequence dataset suggest that the abundant marine nitrite-oxidizer *Nitrospina* form a new deep branching bacterial phylum (*Nitrospinae*) rather than being a member of the *Deltaproteobacteria*, as originally suggested (68). Members of the *Nitrospira*, *Nitrotoga*, and *Nitrobacter* genera seem to be responsible for the bulk of terrestrial nitrite oxidation, while NOB active in oceans are predominantly sublineage IV *Nitrospira*, *Nitrococcus,* and *Nitrospina*. Only recently described *Nitrolancea hollandica* was isolated from sewage, and is likely to significantly contribute to nitrification only at somewhat higher temperatures (69), though more targeted future research might change this view.

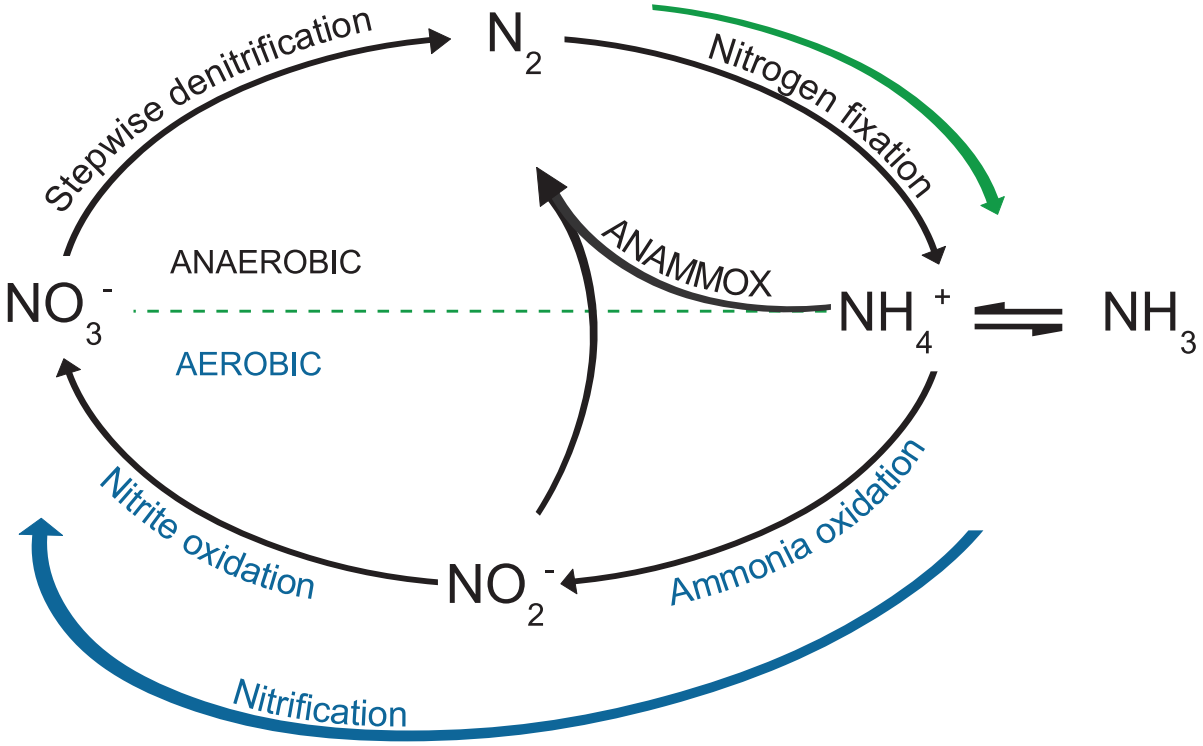

Figure 2: Simplified representation of the nitrogen cycle (N-cycle) showing the major steps in the global nitrogen turnover. The assimilation of NH_4^+ into biomolecules and ammonification has been omitted from the figure. Although the nitrogenase complex is oxygen sensitive, nitrogen fixation can take place in aerobic conditions. Cyanobacteria, for example, developed several efficient mechanisms to separate molecular oxygen from nitrogenase enzyme (48). Denitrification is a stepwise process, in which NO_3^- is reduced to N_2 via several intermediates (NO_2^-, NO and N_2O). The dashed line separates aerobic processes from anaerobic ones.

Much of our knowledge on nitrification stems from the need to better understand the processes in waste water treatment plants (WWTPs), man-made systems that allow the biological turnover of dissolved pollutants (nitrogen, carbon, and phosphorous) into more manageable or inert forms. A central priority of many WWTPs is efficient nitrogen removal. Population growth and concentration in cities has resulted in high amounts of sewage, mostly in the form of urea. Urea is rapidly converted to ammonia either by hydrolysis or microbe-mediated ammonification. Excess nitrogen in is toxic to aquatic life and also leads to eutrophication, which has numerous detrimental effects on the local aquatic ecosystems (52, 56). In addition, some industries (including agriculture) can be a substantial source of environmental pollution with reactive nitrogen forms. In man-made environments exploiting two-step nitrification for sewage treatment, AOB seem to be major players, and despite an occasional presence of archaeal ammonia monooxygenase (*amoA*) genes and members of *Thaumarchaeota* in nitrifying WWTPs, their activity could not be linked to ammonia oxidation (52, 70). In the majority of WWTPs, the nitrite oxidation is a domain of *Nitrospira*, whereas in some plants operated at lower temperatures *Nitrotoga* is found in high numbers (71).

Nitrifying organisms thriving in WWTPs usually grow in tight clusters and are embedded in multispecies biofilm-like flocs. Thus, the cooperation between different microbes involved in nitrogen turnover has received much research attention (72-75). As energy gain during nitrification reactions is low, relatively slow growth is unavoidable for all microbes that gain energy from aerobic nitrification (52). A biofilm embedding and concomitant close co-localization seem to be the strategies that enable an efficient nutrient flow, from which both partners involved in nitrification ultimately benefit. NOB have access to nitrite before it dilutes into the surrounding medium while at the same time they prevent nitrite concentrations reaching levels toxic for the neighboring AOB. Positioning within the biofilm thus allow AOB and NOB to fine-tune the effective substrate and O_2 concentrations (72, 74,

76, 77). In nitrifying flocs, *Nitrospira* clusters typically colocalize with the clusters of AOB (72, 77). The intimacy of this association is influenced by the niche adaptation of different NOB to the nitrite concentrations along the concentration gradient (77). Additionally, Costa et al. proposed that the labor is divided between nitrifying organisms in order to maximize the ATP production rate, optimize enzyme synthesis, and to better cope with toxic metabolism intermediates. Although an organism capable of the complete ammonia oxidation ("comammox") could exist in environments where a slow growth rate and a high ATP yield per substrate would be advantageous, no such organism has been found yet (78).

Nitrifying sludge flocs are populated also by many microbes that are not directly involved in nitrification. That nitrification can be a source of soluble microbial products (SMP), and can support the growth of heterotrophic bacteria is well established (79-81). In experiments where ammonia was the only available energy source, heterotrophic bacteria typically represented 20-50% of the community in nitrifying biofilms (82-84). However, since the initial report of nitrification-powered food web from Rittmann and colleagues (1994), studies focusing on interactions between nitrifiers and accompanying microbes were published only sporadically. Okabe and coworkers could associate the uptake of growth-associated and decay-associated nitrifier products with different phylogenetic groups of bacteria (82, 85). In these two studies, the utilization of SMP has been associated predominately with *Alpha*- and *Gammaproteobacteria*, whereas N-acetyl-D-glucosamine (cell wall component) was consumed by members of *Chloroflexi* and the *Cytophaga-Flavobacterium* cluster. In a follow-up study, *Chloroflexi* consumed decay-associated products, whereas *Cytophaga-Flavobacteria* were linked to growth-associated products secreted by AOB and NOB. No such link could be made for the present *Alpha*- and *Gammaproteobacteria*. Aside from aforementioned studies, little effort has been made to identify the microbes interacting with nitrifiers and to closer illuminate the nature of such cohabitation.

Molecular tools common in symbiosis and nitrification research

Long before molecular tools were designed to analyze microbial communities in natural samples, microbiologists realized that the majority of microbes is not readily cultivated (86). It was therefore impossible, by existing cultivation techniques alone, to obtain an encompassing picture of microbes in natural habitats (i.e. their diversity, their numbers, *in*

situ activities, and finally interactions among them). Nevertheless, the knowledge of natural microbial assemblages, based on cultivation approaches, has been put on a test only when 16S rRNA targeted PCR- and fluorescence *in situ* hybridization (FISH)-based community analysis were introduced (87, 88). For instance, due to their higher growth rates, resistance to higher nitrite concentration and relative ease of cultivation, almost every attempt to cultivate NOB resulted in the isolation of *Nitrobacter* species. In turn, they have been considered to be the main drivers of nitrite oxidation in man-made environments. However, this view started to change when more and more environmental samples were analyzed with molecular techniques (72, 89), and after less than a decade of research, *Nitrospira* were established as the key NOB in WWTPs (90, 91). Both, symbiosis and nitrification research have been exemplary cases of the use of cultivation-independent approaches in microbiology.

In the last 25 years, molecular tools have allowed invaluable insights into the microbial abundances and structure of various communities on global scales (92-94). The full-cycle rRNA approach (86) became the gold standard in experimental design, additionally propelled by the rapidly growing rRNA sequence databases (95-97). PCR with primers targeting conserved sequence regions of marker genes has evolved into an array of tools for the description of community structures (98-100). Lately, the introduction of "next generation" sequencing primarily characterized by (very) high read numbers, spawned numerous studies describing microbial diversity "in depth" and we are currently witnessing a second renaissance in microbial community profiling (101, 102). Further technical developments reduced sequencing costs to the point, where PCR amplification is no longer necessary to retrieve large amounts of 16S sequences from environmental samples (103). However, the presence and/or identity of a given microbe tells little about its activity or function in that environment (104). It is especially frustrating to characterize a species, described only by rRNA sequence, and with no close relative existing as a culture. Cultivation in pure culture was (and sometimes still is) necessary to study the physiology and metabolic potential of a given microbe. Even in enrichment cultures, created by long term selection under conditions selected by the researcher, it may be difficult to show beyond doubt which microbe is responsible for the activity in question. Partially, this problem has been circumvented by metagenomics (also environmental genomics; genomics of mixed community) and its spin-off metatranscriptomics, extending community characterization to functional genes, larger genomic fragments, or even whole genomes extracted from the environment (92, 105, 106). Metagenomics is nowadays an invaluable tool for characterization of the genomic potential in

a microbial community. For example, the genome of key WWTP NOB *Candidatus* Nitrospira defluvii has been assembled from metagenomic data. In addition to the wealth of data elucidating the physiology of this nitrite-oxidizer, a phylogenetic analysis of the nitrite oxidoreductase-like enzymes led to the proposal that nitrite oxidation evolved twice, and the machinery utilized by *Nitrospira* likely has a common origin with ANAMMOX (68, 107, 108). These results further support the conclusions of ultrastructure studies; while proteobacterial members of NOB and *Nitrolancea* have the Nxr (short for nitrite oxidoreductase; the enzyme that catalyzes the oxidation of nitrite to nitrate) complex located on the inner side of their periplasmic membrane, the nitrite oxidation seems to take place in the periplasmic space in *Nitrospira* and *Nitrospina* (107, 109). Despite its obvious advantages, the metagenomics is not without caveats. It can, for example, be difficult to meaningfully connect obtained sequences, especially when using modern NGS technologies that yield high number of relatively short reads. The generation of chimeric sequences complicates the annotation and can create gene (and thus functions) combinations that do not exist in nature. New creative study designs show, however, high promise in minimizing such biases (110). Alternative approach to minimize the likelihood of chimeric sequences is to clone large genomic fragments (into fosmids), but it is laborious and costly, and only seldom used in studies nowadays.

In parallel, FISH is not only essential for microbial enumeration; it is a vital tool for determining the structure of natural microbial assemblages. The close cohabitation of AOB and NOB in WWTPs, visualized with FISH, is a good example of how different microbial-driven processes can be spatially coupled in the environment (72, 77). Furthermore, FISH has been used to estimate microbial activity, exploiting the fact that ribosome content and growth rate are tightly coupled in some microbes (111). FISH (and its applicability) has been extended by introduction of the catalyzed reporter deposition fluorescence *in situ* hybridization (CARD-FISH) technique (Figure 3, for review see 112, 113). In CARD-FISH, oligonucleotides are covalently linked to the horseradish peroxidase (HRP) enzyme rather than to a fluorescent dye like in FISH. After hybridization, HRP catalyzes the oxidation of tyramides (conjugates of tyramine and reporter molecules; Figure 3B), which react with tyrosine residues of proteins and thus covalently link reporter molecules to the biomass. This method is especially valuable when the obtained signal to noise ratios are too small with standard FISH, which is common for cells with a low ribosome content due to dormancy or low activity. As AOA have a relatively low ribosome content, nitrification research has

benefited from the use of CARD-FISH to detect AOA in environmental samples or enrichments, illuminating their physiology, function and interaction with the environment (63, 70, 114).

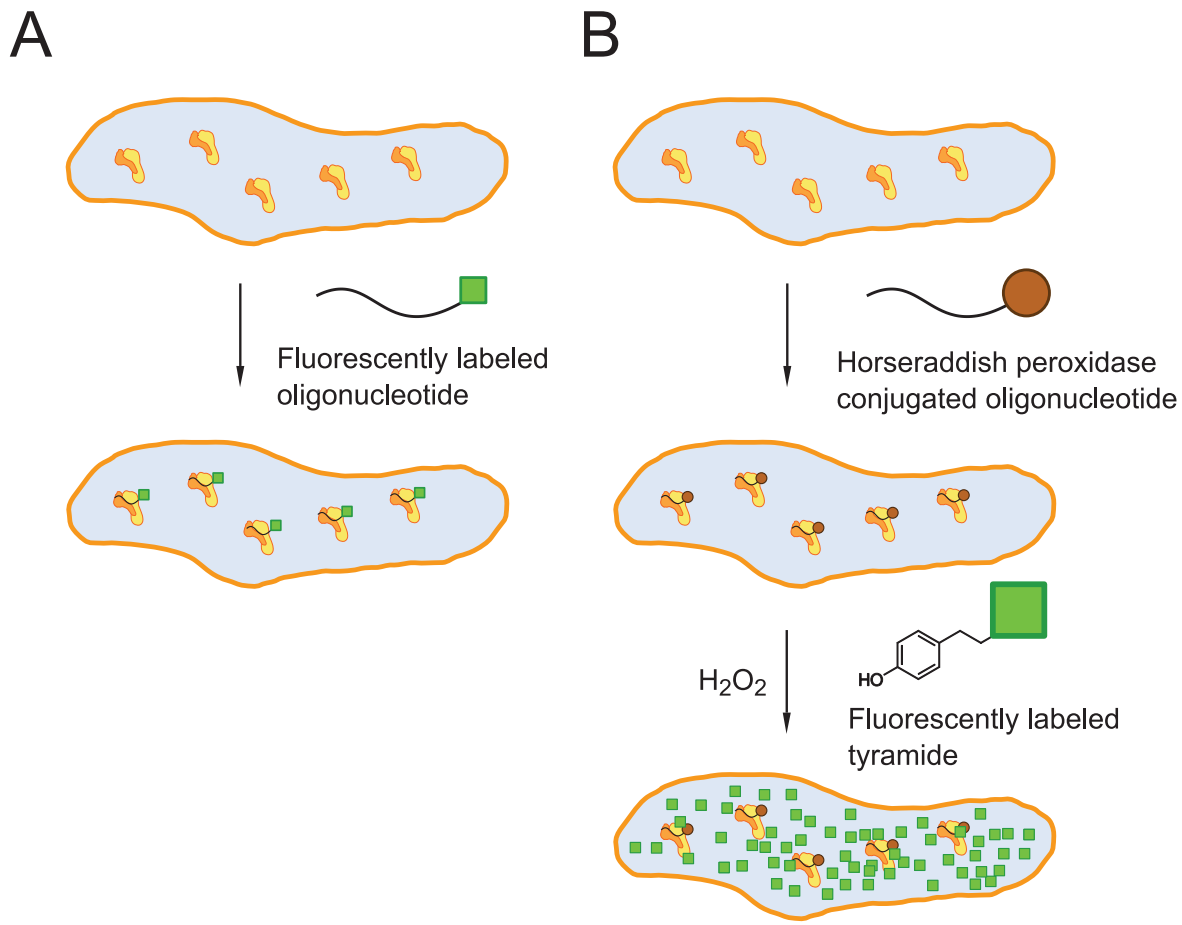

Figure 3: Comparison of rRNA targeted FISH and CARD-FISH. (A) In FISH, oligonucleotides with a covalently linked fluorescent dye are hybridized to the rRNA of the target cell. Given that the density of target rRNA molecules is high enough, labeled cells can be visualized directly. (B) CARD-FISH utilizes an additional amplification step, in which HRP enzyme bound to hybridized oligonucleotides catalyzes a covalent bond formation (or deposition) between fluorescent tyramides and the tyrosine residues of proteins (115). As each HRP can "deposit" several tyramides, the fluorescent signal can be greatly amplified.

To combine the benefits of the functional gene analysis with visualizing community structure, considerable effort has been invested into development of methods that allow detection of mRNA or even single genes (116-121). None of them have, however, found a wide spread in study designs. In general, these methods can hardly be applied "universally" (without specific adaptation to the sample). It is therefore likely that microbial ecologists will continue to look for "single gene FISH" methods that are more rapid, universally applicable,

and possibly even simpler. Advances in nucleotide polymer synthesis, and possibly modified nucleotide bases with improved hybridization properties (that will allow better mismatch discrimination) might assist method developments in the future.

The introduction of isotope-tracer based techniques is considered as a breakthrough in the cultivation-independent characterization of process-relevant microbes (for review see 4, 104). When substrates enriched with suitable isotopes are added (in relevant concentrations) to microbial communities exposed to natural or near-natural conditions, they are metabolized and finally the tracer isotopes are incorporated into biomass. If incorporated isotopes can be detected and at the same time accurately linked to specific community members via a suitable marker, the metabolic function can be linked to the identity of active microbes within the examined community. Such tools are particularly valuable for microbial ecologists, (especially) since the mere presence of microbes, or even the presence of functional genes and their transcripts do not guarantee their activity *in situ* (104). For this purpose, radioactive isotopes were used as tracers well before the wide spread of molecular tools (122, 123). However, only the development of microradiography combined with FISH (FISH-MAR) allowed the simultaneous detection of active microbes in complex samples and their identification with a high phylogenetic resolution (124). Among numerous other studies, FISH-MAR has been used to demonstrate the ability of chemolithoautotrophic members of the *Nitrospira* genus, active in nitrifying sludge, to scavenge some SMP (pyruvate) and use them for growth (91). Over the past 10 years, however, the radioactive tracers have been increasingly complemented by stable isotopes (primarily ^{13}C and ^{15}N). Improved detection possibilities combined with a safer use quickly gained the attention of the research community, and finally resulted in a radiation of stable isotope based methods. Nowadays, phospholipid fatty acids (PLFA), DNA, RNA and protein stable isotope probing (125-128), secondary ion mass spectroscopy (SIMS) imaging (104, 129), and RAMAN microscopy based tracer detection (104, 130) are among the central tools in the environmental microbiologist toolbox. Figure 4 summarizes the tools available to microbial ecologists for activity studies that are based on isotope tracers.

In most stable isotope probing (SIP) approaches, only one cellular component is examined. Increased density of nucleic acids enriched with stable isotopes that have higher atomic mass (^{13}C, ^{15}N and ^{2}H) than abundant isotopes (^{12}C, ^{14}N and ^{1}H) are the basis for the DNA- and RNA-SIP. When a sufficient degree of enrichment is achieved, labeled nucleic acids can be

isolated by density centrifugation and separately analyzed (or rather with less "noise"). Downstream use of rRNA sequencing or suitable fingerprinting technique (e.g. denaturing gradient gel electrophoresis, terminal restriction fragment length polymorphism or high throughput sequencing) allows identification of organisms that incorporated heavy isotopes into their nucleic acids. By combining DNA- or RNA-SIP with targeted metagenomic and metatranscriptomic approaches one may learn more about active community members without much redundant sequencing and analysis efforts (131, 132). In PLFA and protein SIP the markers are isolated from the bulk biomass, and for each specific marker (e.g. protein specific for a certain group of bacteria) the amount of the incorporated isotope is determined by mass spectrometry. Here, only minute amounts of incorporated label can be readily and quantitatively detected. Although targeting rRNA, a method developed by Barbara MacGregor has more in common with PLFA- and protein SIP than with standard DNA- and RNA-SIP techniques (133). It relies on rRNA hybridization to oligonucleotide probes, covalently linked to magnetic beads. Depending on the specificity of the probes used, rRNA from targeted organisms (or targeted groups) can be isolated and its isotopic composition determined by Isotope Ratio Mass Spectroscopy (IRMS). Despite their sensitivity, a considerable disadvantage of the later methods is that one needs prior information on the protein, PLFA, or rRNA composition of microbes in question. In contrast, DNA- and RNA-SIP are true "discovery" methods that do not require prior knowledge of the analyzed microbial community. Indeed, they can be very useful tools to provide preliminary/supporting data and generate hypotheses to be then tested in more targeted experiments.

On the other hand, Raman microspectroscopy enables one to have a holistic look on a cell. Cellular components have their characteristic Raman spectra and, combined together, result in a complex "fingerprint" spectrum that can sometimes be used to identify microbes in a sample without the need for any further reagents or tools (134-136). Raman spectra reflect (many types of) intramolecular bond vibrations, and as these are influenced by an increased atomic mass of stable isotopes, the isotopic composition of marker compounds can be quantitatively determined (104). Thus, Raman microspectroscopy can be a powerful tool for microbial ecologists, especially when combined together with FISH (130) or optical tweezers for single cell sorting (134, 137). Being a nondestructive technique, active cells may be isolated for further cultivation or downstream analysis. In SIMS imaging, sample-dependent secondary ions are formed after bombardment with a focused primary ion beam. Their

detection depends on the instrument and examined sample, but in general it offers very high sensitivity, and can discriminate even between variations in the natural isotopic composition (129). Further technological advancements resulted in NanoSIMS, where current instruments are capable of analyzing samples with a lateral resolution of 50 nm and can simultaneously monitor up to seven different ion species. NanoSIMS has been proven to be a powerful tool in microbial ecology (for review and outlook see 138, 139), and despite its very high purchase and operation costs, the number of instruments available to microbiologists is steadily increasing. The research community has invested a considerable amount of effort into improving the output of NanoSIMS studies, and in addition to "open-source" analysis alternatives (140), several methods to unambiguously identify microbes during NanoSIMS analysis (141-143) emerged in a relatively short time. In SIMSISH, the label (iodine) is bound directly to an oligonucleotide, and can be deployed analogous to fluorescence dyes in FISH. The deposition of the label in "enhanced element labeling-catalyzed reporter deposition fluorescence *in situ* hybridization" (EL-FISH) and "halogen *in situ* hybridization-secondary ion mass spectroscopy" (HISH-SIMS) relies, however, on the modification of the CARD-FISH technique.

Stark difference between SIP approaches lays in the speed and precision of the analysis, and the wealth of information that one can potentially obtain. In DNA- and RNA-SIP, a very limited amount of samples can be processed at once (it takes 4-5 days to completely process four samples, e.g. time points or replicates), however, when combined with modern sequencing approaches, the microbial composition, genomic potential, and even transcription patterns of process-relevant microbes may be analyzed in depth even for very diverse communities. Protein and PFLA-SIP offer very high precision, and if MS instruments offer automatic sampling, they may be optimized to analyze a high number of samples without manual supervision. Raman microspectroscopy (in combination with optical tweezers) may be used to isolate labeled microbes, which can dramatically reduce redundant sequencing when the genomic analysis of active community members is the central part of the study at hand. SIP based on NanoSIMS is notoriously slow, however, data on single cell rather than bulk populations can be obtained. As MS data can be reconstructed as image, SIMS imaging often yields invaluable information on cell interactions with its surroundings (13, 144, 145). With the promise of in-depth sample analysis, the hybridization of RNA to microarrays has been used in combination with radioactive and stable isotopes detection, enabling activity monitoring of a large number of community members simultaneously (146, 147). Although

community profiling with microarrays has been in demise due to modern sequencing technologies, NanoSIMS analysis of microarrays may offer a good compromise between isotope detection sensitivity and the number of phylotypes analyzed in a single run (147). However, as each method brings its own biases and uncertainties, a combination of SIP methods should be used to obtain conclusive and comprehensive results. For example, DNA- or RNA-SIP can provide valuable hypotheses, but, depending on an experimental design, any conclusions should be confirmed (or rejected) by FISH-MAR (148, 149) or another single-cell imaging method.

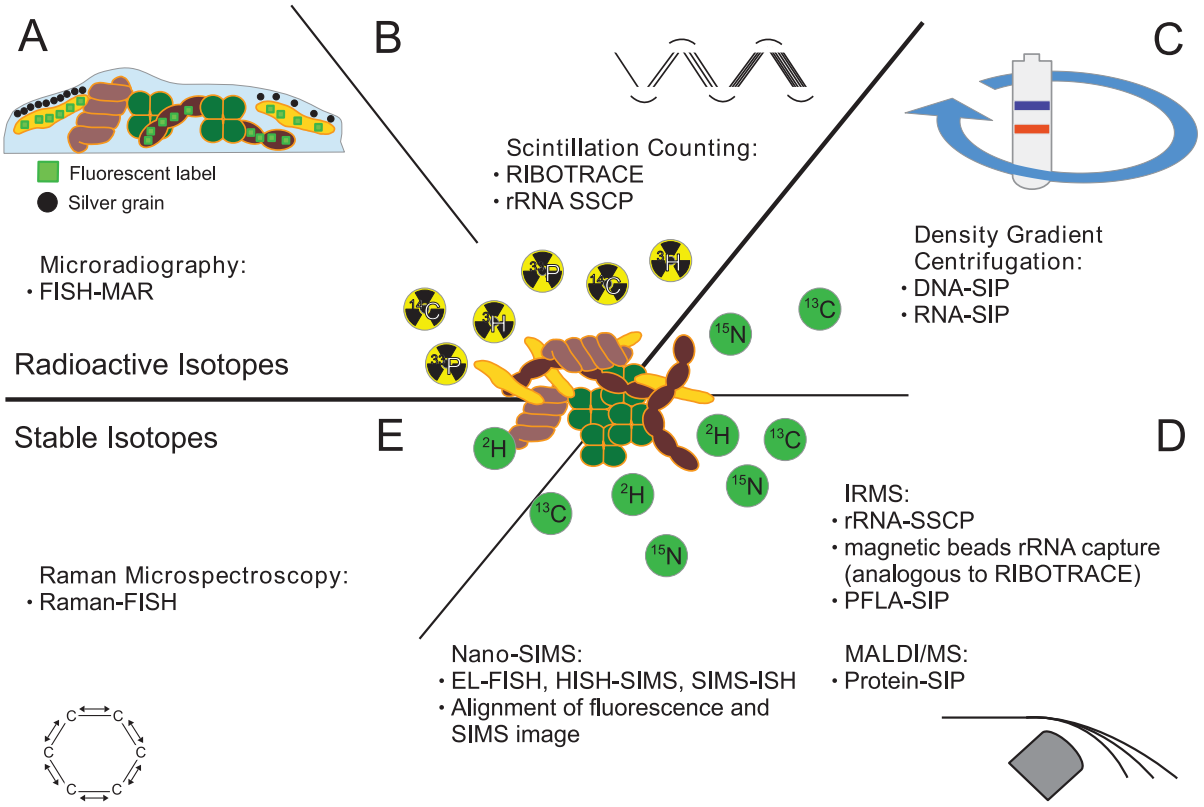

Figure 4: Overview of isotope labeling methods. Bold lines separate methods based on radioactive tracers or stable isotopes. Dashed lines separate conceptually different mechanisms of tracer detection. (A) In FISH-MAR, activity can be linked to identity by parallel visualization of fluorescently labeled cells (by using FISH) and silver grains developed in a photographic emulsion overlaying labeled cells. (B) rRNA originating from target organisms can be specifically isolated by Single-Stranded Conformational Polymorphism (SSCP) or by capture with oligonucleotides attached to magnetic beads (150). Incorporated radioactive tracers are detected and quantified by scintillation counting. As liquid scintillation counters use a photomultiplier, these methods offer very high detection sensitivity. (C) If nucleic acids contain enough stable isotopes with a higher atomic mass than abundant isotopes, they can, due to increase in their density, be separated from unlabeled nucleic acids by density gradient centrifugation. This property is exploited in DNA- and RNA-SIP. (D) Mass Spectrometry (MS) is at the heart of many tracer detection methods. Isotope Ratio Mass Spectroscopy (IRMS) is used to determine stable isotope ratios in rRNA (separated by SSCP or magnetic bead capture), PFLA (pre-separated by chromatography), or even in bulk biomass. Protein-SIP typically relies on the Matrix-Assisted Laser Desorption/Ionization (MALDI)-MS, a method routinely used in proteomics. SIMS imaging can be used to quantitatively determine isotopes incorporated by single cells. Several ISH-based methods have been developed (SIMSISH, EL-FISH and HISH-SIMS) to link the isotopic signature with the identity of the examined cell without the need for (not always straightforward) aligning fluorescent image with SIMS image. (E) The isotopic composition of a molecule influences bond vibrations, and consequently its Raman spectrum. While Raman spectra of whole cells are very complex, heavy isotope-induced shifts (red shifts) of some very distinct peaks may be used to quantify tracer labeling on a single-cell level

Outline

The central objective of this work was to shed light on the ecology of nitrifying bacteria in WWTPs. ***Chapter I*** therefore delineates some basic ecological concepts describing interspecies relations in the microbial world, gives a short introduction to the nitrification and provides the necessary information on modern experimental approaches used in nitrification and symbiosis research. Compared to relatively well studied interactions between AOB and NOB, only a few studies described the fate of carbon fixed by chemolithoautotrophic nitrifying bacteria. Laboratory experiments established that energy harnessed by ammonia and nitrite oxidation can support a diverse and abundant bacterial community. However, since only little information on the type of interactions among the members of nitrifying communities was reported in previous studies, the goal of presented work was to obtain additional insight into the ecology of nitrification driven systems. To this end, RNA-SIP was used to follow the $^{13}CO_2$ fixed during nitrification through the bacterial community and results of the study are presented in ***Chapter II***. However, new approaches can present new challenges. ***Chapter III*** describes the LNAzymes-based method that was developed in order to characterize in detail the ^{13}C labeled nitrifying community, heavily dominated by AOB and NOB, with by Sanger sequencing. As SIP was the central method used in many studies in our department, overcoming challenges of stable isotope detection was a part of daily discussions. At the time a NanoSIMS instrument became available, click chemistry was gaining popularity in molecular biology. To use the potential of click chemistry in facilitating the identification of microbes during NanoSIMS imaging, a novel *in situ* hybridization-based technique was developed, and is described in ***Chapter IV***. The individual studies are connected and additionally discussed in ***Chapter V***. Finally, the ***Appendix 2*** and ***3*** further delineate some aspects of Click-FISH.

References

1. **Schmitz-Esser S, Tischler P, Arnold R, Montanaro J, Wagner M, Rattei T, Horn M.** 2010. The genome of the amoeba symbiont "*Candidatus* Amoebophilus asiaticus" reveals common mechanisms for host cell interaction among amoeba-associated bacteria. J. Bacteriol. **192:**1045-1057.
2. **Sachs JL, Simms EL.** 2006. Pathways to mutualism breakdown. Trends. Ecol. Evol. **21:**585-592.
3. **Sachs JL, Wilcox TP.** 2006. A shift to parasitism in the jellyfish symbiont *Symbiodinium microadriaticum*. Proc. R. Soc. B **273:**425-429.
4. **Orphan VJ.** 2009. Methods for unveiling cryptic microbial partnerships in nature. Curr. Opin. Microbiol. **12:**231-237.
5. **Knittel K, Boetius A.** 2009. Anaerobic oxidation of methane: progress with an unknown process. Annu. Rev. Microbiol. **63:**311-334.
6. **Milucka J, Ferdelman TG, Polerecky L, Franzke D, Wegener G, Schmid M, Lieberwirth I, Wagner M, Widdel F, Kuypers MM.** 2012. Zero-valent sulphur is a key intermediate in marine methane oxidation. Nature **491:**541-546.
7. **McInerney MJ, Sieber JR, Gunsalus RP.** 2009. Syntrophy in anaerobic global carbon cycles. Curr. Opin. Biotechnol. **20:**623-632.
8. **Stams AJ, Plugge CM.** 2009. Electron transfer in syntrophic communities of anaerobic bacteria and archaea. Nature Rev. Microbiol. **7:**568-577.
9. **Summers ZM, Fogarty HE, Leang C, Franks AE, Malvankar NS, Lovley DR.** 2010. Direct exchange of electrons within aggregates of an evolved syntrophic coculture of anaerobic bacteria. Science **330:**1413-1415.
10. **Kato S, Hashimoto K, Watanabe K.** 2012. Microbial interspecies electron transfer via electric currents through conductive minerals. Proc. Natl. Acad. Sci. U. S. A. **109:**10042-10046.
11. **Nielsen LP, Risgaard-Petersen N, Fossing H, Christensen PB, Sayama M.** 2010. Electric currents couple spatially separated biogeochemical processes in marine sediment. Nature **463:**1071-1074.
12. **Pfeffer C, Larsen S, Song J, Dong M, Besenbacher F, Meyer RL, Kjeldsen KU, Schreiber L, Gorby YA, El-Naggar MY, Leung KM, Schramm A, Risgaard-Petersen N, Nielsen LP.** 2012. Filamentous bacteria transport electrons over centimetre distances. Nature **491:**218-221.
13. **Thompson AW, Foster RA, Krupke A, Carter BJ, Musat N, Vaulot D, Kuypers MM, Zehr JP.** 2012. Unicellular cyanobacterium symbiotic with a single-celled eukaryotic alga. Science **337:**1546-1550.
14. **Jurkevitch E.** 2007. Predatory behaviors in bacteria-diversity and transitions. Microbe-American Society for Microbiology **2:**67-70.
15. **Davidov Y, Jurkevitch E.** 2009. Predation between prokaryotes and the origin of eukaryotes. BioEssays: news and reviews in molecular, cellular and developmental biology **31:**748-757.
16. **Berleman JE, Scott J, Chumley T, Kirby JR.** 2008. Predataxis behavior in *Myxococcus xanthus*. Proc. Natl. Acad. Sci. U. S. A. **105:**17127-17132.
17. **Sockett RE.** 2009. Predatory lifestyle of *Bdellovibrio bacteriovorus*. Annu Rev Microbiol **63:**523-539.
18. **Stolp H, Starr MP.** 1963. *Bdellovibrio Bacteriovorus* Gen. Et Sp. N., a predatory, ectoparasitic, and bacteriolytic microorganism. Antonie van Leeuwenhoek **29:**217-248.
19. **Rendulic S, Jagtap P, Rosinus A, Eppinger M, Baar C, Lanz C, Keller H, Lambert C, Evans KJ, Goesmann A, Meyer F, Sockett RE, Schuster SC.** 2004. A predator unmasked: life cycle of *Bdellovibrio bacteriovorus* from a genomic perspective. Science **303:**689-692.
20. **Thomashow MF, Cotter TW.** 1992. *Bdellovibrio* host dependence: the search for signal molecules and genes that regulate the intraperiplasmic growth cycle. J. Bacteriol. **174:**5767-5771.

21. **Dori-Bachash M, Dassa B, Pietrokovski S, Jurkevitch E.** 2008. Proteome-based comparative analyses of growth stages reveal new cell cycle-dependent functions in the predatory bacterium *Bdellovibrio bacteriovorus*. Appl. Environ. Microbiol. **74:**7152-7162.
22. **Lambert C, Ivanov P, Sockett RE.** 2010. A transcriptional "Scream" early response of *E. coli* prey to predatory invasion by *Bdellovibrio*. Curr. Microbiol. **60:**419-427.
23. **Lambert C, Chang CY, Capeness MJ, Sockett RE.** 2010. The first bite--profiling the predatosome in the bacterial pathogen *Bdellovibrio*. PLoS One **5:**e8599.
24. **Liu MY, Kjelleberg S, Thomas T.** 2011. Functional genomic analysis of an uncultured delta-proteobacterium in the sponge *Cymbastela concentrica*. ISME J. **5:**427-435.
25. **Fenton AK, Kanna M, Woods RD, Aizawa SI, Sockett RE.** 2010. Shadowing the actions of a predator: backlit fluorescent microscopy reveals synchronous nonbinary septation of predatory *Bdellovibrio* inside prey and exit through discrete bdelloplast pores. J. Bacteriol. **192:**6329-6335.
26. **Wang Z, Kadouri DE, Wu M.** 2011. Genomic insights into an obligate epibiotic bacterial predator: *Micavibrio aeruginosavorus* ARL-13. BMC Genomics **12:**453.
27. **Lerner TR, Lovering AL, Bui NK, Uchida K, Aizawa S, Vollmer W, Sockett RE.** 2012. Specialized peptidoglycan hydrolases sculpt the intra-bacterial niche of predatory *Bdellovibrio* and increase population fitness. PLoS Pathog. **8:**e1002524.
28. **Pasternak Z, Pietrokovski S, Rotem O, Gophna U, Lurie-Weinberger MN, Jurkevitch E.** 2013. By their genes ye shall know them: genomic signatures of predatory bacteria. ISME J. **7:**756-769.
29. **Karunker I, Rotem O, Dori-Bachash M, Jurkevitch E, Sorek R.** 2013. A global transcriptional switch between the attack and growth forms of *Bdellovibrio bacteriovorus*. PLoS One **8:**e61850.
30. **Lambert C, Morehouse KA, Chang CY, Sockett RE.** 2006. *Bdellovibrio*: growth and development during the predatory cycle. Curr. Opin. Microbiol. **9:**639-644.
31. **Sockett RE, Lambert C.** 2004. *Bdellovibrio* as therapeutic agents: a predatory renaissance? Nature Rev. Microbiol. **2:**669-675.
32. **Lambina VA, Afinogenova AV, Romai Penabad S, Konovalova SM, Pushkareva AP.** 1982. (*Micavibrio admirandus* gen. et sp. nov]. Mikrobiologiia **51:**114-117.
33. **Lambina VA, Afinogenova AV, Romay Penobad Z, Konovalova SM, Andreev LV.** 1983. (New species of exoparasitic bacteria of the genus *Micavibrio* infecting gram-positive bacteria]. Mikrobiologiia **52:**777-780.
34. **Davidov Y, Friedjung A, Jurkevitch E.** 2006. Structure analysis of a soil community of predatory bacteria using culture-dependent and culture-independent methods reveals a hitherto undetected diversity of *Bdellovibrio*-and-like organisms. Environ. Microbiol. **8:**1667-1673.
35. **Davidov Y, Huchon D, Koval SF, Jurkevitch E.** 2006. A new alpha-proteobacterial clade of *Bdellovibrio*-like predators: implications for the mitochondrial endosymbiotic theory. Environ. Microbiol. **8:**2179-2188.
36. **Koval SF, Hynes SH, Flannagan RS, Pasternak Z, Davidov Y, Jurkevitch E.** 2013. *Bdellovibrio exovorus* sp. nov., a novel predator of *Caulobacter crescentus*. Int. J. Syst. Evol. Microbiol. **63:**146-151.
37. **Hector A, Schmid B, Beierkuhnlein C, Caldeira MC, Diemer M, Dimitrakopoulos PG, Finn JA, Freitas H, Giller PS, Good J, Harris R, Hogberg P, Huss-Danell K, Joshi J, Jumpponen A, Korner C, Leadley PW, Loreau M, Minns A, Mulder CP, O'Donovan G, Otway SJ, Pereira JS, Prinz A, Read DJ, et al.** 1999. Plant diversity and productivity experiments in european grasslands. Science **286:**1123-1127.
38. **Zheng G, Wang C, Williams HN, Pineiro SA.** 2008. Development and evaluation of a quantitative real-time PCR assay for the detection of saltwater *Bacteriovorax*. Environ. Microbiol. **10:**2515-2526.
39. **Chauhan A, Cherrier J, Williams HN.** 2009. Impact of sideways and bottom-up control factors on bacterial community succession over a tidal cycle. Proc. Natl. Acad. Sci. U. S. A. **106:**4301-4306.

40. **Pineiro SA, Williams HN, Stine OC.** 2008. Phylogenetic relationships amongst the saltwater members of the genus *Bacteriovorax* using rpoB sequences and reclassification of *Bacteriovorax stolpii* as *Bacteriolyticum stolpii* gen. nov., comb. nov. Int. J. Syst. Evol. Microbiol. **58:**1203-1209.
41. **Pineiro S, Chauhan A, Berhane TK, Athar R, Zheng G, Wang C, Dickerson T, Liang X, Lymperopoulou DS, Chen H, Christman M, Louime C, Babiker W, Stine OC, Williams HN.** 2013. Niche partition of *Bacteriovorax* operational taxonomic units along salinity and temporal gradients in the Chesapeake Bay reveals distinct estuarine strains. Microb. Ecol. **65:**652-660.
42. **Huber H, Hohn MJ, Rachel R, Fuchs T, Wimmer VC, Stetter KO.** 2002. A new phylum of Archaea represented by a nanosized hyperthermophilic symbiont. Nature **417:**63-67.
43. **Jahn U, Gallenberger M, Paper W, Junglas B, Eisenreich W, Stetter KO, Rachel R, Huber H.** 2008. *Nanoarchaeum equitans* and *Ignicoccus hospitalis*: new insights into a unique, intimate association of two archaea. J. Bacteriol. **190:**1743-1750.
44. **Forterre P, Gribaldo S, Brochier-Armanet C.** 2009. Happy together: genomic insights into the unique *Nanoarchaeum*/*Ignicoccus* association. J. Biol. **8:**7.
45. **Guerrero R, Pedros-Alio C, Esteve I, Mas J, Chase D, Margulis L.** 1986. Predatory prokaryotes: predation and primary consumption evolved in bacteria. Proc. Natl. Acad. Sci. U. S. A. **83:**2138-2142.
46. **Larkin JM, Henk MC, Burton SD.** 1990. Occurrence of a *Thiothrix* sp. Attached to Mayfly Larvae and Presence of Parasitic Bacteria in the *Thiothrix* sp. Appl. Environ. Microbiol. **56:**357-361.
47. **Galloway JN, Townsend AR, Erisman JW, Bekunda M, Cai Z, Freney JR, Martinelli LA, Seitzinger SP, Sutton MA.** 2008. Transformation of the nitrogen cycle: recent trends, questions, and potential solutions. Science **320:**889-892.
48. **Zehr JP.** 2011. Nitrogen fixation by marine cyanobacteria. Trends Microbiol. **19:**162-173.
49. **Fowler D, Coyle M, Skiba U, Sutton MA, Cape JN, Reis S, Sheppard LJ, Jenkins A, Grizzetti B, Galloway JN, Vitousek P, Leach A, Bouwman AF, Butterbach-Bahl K, Dentener F, Stevenson D, Amann M, Voss M.** 2013. The global nitrogen cycle in the twenty-first century. Philos. Trans. R. Soc., B **368:**20130164.
50. **Klotz MG, Stein LY.** 2008. Nitrifier genomics and evolution of the nitrogen cycle. FEMS Microbiol. Lett. **278:**146-156.
51. **Zehr JP, Kudela RM.** 2011. Nitrogen cycle of the open ocean: from genes to ecosystems. Annu. Rev. Marine Sci. **3:**197-225.
52. **Daims H, Wagner M.** 2010. The microbiology of nitrogen removal, p. 259-280. *In* Seviour RJ, Nielsen PH (ed.), Microbial Ecology of Activated Sludge. IWA Publishing, London, United Kingdom.
53. **Op den Camp HJ, Kartal B, Guven D, van Niftrik LA, Haaijer SC, van der Star WR, van de Pas-Schoonen KT, Cabezas A, Ying Z, Schmid MC, Kuypers MM, van de Vossenberg J, Harhangi HR, Picioreanu C, van Loosdrecht MC, Kuenen JG, Strous M, Jetten MS.** 2006. Global impact and application of the anaerobic ammonium-oxidizing (anammox) bacteria. Biochem. Soc. Trans. **34:**174-178.
54. **Jetten MS, Niftrik L, Strous M, Kartal B, Keltjens JT, Op den Camp HJ.** 2009. Biochemistry and molecular biology of anammox bacteria. Crit. Rev. Biochem. Mol. Biol. **44:**65-84.
55. **Purkhold U, Pommerening-Roser A, Juretschko S, Schmid MC, Koops HP, Wagner M.** 2000. Phylogeny of all recognized species of ammonia oxidizers based on comparative 16S rRNA and amoA sequence analysis: implications for molecular diversity surveys. Appl. Environ. Microbiol. **66:**5368-5382.
56. **Kowalchuk GA, Stephen JR.** 2001. Ammonia-oxidizing bacteria: a model for molecular microbial ecology. Annu. Rev. Microbiol. **55:**485-529.
57. **Koops H-P, Purkhold U, Pommerening-Röser A, Timmermann G, Wagner M.** 2006. The lithoautotrophic ammonia-oxidizing bacteria, p. 778-811. *In* Dworkin M, Falkow S, Rosenberg E, Schleifer K-H, Stackebrandt E (ed.), The Prokaryotes. Springer, New York, USA.

58. **Stahl DA, de la Torre JR.** 2012. Physiology and diversity of ammonia-oxidizing archaea. Annu. Rev. Microbiol. **66:**83-101.
59. **Prosser JI, Nicol GW.** 2012. Archaeal and bacterial ammonia-oxidisers in soil: the quest for niche specialisation and differentiation. Trends Microbiol. **20:**523-531.
60. **Brochier-Armanet C, Boussau B, Gribaldo S, Forterre P.** 2008. Mesophilic Crenarchaeota: proposal for a third archaeal phylum, the Thaumarchaeota. Nature Rev. Microbiol. **6:**245-252.
61. **Spang A, Hatzenpichler R, Brochier-Armanet C, Rattei T, Tischler P, Spieck E, Streit W, Stahl DA, Wagner M, Schleper C.** 2010. Distinct gene set in two different lineages of ammonia-oxidizing archaea supports the phylum Thaumarchaeota. Trends Microbiol. **18:**331-340.
62. **Konneke M, Bernhard AE, de la Torre JR, Walker CB, Waterbury JB, Stahl DA.** 2005. Isolation of an autotrophic ammonia-oxidizing marine archaeon. Nature **437:**543-546.
63. **Hatzenpichler R, Lebedeva EV, Spieck E, Stoecker K, Richter A, Daims H, Wagner M.** 2008. A moderately thermophilic ammonia-oxidizing crenarchaeote from a hot spring. Proc. Natl. Acad. Sci. U. S. A. **105:**2134-2139.
64. **Lehtovirta-Morley LE, Stoecker K, Vilcinskas A, Prosser JI, Nicol GW.** 2011. Cultivation of an obligate acidophilic ammonia oxidizer from a nitrifying acid soil. Proc. Natl. Acad. Sci. U. S. A. **108:**15892-15897.
65. **Hatzenpichler R.** 2012. Diversity, physiology, and niche differentiation of ammonia-oxidizing archaea. Appl. Environ. Microbiol. **78:**7501-7510.
66. **Sorokin DY, Vejmelkova D, Luecker S, Streshinskaya GM, Rijpstra I, Sinninghe Damste J, Kleerebezem R, Van Loosdrecht M, Muyzer G, Daims H.** 2014. *Nitrolancea hollandica* gen. nov., sp. nov., a chemolithoautotrophic nitrite-oxidizing bacterium from a bioreactor belonging to the phylum Chloroflexi. Int. J. Syst. Evol. Microbiol. 2014 Feb 26. doi: 10.1099/ijs.0.062232-0. (Epub ahead of print]
67. **Daims H, Lücker S, Le Paslier D, Wagner M.** 2011. Diversity, environmental genomics, and ecophysiology of nitrite-oxidizing bacteria, p. 295-322. *In* Ward BB, Arp DJ, Klotz MG (ed.), Nitrification. ASM Press, Washington, DC, USA.
68. **Lucker S, Nowka B, Rattei T, Spieck E, Daims H.** 2013. The genome of *Nitrospina gracilis* illuminates the metabolism and evolution of the major marine nitrite oxidizer. Front. Microbiol. **4:**27.
69. **Sorokin DY, Lucker S, Vejmelkova D, Kostrikina NA, Kleerebezem R, Rijpstra WI, Damste JS, Le Paslier D, Muyzer G, Wagner M, van Loosdrecht MC, Daims H.** 2012. Nitrification expanded: discovery, physiology and genomics of a nitrite-oxidizing bacterium from the phylum Chloroflexi. ISME J. **6:**2245-2256.
70. **Mussmann M, Brito I, Pitcher A, Sinninghe Damste JS, Hatzenpichler R, Richter A, Nielsen JL, Nielsen PH, Muller A, Daims H, Wagner M, Head IM.** 2011. Thaumarchaeotes abundant in refinery nitrifying sludges express *amoA* but are not obligate autotrophic ammonia oxidizers. Proc. Natl. Acad. Sci. U. S. A. **108:**16771-16776.
71. **Lücker S.** 2010. Exploring the ecology and genomics of globally important nitrite-oxidizing bacteria. Ph.D. thesis, University of Vienna, Vienna, Austria.
72. **Schramm A, De Beer D, Wagner M, Amann R.** 1998. Identification and activities *in situ* of *Nitrosospira* and *Nitrospira* spp. as dominant populations in a nitrifying fluidized bed reactor. Appl. Environ. Microbiol. **64:**3480-3485.
73. **Schramm A.** 2003. *In situ* analysis of structure and activity of the nitrifying community in biofilms, aggregates, and sediments. Geomicrobiol. J. **20:**313-333.
74. **Schramm A, De Beer D, Gieseke A, Amann R.** 2000. Microenvironments and distribution of nitrifying bacteria in a membrane-bound biofilm. Environ. Microbiol. **2:**680-686.
75. **Okabe S, Satoh H, Watanabe Y.** 1999. *In situ* analysis of nitrifying biofilms as determined by *in situ* hybridization and the use of microelectrodes. Appl. Environ. Microbiol. **65:**3182-3191.

76. **Stein LY, Arp DJ.** 1998. Loss of ammonia monooxygenase activity in *Nitrosomonas europaea* upon exposure to nitrite. Appl. Environ. Microbiol. **64:**4098-4102.
77. **Maixner F, Noguera DR, Anneser B, Stoecker K, Wegl G, Wagner M, Daims H.** 2006. Nitrite concentration influences the population structure of *Nitrospira*-like bacteria. Environ. Microbiol. **8:**1487-1495.
78. **Costa E, Perez J, Kreft JU.** 2006. Why is metabolic labour divided in nitrification? Trends Microbiol. **14:**213-219.
79. **Rittmann BE, Regan JM, Stahl DA.** 1994. Nitrification as a source of soluble organic substrate in biological treatment. Water Sci. Technol. **30:**1-6.
80. **Ni BJ, Fang F, Xie WM, Yu HQ.** 2008. Growth, maintenance and product formation of autotrophs in activated sludge: taking the nitrite-oxidizing bacteria as an example. Water Res. **42:**4261-4270.
81. **Ni BJ, Rittmann BE, Yu HQ.** 2011. Soluble microbial products and their implications in mixed culture biotechnology. Trends Biotechnol. **29:**454-463.
82. **Kindaichi T, Ito T, Okabe S.** 2004. Ecophysiological interaction between nitrifying bacteria and heterotrophic bacteria in autotrophic nitrifying biofilms as determined by microautoradiography-fluorescence *in situ* hybridization. Appl. Environ. Microbiol. **70:**1641-1650.
83. **Matsumoto S, Katoku M, Saeki G, Terada A, Aoi Y, Tsuneda S, Picioreanu C, van Loosdrecht MC.** 2010. Microbial community structure in autotrophic nitrifying granules characterized by experimental and simulation analyses. Environ. Microbiol. **12:**192-206.
84. **Nogueira R, Elenter D, Brito A, Melo LF, Wagner M, Morgenroth E.** 2005. Evaluating heterotrophic growth in a nitrifying biofilm reactor using fluorescence *in situ* hybridization and mathematical modeling. Water Sci. Technol. **52:**135-141.
85. **Okabe S, Kindaichi T, Ito T.** 2005. Fate of ^{14}C-labeled microbial products derived from nitrifying bacteria in autotrophic nitrifying biofilms. Appl. Environ. Microbiol. **71:**3987-3994.
86. **Amann RI, Ludwig W, Schleifer KH.** 1995. Phylogenetic identification and in situ detection of individual microbial cells without cultivation. Microbiol Rev. **59:**143-169.
87. **DeLong EF, Wickham GS, Pace NR.** 1989. Phylogenetic stains: ribosomal RNA-based probes for the identification of single cells. Science **243:**1360-1363.
88. **Giovannoni SJ, Britschgi TB, Moyer CL, Field KG.** 1990. Genetic diversity in Sargasso Sea bacterioplankton. Nature **345:**60-63.
89. **Wagner M, Rath G, Koops H-P, Flood J, Amann R.** 1996. *In situ* analysis of nitrifying bacteria in sewage treatment plants. Water Sci. Technol. **34:**237-244.
90. **Juretschko S, Timmermann G, Schmid M, Schleifer KH, Pommerening-Roser A, Koops HP, Wagner M.** 1998. Combined molecular and conventional analyses of nitrifying bacterium diversity in activated sludge: *Nitrosococcus mobilis* and *Nitrospira*-like bacteria as dominant populations. Appl. Environ. Microbiol. **64:**3042-3051.
91. **Daims H, Nielsen JL, Nielsen PH, Schleifer KH, Wagner M.** 2001. *In situ* characterization of *Nitrospira*-like nitrite-oxidizing bacteria active in wastewater treatment plants. Appl. Environ. Microbiol. **67:**5273-5284.
92. **Venter JC, Remington K, Heidelberg JF, Halpern AL, Rusch D, Eisen JA, Wu D, Paulsen I, Nelson KE, Nelson W, Fouts DE, Levy S, Knap AH, Lomas MW, Nealson K, White O, Peterson J, Hoffman J, Parsons R, Baden-Tillson H, Pfannkoch C, Rogers YH, Smith HO.** 2004. Environmental genome shotgun sequencing of the Sargasso Sea. Science **304:**66-74.
93. **Suttle CA.** 2007. Marine viruses--major players in the global ecosystem. Nature Rev. Microbiol. **5:**801-812.
94. **Whitman WB, Coleman DC, Wiebe WJ.** 1998. Prokaryotes: the unseen majority. Proc. Natl. Acad. Sci. U. S. A. **95:**6578-6583.

95. **Yilmaz P, Parfrey LW, Yarza P, Gerken J, Pruesse E, Quast C, Schweer T, Peplies J, Ludwig W, Glockner FO.** 2014. The SILVA and "All-species Living Tree Project (LTP)" taxonomic frameworks. Nucleic Acids Res. **42:**D643-648.

96. **McDonald D, Price MN, Goodrich J, Nawrocki EP, DeSantis TZ, Probst A, Andersen GL, Knight R, Hugenholtz P.** 2012. An improved Greengenes taxonomy with explicit ranks for ecological and evolutionary analyses of bacteria and archaea. ISME J. **6:**610-618.

97. **Cole JR, Wang Q, Fish JA, Chai B, McGarrell DM, Sun Y, Brown CT, Porras-Alfaro A, Kuske CR, Tiedje JM.** 2014. Ribosomal Database Project: data and tools for high throughput rRNA analysis. Nucleic Acids Res. **42:**D633-642.

98. **Muyzer G, de Waal EC, Uitterlinden AG.** 1993. Profiling of complex microbial populations by denaturing gradient gel electrophoresis analysis of polymerase chain reaction-amplified genes coding for 16S rRNA. Appl. Environ. Microbiol. **59:**695-700.

99. **Liu WT, Marsh TL, Cheng H, Forney LJ.** 1997. Characterization of microbial diversity by determining terminal restriction fragment length polymorphisms of genes encoding 16S rRNA. Appl. Environ. Microbiol. **63:**4516-4522.

100. **Fisher MM, Triplett EW.** 1999. Automated approach for ribosomal intergenic spacer analysis of microbial diversity and its application to freshwater bacterial communities. Appl Environ Microbiol **65:**4630-4636.

101. **Sogin ML, Morrison HG, Huber JA, Mark Welch D, Huse SM, Neal PR, Arrieta JM, Herndl GJ.** 2006. Microbial diversity in the deep sea and the underexplored "rare biosphere". Proc. Natl.Acad. Sci. U. S. A. **103:**12115-12120.

102. **Caporaso JG, Lauber CL, Walters WA, Berg-Lyons D, Huntley J, Fierer N, Owens SM, Betley J, Fraser L, Bauer M, Gormley N, Gilbert JA, Smith G, Knight R.** 2012. Ultra-high-throughput microbial community analysis on the Illumina HiSeq and MiSeq platforms. ISME J. **6:**1621-1624.

103. **Logares R, Sunagawa S, Salazar G, Cornejo-Castillo FM, Ferrera I, Sarmento H, Hingamp P, Ogata H, de Vargas C, Lima-Mendez G, Raes J, Poulain J, Jaillon O, Wincker P, Kandels-Lewis S, Karsenti E, Bork P, Acinas SG.** 2013. Metagenomic 16S rDNA Illumina tags are a powerful alternative to amplicon sequencing to explore diversity and structure of microbial communities. Environ. Microbiol.

104. **Wagner M.** 2009. Single-cell ecophysiology of microbes as revealed by Raman microspectroscopy or secondary ion mass spectrometry imaging. Annu. Rev. Microbiol. **63:**411-429.

105. **Tyson GW, Chapman J, Hugenholtz P, Allen EE, Ram RJ, Richardson PM, Solovyev VV, Rubin EM, Rokhsar DS, Banfield JF.** 2004. Community structure and metabolism through reconstruction of microbial genomes from the environment. Nature **428:**37-43.

106. **Urich T, Lanzen A, Qi J, Huson DH, Schleper C, Schuster SC.** 2008. Simultaneous assessment of soil microbial community structure and function through analysis of the meta-transcriptome. PLoS One **3:**e2527.

107. **Lucker S, Wagner M, Maixner F, Pelletier E, Koch H, Vacherie B, Rattei T, Damste JS, Spieck E, Le Paslier D, Daims H.** 2010. A *Nitrospira* metagenome illuminates the physiology and evolution of globally important nitrite-oxidizing bacteria. Proc. Natl. Acad. Sci. U. S. A. **107:**13479-13484.

108. **Strous M, Pelletier E, Mangenot S, Rattei T, Lehner A, Taylor MW, Horn M, Daims H, Bartol-Mavel D, Wincker P, Barbe V, Fonknechten N, Vallenet D, Segurens B, Schenowitz-Truong C, Medigue C, Collingro A, Snel B, Dutilh BE, Op den Camp HJ, van der Drift C, Cirpus I, van de Pas-Schoonen KT, Harhangi HR, van Niftrik L, Schmid M, Keltjens J, van de Vossenberg J, Kartal B, Meier H, Frishman D, Huynen MA, Mewes HW, Weissenbach J, Jetten MS, Wagner M, Le Paslier D.** 2006. Deciphering the evolution and metabolism of an anammox bacterium from a community genome. Nature **440:**790-794.

109. **Spieck E, Ehrich S, Aamand J, Bock E.** 1998. Isolation and immunocytochemical location of the nitrite-oxidizing system in *Nitrospira moscoviensis*. Arch. Microbiol. **169:**225-230.
110. **Albertsen M, Hugenholtz P, Skarshewski A, Nielsen KL, Tyson GW, Nielsen PH.** 2013. Genome sequences of rare, uncultured bacteria obtained by differential coverage binning of multiple metagenomes. Nature Biotechnol. **31:**533-538.
111. **Poulsen LK, Ballard G, Stahl DA.** 1993. Use of rRNA fluorescence *in situ* hybridization for measuring the activity of single cells in young and established biofilms. Appl. Environ. Microbiol. **59:**1354-1360.
112. **Kubota K.** 2013. CARD-FISH for environmental microorganisms: technical advancement and future applications. Microbes and environments / JSME **28:**3-12.
113. **Amann R, Fuchs BM.** 2008. Single-cell identification in microbial communities by improved fluorescence *in situ* hybridization techniques. Nature Rev. Microbiol. **6:**339-348.
114. **Radax R, Hoffmann F, Rapp HT, Leininger S, Schleper C.** 2012. Ammonia-oxidizing archaea as main drivers of nitrification in cold-water sponges. Environ. Microbiol. **14:**909-923.
115. **Krieg R, Halbhuber KJ.** 2010. Detection of endogenous and immuno-bound peroxidase--the status quo in histochemistry. Prog. Histochem. Cytochem. **45:**81-139.
116. **Wagner M, Haider S.** 2012. New trends in fluorescence *in situ* hybridization for identification and functional analyses of microbes. Curr. Opin. Biotechnol. **23:**96-102.
117. **Kawakami S, Hasegawa T, Imachi H, Yamaguchi T, Harada H, Ohashi A, Kubota K.** 2012. Detection of single-copy functional genes in prokaryotic cells by two-pass TSA-FISH with polynucleotide probes. J. Microbiol. Methods **88:**218-223.
118. **Moraru C, Lam P, Fuchs BM, Kuypers MM, Amann R.** 2010. GeneFISH--an *in situ* technique for linking gene presence and cell identity in environmental microorganisms. Environ. Microbiol. **12:**3057-3073.
119. **Hoshino T, Tsuneda S, Hirata A, Inamori Y.** 2003. *In situ* PCR for visualizing distribution of a functional gene "*amoA*" in a biofilm regardless of activity. J. Biotechnol. **105:**33-40.
120. **Hoshino T, Schramm A.** 2010. Detection of denitrification genes by *in situ* rolling circle amplification-fluorescence *in situ* hybridization to link metabolic potential with identity inside bacterial cells. Environ. Microbiol. **12:**2508-2517.
121. **Kawakami S, Kubota K, Imachi H, Yamaguchi T, Harada H, Ohashi A.** 2010. Detection of single copy genes by two-pass tyramide signal amplification fluorescence *in situ* hybridization (Two-Pass TSA-FISH) with single oligonucleotide probes. Microbes and environments / JSME **25:**15-21.
122. **Ellis BK, Stanford JA.** 1982. Comparative photoheterotrophy, chemoheterotrophy, and photolithotrophy in a eutrophic reservoir and an oligotrophic lake. Limnol. Oceanogr. **27:**440-454.
123. **Andreasen K, Nielsen PH.** 1997. Application of microautoradiography to the study of substrate uptake by filamentous microorganisms in activated sludge. Appl. Environ. Microbiol. **63:**3662-3668.
124. **Lee N, Nielsen PH, Andreasen KH, Juretschko S, Nielsen JL, Schleifer KH, Wagner M.** 1999. Combination of fluorescent *in situ* hybridization and microautoradiography-a new tool for structure-function analyses in microbial ecology. Appl. Environ. Microbiol. **65:**1289-1297.
125. **Radajewski S, Ineson P, Parekh NR, Murrell JC.** 2000. Stable-isotope probing as a tool in microbial ecology. Nature **403:**646-649.
126. **Manefield M, Whiteley AS, Griffiths RI, Bailey MJ.** 2002. RNA stable isotope probing, a novel means of linking microbial community function to phylogeny. Appl. Environ. Microbiol. **68:**5367-5373.
127. **Jehmlich N, Schmidt F, Hartwich M, von Bergen M, Richnow HH, Vogt C.** 2008. Incorporation of carbon and nitrogen atoms into proteins measured by protein-based stable isotope probing (Protein-SIP). Rapid. Commun. Mass. Spectrom. **22:**2889-2897.

128. **Boschker HTS, Nold SC, Wellsbury P, Bos D, de Graaf W, Pel R, Parkes RJ, Cappenberg TE.** 1998. Direct linking of microbial populations to specific biogeochemical processes by ^{13}C-labelling of biomarkers. Nature **392:**801-805.
129. **Orphan VJ, House CH, Hinrichs KU, McKeegan KD, DeLong EF.** 2001. Methane-consuming archaea revealed by directly coupled isotopic and phylogenetic analysis. Science **293:**484-487.
130. **Huang WE, Stoecker K, Griffiths R, Newbold L, Daims H, Whiteley AS, Wagner M.** 2007. Raman-FISH: combining stable-isotope Raman spectroscopy and fluorescence *in situ* hybridization for the single cell analysis of identity and function. Environ. Microbiol. **9:**1878-1889.
131. **Neufeld JD, Chen Y, Dumont MG, Murrell JC.** 2008. Marine methylotrophs revealed by stable-isotope probing, multiple displacement amplification and metagenomics. Environ. Microbiol. **10:**1526-1535.
132. **Dumont MG, Pommerenke B, Casper P.** 2013. Using stable isotope probing to obtain a targeted metatranscriptome of aerobic methanotrophs in lake sediment. Environ. Microbiol. Rep. **5:**757-764.
133. **MacGregor BJ, Bruchert V, Fleischer S, Amann R.** 2002. Isolation of small-subunit rRNA for stable isotopic characterization. Environ. Microbiol. **4:**451-464.
134. **Chan JW, Esposito AP, Talley CE, Hollars CW, Lane SM, Huser T.** 2004. Reagentless identification of single bacterial spores in aqueous solution by confocal laser tweezers Raman spectroscopy. Anal. Chem. **76:**599-603.
135. **Rosch P, Harz M, Schmitt M, Peschke KD, Ronneberger O, Burkhardt H, Motzkus HW, Lankers M, Hofer S, Thiele H, Popp J.** 2005. Chemotaxonomic identification of single bacteria by micro-Raman spectroscopy: application to clean-room-relevant biological contaminations. Appl. Environ. Microbiol. **71:**1626-1637.
136. **Kloss S, Kampe B, Sachse S, Rosch P, Straube E, Pfister W, Kiehntopf M, Popp J.** 2013. Culture independent Raman spectroscopic identification of urinary tract infection pathogens: a proof of principle study. Anal. Chem. **85:**9610-9616.
137. **Xie C, Mace J, Dinno MA, Li YQ, Tang W, Newton RJ, Gemperline PJ.** 2005. Identification of single bacterial cells in aqueous solution using confocal laser tweezers Raman spectroscopy. Anal. Chem. **77:**4390-4397.
138. **Musat N, Foster R, Vagner T, Adam B, Kuypers MM.** 2012. Detecting metabolic activities in single cells, with emphasis on nanoSIMS. FEMS Microbiol. Rev. **36:**486-511.
139. **Behrens S, Kappler A, Obst M.** 2012. Linking environmental processes to the *in situ* functioning of microorganisms by high-resolution secondary ion mass spectrometry (NanoSIMS) and scanning transmission X-ray microscopy (STXM). Environ. Microbiol. **14:**2851-2869.
140. **Polerecky L, Adam B, Milucka J, Musat N, Vagner T, Kuypers MM.** 2012. Look@NanoSIMS--a tool for the analysis of nanoSIMS data in environmental microbiology. Environ. Microbiol. **14:**1009-1023.
141. **Musat N, Halm H, Winterholler B, Hoppe P, Peduzzi S, Hillion F, Horreard F, Amann R, Jørgensen B, Kuypers M.** 2008. A single-cell view on the ecophysiology of anaerobic phototrophic bacteria. Proc. Natl. Acad. Sci. U.S.A. **105:**17861-17866.
142. **Behrens S, Lösekann T, Pett-Ridge J, Weber P, Ng W-O, Stevenson B, Hutcheon I, Relman D, Spormann A.** 2008. Linking microbial phylogeny to metabolic activity at the single-cell level by using enhanced element labeling-catalyzed reporter deposition fluorescence *in situ* hybridization (EL-FISH) and NanoSIMS. Appl. Environ. Microbiol. **74:**3143-3150.
143. **Li T, Wu TD, Mazeas L, Toffin L, Guerquin-Kern JL, Leblon G, Bouchez T.** 2008. Simultaneous analysis of microbial identity and function using NanoSIMS. Environ. Microbiol. **10:**580-588.
144. **Lechene CP, Luyten Y, McMahon G, Distel DL.** 2007. Quantitative imaging of nitrogen fixation by individual bacteria within animal cells. Science **317:**1563-1566.

145. **Berry D, Stecher B, Schintlmeister A, Reichert J, Brugiroux S, Wild B, Wanek W, Richter A, Rauch I, Decker T, Loy A, Wagner M.** 2013. Host-compound foraging by intestinal microbiota revealed by single-cell stable isotope probing. Proc. Natl. Acad. Sci. U.S.A. **110:**4720-4725.

146. **Adamczyk J, Hesselsoe M, Iversen N, Horn M, Lehner A, Nielsen PH, Schloter M, Roslev P, Wagner M.** 2003. The isotope array, a new tool that employs substrate-mediated labeling of rRNA for determination of microbial community structure and function. Appl. Environ. Microbiol. **69:**6875-6887.

147. **Mayali X, Weber PK, Brodie EL, Mabery S, Hoeprich PD, Pett-Ridge J.** 2012. High-throughput isotopic analysis of RNA microarrays to quantify microbial resource use. ISME J. **6:**1210-1221.

148. **Wagner M.** 2004. Deciphering Functions of Uncultured Microorganisms. Microbe-American Society for microbiology **70:**63-70.

149. **Ginige MP, Hugenholtz P, Daims H, Wagner M, Keller J, Blackall LL.** 2004. Use of stable-isotope probing, full-cycle rRNA analysis, and fluorescence *in situ* hybridization-microautoradiography to study a methanol-fed denitrifying microbial community. Appl. Environ. Microbiol. **70:**588-596.

150. **Van Mooy B, Devol A.** 2008. Assessing nutrient limitation of *Prochlorococcus* in the North Pacific subtropical gyre by using an RNA capture method. Limnol. Oceanogr. **53:**78-88.

Chapter II

Interactions of Nitrifying Bacteria and Heterotrophs: Identification of a *Micavibrio*-Like Putative Predator of Nitrospira spp.

AEM
Journals.ASM.org

Interactions of Nitrifying Bacteria and Heterotrophs: Identification of a *Micavibrio*-Like Putative Predator of *Nitrospira* spp.

Jan Dolinšek,[a] Ilias Lagkouvardos,[a] Wolfgang Wanek,[b] Michael Wagner,[a] Holger Daims[a]

Department of Microbial Ecology, Ecology Centre, University of Vienna, Vienna, Austria[a]; Department of Terrestrial Ecosystem Research, Ecology Centre, University of Vienna, Vienna, Austria[b]

Chemolithoautotrophic nitrifying bacteria release soluble organic compounds, which can be substrates for heterotrophic microorganisms. The identities of these heterotrophs and the specificities of their interactions with nitrifiers are largely unknown. In this study, we incubated nitrifying activated sludge with ^{13}C-labeled bicarbonate and used stable isotope probing of 16S rRNA to monitor the flow of carbon from uncultured nitrifiers to heterotrophs. To facilitate the identification of heterotrophs, the abundant 16S rRNA molecules from nitrifiers were depleted by catalytic oligonucleotides containing locked nucleic acids (LNAzymes), which specifically cut the 16S rRNA of defined target organisms. Among the ^{13}C-labeled heterotrophs were organisms remotely related to *Micavibrio*, a microbial predator of Gram-negative bacteria. Fluorescence *in situ* hybridization revealed a close spatial association of these organisms with microcolonies of nitrite-oxidizing sublineage I *Nitrospira* in sludge flocs. The high specificity of this interaction was confirmed by confocal microscopy and a novel image analysis method to quantify the localization patterns of biofilm microorganisms in three-dimensional (3-D) space. Other isotope-labeled bacteria, which were affiliated with *Thermomonas*, colocalized less frequently with nitrifiers and thus were commensals or saprophytes rather than specific symbionts or predators. These results suggest that *Nitrospira* spp. are subject to bacterial predation, which may influence the abundance and diversity of these nitrite oxidizers and the stability of nitrification in engineered and natural ecosystems. *In silico* screening of published next-generation sequencing data sets revealed a broad environmental distribution of the uncultured *Micavibrio*-like lineage.

Chemolithoautotrophic ammonia- and nitrite-oxidizing microorganisms catalyze nitrification, which is a key process of the biogeochemical nitrogen cycle and important for excess nitrogen elimination from sewage in biological wastewater treatment plants (WWTPs). Key nitrifiers in most domestic and industrial WWTPs are ammonia-oxidizing bacteria (AOB) (1) related to the genera *Nitrosomonas* and *Nitrosospira* (2, 3) and nitrite-oxidizing bacteria (NOB) of the genus *Nitrospira* (3–5). Usually these organisms occur in tight cell clusters, which are embedded in the extracellular matrix of biofilms or activated sludge flocs (5, 6). Aside from the nitrifiers, most nitrifying bioreactors host a great diversity of other organisms, most of which presumably are heterotrophs that feed on organic substrates present in the sewage (7). Interestingly, however, soluble microbial products (SMP) released by the autotrophic AOB and NOB, and decaying nitrifier biomass, also can support the growth of heterotrophs in WWTPs (8) and in other environments such as drinking water treatment facilities (9). Heterotrophic growth supported by nitrifiers as primary producers can be quite extensive, as heterotrophic bacteria represented 50% of the microbial community in a nitrifying biofilm that received ammonia and bicarbonate-CO_2 as the sole energy and carbon sources, respectively (10). Accordingly, the growth of nitrifiers and the resulting increase of heterotrophic biomass can pose serious hygienic problems in sensitive applications such as drinking water treatment (11, 12). Dissecting the flow of nutrients from nitrifiers to heterotrophs is a nontrivial task that requires cultivation-independent methods to detect the *in situ* uptake and assimilation of substrates. Previous studies (10, 13) applied fluorescence *in situ* hybridization with rRNA-targeted probes (FISH) and microautoradiography (MAR) (14) to monitor the cross-feeding of heterotrophs by nitrifiers in biofilm. This elegant approach revealed a niche differentiation among heterotrophs, which fed on different radiolabeled organics (10) and metabolites or cellular decay products of nitrifiers (13). These results, which were based on the use of FISH probes covering large phylogenetic groups, led to the question of how specific such interactions might be at a higher phylogenetic resolution. It would also be interesting to analyze the *in situ* spatial distribution of the nitrifiers and heterotrophs, because localization patterns can provide important hints about the specificity and nature of interactions among microbes in biofilms and flocs (15).

In this study, we combined stable isotope probing of RNA (RNA-SIP) (16) with the full-cycle rRNA approach (17) to specifically identify heterotrophic bacteria that received carbon from nitrifiers in activated sludge. Stable isotope probing has successfully been used to monitor the carbon flow in natural environments (18–23). Following the incubation of activated sludge with $H^{13}CO_3^-$ and NH_4^+ or NO_2^-, ^{13}C-labeled RNA was separated from unlabeled RNA by isopycnic centrifugation. To facilitate the identification of heterotrophs, we used novel locked nucleic acid enzymes (LNAzymes) (24) to specifically deplete the 16S rRNA of AOB and NOB in the complex RNA mixture prior to the isopycnic centrifugation. The 16S rRNA in the separated fractions was reverse transcribed and PCR amplified, and the amplicons were

Received 5 November 2012 **Accepted** 11 January 2013
Published ahead of print 18 January 2013
Address correspondence to Holger Daims, daims@microbial-ecology.net.
Supplemental material for this article may be found at http://dx.doi.org/10.1128/AEM.03408-12.
Copyright © 2013, American Society for Microbiology. All Rights Reserved.
doi:10.1128/AEM.03408-12

characterized by terminal restriction fragment length polymorphism (T-RFLP) analysis, cloning, and sequencing. Once the 16S rRNA sequences of potential cross-feeding heterotrophs had been obtained by RNA-SIP, we designed specific FISH probes to detect the respective organisms *in situ*. Most interestingly, this approach revealed a previously unknown interaction between *Nitrospira*-like NOB and an uncultured alphaproteobacterium. The high specificity of this interaction was demonstrated by quantifying the spatial localization patterns of these organisms in the sludge flocs.

MATERIALS AND METHODS

Sludge sampling and stable isotope labeling. Activated sludge samples were collected from a full-scale nitrifying sequencing batch reactor of the municipal WWTP of Ingolstadt, Germany. The suspended biomass was diluted 1:8 (vol/vol) in sludge supernatant, and 30-ml aliquots of the diluted sludge were incubated in the dark in six 100-ml sterilized crimp-sealed flasks in a water bath set at 23°C (the temperature in the WWTP reactor was 20°C) with horizontal shaking (60 rpm). Ammonium (0.25 mM) was added to two flasks, one containing also $NaH^{13}CO_3$ (2 mM) and the other one $NaH^{12}CO_3$ (2 mM). Two other flasks, also containing either [^{13}C]bicarbonate or [^{12}C]bicarbonate, were amended with 0.25 mM nitrite. During the incubation, ammonium and nitrite were replenished by adding, on average, 50 μl of a NH_4Cl or $NaNO_2$ stock solution (final concentration, 0.25 mM) every 3 h with an automated peristaltic pump. A preliminary experiment had shown that this rate of feeding did not cause accumulation of ammonium or nitrite, respectively (data not shown). These incubations were done to label with ^{13}C first the autotrophic AOB or NOB and subsequently any heterotrophs feeding on ^{13}C-labeled exudates or biomass of nitrifiers. The experiments including [^{12}C]bicarbonate were controls for SIP. To distinguish carbon fixation by AOB or NOB from nitrifier-independent anaplerotic CO_2 fixation (25), the last two flasks were amended only with $NaH^{13}CO_3$ or $NaH^{12}CO_3$ and contained neither ammonium nor nitrite. The headspace of all flasks was aerated, by using an automated air pump, every 4 h for 2 min. The depletion of ammonium in the respective flasks was regularly confirmed colorimetrically (26), whereas the use of nitrite was monitored by using nitrite test stripes (Merckoquant; Merck, Darmstadt, Germany). The pH was adjusted daily to 7.5 by adding appropriate amounts of 175 mM [^{12}C]$NaHCO_3$ or [^{13}C]$NaHCO_3$ (the final concentration of HCO_3^- was 5 to 10 mM). Prior to the start of the incubation and at selected time points (12 h, 36 h, 4.5 days, 12 days, 21 days, and 41 days), 1 ml of each culture was fixed in 2% (vol/vol) formaldehyde for 3 h at 4°C, and 4 ml of each culture was subdivided into four equal aliquots. The sludge in these aliquots was shortly allowed to settle by gravitation, the supernatant was removed, and the concentrated sludge was frozen in liquid N_2. Fixed aliquots were resuspended in a 1:1 mixture of 1× phosphate-buffered saline and 96% (vol/vol) ethanol and kept at −20°C, whereas frozen aliquots were stored at −80°C until further use.

Nucleic acid extraction. Frozen activated sludge pellets were resuspended in 1 ml of TRIzol (Invitrogen, Carlsbad, CA). The suspension was transferred into Lysing Matrix A tubes (MP Biomedicals, Solon, OH), and cells were disrupted in a bead beater (Bio 101, Vista, CA) at 6.5 m/s for 45 s. Subsequently, RNA and DNA were extracted according to the recommendations provided with TRIzol. DNA was removed from RNA preparations by DNase I (Sigma-Aldrich, St. Louis, MO) digestion in a modified (slightly lower pH and addition of $CaCl_2$) DNase I buffer (20 mM Tris-HCl [pH 8.0], 2 mM $MgCl_2$, 0.2 mM $CaCl_2$) for 45 min at 37°C. After the digestion, the RNA was extracted again with TRIzol.

Isotope ratio mass spectrometry (IRMS). The ^{13}C content of total extracted RNA was measured on days 12, 21, and 41 to determine the incorporation of ^{13}C into biomass during the incubations. RNA concentrations were determined using a NanoDrop ND-1000 spetrophotometer (NanoDrop Technologies, Wilmington, DE). An aliquot of 500 ng of RNA was added into a tin capsule already containing 7 μg of unlabeled proline-sucrose solution. This spiking was necessary to increase the total amount of C and to improve the reliability of measuring the ^{13}C content in small amounts of ^{13}C-enriched RNA. Samples were dried at 60°C overnight and analyzed by an elemental analyzer (EA 1110, CE Instruments, Wigan, United Kingdom) coupled via a ConFlo III device to the isotope ratio mass spectrometer (Delta^{PLUS}; Thermo Fisher Scientific). The ^{13}C content of the RNA was calculated according to the following formula: atoms percent $^{13}C_{RNA}$ = (atoms percent $^{13}C_{total} \times C_{total}$ − atoms percent $^{13}C_{spike} \times C_{spike}$)/($C_{total} - C_{spike}$).

LNAzyme digestion. The LNAzymes used in this study were purchased from Exiqon (Vedbaek, Denmark) and are listed in Table S1 in the supplemental material. The LNAzyme-mediated depletion of the native 16S rRNA of AOB and NOB was carried out as described elsewhere (24). We simultaneously applied two LNAzymes with helper probes (see Table S1) to achieve a significant depletion of the target 16S rRNA types of nitrifiers. After cleavage, the LNAzymes were digested with DNase I for 45 min at 37°C. Subsequently, 10 μl of 50 mM EDTA was added, and DNase I was inactivated by heating the mixture to 70°C for 10 min. After this step, the noncleaved rRNA (of microorganisms other than the known nitrifiers) was ready for isopycnic centrifugation.

Isopycnic centrifugation. Cesium trifluoroacetate (GE Healthcare, Munich, Germany) density gradients were prepared as described by Whiteley et al. (27). A total of 500 ng of RNA was added to the gradient solution, which had a starting density of 1.8 g/ml. OptiSeal tubes (4.9 ml) filled with the gradient solution were sealed and spun in a VTi 90 rotor in an Optima L-100 XP ultracentrifuge (Beckman Coulter, Brea, CA) at 130,000 × *g* for 72 h. The gradients were then fractionated by displacing the gradient solution with water by using a syringe pump (World Precision Instruments, Sarasota, FL) at a flow rate of 0.75 ml/min. Fractions were collected at intervals of 20 s, and the density of each fraction was determined by using a digital refractometer (AR 200; Reichert Analytical Instruments, Depew, NY). Glycogen (30 μg; Ambion, Austin, TX) and 2 volumes of ice-cold isopropanol were added to each of the fractions, which then were stored at −20°C until further processing. To precipitate RNA, the samples were centrifuged at 14,000 × *g* at 4°C for 20 min. The supernatant was discarded, and the pellet was washed with 500 μl of ice-cold 70% (vol/vol) ethanol and again centrifuged (14,000 × *g* and 4°C for 5 min). After brief air-drying, the pellet was resuspended in 50 μl of diethyl pyrocarbonate (DEPC)-treated water and stored at −80°C. To treat water with DEPC, 1 ml of DEPC was added to 1 liter of ultrapure water (Milli-Q; Millipore, Bedford, MA) in a prebaked (180°C for 6 h) glass bottle. This water was then stirred for 24 h on a magnetic stirrer and finally autoclaved (121°C for 15 min) before use.

PCR and RT-PCR. All PCRs and reverse transcriptase PCRs (RT-PCRs) were performed as described in reference 24. The primers used in this study for PCR and RT-PCR are listed in Table S1 in the supplemental material and were obtained from Thermo Fisher Scientific (Ulm, Germany). For PCRs and for RT-PCRs, the nucleic acid templates were diluted 1:10 in ultrapure water in order to avoid PCR inhibition by highly concentrated template or inhibitory compounds.

T-RFLP. For T-RFLP analysis, primer 8F (see Table S1 in the supplemental material) labeled with 6-carboxyfluorescein (6-FAM) was used in PCRs or RT-PCRs. Amplicons of the correct size were excised from agarose gels and purified by using the QiaQuick gel extraction kit (Qiagen). BesTRF software (28) was used to determine which restriction enzyme yielded the optimal resolution of T-RFLP for specific phylogenetic groups. Approximately 100 ng of purified amplicons was digested for 3 h at 37°C using either the restriction endonuclease MspI or RsaI (Fermentas). The digestion products were analyzed by using an ABI 3130xl genetic analyzer (Applied Biosystems, Foster City, CA) and PeakScanner 1.0 software (Applied Biosystems). An in-house Perl script was used to remove an artifact peak that was present in all T-RFLP profiles in this and a previous (24) study. Real peaks were distinguished from noise by using the method described by Abdo et al. (29) and by using the Perl and "R" scripts provided on their website (http://www.ibest.uidaho.edu/tools/trflp_stats/index.php).

Cloning, sequencing, and phylogenetic analysis of 16S rRNA genes. Cloning and sequencing of PCR-amplified 16S rRNA genes were performed as described elsewhere (24). The obtained 16S rRNA gene sequences were aligned using the SINA Webaligner (http://www.arb-silva.de/aligner) and imported into ARB (30) using the SILVA 108 sequence database (31). The sequence alignments were refined manually. Phylogenetic trees were computed by maximum likelihood analysis (RAxML [32]) with a 50% conservation filter for *Bacteria*. Chimeric sequences were detected by independent phylogenetic analyses of the first, central, and last ≈300 base positions. Sequences showing unstable phylogenetic affiliations in these tests were further inspected for anomalies by using Mallard software (33).

Next-generation sequencing (NGS) reads of 16S rRNA gene amplicons from environmental samples were extracted from the SRA (34) and VAMPS (http://vamps.mbl.edu/resources/databases.php) databases on 4 and 5 June 2012. The sequence data sets (see Table S4 in the supplemental material) were downloaded manually according to the classification of "ecological metagenomes" provided by the NCBI Taxonomy Browser (http://www.ncbi.nlm.nih.gov/Taxonomy/Browser/wwwtax.cgi?mode=Root). NGS data sets from the same kind of environment were saved in a common folder on disk for subsequent processing. Raw fasta files were produced from fastq files by using the fastq-dump program of the sratoolkit software suite (version 2.2.0), which is available on the SRA website. Sequences longer than 200 bp were then collected in newly created, specific databases for each kind of environment by using tools of the BLAST+ suite (35). These databases were searched by BLAST (36) using the *Micavibrio*-like P7H12 clone sequence (JQ815012), representatives of different *Nitrospira* lineages, and known predatory bacteria as queries (see Table S3 in the supplemental material). To avoid false-positive hits due to partial sequence similarities, the BLAST results were filtered by a self-written Perl script to exclude all NGS reads, whose alignment to the most similar query sequence was shorter than 80% of the NGS read length and whose sequence similarity to the query along this aligned region was below 97%. The 80% alignment length threshold was chosen because the raw NGS reads still contained barcode and primer sequences, and because the sequence read quality was often low toward the 5′ and 3′ ends. The hits which met the minimal alignment length and similarity criteria were counted for each query organism.

Probe design, FISH, and digital image analysis. 16S rRNA-targeted oligonucleotide probes specific for organisms identified in this study were designed by using the "Probe Design" and "Probe Match" tools of ARB (30). To determine the optimal stringent hybridization conditions, formamide concentration series (37) were carried out using the new probes and activated sludge, which was collected during our experiments and contained the respective target organisms according to the T-RFLP data. FISH with rRNA-targeted oligonucleotide probes was performed according to reference 38 with the probes listed in Table S1. Probes labeled with FLUOS or with the dye Cy3 or Cy5 were obtained from Thermo Fisher. Stacked optical sections (z-stacks) of probe-labeled bacteria in sludge flocs were recorded by using a Zeiss LSM 510 Meta confocal laser scanning microscope equipped with two HeNe lasers (543 and 633 nm, respectively) and one argon laser (458, 477, 488, and 514 nm). The xy resolution of the images was 512 by 512 or 1,024 by 1,024 pixels, and the axial distances between the images in the z-stacks were 0.25 to 0.5 μm. Biomass objects of probe-target organisms were detected by three-dimensional (3-D) image segmentation based on voxel intensity thresholding by the RATS-L method (39). The detected 3-D objects (cells and cell aggregates) were counted automatically by using our image analysis software *daime* (39). The spatial arrangement patterns of probe-target organisms were quantified in z-stacks by a new 3-D implementation of the original 2-D "Inflate Algorithm" (15) that is part of the *daime* software. In all these analyses, the *Micavibrio*-like alphaproteobacterium was the "analyzed population." The "reference population" was either sublineage I *Nitrospira* or other NOB (sublineage II *Nitrospira*). In the 3-D version of the algorithm, all biomass objects of the reference population are virtually

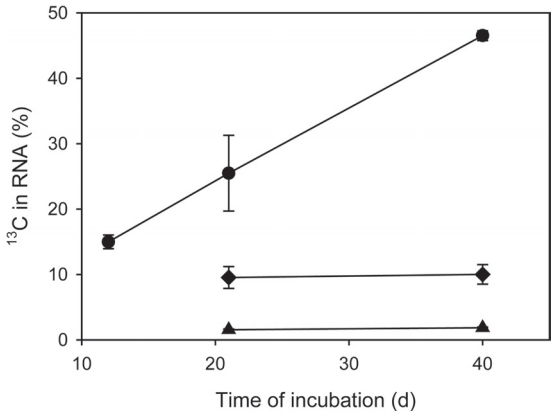

FIG 1 ^{13}C content of RNA, which was extracted from activated sludge incubated with $H^{13}CO_3^-$, as measured by IRMS. Circles represent the experiment with NH_4^+ as the energy source and $H^{13}CO_2^-$ as the carbon source, diamonds the experiment with NO_2^- and $H^{13}CO_2^-$, and triangles the control experiment without any added energy source and $H^{13}CO_2^-$.

and iteratively enlarged ("inflated") in 3-D space by 3-D dilations with a spherical structuring element (see Fig. S1 in the supplemental material). The size of the structuring element determines the increase in size (in μm) of the inflated objects after each dilation. Thus, a given number of dilations also indicates a particular distance in 3-D space from the original, not dilated objects of the "reference" population. After each dilation, the overlapping voxels of the inflated "reference" population and the unmodified "analyzed" population are counted (Fig. S1). From this number, we subtract the number of voxels that overlapped after the previous dilation. The result is divided by the total number of voxels that belong to the analyzed population in the z-stack. This fraction represents the density of the analyzed population at the current distance from the reference population. The current distance (in μm) is inferred from the respective number of dilations (see above). As a null hypothesis, we assume that the populations are randomly distributed. This is tested by repeating the whole procedure with artificial image stacks, which contain the real reference population and an *in silico*-generated and randomly distributed analyzed population, whose overall density in the image stack is equal to that of the real analyzed population. The fractions of overlapping voxels, which have been obtained with the real images, are divided by the respective fractions obtained with these artificial images. Then a value of 1 indicates random distribution of the real analyzed population at the respective distance. Finally, these normalized values are plotted against the corresponding distances (in μm) between the reference and analyzed populations. In these plots, values of 1 indicate random spatial distribution of the populations, values of >1 indicate coaggregation, and values of <1 indicate mutual avoidance. Further details of the algorithm are provided in reference 15. 3-D visualizations of confocal image stacks were rendered by the *daime* software.

Nucleotide sequence accession numbers. The nucleotide sequences obtained in this work have been deposited in the GenBank database (accession numbers JQ814956 to JQ815075).

RESULTS

Stable isotope probing and phylogenetic analyses. A quick prescreening analysis of the extracted (but not LNAzyme-treated) RNA by IRMS showed a substantial increase of its ^{13}C content during the incubation of activated sludge with ammonium (Fig. 1). This increase is consistent with the expected autotrophic fixation of the added [^{13}C]bicarbonate by the nitrifiers. During the incubations with nitrite, the increase of the ^{13}C content was much weaker (Fig. 1), and as expected, no increase was observed in the

absence of ammonia and nitrite (Fig. 1). We assumed that a successful SIP-based identification of heterotrophs that received carbon from nitrifiers would require a considerable incorporation of ^{13}C into their rRNA. Hence, we did not further analyze the samples that were incubated with nitrite due to the relatively weak ^{13}C labeling. Instead, we focused on the incubations with ammonium and on the negative control without any added energy source. RNA extracted from these samples after 21 days of incubation was subjected to isopycnic centrifugation and subsequent bacterial 16S rRNA-specific RT-PCR and T-RFLP analysis. Although the ^{13}C labeling had been even stronger after 41 days (Fig. 1), we did not analyze this time point, because we assumed an increasing amount of rRNA from nonnitrifiers to be labeled due to carbon exchange among heterotrophs instead of direct carbon transfer from the nitrifiers. As expected, after incubation with ammonium and $H^{13}CO_3^-$, the 16S rRNA in the heaviest fractions of the density gradient (density $>$ 1.82 g/ml) was dominated by 16S rRNA of AOB and NOB, as the T-RFLP profiles obtained from these fractions contained prominent peaks characteristic for these organisms (data not shown). This result was confirmed by RT-PCR and cloning of 16S rRNA from these fractions and by sequencing of 45 randomly selected clones, which all carried 16S rRNA genes related to *Nitrosomonas* or *Nitrospira* (data not shown). The dominance of labeled 16S rRNA from nitrifiers complicated the identification of other organisms that were ^{13}C labeled during the experiment and thus had received labeled carbon from the nitrifiers. A conceptually simple solution would be to sequence large numbers of randomly selected clones, possibly after prescreening the clones by restriction fragment length polymorphism analysis or a similar technique, in order to find cloned 16S rRNA genes of nonnitrifiers. We wanted to avoid such a labor-intensive screening and sequencing of many clones and decided to use a method that would further improve the sensitivity of T-RFLP, where dominant nitrifier peaks might mask changes of peaks belonging to other organisms. Therefore, we applied catalytic oligodeoxyribonucleotides containing locked nucleic acids (LNAzymes) that cleave target RNA molecules with a high specificity at a defined site (40, 41). If specific LNAzymes cleave native rRNA molecules between the primer binding sites, the cleaved rRNA is not amplified during RT-PCR (see Fig. S2 in the supplemental material). Hence, appropriate LNAzymes can be used to deplete selected dominant rRNA types in a complex mixture, and this depletion leads to a relative increase in the abundance of rarer sequence types (24). Consequently, we repeated the isopycnic centrifugation of RNA, but prior to this step, we used previously developed LNAzymes targeting the genera *Nitrosomonas* and *Nitrospira* (24) (see Table S1 in the supplemental material) to deplete the 16S rRNA molecules of these nitrifiers. RT-PCR and T-RFLP analysis were performed as described above. Based on a comparison of the resulting T-RFLP profiles to the profiles obtained without LNAzyme treatment, this approach resulted in a 4-fold decrease of the 16S rRNA genes of nitrifiers from the heavy fractions of the density gradient (data not shown). Thus, the identification of other 16S rRNA types was greatly facilitated. Nevertheless, ^{13}C-labeled 16S rRNA from nitrifiers still was abundant in the heavy RNA fractions, showing that the LNAzyme-based digestion of their rRNA was not complete (Fig. 2).

Like for the non LNAzyme-treated sample, a 16S rRNA gene library was established from the heavy fraction (density = 1.823 g/ml) of the LNAzyme-treated RNA sample (incubated for 21 days with $H^{13}CO_3^-$ and NH_4^+) after RT-PCR. Approximately 900-bp-long sequences were obtained from 120 randomly selected clones. Based on a 97% sequence similarity threshold, 37 operational taxonomic units (OTUs) were defined, which were distributed across 10 bacterial phyla (see Table S2 in the supplemental material). The most frequent OTUs in the library represented AOB (OTUs 2 to 4; 10.8% abundance), NOB (OTUs 30 to 32; 45% abundance), *Micavibrio*-related alphaproteobacteria (OTU 9; 5% abundance), *Thermomonas*-related betaproteobacteria (OTU 5; 5% abundance), and a member of the phylum *Bacteroidetes* (OTU 17; 5.8% abundance) (see Table S2).

Based on the 16S rRNA sequences, which had been retrieved from the sample incubated with NH_4^+ and after LNAzyme treatment of the RNA, we could assign additional T-RFLP peaks to organisms in the T-RFLP profiles. As expected, the terminal restriction fragments (T-RFs) belonging to AOB or NOB increased in relative abundance in the heavy fractions after incubation with NH_4^+ and [^{13}C]bicarbonate (Fig. 2). However, if the RT-PCR products were cleaved by the restriction endonuclease MspI, an additional 436-nucleotide-long T-RF was identified to be abundant in the clearly ^{13}C-labeled fractions and also in the lighter fractions (Fig. 2). According to an *in silico* analysis, several different alphaproteobacterial sequences from the clone library could have yielded this T-RF. Analyses of the sequences by BesTRF software (28) showed that the restriction enzyme RsaI would allow us to distinguish these alphaproteobacterial sequences in the T-RFLP profiles. Indeed, T-RFLP analyses using RsaI revealed that the aforementioned prominent T-RF from the ^{13}C-labeled (heavy) fractions represented the *Micavibrio*-like alphaproteobacterial OTU that was also abundant in the 16S rRNA gene library (see Table S2 and Fig. S3 in the supplemental material). Another T-RF representing a gammaproteobacterial, *Thermomonas*-like OTU (see Table S2) was detected mainly in fractions of intermediate density (Fig. 2; see also Fig. S3 in the supplemental material), indicating that this group was not ^{13}C labeled as strongly as the *Micavibrio*-like alphaproteobacterial OTU. The T-RFLP analyses of the density fractions showed that for all other detected organisms, the ratio of labeled to unlabeled RNA was lower than for the *Micavibrio*-like and *Thermomonas*-like OTUs. For example, although a high number (5.8%) of clones from the heavy RNA fraction belonged to the *Bacteroidetes* (see Table S2), the majority of this population was detected in the light fractions and thus was mainly unlabeled (Fig. 2; see also Fig. S3 in the supplemental material).

None of the aforementioned T-RFs increased in relative abundance in the heavy density gradient fractions after incubation of the activated sludge with [^{12}C]bicarbonate (Fig. 2). This result confirmed that the increase, which was observed with [^{13}C]bicarbonate, was not an artifact but resulted from the incorporation of ^{13}C into the RNA of the respective organisms. Consistently, in the control experiments with [^{13}C]bicarbonate but without added NH_4^+ or NO_2^-, the T-RFs of the nitrifiers and of the *Micavibrio*-like bacteria did not increase in the heavy compared to the light fractions (Fig. 2). No T-RF of the *Thermomonas*-like OTU was detected in these experiments. Thus, the labeling of the *Thermomonas*- or *Micavibrio*-like organisms was detectable only after incubation of the sludge with ammonium and was most likely not due to heterotrophic CO_2 fixation, which could in principle also cause positive signals in SIP experiments (25).

***In situ* detection of nitrifiers and heterotrophs.** FISH with

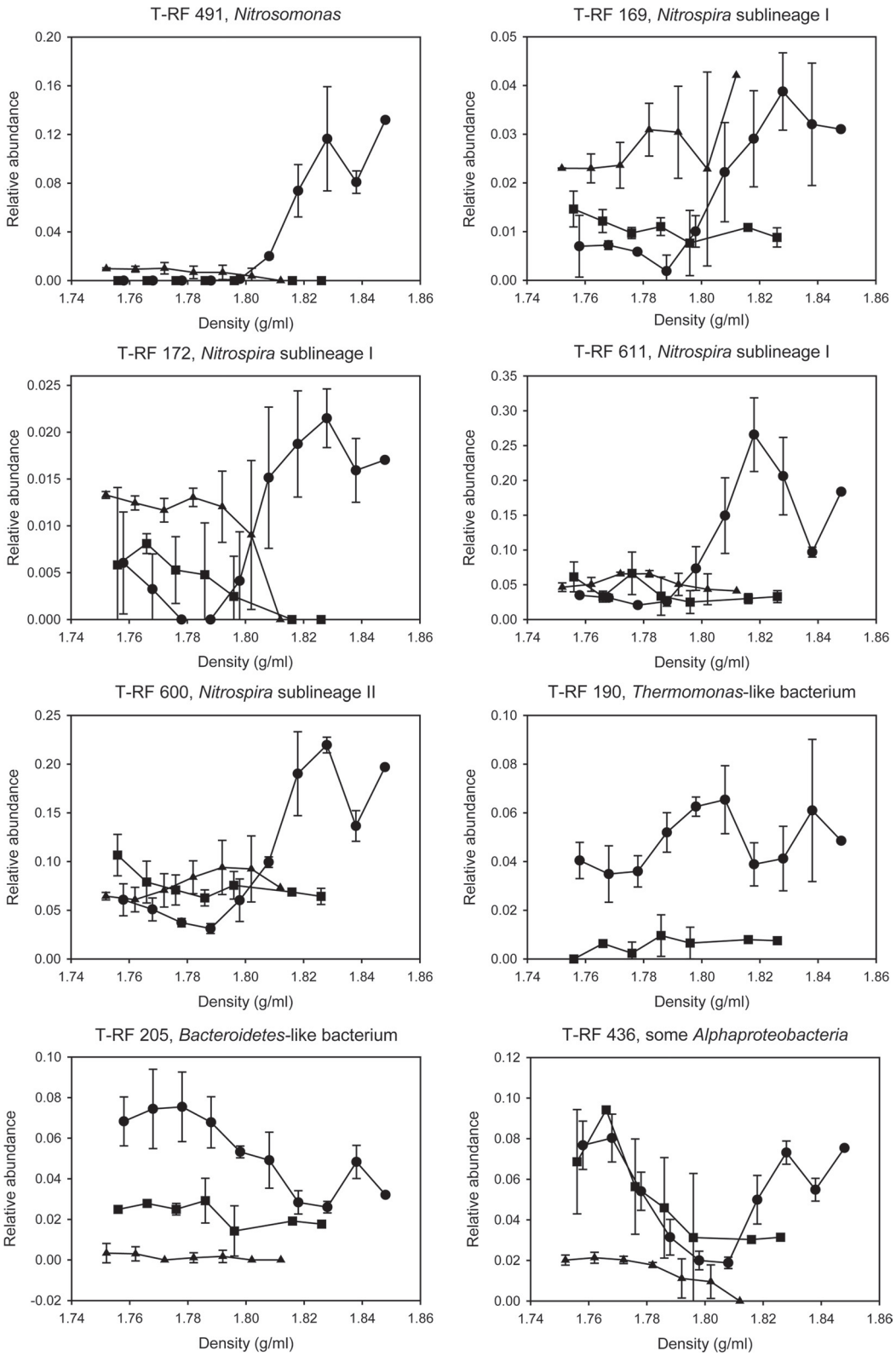

FIG 2 Relative abundances of T-RFs, after digestion with MspI, which represent key nitrifying and heterotrophic populations in the light and heavy fractions of the density gradients after RNA-SIP. The analysis was conducted after the samples had been incubated for 21 days. Error bars show 1 standard deviation (two replicates). Missing data points indicate that no PCR amplicon could be obtained at these gradient densities in the respective experiment. Circles represent the experiment with NH_4^+ as the energy source and $H^{13}CO_2^-$ as the carbon source, squares the control experiment with NH_4^+ and $H^{12}CO_2^-$, and triangles the control experiment without any added energy source and $H^{13}CO_2^-$ (in this control experiment, *Thermomonas* T-RF 190 was not detected above the threshold applied for peak calling). Note the different *y* axis scales in the graphs.

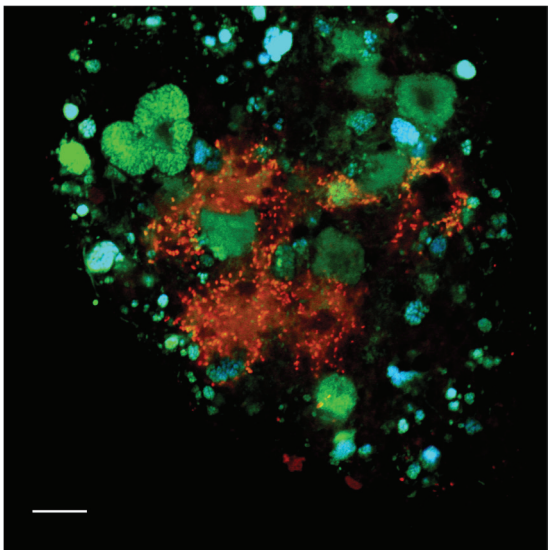

FIG 3 Fluorescence micrograph showing the *Thermomonas*-like organism (red), *Nitrospira* (cyan), and other bacteria (green) detected by FISH in activated sludge. Applied probes were Thmm115 (labeled with Cy3), Ntspa662 (labeled with Cy5), and the EUB338 probe mix (labeled with FLUOS). The *Thermomonas*-like bacterium appears more red than yellow due to a weak EUB338 signal obtained for this organism. Bar = 10 μm.

specific 16S rRNA-targeted oligonucleotide probes (see Table S1 in the supplemental material) was used to confirm that the organisms, which had clearly been labeled by ^{13}C according to SIP, indeed were present in the activated sludge samples. As expected, betaproteobacterial AOB and *Nitrospira*-like NOB were abundant in the original activated sludge from the WWTP and in the incubated samples. By using suitable probes (42), *Nitrospira* of the phylogenetic sublineages I and II of this genus (5) could be distinguished and were found to coexist in the sludge. All detected AOB and NOB formed tight microcolonies embedded in the sludge flocs. They frequently occurred in close spatial vicinity, which reflects their mutualistic symbiosis (4, 43). FISH with the newly designed probe Thmm115, which targets the *Thermomonas*-like betaproteobacterium (see Table S1 in the supplemental material), detected small (1- to 1.3-μm) rod-shaped cells. These organisms did not form aggregates, but they occasionally agglomerated in the neighborhood of nitrifiers (Fig. 3). However, loose aggregations of Thmm115-labeled cells were also found at large distances from any detectable nitrifiers, and no specific spatial coaggregation pattern of these populations was observed. Consistent with the T-RFLP data, the *Thermomonas*-like organism was most abundant in the samples from day 21 of the incubations supplemented with ammonium. It was not detected by FISH and T-RFLP in the original activated sludge.

Both newly designed oligonucleotide probes targeting the *Micavibrio*-like organism (see Table S1 in the supplemental material) detected short (0.7- to 1-μm) cells that were almost exclusively found in the direct vicinity of *Nitrospira* sublineage I cell colonies (Fig. 4). This very close spatial colocalization was observed in all investigated incubated samples and in original activated sludge collected at different time points. While only few of the probe-labeled *Nitrospira* cell aggregates colocalized with the *Micavibrio*-like bacterium, the latter was almost never found at larger distances away from *Nitrospira* sublineage I. Interestingly, we found several *Nitrospira* colonies that were surrounded by *Micavibrio*-like cells, which seemed to be attached to the surface of the *Nitrospira* clusters and sometimes appeared to have migrated or grown into the *Nitrospira* aggregates (Fig. 4A, C, and D). Occasionally, *Micavibrio*-like cells were found close to weakly fluorescent FISH-labeled *Nitrospira* clusters (Fig. 4B). To verify the qualitative observation that the *Micavibrio*-like organism and sublineage I *Nitrospira* specifically coaggregated, we applied digital image analysis to quantify the spatial distribution patterns of the nitrifiers and the *Micavibrio*-like bacteria. Previously developed algorithms for spatial analyses of microbial populations (15, 39) process batches of 2-D images, which must be taken at random x, y, and z positions within a specimen. This approach works best if the target populations are so abundant that they occur in most of the recorded images. The *Micavibrio*-like bacteria, however, were rare in the sludge samples. They would have been found only in a very few of the randomly taken 2-D images, which might not contain sufficient information about localization patterns with other organisms. This problem was solved by a 3-D approach that analyzed a larger volume around the few detected *Micavibrio*-like bacteria and thus lowered the risk of overlooking colocalized other bacteria. We acquired 3-D confocal z-stacks at four positions where the *Micavibrio*-like organism was detected and recorded the fluorescent signals of the different FISH probes targeting this bacterium, sublineage I *Nitrospira*, and sublineage II *Nitrospira*. The recorded volumes ranged from 33,203 to 71,150 μm^3. Automated counting of 3-D objects by the *daime* software revealed that the image stacks together contained at least 538 *Micavibrio*-like cells and small cell aggregates, 236 cell clusters of sublineage I *Nitrospira*, and 502 cell clusters of sublineage II *Nitrospira*. The count of *Micavibrio*-like bacteria is an underestimation, because the software could not split all adjacent *Micavibrio*-like cells in the 3-D images prior to counting. Of the 236 sublineage I *Nitrospira* cell clusters, 9 (3.8%) were surrounded by *Micavibrio*-like bacteria. The multicolor z-stacks were analyzed by a new 3-D implementation of the 2-D "Inflate Algorithm" (15) as described in Materials and Methods. These analyses confirmed a very pronounced coaggregation of the *Micavibrio*-like organism with sublineage I *Nitrospira* within short distances, below 2 μm (Fig. 5A). Beyond this distance range, the density of *Micavibrio* was lower than expected if the populations were randomly distributed (Fig. 5A). As only a few cell clusters of sublineage I *Nitrospira* were surrounded by *Micavibrio*-like cells (see above), this result shows that the tendency to coaggregate was a feature of *Micavibrio* only and not of *Nitrospira*. In contrast, the spatial arrangement pattern of the *Micavibrio*-like bacterium and sublineage II *Nitrospira* lacked any coaggregation signal (Fig. 5B).

Screening of NGS data sets for *Micavibrio*-like bacteria. An *in silico* screening of published NGS data sets detected organisms, which are closely related to the *Micavibrio*-like bacterium analyzed in this study, in other bioreactors and in freshwater, soil, and extreme (e.g., hydrothermal vents) environments (see Fig. S4 in the supplemental material). Interestingly, the percentages of sequence reads from these organisms were similar to the percentages of reads from some known obligate bacterial predators, which were also detected in the same habitat types. However, the frequency of all considered predators ranged over several orders of magnitude in most data sets (see Fig. S4).

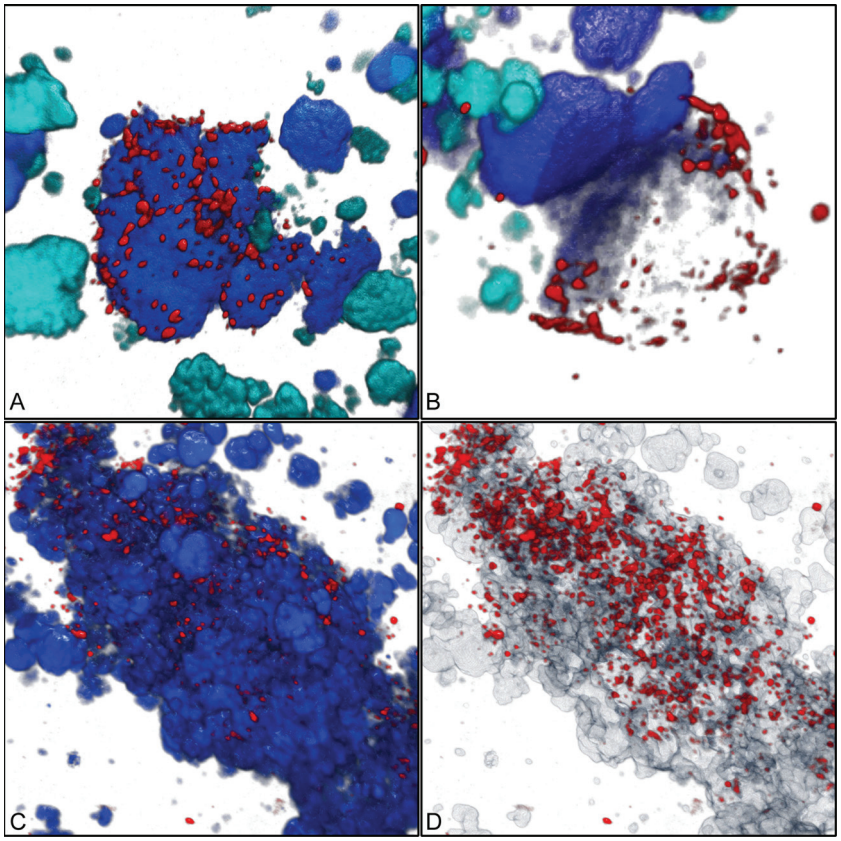

FIG 4 Three-dimensional visualization showing the coaggregation of the *Micavibrio*-like bacterium with sublineage I *Nitrospira*. (A) *Micavibrio*-like cells (red) attached to a cell aggregate of sublineage I *Nitrospira* (blue). Other nitrifiers (AOB and sublineage II *Nitrospira*) are shown in cyan. Applied probes were HSAL723 and HSAL866 (both labeled with Cy3), Ntspa662 (labeled with Cy5, rendered as blue), Ntspa1151 (labeled with FLUOS, rendered as cyan), and NEU, Cluster6a192, and Nso1225 (labeled with FLUOS, rendered as cyan). (B) *Micavibrio*-like cells surrounding a partly dark (possibly degraded) sublineage I *Nitrospira* cell aggregate. Colors and probes are like in panel A. (C) *Micavibrio*-like cells (red) attached to a cell aggregate of *Nitrospira* (probe Ntspa662; blue). (D) Same position as shown in panel C, but *Nitrospira* clusters are rendered semitransparent to show that *Micavibrio*-like cells also penetrated the inner parts of the *Nitrospira* cell colonies.

DISCUSSION

Nitrifying microorganisms, which fix inorganic carbon, can support the growth of heterotrophic organisms by excreting organic compounds or by providing substrates to saprophytes after cell lysis (8, 13). Although nitrifiers might have important functions as primary producers, in addition to their roles in nitrogen cycling, little is known about the specificity and nature of their interactions with heterotrophs in engineered or natural ecosystems. It remains largely unexplored which heterotrophs benefit from AOB and/or NOB and whether these organisms are mutualistic symbionts, merely commensals or saprophytes, or even parasites of the nitrifiers. Experiments using radiolabeled substrates and FISH-MAR successfully started to dissect the complex food web in nitrifying activated sludge (10, 13). This approach is efficient if broad group-specific FISH probes are used in the FISH-MAR experiments, but it lacks the high phylogenetic resolution that may be needed to identify specific biological interactions. An alternative would be to establish from the sample a general 16S rRNA clone library and use this sequence information to design many (possibly hundreds) highly specific FISH probes, which could then be used in numerous FISH-MAR experiments to specifically identify the substrate-labeled organisms. This "brute force" approach would be very tedious and time-consuming and may easily overlook rare organisms that are underrepresented in the clone library. Therefore, we followed a different strategy and applied RNA-SIP, which is a true discovery tool that directly identifies also unknown isotope-labeled organisms and provides access to their 16S rRNA sequences for further analysis. Subsequently, we completed the full-cycle rRNA approach (17) by using FISH with newly designed probes to detect two isotope-labeled putative heterotrophs *in situ*.

Stable isotope probing. Betaproteobacterial AOB and *Nitrospira*-like NOB were expected to be active and fix inorganic carbon during the incubations of activated sludge in the presence of NH_4^+, whereas only NOB should be active nitrifiers during the incubations with NO_2^-. Consistently, 16S rRNA genes of both AOB and NOB were abundant in a clone library established from ^{13}C-labeled RNA after incubation with ammonium and $H^{13}CO_3$. The weak ^{13}C labeling of RNA in the late phase of the incubation with NO_2^- indicates an unexpectedly low carbon fixation and/or ribosome biosynthesis by *Nitrospira* under the applied conditions, although nitrite was removed during this incubation (data not shown) and the supplied nitrite concentration (0.25 mM) should have supported the growth of *Nitrospira* spp. (42), which are adapted to relatively low nitrite concentrations (44–46). This outcome of the incubations with NO_2^- did not impair our study,

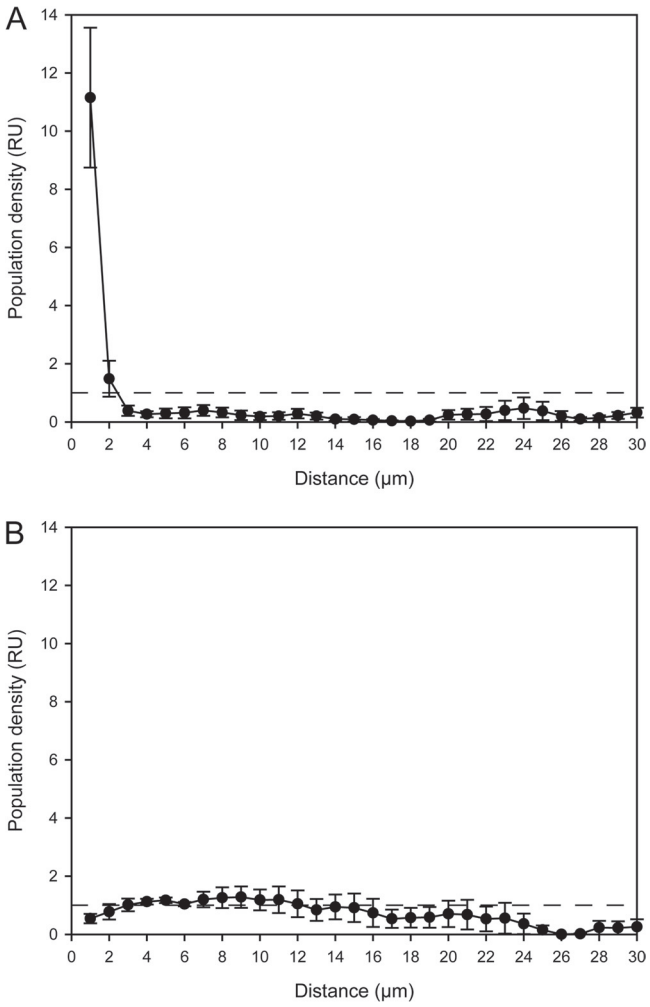

FIG 5 Spatial arrangement pattern analysis of the *Micavibrio*-like organism and nitrifiying bacteria. In either plot the horizontal dashed line ($y = 1$) indicates random distribution at the respective distance. Values above this line indicate coaggregation (i.e., the *Micavibrio*-like cells were more abundant at these distances than expected for randomly distributed populations). Values below this line indicate that the *Micavibrio*-like cells were less abundant at these distances than expected for randomly distributed populations. Error bars show the standard errors of the means ($n = 4$). RU, relative units. (A) Coaggregation of *Micavibrio*-like bacteria with sublineage I *Nitrospira*; (B) lack of coaggregation between *Micavibrio*-like bacteria and sublineage II *Nitrospira*.

because the experiments with NH_4^+ allowed us to analyze interactions of heterotrophs with AOB and NOB.

The 16S rRNA sequences of ^{13}C-labeled heterotrophs were difficult to obtain due to the dominance of 16S rRNA from nitrifiers in the ^{13}C-labeled RNA fraction. This problem was solved by applying LNAzymes, which can strongly facilitate the detection of rare organisms in highly uneven microbial communities (24). In this study, the use of LNAzymes helped us to obtain from the heavy rRNA fraction several sequences of organisms not known to be nitrifiers (see Table S2 in the supplemental material). Two of these organisms, a *Thermomonas*- and a *Micavibrio*-like bacterium, were ^{13}C labeled in the presence of NH_4^+ as indicated by the T-RFLP profiles from the light and heavy fractions and the control experiments (Fig. 2; see also Fig. S3 in the supplemental material). The other organisms (see Table S2) may also have obtained ^{13}C from nitrifiers, but the labeling was too weak to be confirmed by the combination of SIP and T-RFLP analysis. In addition, LNAzyme 215 is not perfectly specific and might thus have cleaved the 16S rRNA of some nonnitrifiers (see Table S1). As the original activated sludge samples and the RNA preparations had not been screened for presence of these nonnitrifiers prior to LNAzyme treatment, we cannot exclude the possibility that unspecific action of LNAzyme 215 hampered their detection in our experiments. To confirm uptake of small amounts of carbon from nitrifiers by the other putative heterotrophs (see Table S2), a more sensitive method like FISH-MAR with $H^{14}CO_3^-$ could be used in future experiments with newly designed FISH probes that target the sequences obtained by SIP.

***In situ* analysis and lifestyle of the *Thermomonas*- and *Micavibrio*-like bacteria.** In this study, we focused on the two potential heterotrophs that were labeled according to SIP. FISH showed that one of these organisms, the *Thermomonas*-like bacterium, sometimes occurred in the spatial neighborhood of nitrifiers (Fig. 3) but also grew far away from any known AOB and NOB. Together with the relatively weak ^{13}C labeling, this distribution pattern suggests that the *Thermomonas*-like organism is not a specific symbiont of nitrifiers but a heterotroph that occasionally takes up soluble organic products excreted by nitrifiers, or substrates set free due to the decay of nitrifier biomass, or extracellular polymeric substances (EPS) that enclose the microcolonies of nitrifiers. This lifestyle would be consistent with the properties of the closely related isolate *Thermomonas brevis*, which was obtained from a denitrifying bioreactor, reduces nitrate and nitrite, and grows on a variety of substrates, including sugars and *N*-acetylglucosamine (47). Its transiently high abundance in our incubations but not the original sludge indicates that this organism was only temporarily favored, either by the incubation conditions or by biotic factors such as the decline and cell lysis of another population in the sludge.

The coaggregation of the *Micavibrio*-like bacterium and *Nitrospira* sublineage I, which was observed in the incubated samples and in the source activated sludge, indicates an interaction of these organisms different from the nonobligate saprophytism or commensalism proposed for *Thermomonas*. The absence of the *Micavibrio*-like organism at larger distances from *Nitrospira* and its quantified strong tendency to tightly coaggregate with sublineage I *Nitrospira* (Fig. 5A), but not with other *Nitrospira* members (Fig. 5B), suggest that this interaction is highly specific and, at least in the examined sludge, also obligate for *Micavibrio*. The characterized members of the genus *Micavibrio* (48) are obligate epibiotic predators of Gram-negative bacteria (49, 50). These motile organisms attach to the outer membrane of their prey, but different from other predators such as *Bdellovibrio*, they do not penetrate the periplasmic space and divide simply by binary fission. The attacked cells are completely consumed (51). Furthermore, *Micavibrio* spp. are able to prey on target bacteria that aggregate within biofilms and thus are not limited to attacking planktonic cells (52, 53). This mode of predation strikingly resembles the direct attachment of the *Micavibrio*-like cells to *Nitrospira* microcolonies in the sludge flocs (Fig. 4) and would lead to ^{13}C labeling of the *Micavibrio*-like population. It would also explain the occasional agglomerations of *Micavibrio*-like bacteria around apparently empty space or weakly probe-labeled sublineage I *Nitrospira* clusters (Fig. 4B). Completely or partly degraded prey cells would not be detectable by FISH, or they would emit only dim fluores-

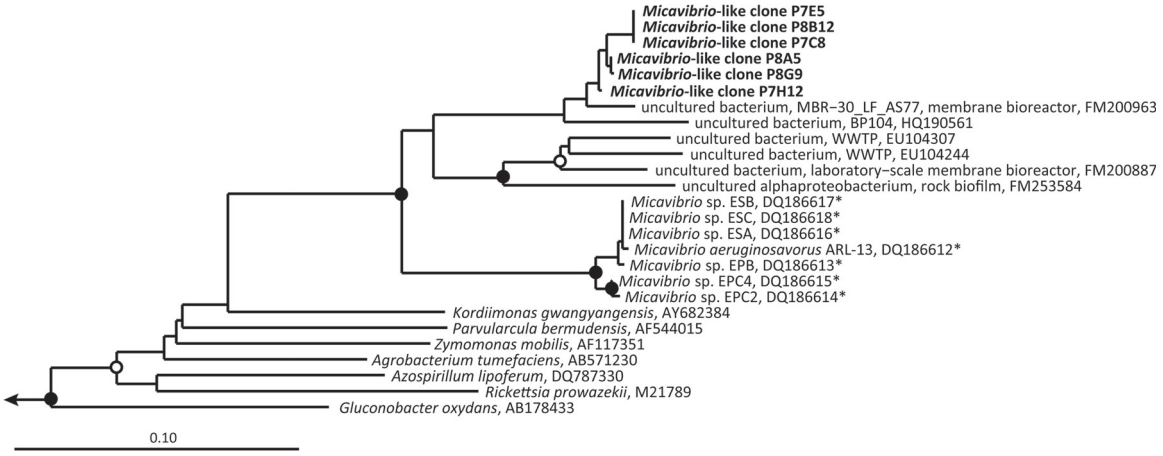

FIG 6 Maximum likelihood tree based on 16S rRNA sequences, which shows the phylogenetic affiliation of the *Micavibrio*-like bacteria detected in this study (in boldface). Strains which are known predators are marked by an asterisk. Sequences retrieved from WWTPs in other studies are marked by "WWTP." Solid circles on tree nodes indicate >90% and open circles >70% maximum likelihood bootstrap support (1,000 iterations). Representative beta- and gammaproteobacteria were used as outgroups. The scale bar indicates 0.1 estimated change per nucleotide.

cence signals due to the degradation or leakage of ribosomes. The high specificity for *Nitrospira* sublineage I is in line with the high prey specificity that has been observed for *Micavibrio* and other bacterial predators (51, 54, 55). The observation that most sublineage I *Nitrospira* microcolonies did not coaggregate with *Micavibrio*-like cells would also be consistent with a predator-prey relationship, where usually only a fraction of the prey population is attacked by the predator at any time. Shemesh and Jurkevitch (56) observed that bacterial prey populations developed a transient resistance to predation by *Bdellovibrio*, which was a plastic phenotypic response rather than a genetic mutation. As this resistance was not total, both the predator and the prey survived (56). It is tempting to speculate that only few sublineage I *Nitrospira* colonies were surrounded by *Micavibrio*-like cells, because the major part of the *Nitrospira* population had developed resistance. Moreover, different T-RFs representing sublineage I *Nitrospira* (Fig. 2) indicate a high microdiversity in this sublineage that was not resolved by the applied FISH probes, which had a broader specificity. Most of these sublineage I populations might not have been susceptible to predation by the *Micavibrio*-like bacteria. Alternatively, many of the *Nitrospira* clusters may have been inaccessible to the *Micavibrio*-like organism if they were deeply embedded in EPS or located in the center of dense activated sludge flocs, or they were simply not encountered yet by *Micavibrio*-like cells seeking prey. Other possible interactions between *Nitrospira* and the *Micavibrio*-like organism would be inconsistent with the current notion that *Micavibrio* spp. are predators but cannot be excluded without direct evidence for predation. For example, the detected transfer of ^{13}C could also be explained by a mutualistic symbiosis that involves the transfer of substrates. Such a mutualistic relationship can also be reflected by a tight spatial coupling of the partners (for example, see reference 57). Moreover, the *Micavibrio*-like organism might be a previously unrecognized autotrophic nitrifier that directly fixed inorganic ^{13}C and colocalized with other nitrifiers, because AOB and NOB are mutualistic symbionts (43) and often coaggregate (4, 42). A mutualistic relationship of any kind, however, would be beneficial for both partners. It should thus be reflected by mutual coaggregation, which was not observed for *Nitrospira* relative to the *Micavibrio*-like bacterium. If the latter indeed was a novel nitrifier, one would also not expect such a highly specific colocalization with only one *Nitrospira* sublineage. It seems to be more likely that the *Micavibrio*-like organism, if not a predator, could be a highly specialized heterotrophic commensal or saprophyte feeding on particular organic products or cell components of sublineage I *Nitrospira*. Further hints could be obtained from chemical and isotopic analyses of sludge pore water and the floc matrix. This could show whether extracellular ^{13}C-labeled compounds are small molecules, which likely have been secreted by living *Nitrospira*, or proteins and other larger cell components that more probably have been released from lysed *Nitrospira* cells. Such analyses could be difficult to conduct with the complex microbial community in activated sludge but should be more straightforward once coenrichment cultures of *Nitrospira* and *Micavibrio*-like bacteria become available. As outlined in reference 49, bacterial predators such as *Micavibrio* might have evolved from saprophytic ancestors, which attached to the envelope of dead cells and secreted lytic enzymes. According to this evolutionary model, the common ancestry with the known predatory *Micavibrio* species (Fig. 6) would be consistent with a saprophytic or a predatory lifestyle of the *Micavibrio*-like organism.

Ecological considerations. This study provides further evidence of a role for autotrophic nitrifiers as primary producers, which supply heterotrophic microbial community members with organic sources of carbon and energy. While such carbon transfer was detectable in the activated sludge samples analyzed in this study, this additional ecological function of nitrifiers likely is more important in oligotrophic environments where the ambient concentrations of organic nutrients are much lower than in wastewater. Examples include drinking water treatment facilities (9, 11, 12) and even cave ecosystems that may be driven primarily by nitrite oxidation (58). As demonstrated for the *Micavibrio*-like organism, interactions of heterotrophic bacteria with nitrifiers can be more specific than previously recognized. So far, only protozoan grazing (23, 59, 60) and bacteriophage attack (61) have been considered biological controls of nitrifier populations. Our results indicate that bacterial predation may be another regulator of nitrification. Whether its impact on the population densities of nitrifiers is marginal or significant, and whether it may account for

nitrification failure in WWTPs, awaits clarification in future research. However, predation could even have positive effects. The specific control of nitrifier populations by predators may prevent any particular nitrifier strain from becoming dominant. Thus, predators could be a selective force toward a high diversity of susceptible and resistant strains within nitrifier communities, which may lead to high functional redundancy and thus improve the overall resistance of a nitrifying WWTP or a natural ecosystem to environmental perturbations (62).

Micavibrio-related 16S rRNA sequences have been retrieved from other bioreactors (7, 10, 63) and from soils (64) (Fig. 6). In addition, our analysis of NGS data sets revealed the presence of these organisms in many kinds of habitats (see Fig. S4 in the supplemental material). Solely based on their phylogenetic affiliation and sequence similarity to known *Micavibrio* spp., one cannot determine whether all these environmental *Micavibrio*-like organisms are predators. Here we show that one member of this group (Fig. 6) is involved in a highly specific interaction with other Gram-negative bacteria (*Nitrospira*). However, the aforementioned screening of NGS data sets did not reveal any correlation between the occurrence of *Micavibrio*-like bacteria and members of the genus *Nitrospira* (data not shown). This may indicate that no biological interactions exist between these organisms in the respective habitats, but the lack of a correlation might also be due to possible biases of nucleic acid extraction or PCR amplification in the respective studies. Future research, possibly including genomic comparisons to already sequenced predators such as *Micavibrio aeruginosavorus* (50) and *Bdellovibrio bacteriovorus* (65), may illuminate the lifestyle of the *Micavibrio*-like bacteria and their impact on the ecological functions of their interaction partners or prey.

ACKNOWLEDGMENTS

We thank Christian Baranyi for technical assistance and Norbert Kohler and Konrad Thoma for providing us with sludge samples from the WWTP Ingolstadt. We thank Margarete Watzka for performing the IRMS analyses.

This work was funded by the Graduate School "Symbiotic Interactions" of the University of Vienna and partly by the Vienna Science and Technology Fund (WWTF, grant LS09-040).

REFERENCES

1. **Mussmann M, Brito I, Pitcher A, Sinninghe Damste JS, Hatzenpichler R, Richter A, Nielsen JL, Nielsen PH, Muller A, Daims H, Wagner M, Head IM.** 2011. Thaumarchaeotes abundant in refinery nitrifying sludges express *amoA* but are not obligate autotrophic ammonia oxidizers. Proc. Natl. Acad. Sci. U. S. A. **108**:16771–16776.
2. **Koops HP, Purkhold U, Pommerening-Röser A, Timmermann G, Wagner M.** 2003. The lithoautotrophic ammonia-oxidizing bacteria, p 778–811. *In* Dworkin M, Falkow S, Rosenberg E, Schleifer KH, Stackebrandt E (ed), The prokaryotes: a handbook on the biology of bacteria, 3rd ed. Springer Science+Business Media, New York, NY.
3. **Schramm A, de Beer D, Wagner M, Amann R.** 1998. Identification and activities in situ of *Nitrosospira* and *Nitrospira* spp. as dominant populations in a nitrifying fluidized bed reactor. Appl. Environ. Microbiol. **64**: 3480–3485.
4. **Juretschko S, Timmermann G, Schmid M, Schleifer K-H, Pommerening-Röser A, Koops H-P, Wagner M.** 1998. Combined molecular and conventional analyses of nitrifying bacterium diversity in activated sludge: *Nitrosococcus mobilis* and *Nitrospira*-like bacteria as dominant populations. Appl. Environ. Microbiol. **64**:3042–3051.
5. **Daims H, Nielsen JL, Nielsen PH, Schleifer KH, Wagner M.** 2001. In situ characterization of *Nitrospira*-like nitrite-oxidizing bacteria active in wastewater treatment plants. Appl. Environ. Microbiol. **67**:5273–5284.
6. **Wagner M, Rath G, Amann R, Koops H-P, Schleifer K-H.** 1995. In situ identification of ammonia-oxidizing bacteria. Syst. Appl. Microbiol. **18**: 251–264.
7. **Juretschko S, Loy A, Lehner A, Wagner M.** 2002. The microbial community composition of a nitrifying-denitrifying activated sludge from an industrial sewage treatment plant analyzed by the full-cycle rRNA approach. Syst. Appl. Microbiol. **25**:84–99.
8. **Rittmann BE, Regan JM, Stahl DA.** 1994. Nitrification as a source of soluble organic substrate in biological treatment. Water Sci. Technol. **30**: 1–8.
9. **Martiny AC, Albrechtsen HJ, Arvin E, Molin S.** 2005. Identification of bacteria in biofilm and bulk water samples from a nonchlorinated model drinking water distribution system: detection of a large nitrite-oxidizing population associated with *Nitrospira* spp. Appl. Environ. Microbiol. **71**: 8611–8617.
10. **Kindaichi T, Ito T, Okabe S.** 2004. Ecophysiological interaction between nitrifying bacteria and heterotrophic bacteria in autotrophic nitrifying biofilms as determined by microautoradiography-fluorescence in situ hybridization. Appl. Environ. Microbiol. **70**:1641–1650.
11. **Regan JM, Harrington GW, Baribeau H, De Leon R, Noguera DR.** 2003. Diversity of nitrifying bacteria in full-scale chloraminated distribution systems. Water Res. **37**:197–205.
12. **Regan JM, Harrington GW, Noguera DR.** 2002. Ammonia- and nitrite-oxidizing bacterial communities in a pilot-scale chloraminated drinking water distribution system. Appl. Environ. Microbiol. **68**:73–81.
13. **Okabe S, Kindaichi T, Ito T.** 2005. Fate of ^{14}C-labeled microbial products derived from nitrifying bacteria in autotrophic nitrifying biofilms. Appl. Environ. Microbiol. **71**:3987–3994.
14. **Lee N, Nielsen PH, Andreasen KH, Juretschko S, Nielsen JL, Schleifer K-H, Wagner M.** 1999. Combination of fluorescent *in situ* hybridization and microautoradiography—a new tool for structure-function analyses in microbial ecology. Appl. Environ. Microbiol. **65**:1289–1297.
15. **Daims H, Wagner M.** 2011. In situ techniques and digital image analysis methods for quantifying spatial localization patterns of nitrifiers and other microorganisms in biofilm and flocs. Methods Enzymol. **496**:185–215.
16. **Manefield M, Whiteley AS, Griffiths RI, Bailey MJ.** 2002. RNA stable isotope probing, a novel means of linking microbial community function to phylogeny. Appl. Environ. Microbiol. **68**:5367–5373.
17. **Amann RI, Ludwig W, Schleifer K-H.** 1995. Phylogenetic identification and in situ detection of individual microbial cells without cultivation. Microbiol. Rev. **59**:143–169.
18. **Chauhan A, Cherrier J, Williams HN.** 2009. Impact of sideways and bottom-up control factors on bacterial community succession over a tidal cycle. Proc. Natl. Acad. Sci. U. S. A. **106**:4301–4306.
19. **Frias-Lopez J, Thompson A, Waldbauer J, Chisholm SW.** 2009. Use of stable isotope-labelled cells to identify active grazers of picocyanobacteria in ocean surface waters. Environ. Microbiol. **11**:512–525.
20. **Glaubitz S, Lueders T, Abraham WR, Jost G, Jurgens K, Labrenz M.** 2009. (13)C-isotope analyses reveal that chemolithoautotrophic Gamma- and Epsilonproteobacteria feed a microbial food web in a pelagic redoxcline of the central Baltic Sea. Environ. Microbiol. **11**:326–337.
21. **Lu YH, Conrad R.** 2005. In situ stable isotope probing of methanogenic archaea in the rice rhizosphere. Science **309**:1088–1090.
22. **Lueders T, Kindler R, Miltner A, Friedrich MW, Kaestner M.** 2006. Identification of bacterial micropredators distinctively active in a soil microbial food web. Appl. Environ. Microbiol. **72**:5342–5348.
23. **Moreno AM, Matz C, Kjelleberg S, Manefield M.** 2010. Identification of ciliate grazers of autotrophic bacteria in ammonia-oxidizing activated sludge by RNA stable isotope probing. Appl. Environ. Microbiol. **76**: 2203–2211.
24. **Dolinšek J, Dorninger C, Lagkouvardos I, Wagner M, Daims H.** Depletion of unwanted nucleic acid templates by selective cleavage: LNAzymes open a new window for detecting rare microbial community members. Appl. Environ. Microbiol., in press.
25. **Feisthauer S, Wick LY, Kastner M, Kaschabek SR, Schlomann M, Richnow HH.** 2008. Differences of heterotrophic (13)CO(2) assimilation by Pseudomonas knackmussii strain B13 and Rhodococcus opacus 1CP and potential impact on biomarker stable isotope probing. Environ. Microbiol. **10**:1641–1651.
26. **Hood-Nowotny R, Hinko-Najera Umana N, Inselbacher E, Oswald-Lachouani P, Wanek W.** 2010. Alternative methods for measuring inorganic, organic, and total dissolved nitrogen in soil. Soil Sci. Soc. Am. J. **74**:1018–1027.

27. **Whiteley AS, Thomson B, Lueders T, Manefield M.** 2007. RNA stable-isotope probing. Nat. Protoc. **2**:838–844.
28. **Stres B, Tiedje JM, Murovec B.** 2009. BEsTRF: a tool for optimal resolution of terminal-restriction fragment length polymorphism analysis based on user-defined primer-enzyme-sequence databases. Bioinformatics **25**:1556–1558.
29. **Abdo Z, Schuette UM, Bent SJ, Williams CJ, Forney LJ, Joyce P.** 2006. Statistical methods for characterizing diversity of microbial communities by analysis of terminal restriction fragment length polymorphisms of 16S rRNA genes. Environ. Microbiol. **8**:929–938.
30. **Ludwig W, Strunk O, Westram R, Richter L, Meier, H, Yadhukumar, Buchner A, Lai T, Steppi S, Jobb G, Förster W, Brettske I, Gerber S, Ginhart AW, Gross O, Grumann S, Hermann S, Jost R, König A, Liss T, Lüßmann R, May M, Nonhoff B, Reichel B, Strehlow R, Stamatakis A, Stuckmann N, Vilbig A, Lenke M, Ludwig T, Bode A, Schleifer K-H.** 2004. ARB: a software environment for sequence data. Nucleic Acids Res. **32**:1363–1371.
31. **Pruesse E, Quast C, Knittel K, Fuchs BM, Ludwig W, Peplies J, Glockner FO.** 2007. SILVA: a comprehensive online resource for quality checked and aligned ribosomal RNA sequence data compatible with ARB. Nucleic Acids Res. **35**:7188–7196.
32. **Stamatakis A, Ludwig T, Meier H.** 2005. RAxML-III: a fast program for maximum likelihood-based inference of large phylogenetic trees. Bioinformatics **21**:456–463.
33. **Ashelford KE, Chuzhanova NA, Fry JC, Jones AJ, Weightman AJ.** 2006. New screening software shows that most recent large 16S rRNA gene clone libraries contain chimeras. Appl. Environ. Microbiol. **72**:5734–5741.
34. **Kodama Y, Shumway M, Leinonen R.** 2012. The Sequence Read Archive: explosive growth of sequencing data. Nucleic Acids Res. **40**:D54–D56. doi:10.1093/nar/gkr854.
35. **Camacho C, Coulouris G, Avagyan V, Ma N, Papadopoulos J, Bealer K, Madden TL.** 2009. BLAST+: architecture and applications. BMC Bioinformatics **10**:421.
36. **Altschul SF, Gish W, Miller W, Myers EW, Lipman DJ.** 1990. Basic local alignment search tool. J. Mol. Biol. **215**:403–410.
37. **Daims H, Brühl A, Amann R, Schleifer K-H, Wagner M.** 1999. The domain-specific probe EUB338 is insufficient for the detection of all *Bacteria*: development and evaluation of a more comprehensive probe set. Syst. Appl. Microbiol. **22**:434–444.
38. **Daims H, Stoecker K, Wagner M.** 2005. Fluorescence in situ hybridisation for the detection of prokaryotes, p 213–239. *In* Osborn AM, Smith CJ (ed), Molecular microbial ecology. Bios-Garland, Abingdon, United Kingdom.
39. **Daims H, Lücker S, Wagner M.** 2006. *daime*, a novel image analysis program for microbial ecology and biofilm research. Environ. Microbiol. **8**:200–213.
40. **Santoro SW, Joyce GF.** 1997. A general purpose RNA-cleaving DNA enzyme. Proc. Natl. Acad. Sci. U. S. A. **94**:4262–4266.
41. **Vester B, Lundberg LB, Sorensen MD, Babu BR, Douthwaite S, Wengel J.** 2004. Improved RNA cleavage by LNAzyme derivatives of DNAzymes. Biochem. Soc. Trans. **32**:37–40.
42. **Maixner F, Noguera DR, Anneser B, Stoecker K, Wegl G, Wagner M, Daims H.** 2006. Nitrite concentration influences the population structure of *Nitrospira*-like bacteria. Environ. Microbiol. **8**:1487–1495.
43. **Stein LY, Arp DJ.** 1998. Loss of ammonia monooxygenase activity in *Nitrosomonas europaea* upon exposure to nitrite. Appl. Environ. Microbiol. **64**:4098–4102.
44. **Bartosch S, Hartwig C, Spieck E, Bock E.** 2002. Immunological detection of Nitrospira-like bacteria in various soils. Microb. Ecol. **43**:26–33.
45. **Schramm A, de Beer D, van den Heuvel JC, Ottengraf S, Amann R.** 1999. Microscale distribution of populations and activities of *Nitrosospira* and *Nitrospira* spp. along a macroscale gradient in a nitrifying bioreactor: quantification by in situ hybridization and the use of microsensors. Appl. Environ. Microbiol. **65**:3690–3696.
46. **Lücker S, Wagner M, Maixner F, Pelletier E, Koch H, Vacherie B, Rattei T, Damsté JS, Spieck E, Le Paslier D, Daims H.** 2010. A *Nitrospira* metagenome illuminates the physiology and evolution of globally important nitrite-oxidizing bacteria. Proc. Natl. Acad. Sci. U. S. A. **107**:13479–13484.
47. **Mergaert J, Cnockaert MC, Swings J.** 2003. *Thermomonas fusca* sp. nov. and *Thermomonas brevis* sp. nov., two mesophilic species isolated from a denitrification reactor with poly(epsilon-caprolactone) plastic granules as fixed bed, and emended description of the genus *Thermomonas*. Int. J. Syst. Evol. Microbiol. **53**:1961–1966.
48. **Lambina VA, Afinogenova AV, Lenabad SR, Konovalova SM, Pushkareva AP.** 1982. *Micavibrio admirandus* new-genus new-species. Mikrobiologiia **51**:114–117.
49. **Jurkevitch E.** 2007. Predatory behaviors in bacteria—diversity and transitions. Microbe **2**:67–73.
50. **Wang Z, Kadouri DE, Wu M.** 2011. Genomic insights into an obligate epibiotic bacterial predator: *Micavibrio aeruginosavorus* ARL-13. BMC Genomics **12**:453. doi:10.1186/1471-2164-12-453.
51. **Davidov Y, Huchon D, Koval SF, Jurkevitch E.** 2006. A new alpha-proteobacterial clade of *Bdellovibrio*-like predators: implications for the mitochondrial endosymbiotic theory. Environ. Microbiol. **8**:2179–2188.
52. **Dashiff A, Junka RA, Libera M, Kadouri DE.** 2011. Predation of human pathogens by the predatory bacteria *Micavibrio aeruginosavorus* and *Bdellovibrio bacteriovorus*. J. Appl. Microbiol. **110**:431–444.
53. **Kadouri D, Venzon NC, O'Toole GA.** 2007. Vulnerability of pathogenic biofilms to *Micavibrio aeruginosavorus*. Appl. Environ. Microbiol. **73**:605–614.
54. **Guerrero R, Pedrosalio C, Esteve I, Mas J, Chase D, Margulis L.** 1986. Predatory prokaryotes: predation and primary consumption evolved in bacteria. Proc. Natl. Acad. Sci. U. S. A. **83**:2138–2142.
55. **Rashidan KK, Bird DF.** 2001. Role of predatory bacteria in the termination of a cyanobacterial bloom. Microb. Ecol. **41**:97–105.
56. **Shemesh Y, Jurkevitch E.** 2004. Plastic phenotypic resistance to predation by *Bdellovibrio* and like organisms in bacterial prey. Environ. Microbiol. **6**:12–18.
57. **Orphan VJ, House CH, Hinrichs KU, McKeegan KD, DeLong EF.** 2001. Methane-consuming archaea revealed by directly coupled isotopic and phylogenetic analysis. Science **293**:484–487.
58. **Holmes AJ, Tujula NA, Holley M, Contos A, James JM, Rogers P, Gillings MR.** 2001. Phylogenetic structure of unusual aquatic microbial formations in Nullarbor caves, Australia. Environ. Microbiol. **3**:256–264.
59. **Graham DW, Knapp CW, Van Vleck ES, Bloor K, Lane TB, Graham CE.** 2007. Experimental demonstration of chaotic instability in biological nitrification. ISME J. **1**:385–393.
60. **Moussa MS, Hooijmans CM, Lubberding HJ, Gijzen HJ, van Loosdrecht MC.** 2005. Modelling nitrification, heterotrophic growth and predation in activated sludge. Water Res. **39**:5080–5098.
61. **Choi JD, Kotay SM, Goel R.** 2010. Various physico-chemical stress factors cause prophage induction in *Nitrosospira multiformis* 25196—an ammonia oxidizing bacteria. Water Res. **44**:4550–4558.
62. **Daims H, Purkhold U, Bjerrum L, Arnold E, Wilderer PA, Wagner M.** 2001. Nitrification in sequencing biofilm batch reactors: lessons from molecular approaches. Water Sci. Technol. **43**:9–18.
63. **Huang LN, De Wever H, Diels L.** 2008. Diverse and distinct bacterial communities induced biofilm fouling in membrane bioreactors operated under different conditions. Environ. Sci. Technol. **42**:8360–8366.
64. **Davidov Y, Friedjung A, Jurkevitch E.** 2006. Structure analysis of a soil community of predatory bacteria using culture-dependent and culture-independent methods reveals a hitherto undetected diversity of Bdellovibrio-and-like organisms. Environ. Microbiol. **8**:1667–1673.
65. **Rendulic S, Jagtap P, Rosinus A, Eppinger M, Baar C, Lanz C, Keller H, Lambert C, Evans KJ, Goesmann A, Meyer F, Sockett RE, Schuster SC.** 2004. A predator unmasked: life cycle of *Bdellovibrio bacteriovorus* from a genomic perspective. Science **303**:689–692.

Supplemental material

Interactions of Nitrifying Bacteria and Heterotrophs: Identification of a *Micavibrio*-Like Putative Predator of *Nitrospira* spp.

Jan Dolinšek[a], Ilias Lagkouvardos[a], Wolfgang Wanek[b], Michael Wagner[a], Holger Daims[a]

[a] Department of Microbial Ecology, Ecology Centre, University of Vienna, Vienna, Austria;
[b] Department of Terrestrial Ecosystem Research, Ecology Centre, University of Vienna, Vienna, Austria

Appl. Environ. Microbiol., March 2013, vol. 79, no. 6, p. 2027-2037

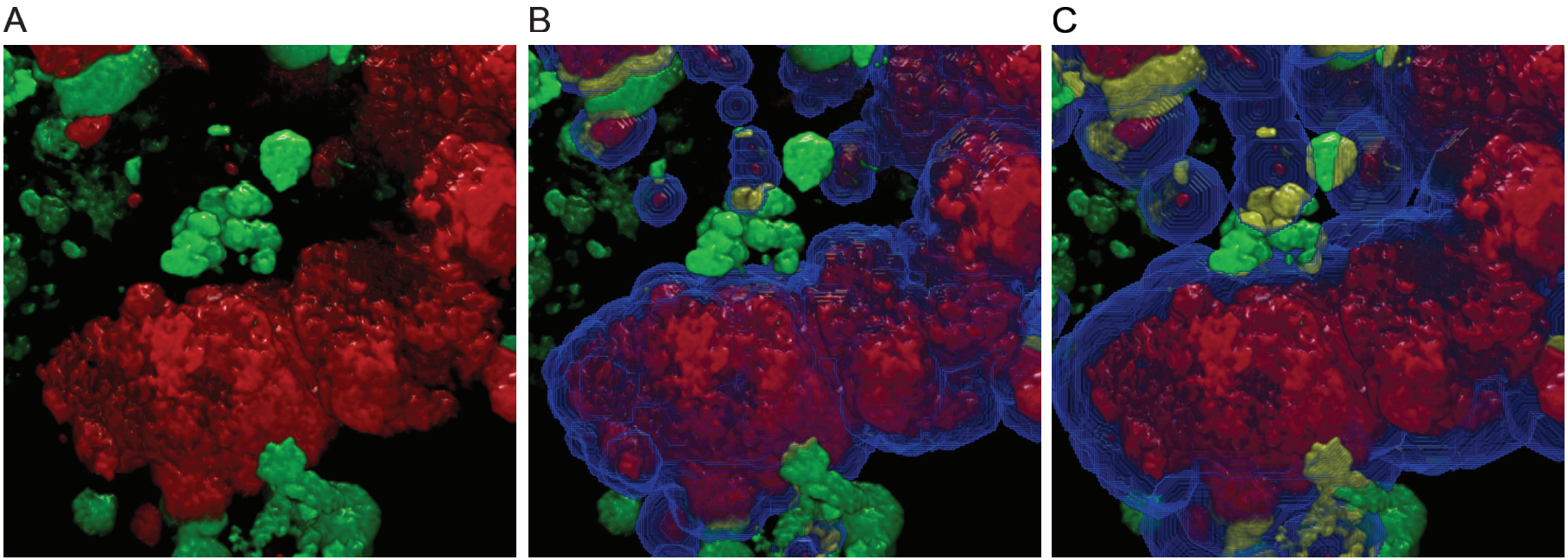

Fig. S1. Illustration of the 3-D Inflate Algorithm for the spatial arrangement analysis of microbial populations. (A) 3-D visualization of two bacterial populations labeled by specific FISH probes in biofilm. (B) The red population has been virtually enlarged ("inflated"; indicated by blue contours). Overlapping voxels with the green population are shown in yellow. These voxels are counted. The distance (in µm), by which the red population has been enlarged, is known. (C) The red population has been further enlarged, and more voxels of this enlarged population overlap with the green population (shown in yellow). These overlapping voxels are counted again. All counts of overlapping voxels are stored in computer memory together with the respective distances (in µm).

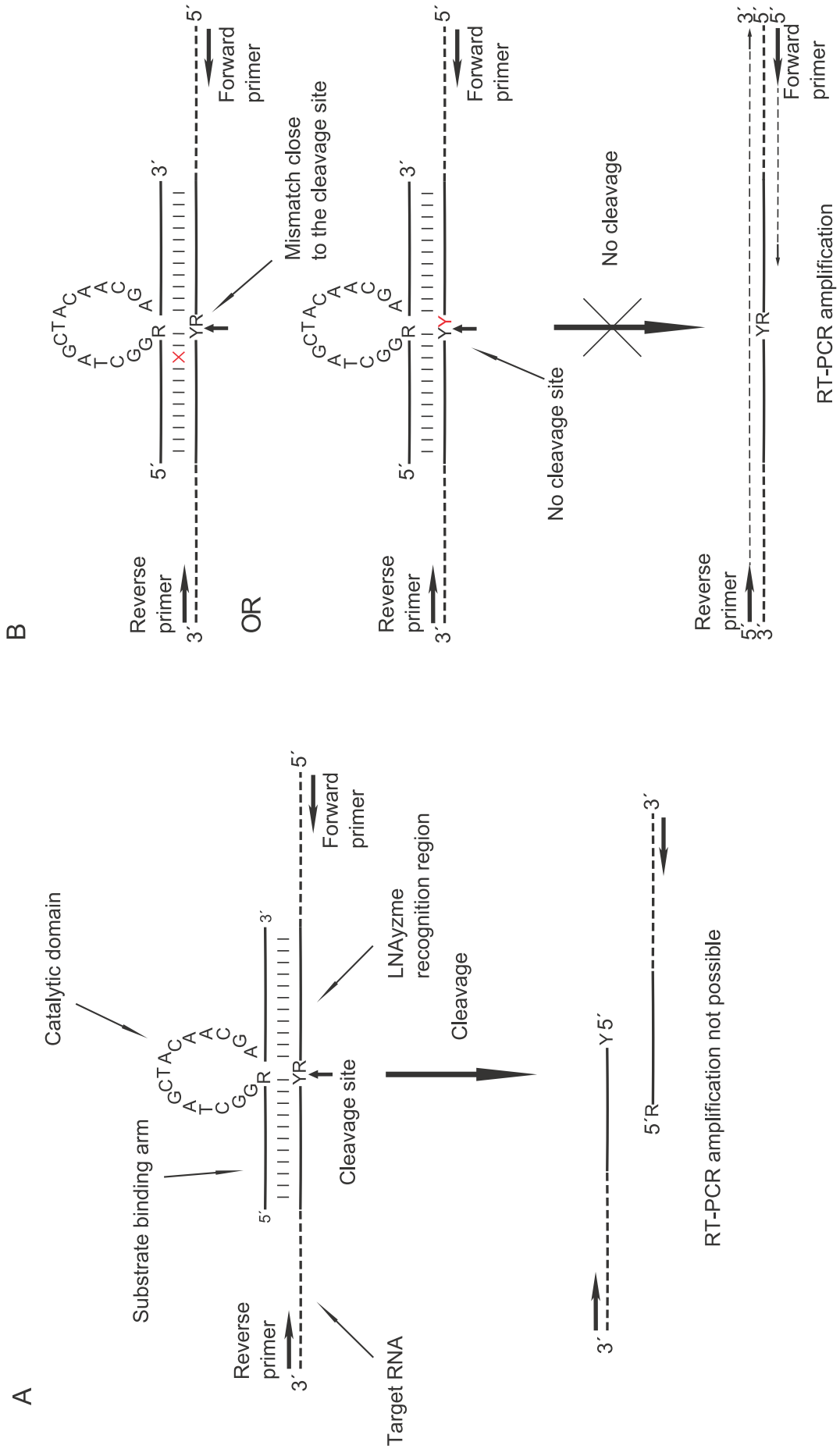
A
Catalytic domain
Substrate binding arm
Reverse primer
Target RNA
Cleavage site
LNAyzme recognition region
Cleavage
Forward primer
RT-PCR amplification not possible
B
Reverse primer
Mismatch close to the cleavage site
OR
No cleavage site
No cleavage
Forward primer
RT-PCR amplification

Fig. S2. Illustration of the specific, LNAzyme-facilitated depletion of predominant RNA templates. (A) LNAzymes bind specifically to their RNA targets by hybridization of the substrate-binding arms to the regions adjacent to the cleavage site. Cleavage of the target results in a failure of RT-PCR amplification. (B) Base mismatches (red) between a non-target RNA and an LNAzyme prevent cleavage, even if hybridization occurs. Non-target templates, which do not contain an RY cleavage site, are not cleaved either (red). Intact non-target templates can be amplified by RT-PCR and the amplicons be used for downstream analyses or cloning. Figure modified from (1).

References

1. **Dolinšek J, Dorninger C, Lagkouvardos I, Wagner M, Daims H.** in press. Depletion of unwanted nucleic acid templates by selective cleavage: LNAzymes open a new window for detecting rare microbial community members. Appl. Environ. Microbiol.

T-RF 578, *Nitrosomonas,* clones P7D8 and P8H6

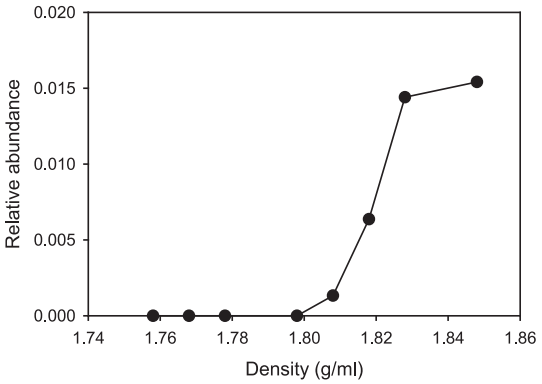

T-RF 879, *Nitrosomonas* sp. JL21 related

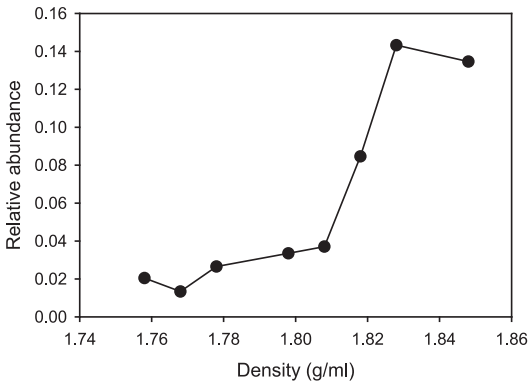

T-RF 163, *Nitrospira* sublineage I

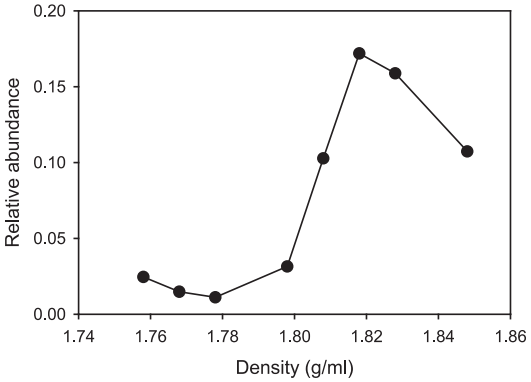

T-RF 471, *Nitrospira* sublineage II

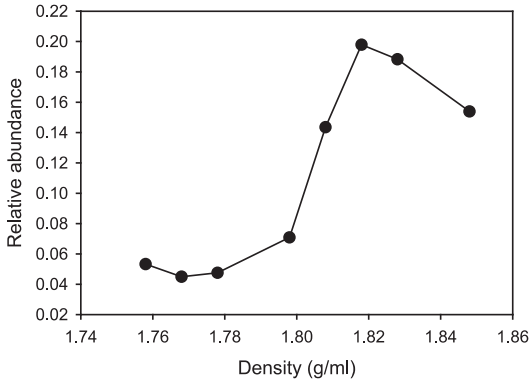

T-RF 156, *Thermomonas*-like bacterium

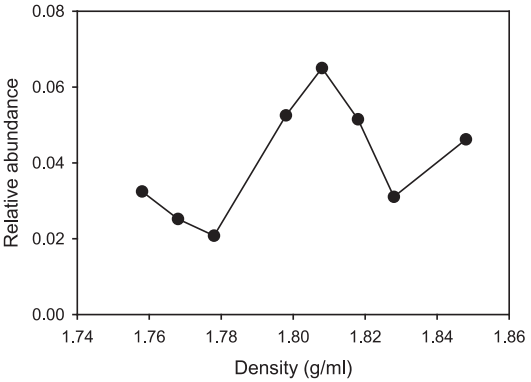

T-RF 310, *Bacteroidetes*-like bacterium

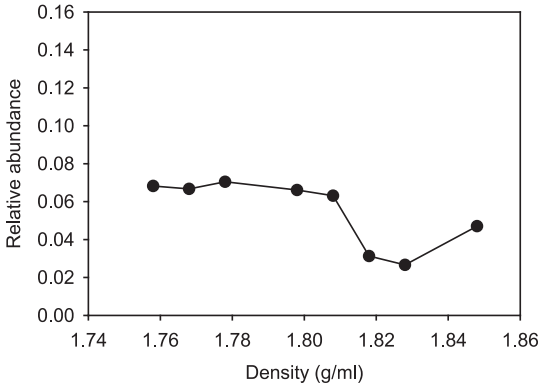

T-RF 826, *Micavibrio*-like bacterium

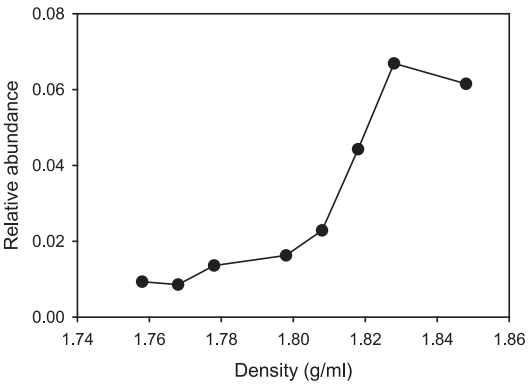

Fig. S3. Relative abundances of terminal restriction fragments (T-RFs) (after digestion with the restriction endonuclease RsaI), which represent key nitrifying and heterotrophic populations, in the light and heavy fractions of the density gradients after SIP. The analysis was conducted after the samples had been incubated with NH_4^+ and $^{13}CO_2^-$ for 21 days.

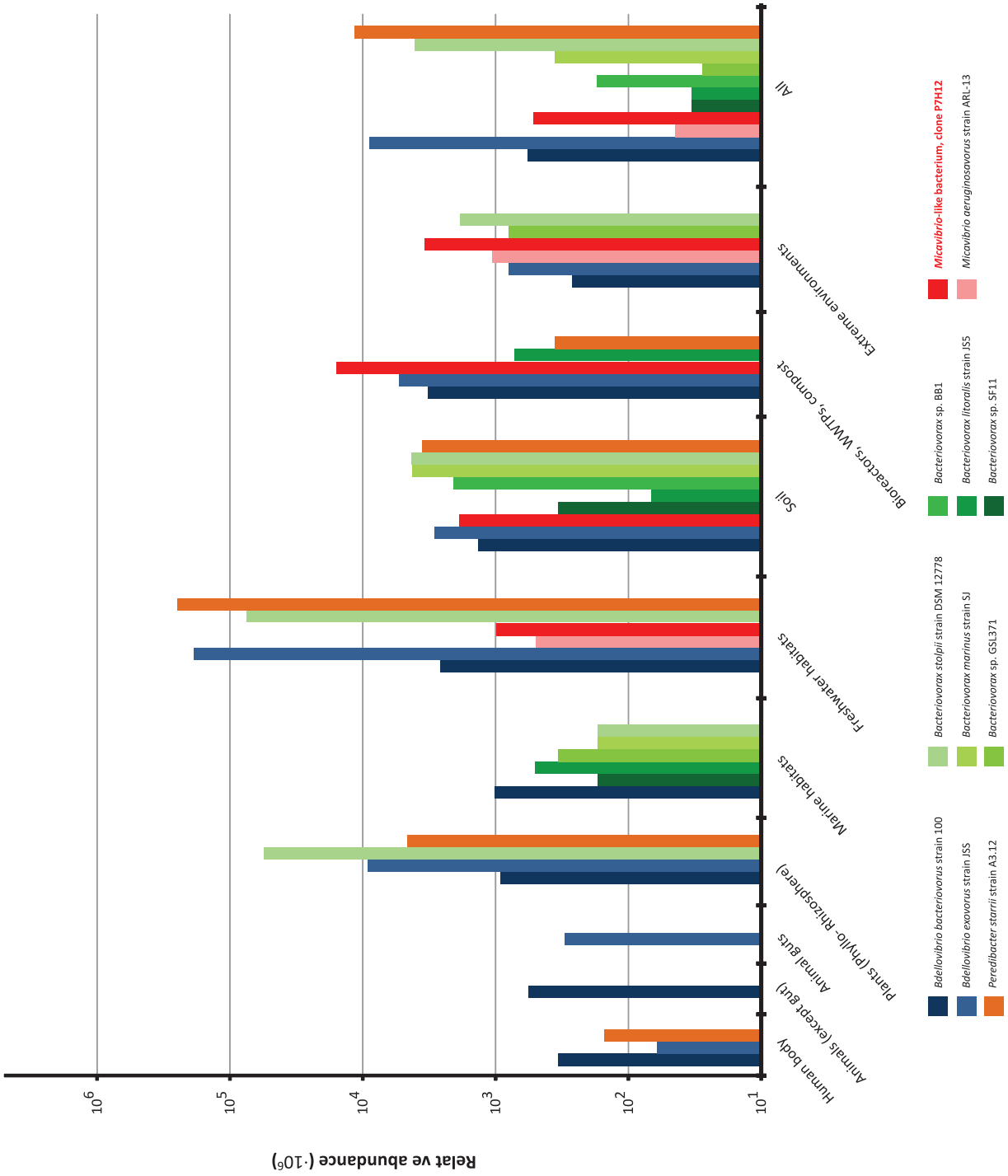
Relat ve abundance (·10⁶)
10⁶
10⁵
10⁴
10³
10²
10¹
Human body
Animals (except gut)
Animal guts
Plants (Phyllo- Rhizosphere)
Marine habitats
Freshwater habitats
Soil
Bioreactors, WWTPs, compost
Extreme environments
All
Micavibrio-like bacterium, clone P7H12
Micavibrio aeruginosavorus strain ARL-13
Bacteriovorax sp. BB1
Bacteriovorax litoralis strain JS5
Bacteriovorax sp. SF11
Bacteriovorax stolpii strain DSM 12778
Bacteriovorax marinus strain SJ
Bacteriovorax sp. GSL371
Bdellovibrio bacteriovorus strain 100
Bdellovibrio exovorus strain JSS
Peredibacter starrii strain A3.12

Fig. S4. Screening of published 16S rRNA amplicon NGS datasets for close relatives of known bacterial predators and of the *Micavibrio*-like organism analyzed in this study (marked in red). Each habitat type represents a collection of different NGS datasets from similar environmental or medical samples. Relative abundances of predators are shown as per cent, based on the total number of sequence reads in all NGS datasets for the respective habitat type. The values were multiplied by 10^6 to avoid negative values on the logarithmic y-axis for fractions below 1%. "All" shows the relative abundances of predators in all habitat types, based on the total number of sequence reads in all screened NGS datasets. Habitat types, where no relatives of the shown predators were detected in any NGS dataset, were excluded.

Table S1. Primers, oligonucleotide probes, and LNAzymes used in this study. FA=Formamide in the hybridization buffer (FISH probes only).

Oligonucleotide	Sequence (5´- 3´)	Target group	FA (%)	Reference
Probes used for FISH				
EUB338	GCT GCC TCC CGT AGG AGT	most *Bacteria*	0-50	(1)
EUB338-II	GCA GCC ACC CGT AGG TGT	*Planctomycetales*	0-50	(2)
EUB338-III	GCT GCC ACC CGT AGG TGT	*Verrucomicrobiales*	0-50	(2)
Ntspa662	GGA ATT CCG CGC TCC TCT	genus *Nitrospira*	35	(3)
Competitor for Ntspa662	GGA ATT CCG CTC TCC TCT		35	(3)
Ntspa1151	TTC TCC TGG GCA GTC TCT CC	Sublineage II of the genus *Nitrospira*	35-40	(4)
Ntspa1431	TTG GCT TGG GCG ACT TC	Sublineage I of the genus *Nitrospira*	35	(4)
NEU	CCC CTC TGC TGC ACT CTA	Most halophilic and halotolerant *Nitrosomonas* spp.	35-40	(5)
Competitor for NEU	TTC CAT CCC CCT CTG CCG		35-40	(5)
Cluster6a192	GCA TAA GGT CTT TCG AT	*Nitrosomonas oligotropha* lineage (Cluster 6a)	35	(6)
Nso1225	CGC CAT TGT ATT ACG TGT GA	Betaproteobacterial ammonia-oxidizing bacteria	35	(7)
HSAL723	GCC CAG TTA GCT GCC TAC GCC	*Micavibrio*-like alphaproteobacterium	35	this study
HSAL866	CCC AGG CGG TGT GCT AAT CAC T	*Micavibrio*-like alphaproteobacterium	35	this study
Thmm115	GGC AGA TTC CCA TGT ATT CCT C	some *Xanthomonadaceae* and most *Thermomonas*	35	this study

PCR Primers			
1492R	GAC GGG CGG TGT GTA CAA	most *Bacteria*	(8)
8F	AGA GTT TGA TYM TGG CTC	most *Bacteria*	(9, 10)
907R	CCG TCA ATT CMT TTG AGT TT	most *Bacteria*	(8)
LNAzymes			
LNAzyme Ntspa665	C<u>C</u>G CTA CAC <u>C</u>GG GAA GGC TAG CTA CAA CGA TCC G<u>C</u>G CTC CTC T<u>C</u>C[1]	genus *Nitrospira*	(11)
LNAzyme Nso215	AAC TA<u>G</u> CTA AT<u>C</u> AGA GGC TAG CTA CAA CGA ATC GG<u>C</u> CR<u>C</u> TCC[1]	most *Nitrosomonadales*, most *Cupravidus* and *Ralstonia*, some *Massillia* (all *Burkholderiales*)	(11)
Helper probes for LNAzymes			
Ntspa630help	CCT CTA GCC KRG CAG TMC CCT CYG CRC TTT CC	genus *Nitrospira*	(11)
Ntspa700help	GCC ACC GGC CTT CCT CCC GAT CTC TAC GC	genus *Nitrospira*	(11)

[1] LNA nucleotides are underlined.

References

1. **Amann RI, Binder BJ, Olson RJ, Chisholm SW, Devereux R, Stahl DA.** 1990. Combination of 16S rRNA-targeted oligonucleotide probes with flow cytometry for analyzing mixed microbial populations. Appl. Environ. Microbiol. **56:**1919-1925.
2. **Daims H, Brühl A, Amann R, Schleifer K-H, Wagner M.** 1999. The domain-specific probe EUB338 is insufficient for the detection of all *Bacteria*: Development and evaluation of a more comprehensive probe set. System. Appl. Microbiol. **22:**434-444.
3. **Daims H, Nielsen JL, Nielsen PH, Schleifer KH, Wagner M.** 2001. In situ characterization of *Nitrospira*-like nitrite-oxidizing bacteria active in wastewater treatment plants. Appl. Environ. Microbiol. **67:**5273-5284.
4. **Maixner F, Noguera DR, Anneser B, Stoecker K, Wegl G, Wagner M, Daims H.** 2006. Nitrite concentration influences the population structure of *Nitrospira*-like bacteria. Environ. Microbiol. **8:**1487-1495.
5. **Wagner M, Rath G, Amann R, Koops H-P, Schleifer K-H.** 1995. In situ identification of ammonia-oxidizing bacteria. System. Appl. Microbiol. **18:**251-264.
6. **Adamczyk J, Hesselsoe M, Iversen N, Horn M, Lehner A, Nielsen PH, Schloter M, Roslev P, Wagner M.** 2003. The isotope array, a new tool that employs substrate-mediated labeling of rRNA for determination of microbial community structure and function. Appl. Environ. Microbiol. **69:**6875-6887.
7. **Mobarry BK, Wagner M, Urbain V, Rittmann BE, Stahl DA.** 1996. Phylogenetic probes for analyzing abundance and spatial organization of nitrifying bacteria. Appl. Environ. Microbiol. **62:**2156-2162.
8. **Lane DJ.** 1991. 16S/23S rRNA sequencing, p. 115-175. *In* Stackebrandt E, Goodfellow M (ed.), Nucleic acid techniques in bacterial systematics. John Wiley & Sons, Inc., New York.
9. **Hicks RE, Amann RI, Stahl DA.** 1992. Dual staining of natural bacterioplankton with 4',6-diamidino-2-phenylindole and fluorescent oligonucleotide probes targeting kingdom-level 16S rRNA sequences. Appl. Environ. Microbiol. **58:**2158-2163.
10. **Juretschko S, Timmermann G, Schmid M, Schleifer K-H, Pommerening-Röser A, Koops H-P, Wagner M.** 1998. Combined molecular and conventional analyses of nitrifying bacterium diversity in activated sludge: *Nitrosococcus mobilis* and *Nitrospira*-like bacteria as dominant populations. Appl. Environ. Microbiol. **64:**3042-3051.
11. **Dolinšek J, Dorninger C, Lagkouvardos I, Wagner M, Daims H.** in press. Depletion of unwanted nucleic acid templates by selective cleavage: LNAzymes open a new window for detecting rare microbial community members. Appl. Environ. Microbiol.

Table S2. Cloned partial 16S rRNA genes retrieved, after RNA-SIP, from the heavy fraction of the LNAzyme-treated RNA sample (incubation of activated sludge with ammonia). See main text for details.

Clone no.	Clone ID	Phylum or class	Similarity to closest cultured relative (%)	Closest cultured relative (according to parsimony analysis)	Similarity to closest uncultured relative (%)	Closest uncultured relative (according to parsimony analysis)	Similarity to closest relative (according to BLAST search) (%)	Closest relative (according to BLAST search), GenBank accession number	Same closest relatives found by BLAST and parsimony analyses	OTU (>=97%) number
1	P8C2	*Betaproteobacteria*	89.4	*Nitrosospira multiformis* ATCC 25196	99.3	Unc00gte EBPR sludge DQ413076				1
2	P8A6	*Betaproteobacteria*	96.9	*Nitrosomonas* sp. JL21			97	AB000700	*	2
3	P8H7	*Betaproteobacteria*	96.8	*Nitrosomonas* sp. JL21			97	AB000700	*	2
4	P7C11	*Betaproteobacteria*	96.8	*Nitrosomonas* sp. JL21			97	AB000700	*	2
5	P8E2	*Betaproteobacteria*	96.9	*Nitrosomonas* sp. JL21			97	AB000700	*	2
6	P7E11	*Betaproteobacteria*	96.8	*Nitrosomonas* sp. JL21			97	AB000700	*	2
7	P7H7	*Betaproteobacteria*	96.7	*Nitrosomonas* sp. JL21			97	AB000700	*	2
8	P7H8	*Betaproteobacteria*	96.9	*Nitrosomonas* sp. JL21			97	AB000700	*	2
9	P8A7	*Betaproteobacteria*	96.6	*Nitrosomonas* sp. JL21			96	AB000700	*	2
10	P7A12	*Betaproteobacteria*	96.8	*Nitrosomonas* sp. JL21			97	AB000700	*	2
11	P8A11	*Betaproteobacteria*	96.7	*Nitrosomonas* sp. JL21			97	AB000700	*	2
12	P7D8	*Betaproteobacteria*	94.4	*Nitrosomonas* sp. JL21			99	FJ933399		3
13	P8H6	*Betaproteobacteria*	94.6	*Nitrosomonas* sp. JL21			99	FJ933399		3
14	P7E12	*Betaproteobacteria*	98.5	*Nitrosomonas* sp. NL7	99.6	Unc01azw batch reactor AY343318	99	HQ221930		4
15	P7E10	*Gammaproteobacteria*	96.6	*Thermomonas fusca*	99.8	*Xanthomonas* sp. R-20819	99	AJ786786	*	5
16	P7H10	*Gammaproteobacteria*	96.3	*Thermomonas fusca*	99.6	*Xanthomonas* sp. R-20819	99	AJ786786	*	5
17	P7D4	*Gammaproteobacteria*	96.7	*Thermomonas fusca*	99.9	*Xanthomonas* sp. R-20819	99	AJ786786	*	5
18	P7D2	*Gammaproteobacteria*	96.7	*Thermomonas fusca*	99.9	*Xanthomonas* sp. R-20819	99	AJ786786	*	5
19	P8C4	*Gammaproteobacteria*	96.7	*Thermomonas fusca*	99.9	*Xanthomonas* sp. R-20819	99	AJ786786	*	5
20	P8D1	*Gammaproteobacteria*	96.8	*Thermomonas fusca*	100	*Xanthomonas* sp. R-20819	99	AJ786786	*	5
21	P8D7	*Gammaproteobacteria*	88.5	*Cycloclasticus pugetii*	96.7	Unc0391c Sludge taken from N2O oxidation system AB619696	99	AM910088		6
22	P8D5	*Alphaproteobacteria*	85.1	*Henriciella marina*	99.1	Unc00igx aerobic sequencing batch reactor (SBR)	99	DQ376579	*	7
23	P8E10	*Alphaproteobacteria*	99.1	*Bradyrhizobium japonicum*	99.1	Unc03no9 boiling pool (86 C) sediment uncultured bacterium GU437259	99	HQ385597		8
24	P7H12	*Alphaproteobacteria*	86.6	*Micavibrio* sp. EPC2			99	FM200963		9
25	P8A5	*Alphaproteobacteria*	86.7	*Micavibrio* sp. EPC2			95	FM200963		9
26	P8G9	*Alphaproteobacteria*	86.6	*Micavibrio* sp. EPC2			99	FM200963		9
27	P7C8	*Alphaproteobacteria*	86.8	*Micavibrio* sp. EPC2			99	FM200963		9
28	P8B12	*Alphaproteobacteria*	86.8	*Micavibrio* sp. EPC2			99	FM200963		9
29	P7E5	*Alphaproteobacteria*	86.8	*Micavibrio* sp. EPC2			99	FM200963		9
30	P8G12	*Alphaproteobacteria*	96.1	*Rhodovastum atsumiense*			98	FQ658941		10
31	P7D6	*Alphaproteobacteria*	84.3	*Candidatus* Midichloria sp. Ixholo1	94.9	Unc039io aquatic moss pillars	95	AB630443	*	11
32	P8F12	*Alphaproteobacteria*	83.7	*Candidatus* Midichloria sp. Ixholo1	94.3	Unc039io aquatic moss pillars	95	AB630443	*	11
33	P7D3	*Alphaproteobacteria*	79.1	*Candidatus* Hepatinicola porcellionum	91.3	Unc04017 hydrocarbon contaminated saline-alkali soil HQ697715	91	HQ218452		12
34	P7H3	*Alphaproteobacteria*	97.6	*Stella vacuolata*	99.3	Unc01g4c mesophilic anaerobic digester which treats municipal wastewater sludge	99	CU921148	*	13
35	P8C12	*Alphaproteobacteria*	88.1	*Defluviicoccus vanus*	99.1	Unc01wbm pilot-scale bioremediation process of a hydrocarbon-contaminated soil	99	FM209132	*	14
36	P7B5	*Deltaproteobacteria*	89.8	*Polyangium fumosum*	99.2	UncD3051 rhizosphere soil JF319212	99	JN038718		15
37	P7B9	*Deltaproteobacteria*	90.2	*Polyangium fumosum*	95	Unc22462 soil from an undisturbed mixed grass prairie preserve EU134499	95	JN408874		16
38	P7G7	*Deltaproteobacteria*	90.5	*Polyangium fumosum*	95	Unc22462 soil from an undisturbed mixed grass prairie preserve EU134499	95	JN408874		16
39	P8D10	*Bacteroidetes*	81.5	*Olivibacter soli*	99.1	UniBa173 activated sludge	99	JF503089		17
40	P8E8	*Bacteroidetes*	81.5	*Olivibacter soli*	99.1	UniBa173 activated sludge	99	JF503089		17
41	P7G3	*Bacteroidetes*	81.5	*Olivibacter soli*	99.1	UniBa173 activated sludge	99	JF503089		17
42	P8H3	*Bacteroidetes*	81.6	*Olivibacter soli*	99.2	UniBa173 activated sludge	99	JF503089		17
43	P7H2	*Bacteroidetes*	81.6	*Olivibacter soli*	99.1	UniBa173 activated sludge	99	JF503063		17
44	P7G1	*Bacteroidetes*	81.6	*Olivibacter soli*	99.1	UniBa173 activated sludge	99	JF503063		17
45	P8E9	*Bacteroidetes*	81.7	*Olivibacter soli*	99.1	UniBa173 activated sludge	99	JF503063		17
46	P8C11	*Bacteroidetes*	83.1	*Haliscomenobacter hydrossis* DSM 1100	94.5	Unc50655 AF314434	95	HQ609662		18
47	P7G12	*Bacteroidetes*	85.5	*Haliscomenobacter hydrossis* DSM 1100			99	AB567838		19
48	P7H6	*Bacteroidetes*	85.5	*Haliscomenobacter hydrossis* DSM 1100			99	AB567838		19
49	P7F6	*Bacteroidetes*	85.5	*Haliscomenobacter hydrossis* DSM 1100			99	AB567838		19
50	P8C8	*Bacteroidetes*	84	*Flexibacter flexis*	93.8	Unc51624 variably weathered outcrop HQ674889	97	EU593771		20
51	P7C3	*Chlorobi*	81.9	*Ignavibacterium album*			99	AB286378	*	21
52	P7F10	*Chlorobi*	82	*Ignavibacterium album*			99	AB286378	*	21
53	P8A12	*Verrucomicrobia*	93.8	*Opitutus terrae PB90-1*			98	FM200925		22
54	P8D8	*Planctomycetes*	83.6	*Planctomyces maris* DSM 8797	89.2	Unc01g7t mesophilic anaerobic digester which treats municip CU921652	93	EF540354		23
55	P8F9	*Planctomycetes*	89.6	*Planctomyces maris* DSM 8797			97	HQ120305		24
56	P8A3	*Planctomycetes*	87.5	*Planctomyces maris* DSM 8797			99	EU589253		25
57	P8E4	*Planctomycetes*	87.5	*Planctomyces maris* DSM 8797			99	EU589253		25
58	P8C7	*Planctomycetes*	74.8	*Phycisphaera mikrensis*	88.2	Unc011w4 supporting materials in a packed-bed reactor degra AB274517	98	FQ659770		26
59	P7B12	*Planctomycetes*	74.1	*Phycisphaera mikrensis*	92.5	Unc03yex partial nitrifying-ANAMMOX municipal wastewater re HQ640613	99	EF522843		27
60	P7B2	*Planctomycetes*	78.5	*Phycisphaera mikrensis*	87.2	UncPl109 farm soil adjacent to a silage storage bunker AY921845	91	JF922439		28
61	P8E1	*Acidobacteria*	90	*Bryobacter aggregatus*	98.8	Unc001no activated sludge from dairy wastewater treatment plant	99	DQ478938	*	29
62	P7A5	*Nitrospirae*	97.5	*Nitrospira moscoviensis*			99	FN687453		30
63	P8E6	*Nitrospirae*	97.5	*Nitrospira moscoviensis*			99	FN687453		30
64	P8G8	*Nitrospirae*	97.5	*Nitrospira moscoviensis*			99	FN687453		30
65	P7C6	*Nitrospirae*	97.5	*Nitrospira moscoviensis*			99	FN687453		30
66	P8C5	*Nitrospirae*	97.2	*Nitrospira moscoviensis*			99	FN687453		30
67	P8E12	*Nitrospirae*	97.2	*Nitrospira moscoviensis*			99	FN687453		30
68	P8G7	*Nitrospirae*	97.6	*Nitrospira moscoviensis*			99	FN687453		30
69	P7B4	*Nitrospirae*	97.4	*Nitrospira moscoviensis*			99	FN687453		30
70	P7F2	*Nitrospirae*	97.6	*Nitrospira moscoviensis*			99	FN687453		30
71	P7D11	*Nitrospirae*	97.5	*Nitrospira moscoviensis*			99	FN687453		30
72	P8F7	*Nitrospirae*	97.2	*Nitrospira moscoviensis*			99	DQ414437		30
73	P8H5	*Nitrospirae*	97.6	*Nitrospira moscoviensis*			99	DQ414437		30
74	P7E9	*Nitrospirae*	97.5	*Nitrospira moscoviensis*			99	DQ414437		30
75	P7G5	*Nitrospirae*	97.6	*Nitrospira moscoviensis*			99	FN687453		30
76	P8B3	*Nitrospirae*	97.6	*Nitrospira moscoviensis*			99	FN687453		30
77	P7C10	*Nitrospirae*	97.4	*Nitrospira moscoviensis*			99	FJ439876		30
78	P7F4	*Nitrospirae*	97.2	*Nitrospira moscoviensis*			99	FJ439876		30
79	P8C9	*Nitrospirae*	97.5	*Nitrospira moscoviensis*			99	FJ439876		30

Clone no.	Clone ID	Phylum or class	Similarity to closest cultured relative (%)	Closest cultured relative (according to parsimony analysis)	Similarity to closest uncultured relative (%)	Closest uncultured relative (according to parsimony analysis)	Similarity to closest relative (according to BLAST search) (%)	Closest relative (according to BLAST search), GenBank accession number	Same closest relatives found by BLAST and parsimony analyses	OTU (>=97%) number
80	P8B10	*Nitrospirae*	97.4	*Nitrospira moscoviensis*			99	FJ439876		30
81	P8A8	*Nitrospirae*	97.7	*Nitrospira moscoviensis*			99	FJ439876		30
82	P8E11	*Nitrospirae*	97.5	*Nitrospira moscoviensis*			99	FJ439876		30
83	P7F9	*Nitrospirae*	99	*Candidatus* Nitrospira defluvii			99	Y14639		31
84	P8G3	*Nitrospirae*	99	*Candidatus* Nitrospira defluvii			99	Y14639		31
85	P8G2	*Nitrospirae*	98.9	*Candidatus* Nitrospira defluvii			99	Y14639		31
86	P7F3	*Nitrospirae*	98.9	*Candidatus* Nitrospira defluvii			99	Y14639		31
87	P8F4	*Nitrospirae*	98.7	*Candidatus* Nitrospira defluvii			99	Y14639		31
88	P8G1	*Nitrospirae*	98.8	*Candidatus* Nitrospira defluvii			99	Y14639		31
89	P7H1	*Nitrospirae*	98.9	*Candidatus* Nitrospira defluvii			99	Y14639		31
90	P7G9	*Nitrospirae*	99	*Candidatus* Nitrospira defluvii			99	Y14639		31
91	P7H11	*Nitrospirae*	99	*Candidatus* Nitrospira defluvii			99	Y14639		31
92	P7C1	*Nitrospirae*	98.9	*Candidatus* Nitrospira defluvii			99	Y14639		31
93	P7A8	*Nitrospirae*	98.8	*Candidatus* Nitrospira defluvii			99	HQ538637		31
94	P7D7	*Nitrospirae*	99	*Candidatus* Nitrospira defluvii			99	HQ538637		31
95	P7G11	*Nitrospirae*	99.3	*Candidatus* Nitrospira defluvii			99	HQ538637		31
96	P8A10	*Nitrospirae*	99.2	*Candidatus* Nitrospira defluvii			99	JN217071		31
97	P7G2	*Nitrospirae*	99.3	*Candidatus* Nitrospira defluvii			99	JN217071		31
98	P7D9	*Nitrospirae*	99.3	*Candidatus* Nitrospira defluvii			99	JN217071		31
99	P8D9	*Nitrospirae*	99.1	*Candidatus* Nitrospira defluvii			99	JN217071		31
100	P8A9	*Nitrospirae*	99	*Candidatus* Nitrospira defluvii			99	JN217071		31
101	P8B7	*Nitrospirae*	98.9	*Candidatus* Nitrospira defluvii			99	JN217071		31
102	P8H2	*Nitrospirae*	99.1	*Candidatus* Nitrospira defluvii			99	JN217071		31
103	P7G4	*Nitrospirae*	99.2	*Candidatus* Nitrospira defluvii			99	JN217071		31
104	P7A6	*Nitrospirae*	99.3	*Candidatus* Nitrospira defluvii			99	JN217071		31
105	P8B1	*Nitrospirae*	99.4	*Candidatus* Nitrospira defluvii			99	JN217071		31
106	P8C10	*Nitrospirae*	99.4	*Candidatus* Nitrospira defluvii			99	FJ660512		31
107	P8B9	*Nitrospirae*	99.2	*Candidatus* Nitrospira defluvii			99	FJ660512		31
108	P8F1	*Nitrospirae*	96.8	*Candidatus* Nitrospira defluvii	99.7	MixGranu mixed granule from anammox reactor	99	EF594048	*	32
109	P8H11	*Nitrospirae*	96.8	*Candidatus* Nitrospira defluvii	99.7	MixGranu mixed granule from anammox reactor	99	JQ003189		32
110	P8A4	*Nitrospirae*	96.8	*Candidatus* Nitrospira defluvii	99.7	MixGranu mixed granule from anammox reactor	99	EF594048	*	32
111	P8H10	*Nitrospirae*	96.8	*Candidatus* Nitrospira defluvii	99.7	MixGranu mixed granule from anammox reactor	100	JQ003189		32
112	P7E3	*Nitrospirae*	96.9	*Candidatus* Nitrospira defluvii	99.8	MixGranu mixed granule from anammox reactor	100	JQ003189		32
113	P7E2	*Nitrospirae*	96.3	*Candidatus* Nitrospira defluvii	99.7	MixGranu mixed granule from anammox reactor	100	JQ003189		32
114	P7E21	*Nitrospirae*	96.2	*Candidatus* Nitrospira defluvii	99.7	MixGranu mixed granule from anammox reactor	100	JQ003189		32
115	P7G6	*Nitrospirae*	97	*Candidatus* Nitrospira defluvii	99.9	MixGranu mixed granule from anammox reactor	100	EF594048	*	32
116	P7C12	*TM6*			90.3	Unc01pzj Green Lake surface sediments at 16.5 m water depth FJ437950	91	FJ437950		33
117	P8E7	*Actinobacteria*	91	*Fodinicola feengrottensis*	97.8	**(* cultured isolate)** BctrmRJ7 bacterium rJ7 phenol-degrading activated sludge AB021325	98	AB355058		34
118	P8C6	*Actinobacteria*	97.8	*Nocardioides ganghwensis*	99.8	Unc02wxz floor dust FM873011	99	HM005239		35
119	P7B10	*Chloroflexi*	87.7	*Longilinea arvoryzae*	98.5	Unc01glt mesophilic anaerobic digester which treats municipal wastewater sludge CU923588	99	CU923478		36
120	P8F2	*Elusimicrobia*	76.2	*Elusimicrobium minutum*			95	HQ684547		37

Table S3. 16S rRNA genes used as queries for screening NGS datasets.

Organism	GenBank accession number
Obligate predatory bacteria	
Bdellovibrio bacteriovorus strain 100	AF084850
Bdellovibrio exovorus strain JSS	EF687743
Micavibrio aeruginosavorus strain ARL-13	DQ186612
Micavibrio-like bacterium, clone P7H12	JQ815012
Bacteriovorax sp. SF11	DQ631733
Bacteriovorax litoralis strain JS5	NR_028724
Bacteriovorax sp. BB1	DQ631713
Bacteriovorax sp. GSL371	DQ631765
Bacteriovorax marinus strain SJ	NR_028723
Bacteriovorax stolpii strain DSM 12778	NR_042023
Peredibacter starrii strain A3.12	NR_024943
Nitrite-oxidizing bacteria (*Nitrospira*)	
Candidatus Nitrospira defluvii (*Nitrospira* sublineage I)	NC_014355
Nitrospira moscoviensis (*Nitrospira* sublineage II)	X82558
Nullarbor caves clone wb1_C17 (*Nitrospira* sublineage III)	AF317762
Nitrospira marina Nb-295 (*Nitrospira* sublineage IV)	X82559
Candidatus Nitrospira bockiana (*Nitrospira* sublineage V)	EU084879
Nitrospira calida (*Nitrospira* sublineage VI)	HM485589

Chapter III

Depletion of Unwanted Nucleic Acid Templates by Selective Cleavage: LNAzymes, Catalytically Active Oligonucleotides Containing Locked Nucleic Acids, Open a New Window for Detecting Rare Microbial Community Members

AEM
Journals.ASM.org

Depletion of Unwanted Nucleic Acid Templates by Selective Cleavage: LNAzymes, Catalytically Active Oligonucleotides Containing Locked Nucleic Acids, Open a New Window for Detecting Rare Microbial Community Members

Jan Dolinšek, Christiane Dorninger, Ilias Lagkouvardos, Michael Wagner, Holger Daims

Department of Microbial Ecology, Vienna Ecology Centre, University of Vienna, Vienna, Austria

Many studies of molecular microbial ecology rely on the characterization of microbial communities by PCR amplification, cloning, sequencing, and phylogenetic analysis of genes encoding rRNAs or functional marker enzymes. However, if the established clone libraries are dominated by one or a few sequence types, the cloned diversity is difficult to analyze by random clone sequencing. Here we present a novel approach to deplete unwanted sequence types from complex nucleic acid mixtures prior to cloning and downstream analyses. It employs catalytically active oligonucleotides containing locked nucleic acids (LNAzymes) for the specific cleavage of selected RNA targets. When combined with *in vitro* transcription and reverse transcriptase PCR, this LNAzyme-based technique can be used with DNA or RNA extracts from microbial communities. The simultaneous application of more than one specific LNAzyme allows the concurrent depletion of different sequence types from the same nucleic acid preparation. This new method was evaluated with defined mixtures of cloned 16S rRNA genes and then used to identify accompanying bacteria in an enrichment culture dominated by the nitrite oxidizer "*Candidatus* Nitrospira defluvii." *In silico* analysis revealed that the majority of publicly deposited rRNA-targeted oligonucleotide probes may be used as specific LNAzymes with no or only minor sequence modifications. This efficient and cost-effective approach will greatly facilitate tasks such as the identification of microbial symbionts in nucleic acid preparations dominated by plastid or mitochondrial rRNA genes from eukaryotic hosts, the detection of contaminants in microbial cultures, and the analysis of rare organisms in microbial communities of highly uneven composition.

The "rRNA approach" (1–5), i.e., the PCR amplification, cloning, sequencing, and phylogenetic analysis of rRNA genes, has been fundamental for our current understanding of natural microbial diversity. By revealing a huge number of as-yet-uncultured microbes and novel phylogenetic lineages that have been overlooked by traditional cultivation-based methods of microbiology (reviewed in references 6, 7, 8, and 9), this approach has substantially influenced our perception of microbial communities in the environment. Moreover, variations of the same principle using suitable functional marker genes have become the gold standard for diversity analyses of selected microbial guilds (e.g., see references 10, 11, 12, 13, and 14).

In all of these approaches, a highly uneven abundance of the target organisms in the sample, different target gene copy numbers per genome (15), mismatches between primers and some templates, and other PCR biases can lead to the dominance of a few sequence types in the resulting clone libraries. In such cases, an encompassing diversity census of the microbial consortium to be analyzed would require extensive redundant DNA sequencing to retrieve sequences that occur less frequently in the clone library. Rare sequences in a library can be more easily retrieved by the separation of PCR amplicons using denaturing gradient gel electrophoresis (DGGE) prior to cloning and sequencing or by the prescreening of clone libraries by restriction fragment length polymorphism (RFLP) or other fingerprinting methods (16, 17). However, these and related methods can be time-consuming and have their own limitations, such as problems in distinguishing organisms that are represented by highly similar or identical RFLP patterns or by comigrating bands in DGGE gels.

Other approaches to reduce the workload for microbial community analyses prevent the PCR amplification of selected (usually dominant) templates in DNA extracts made from environmental samples (18, 19). Here we present a novel method to specifically remove such unwanted targets that can be applied to either RNA or DNA extracts. It employs catalytically active, locked nucleic acid (LNA)-containing oligonucleotides ("LNAzymes") that hybridize to their target RNA and cleave it at a specific site. This approach is based on the discovery of Breaker and Joyce (20), who used *in vitro* selection to isolate the first catalytically active molecule that was completely composed of deoxyribonucleotides (a "DNAzyme") and that was able to cleave RNA in the presence of Pb^{2+} ions. In 1997, Santoro and Joyce (21) isolated two DNAzymes capable of cleaving RNA at specific sites under simulated *in vivo* conditions. Since then, two DNAzyme sequence motifs, referred to as "8-17" and "10-23," have been used in many applications in molecular biology (22, 23). DNAzymes with the motif 10-23, named after the 23rd clone of the 10th round of *in vitro* selection (21), consist of a 15-nucleotide catalytic domain

Received 5 November 2012 **Accepted** 17 December 2012
Published ahead of print 21 December 2012
Address correspondence to Holger Daims, daims@microbial-ecology.net.
Supplemental material for this article may be found at http://dx.doi.org/10.1128/AEM.03392-12.
Copyright © 2013, American Society for Microbiology. All Rights Reserved.
doi:10.1128/AEM.03392-12

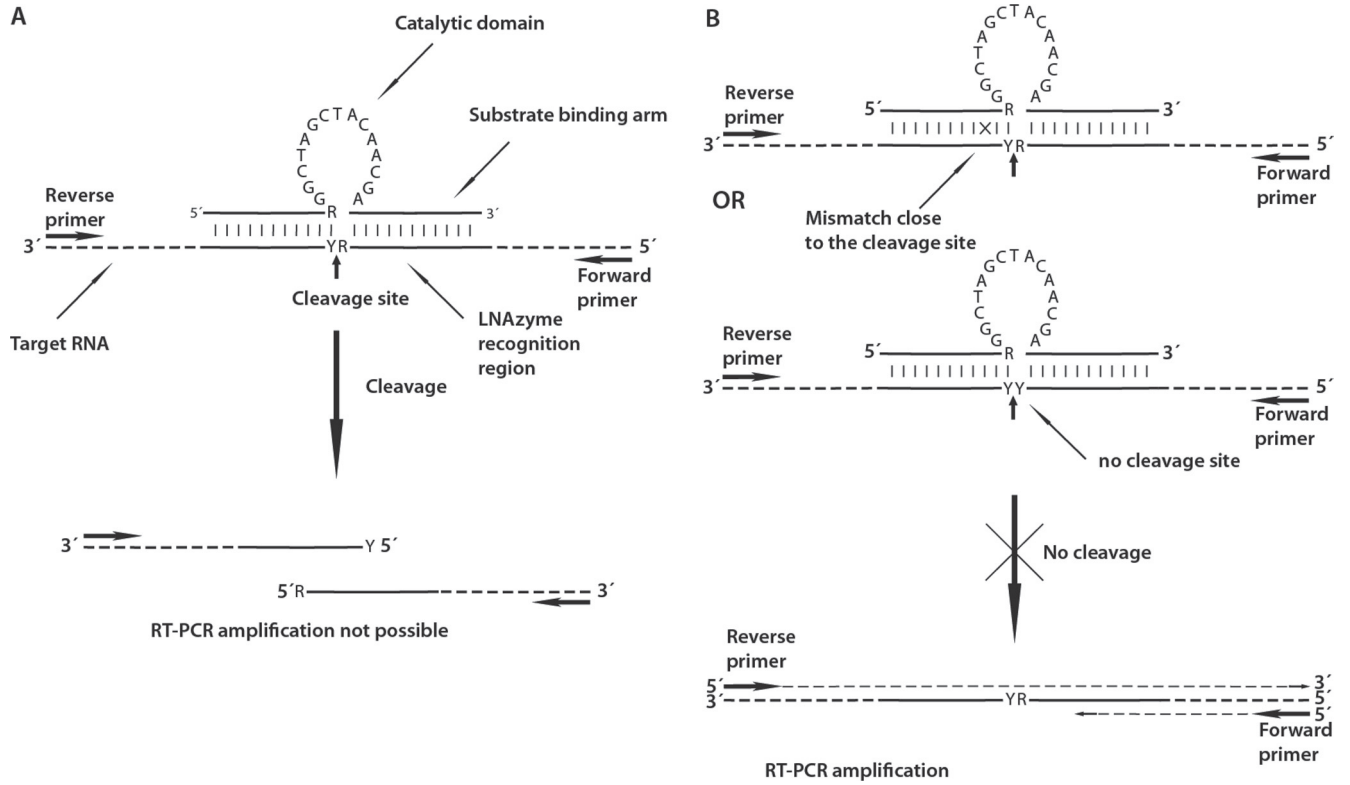

FIG 1 Mechanism of LNAzyme-mediated depletion of specific RNA templates. (A) Binding of the LNAzyme to its target due to hybridization of the substrate-binding arms up- and downstream of the cleavage site, followed by specific cleavage of the target and the resulting failure of RT-PCR amplification. (B) Base mismatches between the substrate-binding arms of the LNAzyme and a nontarget RNA template prevent the cleavage even if hybridization occurs. Nontarget templates, which are identical in sequence to the substrate-binding arms but do not contain any RY (purine-pyrimidine) cleavage site in the binding region of the LNAzyme, are also not cleaved. In either case, the nontarget template remains intact for subsequent RT-PCR amplification and downstream analyses or cloning. This figure is partly based on illustrations of DNAzymes by Santoro and Joyce (29), Cairns et al. (24), and Suenaga et al. (30).

that is flanked by two substrate-binding arms (Fig. 1). The catalytic domain usually is not amenable to any sequence changes without losing its activity. However, the sequences of the substrate-binding arms, which usually consist of 7 to 11 nucleotides, can be freely modified. DNAzymes of type 10-23 cut the phosphodiester bond in RNA at a purine-pyrimidine (R-Y) junction (Fig. 1A), with the efficiency of cleavage following the scheme AU ≈ GU > GC ≫ AC (24). If the substrate-binding arms contain LNA or 2-*O*-methyl RNA nucleotides, the efficiency is significantly improved, especially for cutting RNA molecules that form secondary structures. Locked nucleic acids contain at least one nucleotide whose sugar moiety is modified and has a bicyclic structure, which "locks" the conformation of the sugar (25). Due to the higher binding affinity of LNA nucleotides, LNAzymes can better resolve and hybridize to complex RNA structures. This leads to an improved efficiency of cleavage without compromising the specificity for a particular target (26–28). Interestingly, DNAzymes and LNAzymes are highly sensitive to base mismatches to the substrate RNA in one of the substrate-binding arms. Just one strong mismatch close to the cleavage site is sufficient to dramatically reduce the cleavage efficiency (29, 30) (Fig. 1B).

To date, DNAzymes and LNAzymes have seldom been used in molecular microbial ecology (30). Our approach to deplete unwanted sequence types relies on LNAzymes whose substrate-binding arms are sequence complementary to specific target sites on the RNA molecules to be cleaved. We evaluated the specificity and performance of this method by using defined mixtures of 16S rRNA genes, and subsequently, we demonstrated its usefulness for identifying rare members of a microbial community that is dominated by one organism.

MATERIALS AND METHODS

Outline of the protocol for selective template removal. As LNAzymes cleave RNA exclusively, they can be applied directly to RNA preparations from environmental samples for the specific removal of unwanted RNA molecules (Fig. 2). However, by implementing additional steps in the workflow, LNAzymes can also be used with DNA preparations, which more commonly serve as templates for the PCR amplification of rRNA genes in the "rRNA approach." In this case, the forward (sense) PCR primer must contain a T3 or T7 RNA polymerase promoter at its 5′ end. The obtained PCR amplicons subsequently serve as templates for *in vitro* transcription (IVT) to RNA. The resulting mixture of RNA molecules is then subjected to the specific cleavage of unwanted targets by LNAzymes. The remaining intact RNAs are converted back to DNA by reverse transcriptase PCR (RT-PCR), whereas the cleaved RNAs do not serve as templates for RT-PCR (Fig. 1 and 2). Thus, the obtained DNA is depleted in those targets that were cleaved by the LNAzymes. If a forward primer with a T3 or T7 RNA polymerase promoter is also used in the RT-PCR step, the procedure can be repeated for further depletion of the unwanted targets (Fig. 2).

Nucleic acid extraction. The nitrite-oxidizing enrichment culture of "*Candidatus* Nitrospira defluvii" was maintained as described previously (31). An aliquot of 50 ml of the culture was centrifuged at 6,000 × *g* at

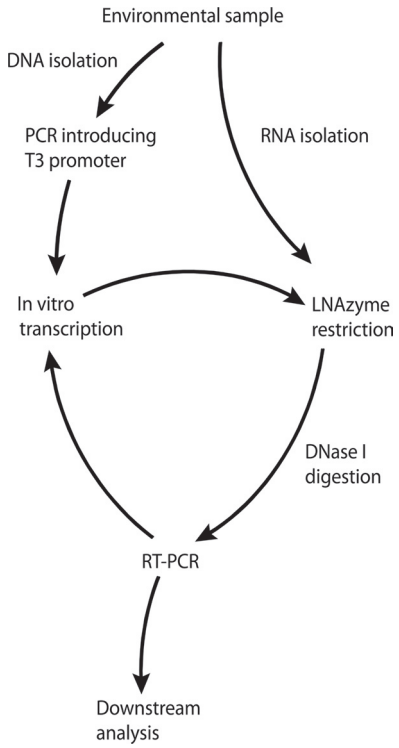

FIG 2 Schematic illustration of the workflow for the specific depletion of unwanted templates using LNAzymes. The procedure starts with the extraction of DNA or RNA from an environmental sample and results in a final PCR product, which is suitable for cloning or analyses by fingerprinting techniques such as T-RFLP.

room temperature for 4 min, and the pellet was resuspended in 1 ml of TRIzol (Invitrogen, Carlsbad, CA). Activated sludge samples were collected from a nitrifying sequencing batch reactor at the municipal wastewater treatment plant of Ingolstadt, Germany. Sludge flocs were allowed to settle, liquid supernatant was removed, and the concentrated sludge was frozen in liquid N_2. Aliquots were stored at −80°C and, before use, were resuspended in 1 ml of TRIzol. The suspensions ("*Ca.* Nitrospira defluvii" enrichment culture or activated sludge) were then transferred into Lysing Matrix A tubes (MP Biomedicals, Solon, OH), and cells were disrupted in a bead beater (Bio 101, Vista, CA) set at 6.5 m s^{-1} for 45 s. RNA and DNA were extracted according to recommendations provided with TRIzol. As a gelatinous matrix was coextracted with the RNA, 0.25 ml of a salt solution (2 M NaCl, 0.2 M LiCl) per ml of TRIzol was added to the aqueous phase prior to precipitation with 2-propanol to obtain pure RNA. Any DNA present in the RNA preparation was removed by DNase I (Sigma-Aldrich, St. Louis, MO) digestion in a modified DNase I buffer (20 mM Tris-HCl [pH 8.0], 2 mM $MgCl_2$, 0.2 mM $CaCl_2$) for 45 min at 37°C. Following digestion, the RNA was extracted again with TRIzol. DNA extracted with TRIzol was further purified by using the AllPrep DNA/RNA minikit (Qiagen, Hilden, Germany).

PCR and RT-PCR. All PCRs were performed according to the following scheme: DNA was denatured at 94°C for 2 min, followed by 25 cycles of denaturation at 94°C for 30 s, primer annealing at 54°C for 45 s, and elongation at 72°C for 90 s. Cycling was completed with a final elongation step at 72°C for 10 min. The reaction mixtures contained 1× enzyme buffer, 2 mM $MgCl_2$, 0.2 mM deoxynucleoside triphosphates (dNTPs), 0.5 μM each primer, 0.75 U of *Taq* polymerase, 0.05 mg ml^{-1} bovine serum albumin (all from Fermentas, St. Leon-Rot, Germany), and 2 μl of template DNA in a final volume of 25 μl. For RT-PCR, the Access One Step RT-PCR kit (Promega, Madison, WI) was used. Briefly, cDNA was synthesized at 45°C for 45 min, followed by denaturation at 94°C for 2 min and by 25 cycles of denaturation at 94°C for 30 s, primer annealing at 54°C for 45 s, and elongation at 68°C for 2 min. Cycling was finished with a final elongation step at 68°C for 7 min. The absence of DNA in all RNA templates was confirmed by PCR without reverse transcription. All primers used in this study for PCR and RT-PCR are listed in Table S1 in the supplemental material. Primers were obtained from Thermo Fisher (Thermo Fisher Scientific, Ulm, Germany). For PCRs and for RT-PCR, the nucleic acid templates were diluted 1:50 in ultrapure water in order to avoid PCR inhibition by highly concentrated template or inhibitory compounds.

***In vitro* transcription.** PCR-amplified 16S rRNA genes containing a 5′ T3 promoter, for *in vitro* transcription by T3 RNA polymerase, were obtained by PCR with primers T3-8F and 907R. These amplicons were analyzed by agarose gel electrophoresis, and bands of the correct size were excised from the gels and purified with the QiaQuick gel extraction kit (Qiagen). The reaction mixture for *in vitro* transcription contained 1× T3 polymerase transcription buffer (Fermentas), 10 mM dithiothreitol (DTT) (Carl Roth, Karlsruhe, Germany), 1 U of T3 polymerase (Fermentas), 0.5 mM nucleoside triphosphates (NTPs) (Hoffmann-La Roche, Basel, Switzerland), and 100 to 200 ng of purified PCR product. The final volume was 20 μl. The mixture was incubated at 37°C for 4 h.

LNAzyme design and digestion of target rRNAs. Already existing 16S rRNA-targeted probes for fluorescence *in situ* hybridization (FISH) were used as a starting point for the design of specific LNAzymes, which was accomplished by using the software package ARB (32). In particular, the ARB "Probe Match" tool was applied to find optimal LNAzyme cleavage positions in the target rRNAs. For this purpose, the FISH probe sequences were entered and then elongated and/or shortened at their 5′ or 3′ ends to shift the probe-binding sites along the target rRNA sequence until a suitable cleavage (AU or GU) site was reached. The candidate LNAzymes obtained from this procedure were checked for unwanted base mismatches to the target bacteria and for required mismatches to nontarget organisms as well as for self-complementary regions that could reduce cleavage efficiency due to hairpin formation or LNAzyme dimerization.

In this study, we designed three 16S rRNA-targeted LNAzymes specific for ammonia-oxidizing bacteria (AOB) or nitrite-oxidizing bacteria (NOB) (see Table S1 in the supplemental material). All three LNAzymes contain the 10-23 motif. LNAzyme Nso215 covers the AOB *Nitrosomonas oligotropha*, *N. europaea*, *N. ureae*, *N. halophila*, *N. cryotolerans*, *Nitrosomonas* sp. Nm143 and Nm84, *Nitrosococcus* (*Nitrosomonas*) *mobilis*, and most environmental sequences related to these cultured strains in the SILVA, release 102, full-length, nonredundant database. The 16S rRNA sequences of other nitrosomonads have base mismatches to the substrate-binding arms that most likely decrease the cleavage efficiency of this LNAzyme. The target region of Nso215 on the 16S rRNA overlaps the target site of probe Nmo218 that is commonly used for the FISH detection of *N. oligotropha*-related AOB (33). The cleavage site of Nso215 is GU, and the substrate-binding arms, determining the specificity of the LNAzyme, contain four LNA nucleotides (see Table S1 and Fig. S1 in the supplemental material). The LNA nucleotides were placed at the mismatch positions to most nontarget organisms that had a similar target sequence in the SILVA, release 102, database (34), because LNAs provide better discrimination against single-base mismatches (25). The LNAzymes Ntspa668 and Ntspa665, both targeting NOB of the genus *Nitrospira*, were derived from the *Nitrospira*-specific FISH probe Ntspa662 (35). This probe was elongated in the 5′ direction along the target 16S rRNA, resulting in a suitable AU cleavage site being flanked by the substrate-binding arms (see Table S1 and Fig. S1 in the supplemental material). Both LNAzymes cover all known sublineages of the genus *Nitrospira* (35–37), except for some members of marine lineage IV. The substrate-binding arms of Ntspa665 are longer (15 nucleotides up- and downstream of the cleavage site, instead of 12 and 10 nucleotides in Ntspa668). In addition, Ntspa665 contains only cytosine LNA nucleotides, which do not form base pairs with each other and thus greatly reduce the likelihood of intramolecular strong secondary structure formation. In both LNAzymes, the four LNA nucle-

otides were placed at positions of frequent mismatches to nontarget organisms.

The LNAzymes were obtained from Exiqon (Vedbaek, Denmark). We observed that both highly concentrated stocks as well as working solutions of LNAzymes partly lose their activity after storage at −20°C for several months. This problem was avoided by storing them in concentrated aliquots at −80°C. The LNAzyme digestion buffer contained 100 mM NaCl, 50 mM RNase-free Tris (pH 8.0) (Ambion, Austin, TX), 10 mM LiCl, 1 μM LNAzyme, and 5 μl of an *in vitro* transcription reaction mixture containing the transcribed RNA (see above). The final volume of the reaction mixture was 60 μl. All reagents except Tris were treated with 0.1% (vol/vol) diethylpyrocarbonate (DEPC) to inactivate nucleases. Previous studies found that Mg^{2+} or other divalent cations are required for DNAzyme activity (21, 29). Good LNAzyme efficiency was obtained even though Mg^{2+} was not added to the LNAzyme digestion buffer in an effort to preserve the integrity of RNA at elevated temperatures (see Results). However, we cannot exclude that the buffer contained trace amounts of divalent cations, because no chelating agent was added.

The efficiency of LNAzyme-mediated cleavage was improved by repeated heating and cooling of the reaction mixture (38). The mixture was incubated first for 90 s at 90°C for RNA denaturation, then for 30 s at 60°C to allow for annealing of LNAzymes to their target RNA molecules, and finally for 45 min at 37°C for the actual cleavage. These steps were repeated three times, resulting in four identical cycles of denaturation, annealing, and cleavage. PCR products (DNA), which had served as templates in the previous *in vitro* transcription step and which had been carried over into the LNAzyme reaction mixture, were then digested with DNase I for 45 min at 37°C. This digestion step also removed residual oligonucleotides (PCR primers) and the LNAzymes. Subsequently, 6 μl of 50 mM EDTA was added, and DNase I was inactivated by heating the mixture to 70°C for 10 min. After this step, the noncleaved RNA was ready for use as the template for RT-PCR.

T-RFLP. For terminal restriction fragment length polymorphism (T-RFLP) analysis, primer 8F labeled with 6-carboxyfluorescein (6-FAM) was used for PCR or RT-PCRs. Amplicons of the correct size were excised from agarose gels and purified by using the QiaQuick gel extraction kit (Qiagen), and approximately 100 ng of purified amplicons was digested for 3 h at 37°C by using the restriction endonuclease MspI (Fermentas). The digestion products were analyzed by using an ABI 3130xl genetic analyzer (Applied Biosystems, Foster City, CA) and PeakScanner 1.0 software (Applied Biosystems). Real peaks were distinguished from noise by using methods described previously by Abdo et al. (39) and by using the Perl and "R" scripts provided on their website (http://www.ibest.uidaho.edu/tools/trflp_stats/index.php). The effects of the LNAzyme treatments were tested for significance by one-way analysis of variance (ANOVA) including Tukey's honestly significant difference (HSD) *post hoc* test, which was performed by using the PASW Statistics 17 software package (IBM SPSS, Armonk, NY).

Cloning, sequencing, and phylogenetic analysis of 16S rRNA genes. One clone library was established from the "*Ca.* Nitrospira defluvii" enrichment using DNA as the initial template, by applying LNAzyme Ntspa668 (see Table S1 in the supplemental material) after PCR and IVT and by performing RT-PCR with primer pair 8F/907R (Fig. 2). Two clone libraries were constructed by using RNA as the initial template, which was treated with LNAzyme Ntspa665 and the helper probes (see Table S1 in the supplemental material). For one of these "RNA-based" libraries, primer pair 8F/907R was used for RT-PCR, whereas primer pair 8F/1492R was applied for the other library, which thus contained almost full-length 16S rRNA genes. For comparison, a fourth library was made by using DNA extracted from the enrichment culture as the template for PCR with primer pair 8F/907R and without any LNAzyme treatment.

PCR products of the correct size were excised from agarose gels, purified with the QiaQuick gel extraction kit (Qiagen), and cloned by using the TOPO TA cloning system (Invitrogen). Cloned genes were subjected to RFLP analysis with the restriction endonuclease MspI (Fermentas). Based on the obtained band patterns in agarose gels, Good's coverage of the clone libraries was calculated as

$$C = 1 - \frac{n_1}{N}$$

where n_1 is the number of RFLP patterns that occurred only once and N is the total number of clones analyzed. The Simpson diversity index was calculated as follows

$$1 - \frac{\sum_{i=1}^{R} n_i(n_i - 1)}{N(N - 1)}$$

where R is the number of different RFLP profiles observed and n_i is the number of clones with a particular RFLP pattern. A subset of the clones was selected for sequencing based upon the RFLP patterns. Sanger sequencing was performed by using BigDye Terminator cycle sequencing kit v3.1 and an ABI 3130xl genetic analyzer (Applied Biosystems), according to the manufacturer's instructions. The obtained 16S rRNA gene sequences were aligned with SINA Webaligner (http://www.arb-silva.de/aligner) and further analyzed by using ARB software (32) with the SSU Ref 108 SILVA NR sequence database (34). Automatically generated sequence alignments were manually refined. The phylogenetic affiliation of each sequence was determined by adding the sequences to the tree "tree_SSURef_1200_99_slv_108," which is included in the database, by using the ARB parsimony function and the "pos_var_ssuref:bacteria" sequence conservation filter that is also included in the database. Prior to adding the new sequences, all sequences with a Pintail (40) score below 80 were removed from the tree. Putative chimeric sequences were identified by independent phylogenetic analyses of the first 513 5′ base positions, the central 513 base positions, and the last 513 3′ base positions of the sequences. Sequences that showed an unstable phylogenetic affiliation in these tests were further checked for anomalies with Pintail software (40).

Fluorescence *in situ* hybridization. Bacteria in the "*Ca.* Nitrospira defluvii" enrichment culture were visualized by FISH with rRNA-targeted oligonucleotide probes (see Table S1 in the supplemental material), as described previously (41). Fluorescence-labeled oligonucleotide probes were obtained from Thermo Fisher. Microscopic observation and documentation were performed with an LSM 510 confocal laser scanning microscope and the provided software (Zeiss, Oberkochen, Germany). The relative biovolume of accompanying bacteria in the enrichment culture (i.e., cells that were labeled by the EUB338 probe mix but not by probe Ntspa1431) was quantified by FISH and digital image analysis (42) and by using daime software (43).

Nucleotide sequence accession numbers. The sequences obtained in this study have been deposited in the GenBank database under accession no. JF449905 to JF449947. The sequences of the 16S rRNA genes in Table 1 have been deposited in the GenBank database under accession no. JQ068103 to JQ068106.

RESULTS

Evaluation of the protocol and the LNAzymes. The newly designed LNAzymes and our protocol for the specific removal of unwanted template nucleic acids (Fig. 2) were tested with artificial mixtures containing template DNAs from target and nontarget organisms. For this purpose, we used four cloned partial 16S rRNA genes that had been retrieved from a nitrifying activated sludge and belonged to bacteria related to the *Nitrosomonas oligotropha* lineage (44), *Comamonas aquatica*, the phylum *Chloroflexi*, and *Nitrospira* lineage I (35), respectively. The plasmid vectors, which contained these cloned genes, were mixed in defined ratios (Table 1). The mixed 16S rRNA genes were then PCR amplified by using primers 8F (with a 5′ T3 promoter) and 907R (see Table S1 in the supplemental material). Subsequently, RNA was obtained by IVT of the mixed PCR amplicons. Further following the scheme in Fig. 2, this *in vitro*-synthesized RNA was incubated with

TABLE 1 Concentration ratios of plasmid vectors carrying the respective partial 16S rRNA genes in the artificial mixtures that were used to evaluate the LNAzymes and the protocol developed in this study

Mixture	Concn ratio			
	Nitrosomonas sp.	*Nitrospira* sp.	*Chloroflexi* sp.	*Comamonas* sp.
A	100	15	10	1
B	15	100	1	10
C	100	1	1	1
D	200	100	1	1

the LNAzymes and was then converted back to cDNA and amplified by RT-PCR with primers 8F and 907R. Finally, T-RFLP analysis was used to determine the composition of the resulting PCR product mixture and to assess how efficiently the respective targets had been depleted by the LNAzyme approach.

LNAzyme-mediated RNA cleavage led to the depletion of specific targets in four different mixtures of the 16S rRNA genes (Fig. 3). LNAzyme Nso215 cleaved the partial 16S rRNA derived from the *Nitrosomonas*-related clone with high efficiency, and a single iteration of the protocol was sufficient to drastically reduce the abundance of this target (Fig. 3A and C). A second iteration of the protocol resulted in an almost complete elimination of the *Nitrosomonas*-related 16S rRNA gene from mixtures that originally contained large relative amounts of this target (Fig. 3A and C and Table 1). Concomitantly, the relative abundances of the other three 16S rRNA types increased in the mixtures (Fig. 3A and C), with the sole exception being the *Comamonas*-related 16S rRNA in mixture "A" (Table 1), whose relative abundance remained constant throughout the experiment (Fig. 3A). In contrast, the relative abundance of this 16S rRNA type increased in the experiment with mixture "C" (Table 1 and Fig. 3C), where the same LNAzyme, Nso215, was used to deplete *Nitrosomonas*-related 16S rRNA.

The *Nitrospira*-specific LNAzyme Ntspa668 was also successful at strongly depleting *Nitrospira*-related 16S rRNA (Fig. 3B). How-

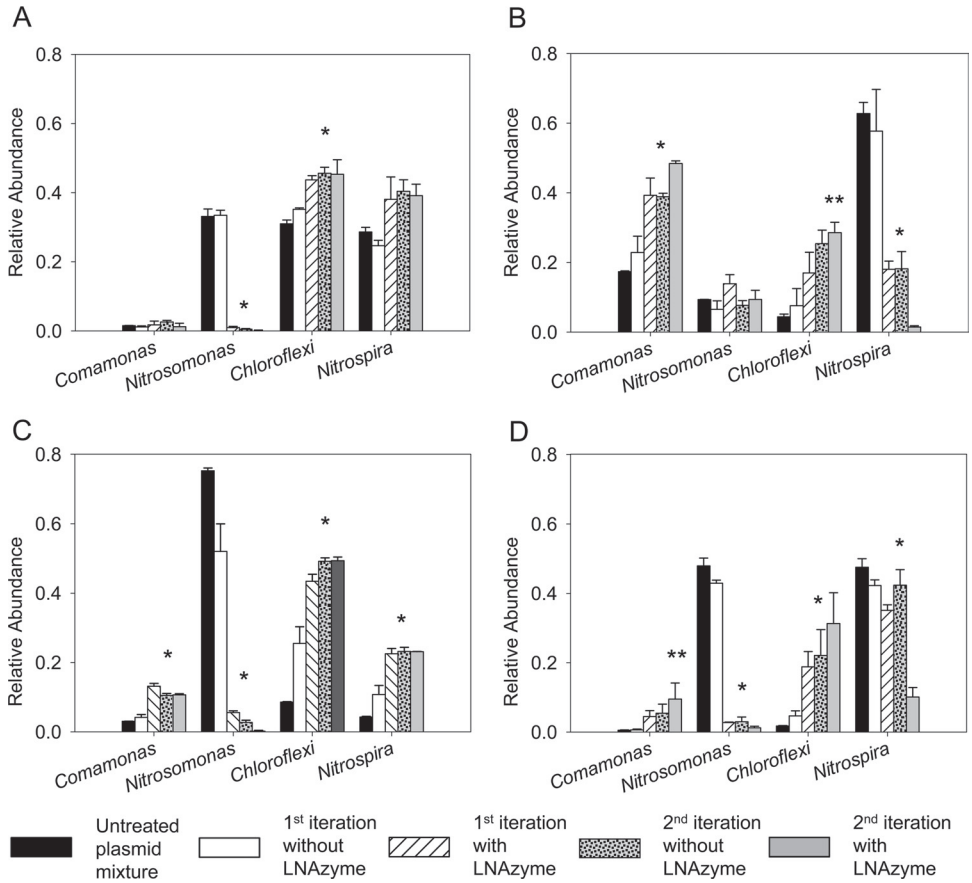

FIG 3 Evaluation of the LNAzyme cleavage protocol with artificial mixtures of cloned partial 16S rRNA genes (Table 1). The bars show the relative abundances of the rRNA genes in the mixtures before and after one or two iterations of the LNAzyme-mediated depletion of the *Nitrosomonas* and/or *Nitrospira* rRNA. Data for control experiments without added LNAzymes are also shown (the second iteration without LNAzyme was performed after a first iteration with LNAzyme). The relative abundances were determined by T-RFLP analysis. Only the relevant T-RFLP peaks are shown; for the complete T-RFLP profiles, please refer to Fig. S2 in the supplemental material. (A) Depletion of the *Nitrosomonas*-related 16S rRNA gene by LNAzyme Nso215 using 16S rRNA gene plasmid mixture "A" (Table 1). (B) Depletion of the *Nitrospira*-related 16S rRNA gene by LNAzyme Ntspa668 using plasmid mixture "B" (Table 1). (C) Like panel A but with a different initial abundance of the *Nitrosomonas*-related and other 16S rRNA genes in the mixture (mixture "C" in Table 1). (D) Simultaneous depletion of the *Nitrosomonas*- and the *Nitrospira*-related 16S rRNA genes by LNAzymes Nso215 and Ntspa668 (mixture "D" in Table 1). Error bars depict standard deviations from three replicate experiments. One asterisk above the bars indicates that a single iteration of target depletion was sufficient to obtain a significant ($P < 0.05$) difference compared to the untreated plasmid mixture. Two asterisks mark cases in which two iterations of target depletion were needed to achieve a significant difference.

ever, in this case, the difference between the first and second iterations of the protocol was more pronounced than with LNAzyme Nso215 (Fig. 3B). Finally, we tested whether two different LNAzymes can be combined in the same experiment for depleting different targets. For this purpose, the LNAzymes Nso215 and Ntspa668 were used simultaneously with an artificial mixture containing large relative amounts of *Nitrosomonas*- and *Nitrospira*-related 16S rRNA genes but very small relative amounts of the *Comamonas*- and *Chloroflexi*-related rRNA genes. Both LNAzymes cleaved their respective targets with efficiencies that were similar to those observed for single LNAzyme experiments (Fig. 3D). It is important to note that the apparently weak decrease of the *Nitrospira*-like 16S rRNA levels during the first iteration (Fig. 3D) did not result from a low efficiency of LNAzyme Ntspa668. The very pronounced depletion of the *Nitrosomonas*-like 16S rRNA (Fig. 3D) must have increased the relative amounts of the other 16S rRNA types in the mixture, including *Nitrospira*. This relative increase in the amount of the *Nitrospira*-like 16S rRNA was neutralized by Ntspa668. After two iterations, the activity of this LNAzyme led to the strong depletion of the *Nitrospira*-like 16S rRNA, which was not observed in the control experiment without Ntspa668 (Fig. 3D).

In preliminary experiments, the obtained T-RFLP profiles contained numerous peaks apparently belonging to short fragments, which were inconsistent with the known positions of restriction endonuclease cleavage sites in the 16S rRNA gene sequences. The number of those peaks increased after each iteration of the LNAzyme cleavage protocol (data not shown). These artifacts were eliminated by agarose gel electrophoresis of the PCR products and excision of the correct bands prior to IVT or T-RFLP analysis (see also Materials and Methods).

Identification of accompanying bacteria in a *Nitrospira* enrichment culture. After the new LNAzymes and the cleavage protocol had been tested with artificial template mixtures, the method was used to identify accompanying bacteria ("contaminants") in an enrichment culture of the nitrite-oxidizing bacterium "*Candidatus* Nitrospira defluvii" (31). This enrichment culture consisted mainly of "*Ca.* Nitrospira defluvii" and had been used for sequencing of the genome of this nitrifier by environmental genomics (45) but still contained minor amounts of bacteria that do not belong to the genus *Nitrospira* according to FISH with rRNA-targeted probes (31). The presence of contaminants in the *Nitrospira* culture, which was used for this study, was confirmed by quantitative FISH, revealing that 13% of the bacterial community in this enrichment culture did not hybridize to any *Nitrospira*-specific FISH probe but was detected by the *Bacteria*-specific EUB338 probe mix.

DNA and RNA were extracted and purified from aliquots of the "*Ca.* Nitrospira defluvii" enrichment culture. Subsequently, the 16S rRNA of *Nitrospira* was depleted by using LNAzymes and the protocol (Fig. 2), with either DNA or RNA as the initial template. When the procedure started with DNA, most of the *Nitrospira* target was already removed after the first iteration using LNAzyme Ntspa668 (Fig. 4A). This led to higher relative abundances of other 16S rRNA types, which was evident from the increasing areas of some peaks in the T-RFLP profile (Fig. 4A).

Interestingly, LNAzyme Ntspa668 cleaved native 16S rRNA of *Nitrospira* with poor efficiency (Fig. 4B). This result was in contrast to the good performance of this LNAzyme when cleaving RNA that had been produced by IVT of a DNA template (Fig. 3B and 4A). Therefore, the second *Nitrospira*-specific LNAzyme (Ntspa665) was designed with longer substrate-binding arms and different LNA nucleotides (see above). Application of Ntspa665 to the native RNA resulted in a significantly stronger relative decrease in the level of the *Nitrospira* target than achieved by Ntspa668 (Fig. 4B). As we assumed that secondary structures of the native 16S rRNA hampered LNAzyme-mediated cleavage, we combined the LNAzymes with helper probes (46) that were newly developed and targeted *Nitrospira* lineages I and II, Ntspa630help and Ntspa700help (see Table S1 in the supplemental material). These helper probes were supposed to bind to the *Nitrospira* 16S rRNA adjacent to the target sites of the LNAzymes, thereby resolving secondary structures and facilitating hybridization of the LNAzymes to their target. Indeed, the helper probes improved the depletion of native *Nitrospira* 16S rRNA by both LNAzymes Ntspa668 and Ntspa665 (Fig. 4B). As observed when DNA was used as an initial template (Fig. 4A), the relative abundances of other 16S rRNA types increased as the abundance of *Nitrospira* 16S rRNA decreased (Fig. 4B). However, this shift was less pronounced, most likely due to the lower efficiency of both *Nitrospira*-specific LNAzymes when cleaving native 16S rRNA, even in the presence of helper probes.

To identify the accompanying bacteria in the enrichment culture, 16S rRNA genes were cloned after the depletion of the *Nitrospira* 16S rRNA. Between 40 and 50 randomly selected clones from each library were subjected to RFLP analysis to determine the proportion of cloned *Nitrospira* 16S rRNA genes. As expected, their frequency was much lower in all libraries produced from LNAzyme-treated templates than in the library that was made from untreated template DNA (Table 2). Analysis of the 31 obtained 16S rRNA gene sequences (after LNAzyme treatment) revealed a surprising diversity of accompanying bacteria in the "*Ca.* Nitrospira defluvii" enrichment culture, comprising representatives of seven bacterial phyla (see Table S2 in the supplemental material).

DISCUSSION

Rank-abundance analyses have shown that complex microbial communities can be dominated by relatively few and highly abundant community members, whereas the bulk of diversity (richness) is "hidden" in a large number of rare taxa (47). This uneven structure is mirrored in the composition of cloned rRNA gene libraries established from samples of these communities. Similarly, rRNA gene libraries made from associations between microorganisms and eukaryotes are often dominated by clones carrying plastid or mitochondrial rRNA genes that were targeted by the applied *Bacteria*-specific PCR primers (e.g., see reference 48). To facilitate the detection of less frequent sequence types, a few methods have been developed for the specific depletion of unwanted (dominant) targets before or during PCR amplification (18, 19, 49). A common motif for these approaches is the use of nucleic acid oligomers, which must specifically hybridize to DNA templates that should not be amplified during PCR. The optimal hybridization conditions must be determined for each oligomer to avoid unspecific binding to nontarget DNA and inefficient hybridization to the target. The parallel elimination of more than one unwanted target would be complicated if the required stringent hybridization conditions prohibit the simultaneous application of different target-specific oligomers.

In this study, we developed an alternative approach that em-

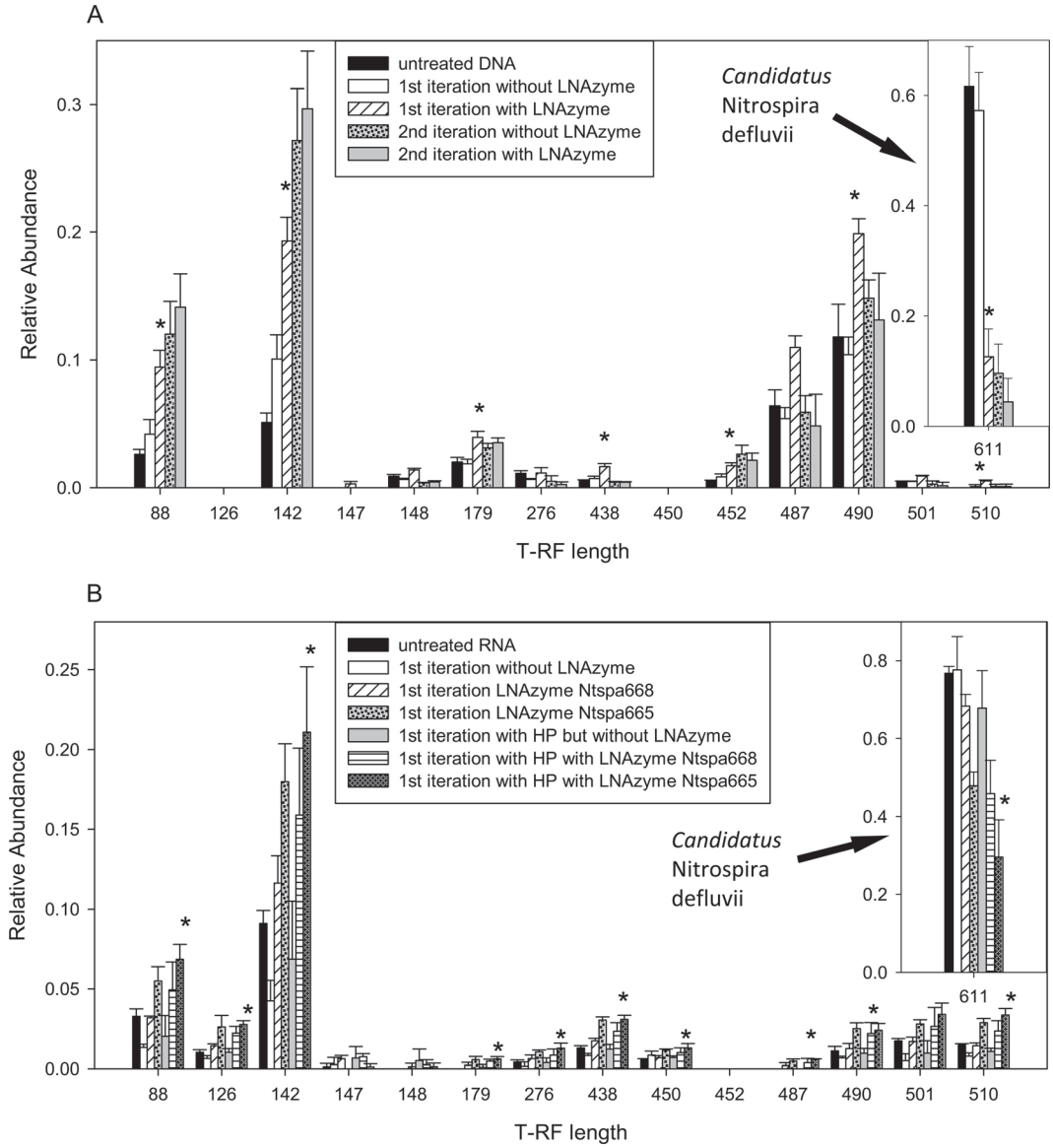

FIG 4 Depletion of 16S rRNA of "*Ca.* Nitrospira defluvii" from DNA (A) or native RNA (B) that was extracted from the "*Ca.* Nitrospira defluvii" enrichment culture. The bars show the relative abundances of the 16S rRNA genes of "*Ca.* Nitrospira defluvii" and of other bacteria, as determined by T-RFLP analysis, before and after one or two iterations of the LNAzyme-mediated depletion. Data for control experiments without added LNAzymes are also shown (the second iteration without LNAzyme was performed after a first iteration with LNAzyme). Only selected T-RFLP peaks are shown; for the complete T-RFLP profiles, please refer to Fig. S3 in the supplemental material. Applied LNAzymes were Ntspa668 (A) and Ntspa668 or Ntspa665 (B) (which also shows the effects of additional helper probes [HP] on the efficiency of target depletion). The decrease of the peaks at positions 487 and 490 (A) in the second iteration probably reflects artifacts of PCR or IVT. Error bars depict standard deviations from three replicate experiments. Asterisks above bars indicate that a significant ($P < 0.05$) difference compared to the untreated DNA or RNA was obtained. Where this was achieved in the experiment with DNA (A), a single iteration of target depletion was sufficient. In panel B, the results of the significance test are shown for the treatment with helper probes and LNAzyme Ntspa665.

ploys catalytically active LNAzymes (Fig. 1). The LNAzymes must also hybridize to their respective target, but the cleaving efficiency highly depends on perfect base complementarity close to the cleaving site. Hence, as demonstrated by previous fundamental work on the properties of DNAzymes and LNAzymes, even unspecific hybridization to a nontarget template (which has mismatches) would not lead to significant cleavage (24, 29, 30, 50). By including *in vitro* transcription, we demonstrated that the RNA-cleaving LNAzymes can also be used if DNA is the initial template.

The experiments with artificial mixtures of four different 16S rRNA genes confirmed that the newly designed LNAzymes Nso215 and Ntspa668 cleaved their respective targets efficiently and with high specificity. The depletion of their targets led to a relative increase of the initially less frequent sequence types (Fig. 3). The absence of such an increase in two cases (*Comamonas* [Fig. 3A] and *Nitrosomonas* [Fig. 3B]) may be due to biases of IVT or one of the amplification steps in the protocol. The increase of the *Comamonas*-like template in another experiment with the same LNAzyme, Nso215 (Fig. 3C), suggests that such biases can be stochastic and are unlikely to hamper the approach in general. In

TABLE 2 Frequencies of the 16S rRNA genes of "*Ca*. Nitrospira defluvii" and other bacteria in clone libraries established with and without preceding treatment by LNAzymes[e]

Treatment[a]	No. of distinct RFLP patterns (no. of singletons)[d]	No. of clones assigned to "*Ca*. Nitrospira defluvii"	No. of clones assigned to other bacteria	Frequency of "*Ca*. Nitrospira defluvii" (%)	Good's coverage (%)	Simpson diversity index
Untreated DNA 907R	4 (2)	40	11	78.4	96.1	0.36
DNA 907R[b]	12 (5)	3	39	7.1	88.1	0.8
RNA 907R[c]	14 (9)	9	35	20.5	79.6	0.76
RNA 1492R[c]	14 (9)	1	45	2.2	80.4	0.84

[a] DNA, DNA was used as the initial template; RNA, RNA was used as the initial template. 907R and 1492R are the reverse primers used for 16S rRNA gene-specific PCR.
[b] Treatment by LNAzyme Ntspa668 prior to cloning.
[c] Treatment by LNAzyme Ntspa665 prior to cloning.
[d] Singletons are RFLP patterns that occurred only once.
[e] Assignments of cloned genes to "*Ca*. Nitrospira defluvii" or other bacteria were based on RFLP band patterns, exploiting the fact that "*Ca*. Nitrospira defluvii" has a characteristic RFLP pattern after digestion of its 16S rRNA gene amplicon with the endonuclease MspI (this was confirmed by sequencing of selected clones showing this RFLP pattern).

addition, we noticed that the T-RFLP profiles obtained for the untreated plasmid mixtures did not correctly reflect the initial composition of these mixtures (Fig. 3 and Table 1). This result was expected because T-RFLP profiles often do not represent the quantitative structure of microbial communities because of biases in PCR, enzymatic digestion, and capillary electrophoresis (see reference 51 and references therein). However, relative changes in the composition of the same microbial community are accurately detected by T-RFLP analysis (51). Thus, this method is suitable for monitoring the shifts in relative abundance caused by the LNAzyme-mediated depletion of selected targets. We also noticed that even without the use of any LNAzyme, the IVT and RT-PCR steps can slightly modify the relative abundances of the templates (Fig. 3). Altogether, these observations show that our protocol may not be able to detect all rare sequence types in a complex mixture and that it, like other approaches using nonquantitative IVT or PCR (52), would not be suitable for a quantitative census of the sequence types in a mixture of different templates.

The *Nitrospira*-specific LNAzyme Ntspa668 was less efficient than the *Nitrosomonas*-targeting LNAzyme Nso215 (Fig. 3A, B, and D). Aside from base mismatches, factors reported to affect the efficiency of DNAzymes and LNAzymes include secondary structures of complex RNA substrates (27, 53) and the thermodynamic stability of the enzyme-substrate complex (29). Although less efficient, the *Nitrospira*-like 16S rRNA gene was almost completely depleted after a second iteration of the cleavage protocol with Ntspa668 (Fig. 3B and D). Thus, repeating the procedure (Fig. 2) can overcome difficulties with less efficient LNAzymes and problematic target sites. The efficiency can easily be monitored over successive iterations by a fingerprinting technique such as T-RFLP. The experiment with both LNAzymes Nso215 and Ntspa668 (Fig. 3D) confirmed that two LNAzymes can be combined in the same workflow step and under the same conditions to simultaneously deplete different unwanted targets. Future experiments should test whether more LNAzymes can be used together for the depletion of multiple targets from complex mixtures.

Enrichment cultures of an organism that still contain accompanying bacteria ("contaminants") are prime examples of highly uneven communities. Here we used LNAzymes to identify contaminants in the enrichment of "*Ca.* Nitrospira defluvii" (31), which still contained small amounts of other bacteria. For this purpose, the entire approach was started with either DNA or native RNA as the initial template in order to compare the results and identify possible difficulties with the method. Additional helper probes were needed to facilitate the LNAzyme-mediated cleavage of native 16S rRNA from "*Ca.* Nitrospira defluvii" (Fig. 4B), whereas no helper probes were required with DNA as the initial template (Fig. 4A). Thus, target site accessibility influences the efficiency of LNAzymes, at least when they cleave native rRNA. Although a pronounced relative increase was not achieved for all rare 16S rRNA sequence types in the enrichment culture (Fig. 4), the selection of non-*Nitrospira* clones required little effort after the LNAzyme treatments. All gene libraries were reasonably well covered by the analyzed sets of clones, but analyses of similar clone numbers retrieved a much higher level of diversity of 16S rRNA types from the libraries that were established after the use of LNAzymes (Table 2). Nevertheless, the detected phylotypes were not evenly distributed among the clones selected from these three libraries (see Table S2 in the supplemental material). This might be caused by nonexhaustive sequencing of non-*Nitrospira* clones from each library or by other factors, such as an unequal coverage of the organisms by the different PCR primers applied. The frequencies of the different sequence types in the "RNA-based" libraries may also be affected by secondary structures of the template rRNA interfering with RT-PCR or by the cellular ribosome content. The LNAzyme-based approach led to the discovery of a surprisingly high level of diversity of cocultured bacteria that are possibly involved in biological interactions with *Nitrospira* (discussed in the supplemental material).

In general, similar criteria must be considered for the design of rRNA-targeted DNAzymes (or LNAzymes) and of rRNA-targeted oligonucleotide probes that are used for hybridization techniques such as FISH. The sites containing mismatches to nontarget organisms should be located near the center of the binding region to achieve an optimal specificity of the probe or LNAzyme. Second, LNAzymes and probes should cover all or at least most members of their phylogenetic target groups. Moreover, the secondary structure of the rRNA is likely to influence the binding of LNAzymes to their target site, as it affects the hybridization efficiency of FISH probes (54). Good target sites for FISH (54, 55) could also be suitable for LNAzymes, although this might not always apply, because FISH targets fixed intact ribosomes, whereas the LNAzymes in our protocol bind to isolated rRNA. Therefore, we suggest starting the design of new rRNA-targeted LNAzymes by screening a resource, such as probeBase (56), for existing FISH probes that are specific for the respective target or-

ganisms and have been tested in previous studies. The next step is to identify a suitable LNAzyme cleavage site in the probe sequence or in adjacent regions of the target rRNA. If a cleavage site is found, the probe, if necessary, can be shifted and/or extended in the 5′ and 3′ directions *in silico* along the rRNA. Either substrate-binding arm must be long enough for efficient hybridization and cleavage (29). In preliminary experiments using native 23S rRNA of *Escherichia coli* and an LNAzyme based on the FISH probe Gam42a, we observed good cleavage efficiency with substrate-binding arms of 8 and 9 nucleotides, respectively (data not shown). The LNAzymes used here to target nitrifiers had arms of 12 and 10 nucleotides (Ntspa668), 15 and 15 nucleotides (Ntspa655), and 15 and 12 nucleotides (Nso215). Finally, the specificity and coverage of the resulting LNAzyme should be evaluated by tools such as the "Probe Match" function of ARB software (32), probeCheck (57), or TestProbe (http://www.arb-silva.de/search/testprobe).

We evaluated all probes deposited in probeBase until 9 March 2010 to determine how suitable they would be for LNAzyme design. Among these 2,479 probes, 2,270 target an rRNA region that contains a potential RU cleavage site, which results in the highest cutting efficiency (24). No less than 807 probes would lead, without any sequence modifications, to LNAzymes with two substrate-binding arms of at least 8 nucleotides (see Fig. S4 in the supplemental material). An additional 703 probes would lead to LNAzymes with one substrate-binding arm of at least 6 nucleotides and the other arm of at least 8 nucleotides (see Fig. S4 in the supplemental material). Thus, only slight modifications (elongation of one arm by up to 2 nucleotides) might be needed to design an efficient LNAzyme based on these probes. In total, 61% of all probes in probeBase could be converted to efficient LNAzymes with few or no sequence changes, mostly preserving the already evaluated coverage of these probes and, due to the LNA nucleotides, possibly even increasing their specificity. However, the different cleavage efficiencies of Ntspa668 and Ntspa665 (see above) show that particular LNAzymes and/or target sites may require additional optimization and that tests to evaluate newly designed LNAzymes should be carried out prior to their use in critical experiments.

In summary, our LNAzyme-based protocol has proven useful for the depletion of unwanted targets in mixtures of 16S rRNA genes and native 16S rRNA types. The method lends itself to analyses of highly uneven communities, whose dominant members can easily be identified prior to the selection or design of suitable LNAzymes. Depending on the choice of primers for the PCR steps (Fig. 2), nearly full-length sequences can be obtained. Furthermore, the possibility of starting the approach with either DNA or RNA as the initial template offers much flexibility for applications in microbial ecology. For example, stable isotope probing (SIP) of RNA is a sensitive tool to identify uncultured microbes that take up and assimilate a specific substrate (58). The resulting stable isotope-labeled RNA fraction, however, may be dominated by rRNA from the largest or most active population that used the offered tracer. In such a situation, the specific cleavage and depletion, by LNAzymes, of this dominant rRNA would facilitate the analysis of less abundant rRNA types and thus provide a more complete picture of the functionally relevant microbial community members. Recently, we used such a combination of RNA-SIP and LNAzymes to study interactions of heterotrophic bacteria with autotrophic nitrifiers (data not shown). If DNA-SIP is more appropriate, the same LNAzymes may be used with few modifications of the protocol, as shown in Fig. 2. Another application for LNAzymes could be purity checks of microbial isolates. Microscopy-based tools such as FISH are insufficient for this purpose, because rare contaminants would be overlooked due to the high detection limit of 1,000 to 10,000 cells per ml (59). Even PCR and DGGE analysis of 16S rRNA genes may not detect populations whose abundance is below 1% of the total community (17). The use of a 16S rRNA-directed LNAzyme, which is specific for the organism to be purified, would deplete this most abundant target and facilitate the detection of other organisms. As the application of LNAzymes does not require expensive or specialty equipment, the method should be usable in most laboratories where basic infrastructure for molecular work is available.

Recently developed high-throughput sequencing techniques allow the detection of the "rare biosphere" by providing large numbers of sequence reads per sample (e.g., see references 4 and 5). These methods undoubtedly mark a new era of microbial diversity analyses. However, their use for routine applications and smaller projects is still limited by the computational efforts needed to analyze the massive amounts of data and to compensate for methodical biases (60, 61) and by the relatively high costs per sequencing run. Moreover, current deep-sequencing techniques cannot be applied if (nearly) full-length rRNA gene sequences are needed for phylogenetic analyses or probe and primer design and if new probes or primers must be evaluated in experiments using the cloned target genes. In such cases, the LNAzyme-based approach complements the deep-sequencing methods, because it facilitates the cloning of full-length rRNA genes of rare organisms. Moreover, diversity analyses by deep sequencing of uneven microbial communities could benefit from LNAzyme-mediated depletion of the most dominant sequence types prior to the sequencing step. This would increase the number of sequence reads from rarer organisms and thus improve the coverage of the rare portion of the community.

The characterization of rare biosphere organisms is a difficult but important challenge for microbial ecology. Despite their low abundance, these microbes can be key players in ecosystems, like a rare *Desulfosporosinus* species that represented only 0.006% of the total microbial community but turned out to be an important sulfate reducer in a peatland (62). LNAzymes are a promising tool that offers more direct access to these often overlooked community members and thus will help to achieve a more complete understanding of their functions.

ACKNOWLEDGMENTS

We thank Eva Spieck for providing "*Ca.* Nitrospira defluvii" enrichment biomass, Christian Baranyi for technical assistance, and David Berry for critically reading the manuscript.

J.D. and I.L. were funded by the Graduate School Symbiotic Interactions of the University of Vienna. This work was also partly funded by the Austrian Science Fund (FWF) (grants S10002-B17 and I44-B06) and by the Vienna Science and Technology Fund (WWTF) (grant LS09-040).

REFERENCES

1. **Amann RI.** 1995. *In situ* identification of micro-organisms by whole cell hybridization with rRNA-targeted nucleic acid probes, p 1–15. *In* Akkeman ADC, van Elsas JD, de Bruigin FJ (ed), Molecular microbial ecology manual, vol 3.3.6. Kluwer Academic Publishers, Dordrecht, Netherlands.
2. **Giovannoni SJ, Britschgi TB, Moyer CL, Field KG.** 1990. Genetic diversity in Sargasso Sea bacterioplankton. Nature **345**:60–63.

3. **Hugenholtz P, Pace NR.** 1996. Identifying microbial diversity in the natural environment: a molecular phylogenetic approach. Trends Biotechnol. **14**:190–197.
4. **Sogin ML, Morrison HG, Huber JA, Welch DM, Huse SM, Neal PR, Arrieta JM, Herndl GJ.** 2006. Microbial diversity in the deep sea and the underexplored "rare biosphere." Proc. Natl. Acad. Sci. U. S. A. **103**:12115–12120.
5. **Webster NS, Taylor MW, Behnam F, Lücker S, Rattei T, Whalan S, Horn M, Wagner M.** 2010. Deep sequencing reveals exceptional diversity and modes of transmission for bacterial sponge symbionts. Environ. Microbiol. **12**:2070–2082.
6. **Achtman M, Wagner M.** 2008. Microbial diversity and the genetic nature of microbial species. Nat. Rev. Microbiol. **6**:431–440.
7. **Hugenholtz P, Goebel BM, Pace NR.** 1998. Impact of culture-independent studies on the emerging phylogenetic view of bacterial diversity. J. Bacteriol. **180**:4765–4774.
8. **Rappé MS, Giovannoni SJ.** 2003. The uncultured microbial majority. Annu. Rev. Microbiol. **57**:369–394.
9. **Schloss PD, Handelsman J.** 2004. Status of the microbial census. Microbiol. Mol. Biol. Rev. **68**:686–691.
10. **Braker G, Fesefeldt A, Witzel K-P.** 1998. Development of PCR primer systems for amplification of nitrite reductase genes (*nirK* and *nirS*) to detect denitrifying bacteria in environmental samples. Appl. Environ. Microbiol. **64**:3769–3775.
11. **Minz D, Flax JL, Green SJ, Muyzer G, Cohen Y, Wagner M, Rittmann BE, Stahl DA.** 1999. Diversity of sulfate-reducing bacteria in oxic and anoxic regions of a microbial mat characterized by comparative analysis of dissimilatory sulfite reductase genes. Appl. Environ. Microbiol. **65**:4666–4671.
12. **Purkhold U, Pommering-Röser A, Juretschko S, Schmid MC, Koops H-P, Wagner M.** 2000. Phylogeny of all recognized species of ammonia oxidizers based on comparative 16S rRNA and amoA sequence analysis: implications for molecular diversity surveys. Appl. Environ. Microbiol. **66**:5368–5382.
13. **Semrau JD, Chistoserdov A, Lebron J, Costello A, Davagnino J, Kenna E, Holmes AJ, Finch R, Murrell JC, Lidstrom ME.** 1995. Particulate methane monooxygenase genes in methanotrophs. J. Bacteriol. **177**:3071–3079.
14. **Zehr JP, Jenkins BD, Short SM, Steward GF.** 2003. Nitrogenase gene diversity and microbial community structure: a cross-system comparison. Environ. Microbiol. **5**:539–554.
15. **Farrelly V, Rainey FA, Stackebrandt E.** 1995. Effect of genome size and rrn gene copy number on PCR amplification of 16S rRNA genes from a mixture of bacterial species. Appl. Environ. Microbiol. **61**:2798–2801.
16. **Hugenholtz P, Pitulle C, Hershberger KL, Pace NR.** 1998. Novel division level bacterial diversity in a Yellowstone hot spring. J. Bacteriol. **180**:366–376.
17. **Muyzer G, de Waal EC, Uitterlinden AG.** 1993. Profiling of complex microbial populations by denaturing gradient gel electrophoresis analysis of polymerase chain reaction-amplified genes coding for 16S rRNA. Appl. Environ. Microbiol. **59**:695–700.
18. **Green SJ, Minz D.** 2005. Suicide polymerase endonuclease restriction, a novel technique for enhancing PCR amplification of minor DNA templates. Appl. Environ. Microbiol. **71**:4721–4727.
19. **von Wintzingerode F, Landt O, Ehrlich A, Gobel UB.** 2000. Peptide nucleic acid-mediated PCR clamping as a useful supplement in the determination of microbial diversity. Appl. Environ. Microbiol. **66**:549–557.
20. **Breaker RR, Joyce GF.** 1994. A DNA enzyme that cleaves RNA. Chem. Biol. **1**:223–229.
21. **Santoro SW, Joyce GF.** 1997. A general purpose RNA-cleaving DNA enzyme. Proc. Natl. Acad. Sci. U. S. A. **94**:4262–4266.
22. **Schlosser K, Li Y.** 2009. Biologically inspired synthetic enzymes made from DNA. Chem. Biol. **16**:311–322.
23. **Silverman SK.** 2005. In vitro selection, characterization, and application of deoxyribozymes that cleave RNA. Nucleic Acids Res. **33**:6151–6163.
24. **Cairns MJ, King A, Sun LQ.** 2003. Optimisation of the 10-23 DNAzyme-substrate pairing interactions enhanced RNA cleavage activity at purine-cytosine target sites. Nucleic Acids Res. **31**:2883–2889.
25. **Vester B, Wengel J.** 2004. LNA (locked nucleic acid): high-affinity targeting of complementary RNA and DNA. Biochemistry **43**:13233–13241.
26. **Schubert S, Gul DC, Grunert HP, Zeichhardt H, Erdmann VA, Kurreck J.** 2003. RNA cleaving '10-23' DNAzymes with enhanced stability and activity. Nucleic Acids Res. **31**:5982–5992.
27. **Vester B, Hansen LH, Lundberg LB, Babu BR, Sorensen MD, Wengel J, Douthwaite S.** 2006. Locked nucleoside analogues expand the potential of DNAzymes to cleave structured RNA targets. BMC Mol. Biol. **7**:19. doi:10.1186/1471-2199-7-19.
28. **Vester B, Lundberg LB, Sorensen MD, Babu BR, Douthwaite S, Wengel J.** 2004. Improved RNA cleavage by LNAzyme derivatives of DNAzymes. Biochem. Soc. Trans. **32**:37–40.
29. **Santoro SW, Joyce GF.** 1998. Mechanism and utility of an RNA-cleaving DNA enzyme. Biochemistry **37**:13330–13342.
30. **Suenaga H, Liu R, Shiramasa Y, Kanagawa T.** 2005. Novel approach to quantitative detection of specific rRNA in a microbial community, using catalytic DNA. Appl. Environ. Microbiol. **71**:4879–4884.
31. **Spieck E, Hartwig C, McCormack I, Maixner F, Wagner M, Lipski A, Daims H.** 2006. Selective enrichment and molecular characterization of a previously uncultured *Nitrospira*-like bacterium from activated sludge. Environ. Microbiol. **8**:405–415.
32. **Ludwig W, Strunk O, Westram R, Richter L, Meier H, Yadhu K, Buchner A, Lai T, Steppi S, Jobb G, Förster W, Brettske I, Gerber S, Ginhart AW, Gross O, Grumann S, Hermann S, Jost R, König A, Lüßmann TLR, May M, Nonhoff B, Reichel B, Strehlow R, Stamatakis A, Stuckmann N, Vilbig A, Lenke M, Ludwig T, Bode A, Schleifer KH.** 2004. ARB: a software environment for sequence data. Nucleic Acids Res. **32**:1363–1371.
33. **Gieseke A, Purkhold U, Wagner M, Amann R, Schramm A.** 2001. Community structure and activity dynamics of nitrifying bacteria in a phosphate-removing biofilm. Appl. Environ. Microbiol. **67**:1351–1362.
34. **Pruesse E, Quast C, Knittel K, Fuchs BM, Ludwig W, Peplies J, Glöckner FO.** 2007. SILVA: a comprehensive online resource for quality checked and aligned ribosomal RNA sequence data compatible with ARB. Nucleic Acids Res. **35**:7188–7196.
35. **Daims H, Nielsen JL, Nielsen PH, Schleifer KH, Wagner M.** 2001. In situ characterization of *Nitrospira*-like nitrite-oxidizing bacteria active in wastewater treatment plants. Appl. Environ. Microbiol. **67**:5273–5284.
36. **Lebedeva EV, Alawi M, Maixner F, Jozsa PG, Daims H, Spieck E.** 2008. Physiological and phylogenetical characterization of a new lithoautotrophic nitrite-oxidizing bacterium '*Candidatus* Nitrospira bockiana' sp. nov. Int. J. Syst. Evol. Microbiol. **58**:242–250.
37. **Lebedeva EV, Off S, Zumbragel S, Kruse M, Shagzhina A, Lucker S, Maixner F, Lipski A, Daims H, Spieck E.** 2011. Isolation and characterization of a moderately thermophilic nitrite-oxidizing bacterium from a geothermal spring. FEMS Microbiol. Ecol. **75**:195–204.
38. **Hengesbach M, Meusburger M, Lyko F, Helm M.** 2008. Use of DNAzymes for site-specific analysis of ribonucleotide modifications. RNA **14**:180–187.
39. **Abdo Z, Schuette UM, Bent SJ, Williams CJ, Forney LJ, Joyce P.** 2006. Statistical methods for characterizing diversity of microbial communities by analysis of terminal restriction fragment length polymorphisms of 16S rRNA genes. Environ. Microbiol. **8**:929–938.
40. **Ashelford KE, Chuzhanova NA, Fry JC, Jones AJ, Weightman AJ.** 2005. At least 1 in 20 16S rRNA sequence records currently held in public repositories is estimated to contain substantial anomalies. Appl. Environ. Microbiol. **71**:7724–7736.
41. **Daims H, Stoecker K, Wagner M.** 2005. Fluorescence in situ hybridisation for the detection of prokaryotes, p 213–239. *In* Osborn AM, Smith CJ (ed), Molecular microbial ecology. Bios-Garland, Abingdon, United Kingdom.
42. **Daims H, Wagner M.** 2007. Quantification of uncultured microorganisms by fluorescence microscopy and digital image analysis. Appl. Microbiol. Biotechnol. **75**:237–248.
43. **Daims H, Lücker S, Wagner M.** 2006. *daime*, a novel image analysis program for microbial ecology and biofilm research. Environ. Microbiol. **8**:200–213.
44. **Purkhold U, Wagner M, Timmermann G, Pommerening-Röser A, Koops HP.** 2003. 16S rRNA- and *amoA*-based phylogeny of 12 novel betaproteobacterial ammonia oxidizing isolates: extension of the data set and proposal of a new lineage within the nitrosomonads. Int. J. Syst. Evol. Microbiol. **53**:1485–1494.
45. **Lücker S, Wagner M, Maixner F, Pelletier E, Koch H, Vacherie B, Rattei T, DamstÉ JS, Spieck E, Le Paslier D, Daims H.** 2010. A *Nitrospira* metagenome illuminates the physiology and evolution of globally important nitrite-oxidizing bacteria. Proc. Natl. Acad. Sci. U. S. A. **107**:13479–13484.
46. **Fuchs BM, Glöckner FO, Wulf J, Amann R.** 2000. Unlabeled helper

oligonucleotides increase the in situ accessibility to 16S rRNA of fluorescently labeled oligonucleotide probes. Appl. Environ. Microbiol. **66**:3603–3607.
47. **Pedros-Alio C.** 2006. Marine microbial diversity: can it be determined? Trends Microbiol. **14**:257–263.
48. **Nikolausz M, Marialigeti K, Kovacs G.** 2004. Comparison of RNA- and DNA-based species diversity investigations in rhizoplane bacteriology with respect to chloroplast sequence exclusion. J. Microbiol. Methods **56**:365–373.
49. **Liles MR, Manske BF, Bintrim SB, Handelsman J, Goodman RM.** 2003. A census of rRNA genes and linked genomic sequences within a soil metagenomic library. Appl. Environ. Microbiol. **69**:2684–2691.
50. **Fluiter K, Frieden M, Vreijling J, Koch T, Baas F.** 2005. Evaluation of LNA-modified DNAzymes targeting a single nucleotide polymorphism in the large subunit of RNA polymerase II. Oligonucleotides **15**:246–254.
51. **Hartmann M, Widmer F.** 2008. Reliability for detecting composition and changes of microbial communities by T-RFLP genetic profiling. FEMS Microbiol. Ecol. **63**:249–260.
52. **Suzuki MT, Giovannoni SJ.** 1996. Bias caused by template annealing in the amplification of mixtures of 16S rRNA genes by PCR. Appl. Environ. Microbiol. **62**:625–630.
53. **Donini S, Clerici M, Wengel J, Vester B, Peracchi A.** 2007. The advantages of being locked. Assessing the cleavage of short and long RNAs by locked nucleic acid-containing 8-17 deoxyribozymes. J. Biol. Chem. **282**:35510–35518.
54. **Fuchs BM, Wallner G, Beisker W, Schwippl I, Ludwig W, Amann R.** 1998. Flow cytometric analysis of the in situ accessibility of Escherichia coli 16S rRNA for fluorescently labeled oligonucleotide probes. Appl. Environ. Microbiol. **64**:4973–4982.
55. **Fuchs BM, Syutsubo K, Ludwig W, Amann R.** 2001. In situ accessibility of Escherichia coli 23S rRNA to fluorescently labeled oligonucleotide probes. Appl. Environ. Microbiol. **67**:961–968.
56. **Loy A, Maixner F, Wagner M, Horn M.** 2007. probeBase—an online resource for rRNA-targeted oligonucleotide probes: new features 2007. Nucleic Acids Res. **35**:D800–D804. doi:10.1093/nar/gkl856.
57. **Loy A, Arnold R, Tischler P, Rattei T, Wagner M, Horn M.** 2008. probeCheck—a central resource for evaluating oligonucleotide probe coverage and specificity. Environ. Microbiol. **10**:2894–2898.
58. **Manefield M, Whiteley AS, Griffiths RI, Bailey MJ.** 2002. RNA stable isotope probing, a novel means of linking microbial community function to phylogeny. Appl. Environ. Microbiol. **68**:5367–5373.
59. **Amann RI, Ludwig W, Schleifer K-H.** 1995. Phylogenetic identification and in situ detection of individual microbial cells without cultivation. Microbiol. Rev. **59**:143–169.
60. **Kunin V, Engelbrektson A, Ochman H, Hugenholtz P.** 2010. Wrinkles in the rare biosphere: pyrosequencing errors can lead to artificial inflation of diversity estimates. Environ. Microbiol. **12**:118–123.
61. **Quince C, Lanzen A, Curtis TP, Davenport RJ, Hall N, Head IM, Read LF, Sloan WT.** 2009. Accurate determination of microbial diversity from 454 pyrosequencing data. Nat. Methods **6**:639–641.
62. **Pester M, Bittner N, Deevong P, Wagner M, Loy A.** 2010. A 'rare biosphere' microorganism contributes to sulfate reduction in a peatland. ISME J. **4**:1591–1602.

Supplemental material

Depletion of Unwanted Nucleic Acid Templates by Selective Cleavage: LNAzymes, Catalytically Active Oligonucleotides Containing Locked Nucleic Acids, Open a New Window for Detecting Rare Microbial Community Members

Jan Dolinšek, Christiane Dorninger, Ilias Lagkouvardos, Michael Wagner, Holger Daims

Department of Microbial Ecology, Ecology Centre, University of Vienna, Vienna, Austria;

Appl. Environ. Microbiol., March 2013, vol. 79, no. 5, p. 1534-1544

Supplemental Text: Discussion

Many of the accompanying organisms detected in the *Ca*. N. defluvii enrichment were closely related to cultured bacteria or to 16S rRNA gene sequences retrieved in other studies from wastewater treatment facilities such as nitrifying or denitrifying bioreactors (Table S2). As *Ca*. N. defluvii has been enriched from activated sludge (1), these results suggest that most members of the accompanying community also stem from the original inoculum and were not introduced by later contamination of the enrichment in the laboratory or by us via contaminated reagents used for the various steps in the protocol prior to the final RT-PCR (2). The enrichment of *Ca*. N. defluvii was started in the year 1997 (1), so that most accompanying populations may have been co-cultured with *Nitrospira* for more than a decade. The amounts of non-*Nitrospira* cells in the enrichment varied during this period (1; and unpublished data of the authors), but despite extended efforts, these organisms could not be completely removed to obtain a pure culture of *Ca*. N. defluvii. Thus, it is tempting to speculate that they are persistent commensals or even mutualistic symbionts of *Nitrospira*. The closest cultured relatives of some accompanying organisms are heterotrophs growing on a broad range of organic substrates including carbohydrates, which may be components of the extracellular matrix formed by *Ca*. N. defluvii (1). Members of the *Bacteroidetes*, for example, are known to degrade biopolymers and high-molecular-weight dissolved organic matter (3), and were present in the *Ca.* N. defluvii enrichment (Table S2). Heterotrophic commensals may also feed on lysed *Nitrospira* biomass or may use soluble organic compounds released by the autotrophic nitrifiers (4, 5). Two of the cultured heterotrophic relatives, *Afipia birgiae* and *Terrimonas lutea* (Table S2), are known to reduce nitrate (6, 7). Nitrate reducers would benefit from the nitrate produced by *Nitrospira* from nitrite, especially if they grow in the possibly oxygen-depleted central regions of the large flocs formed by *Nitrospira* in this culture. In addition, nitrate reduction by such organisms could

attenuate end-product inhibition by nitrate of *Nitrospira*, which has been observed for *N. moscoviensis* (8) and also for *Ca.* N. defluvii whose microcolonies disintegrate after nitrate accumulation (1).

References

1. **Spieck E, Hartwig C, McCormack I, Maixner F, Wagner M, Lipski A, Daims H.** 2006. Selective enrichment and molecular characterization of a previously uncultured *Nitrospira*-like bacterium from activated sludge. Environ. Microbiol. **8:**405-415.
2. **Tanner MA, Goebel BM, Dojka MA, Pace NR.** 1998. Specific ribosomal DNA sequences from diverse environmental settings correlate with experimental contaminants. Appl. Environ. Microbiol. **64:**3110-3113.
3. **Cottrell MT, Kirchman DL.** 2000. Natural assemblages of marine proteobacteria and members of the *Cytophaga-Flavobacter* cluster consuming low- and high-molecular-weight dissolved organic matter. Appl. Environ. Microbiol. **66:**1692-1697.
4. **Kindaichi T, Ito T, Okabe S.** 2004. Ecophysiological interaction between nitrifying bacteria and heterotrophic bacteria in autotrophic nitrifying biofilms as determined by microautoradiography-fluorescence in situ hybridization. Appl. Environ. Microbiol. **70:**1641-1650.
5. **Rittmann BE, Regan JM, Stahl DA.** 1994. Nitrification as a source of soluble organic substrate in biological treatment. Water Sci. Technol. **30:**1-8.
6. **La Scola B, Mallet MN, Grimont PA, Raoult D.** 2002. Description of *Afipia birgiae* sp. nov. and *Afipia massiliensis* sp. nov. and recognition of *Afipia felis* genospecies A. Int. J. Syst. Evol. Microbiol. **52:**1773-1782.

7. **Xie CH, Yokota A.** 2006. Reclassification of [*Flavobacterium*] *ferrugineum* as *Terrimonas ferruginea* gen. nov., comb. nov., and description of *Terrimonas lutea* sp. nov., isolated from soil. Int. J. Syst. Evol. Microbiol. **56:**1117-1121.

8. **Ehrich S, Behrens D, Lebedeva E, Ludwig W, Bock E.** 1995. A new obligately chemolithoautotrophic, nitrite-oxidizing bacterium, *Nitrospira moscoviensis* sp. nov. and its phylogenetic relationship. Arch. Microbiol. **164:**16-23.

Table S1. Primers, oligonucleotide probes, and LNAzymes used in this study.

Oligonucleotide	Sequence (5´- 3´)
Probes used for FISH	
Ntspa1431 (6)	TTG GCT TGG GCG ACT TC
EUB338 (1)	GCT GCC TCC CGT AGG AGT
EUB338-II (2)	GCA GCC ACC CGT AGG TGT
EUB338-III (2)	GCT GCC ACC CGT AGG TGT
PCR Primers	
1492R (5)	GGY TAC CTT GTT ACG ACT T
8F (modified) (3, 4)	AGA GTT TGA TYM TGG CTC
T3-8F (7)	AAT TAA CCC TCA CTA AAG GG AGA GTT TGA TYM TGG CTC
907R (5)	CCG TCA ATT CMT TTG AGT TT
LNAzymes	
Ntspa668 (this study)[1]	**CTA CAC CGG GAA** GGC TAG CTA CAA CGA **TCC GCG CTC C**
Ntspa665 (this study)[1]	**CCG CTA CAC CGG GAA** GGC TAG CTA CAA CGA **TCC GCG CTC CTC TCC**
Nso215 (this study)[1]	**AAC TAG CTA ATC AGA** GGC TAG CTA CAA CGA **ATC GGC CRC TCC**
Helper probes	
Ntspa630help (this study)	CCT CTA GCC KRG CAG TMC CCT CYG CRC TTT CC
Ntspa700help (this study)	GCC ACC GGC CTT CCT CCC GAT CTC TAC GC

[1] LNA nucleotides are underlined and substrate-binding arms are in boldface.

References

1. **Amann, R. I., B. J. Binder, R. J. Olson, S. W. Chisholm, R. Devereux, and D. A. Stahl.** 1990. Combination of 16S rRNA-targeted oligonucleotide probes with flow cytometry for analyzing mixed microbial populations. Appl. Environ. Microbiol. **56:**1919-1925.
2. **Daims, H., A. Brühl, R. Amann, K.-H. Schleifer, and M. Wagner.** 1999. The domain-specific probe EUB338 is insufficient for the detection of all *Bacteria*: Development and evaluation of a more comprehensive probe set. System. Appl. Microbiol. **22:**434-444.
3. **Hicks, R. E., R. I. Amann, and D. A. Stahl.** 1992. Dual staining of natural bacterioplankton with 4',6-diamidino-2-phenylindole and fluorescent oligonucleotide probes targeting kingdom-level 16S rRNA sequences. Appl. Environ. Microbiol. **58:**2158-2163.
4. **Juretschko, S., G. Timmermann, M. Schmid, K.-H. Schleifer, A. Pommerening-Röser, H.-P. Koops, and M. Wagner.** 1998. Combined molecular and conventional analyses of nitrifying bacterium diversity in activated sludge: *Nitrosococcus mobilis* and *Nitrospira*-like bacteria as dominant populations. Appl. Environ. Microbiol. **64:**3042-3051.
5. **Lane, D. J.** 1991. 16S/23S rRNA sequencing, p. 115-175. *In* E. Stackebrandt and M. Goodfellow (ed.), Nucleic acid techniques in bacterial systematics. John Wiley & Sons, Inc., New York.
6. **Maixner, F., D. R. Noguera, B. Anneser, K. Stoecker, G. Wegl, M. Wagner, and H. Daims.** 2006. Nitrite concentration influences the population structure of *Nitrospira*-like bacteria. Environ. Microbiol. **8:**1487-1495.
7. **Steger, D., D. Berry, S. Haider, M. Horn, M. Wagner, R. Stocker, and A. Loy.** 2011. Systematic spatial bias in DNA microarray hybridization is caused by probe spot position-dependent variability in lateral diffusion. PLoS ONE **6:**e23727.

Table S2. 16S rRNA sequences retrieved from clone libraries that were established from the Ca. Nitrospira deluvii enrichment with preceding treatment by LNAzymes targeting Ca. N. defluvii.

Next cultured relative (identity)	Next uncultured relative, GenBank accession no. (identity)	Sequences from 8F - 907R RNA library	Sequences from 8F - 1492R RNA library	Sequences from 8F - 907R DNA library
Betaproteobacteria				
Methyloversatilis universalis (99.1 %)	denitrifying sequencing batch reactor clone, HQ703525 (99.9 %)		2	
Methyloversatilis universalis (98.6 %)	denitrifying fluidized bed reactor clone, DQ202141 (99.7 %)	1		1
Rubrivivax gelatinosus (96.5 %)	activated sludge clone, EU283352 (98.7 %)		1	
Denitratisoma oestradiolicum (91.9 %)	denitrifying bioreactor clone, FJ167494 (99.7 %)		1	
Variovorax paradoxus (99.8 %)	biofilm on oxygen-transfer membrane clone, AY444994 (99.8 %)			1
Alphaproteobacteria				
Meganema perideroedes (90.8 %)	soil clone, GQ169020 (98.2 %)	1	1	2
Caedibacter caryophilus (88.0 %)	autotrophic nitrifying biofilm reactor clone, FJ529966 (94.9 %)	1		
Geminicoccus roseus (85.5 %)	activated sludge clone, HQ385549 (98.8 %)	1		
Rhodobacter litoralis (95.4 %)	autotrophic nitrifying biofilm reactor clone, FJ529978 (98.4 %)		2	
Pelagibius litoralis (93.1 %)	soil clone, HQ727620 (96.13 %)		1	
Afipia birgiae (99.6 %)	clean room clone, EU071489 (99.9 %)			1
Bacteroidetes				
Terrimonas lutea (95.0 %)	activated sludge clone, FJ536929 (99.3 %)	2		2
Flexibacter flexilis (83.8 %)	Hanford site subsurface clone, HM186924 (91.8 %)	4	5	4
Chlorobi				
N.A.	iron snow from acidic coal clone, FR667812 (92.9 %)	2		
Gemmatimonadetes				
Gemmatimonas aurantiaca (90.1 %)	oil seep clone, EF157193 (96.6 %)		1	
Actinobacteria				
Mycobacterium austroafricanum (99.8 %)	indoor dust clone, AM697434 (98.8 %)	2		
Cyanobacteria				
Gloeobacter violaceus (82.7 %)	human skin clone, JF219539 (100 %)	2		
Deinococcus-Thermus				
Meiothermus ruber (90.7 %)	compost clone, FN667273 (90.4 %)			2

Figure S1

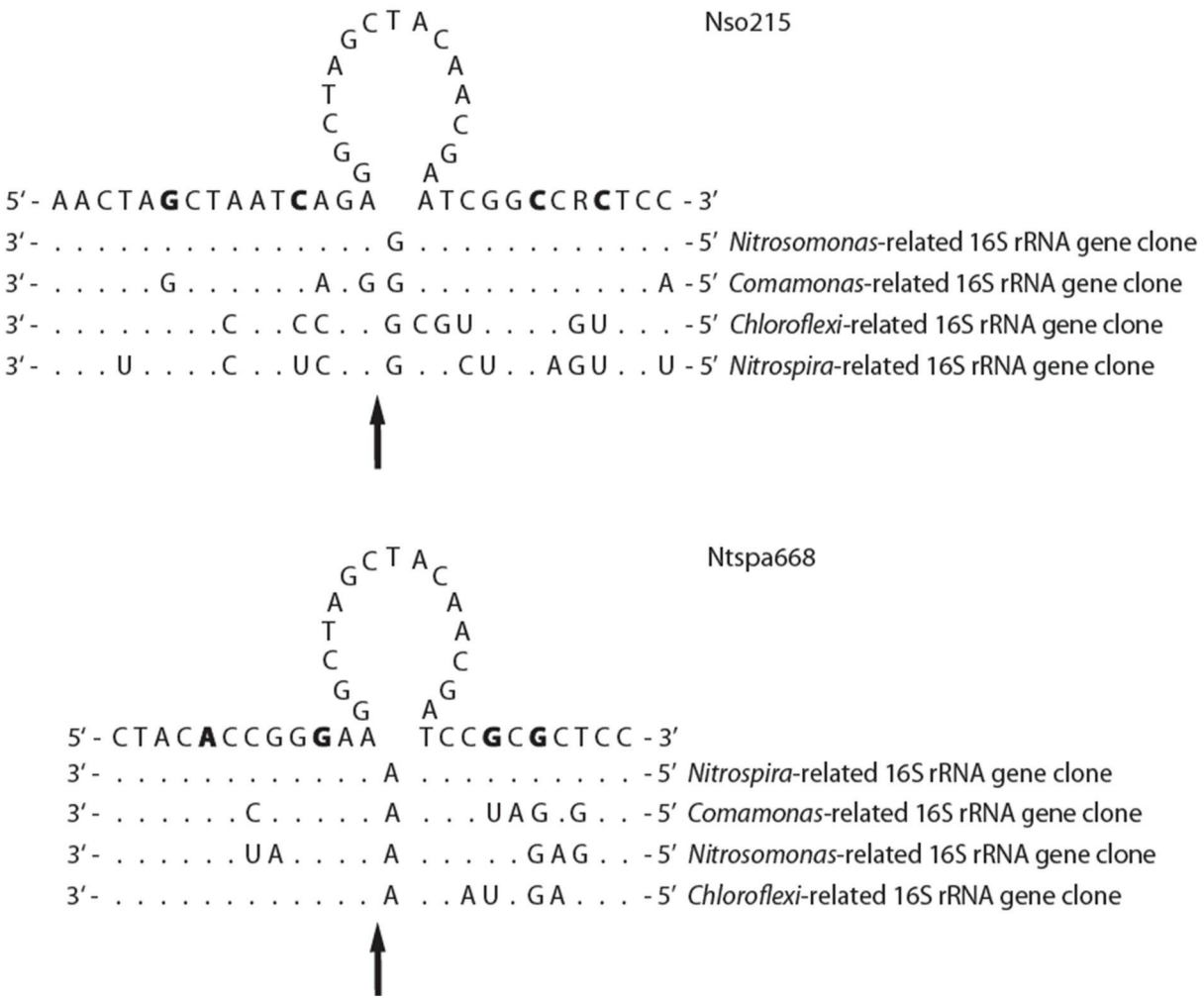

Fig. S1. Sequence alignments of the LNAzymes Nso215 and Ntspa668 to the respective binding regions on the four 16S rRNA genes, which were used in artificial mixtures to evaluate the LNAzymes and the cleavage protocol (see also Table 1 and Fig. 3 in the main text). LNA residues are printed in boldface. Base mismatches between the substrate-binding arms of the LNAzymes and the 16S rRNA sequences are indicated by capital letters, whereas full matches (complementary bases) are indicated by dots. Arrows indicate the cleavage sites.

Figure S2 A

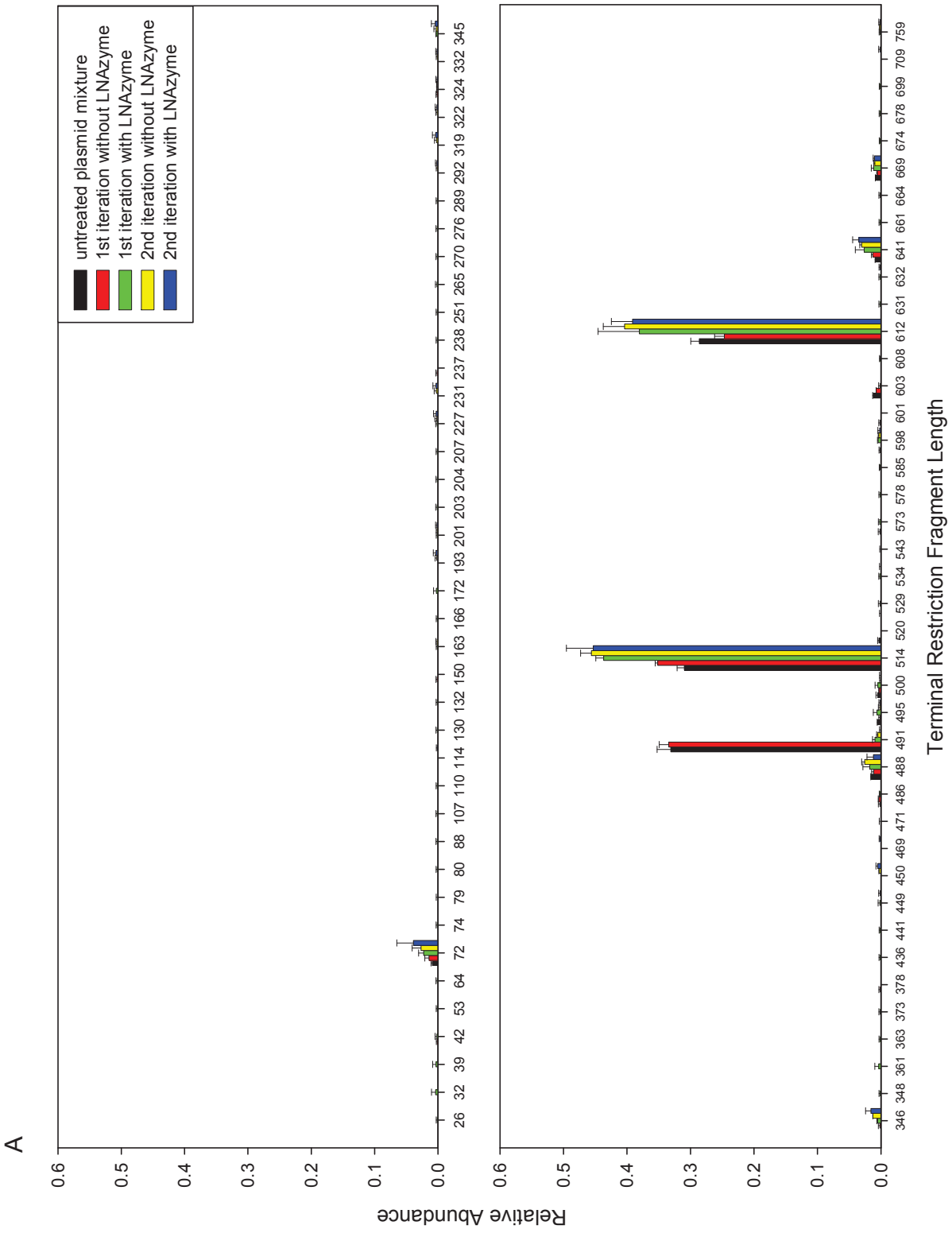
A
untreated plasmid mixture
1st iteration without LNAzyme
1st iteration with LNAzyme
2nd iteration without LNAzyme
2nd iteration with LNAzyme
Relative Abundance
Terminal Restriction Fragment Length

Figure S2 B

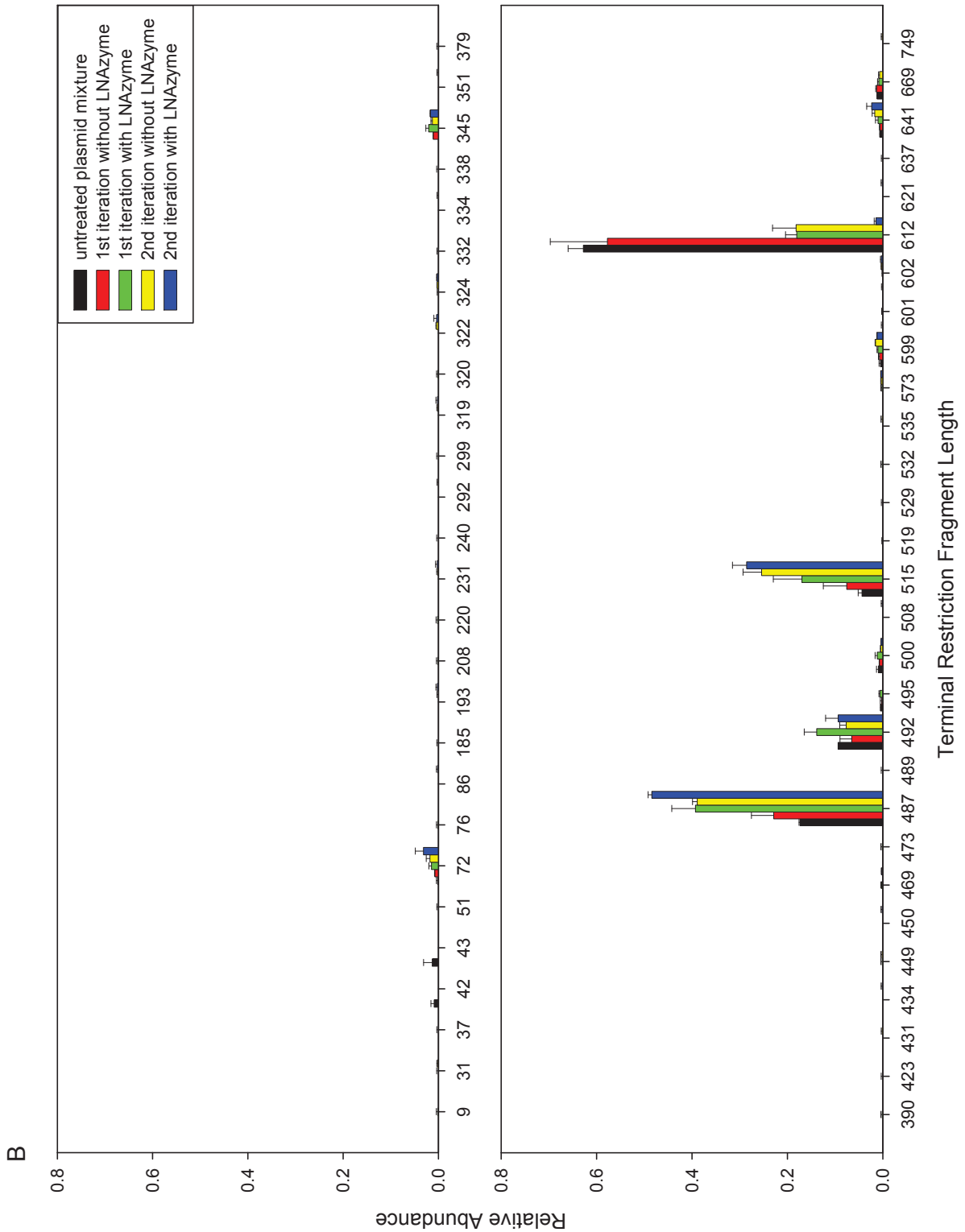
B
untreated plasmid mixture
1st iteration without LNAzyme
1st iteration with LNAzyme
2nd iteration without LNAzyme
2nd iteration with LNAzyme
Relative Abundance
0.0
0.2
0.4
0.6
0.8
9 31 37 42 43 51 72 76 86 185 193 208 220 231 240 292 299 319 320 322 324 332 334 338 345 351 379
390 423 431 434 449 450 469 473 487 489 492 495 500 508 515 519 529 532 535 573 599 601 602 612 621 637 641 669 749
Terminal Restriction Fragment Length

Figure S2 C

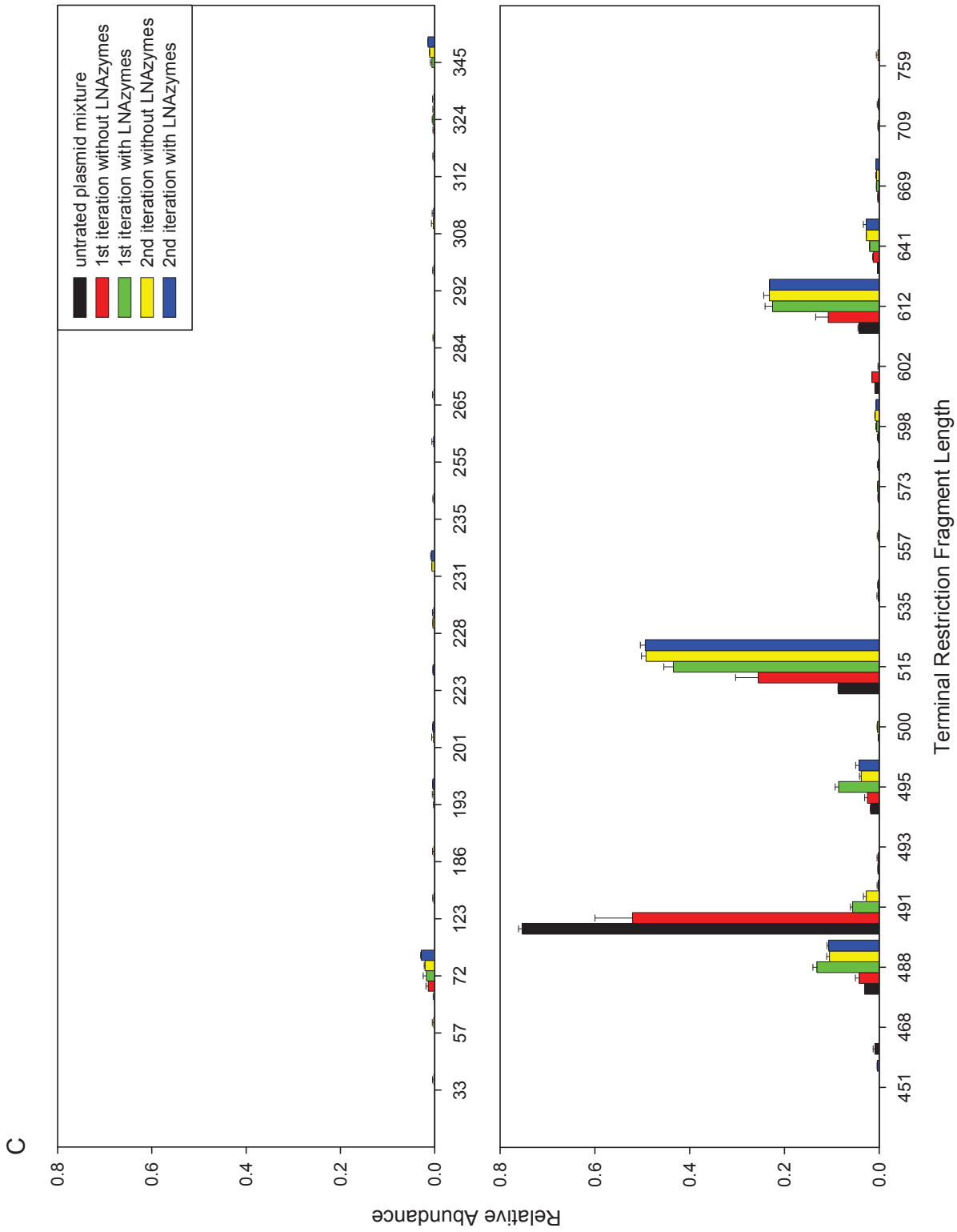
C
untrated plasmid mixture
1st iteration without LNAzymes
1st iteration with LNAzymes
2nd iteration without LNAzymes
2nd iteration with LNAzymes
Relative Abundance
0.0
0.2
0.4
0.6
0.8
33
57
72
123
186
193
201
223
228
231
235
255
265
284
292
308
312
324
345
451
468
488
491
493
495
500
515
535
557
573
598
602
612
641
669
709
759
Terminal Restriction Fragment Length

Figure S2 D

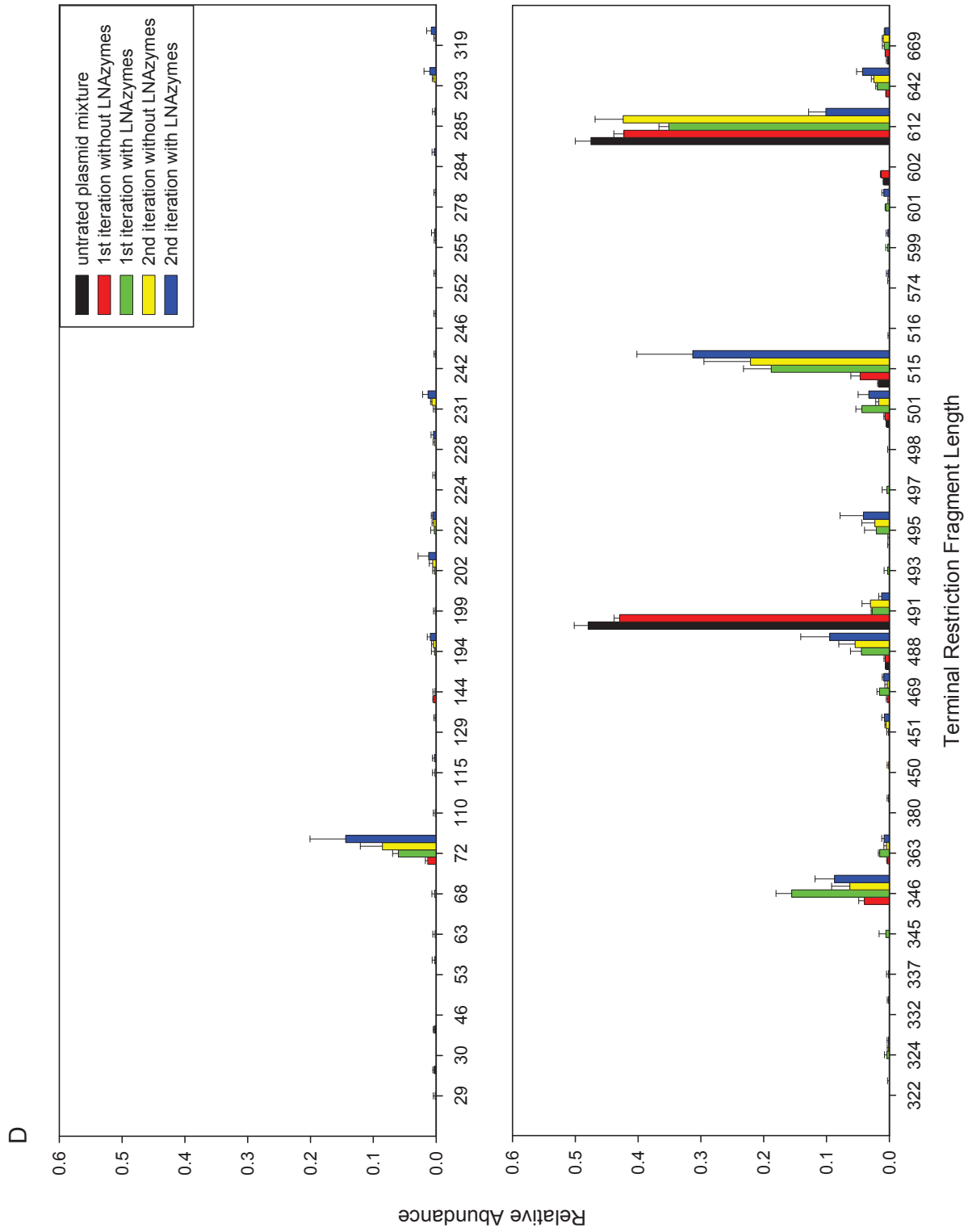
D
untrated plasmid mixture
1st iteration without LNAzymes
1st iteration with LNAzymes
2nd iteration without LNAzymes
2nd iteration with LNAzymes
Relative Abundance
Terminal Restriction Fragment Length

Fig. S2. Evaluation of the LNAzyme cleavage protocol with artificial mixtures of cloned partial 16S rRNA genes (see Table 1 in the main text). The bars show the relative abundances of the rRNA genes in the mixtures before and after one or two iterations of the LNAzyme-mediated depletion of the *Nitrosomonas* and/or *Nitrospira* rRNA. Control experiments without added LNAzymes are also shown (the second iteration without LNAzyme was performed after a first iteration with LNAzyme). The relative abundances were determined by T-RFLP analysis. This figure shows the complete T-RFLP profiles, whereas Fig. 3 (main text) contains the relevant peaks only. Terminal restriction fragment lengths were determined to be 488 bases for *Commamonas*, 492 bases for *Nitrosomonas*, 515 bases for the *Chloroflexi*-related organism, and 612 bases for *Nitrospira*. Panels (A)-(D) show the same experiments as the respective panels of Fig. 3 (main text). The non-target peaks represent artifacts, which are common in T-RFLP analyses of mixed templates and may be caused by the presence of single-stranded PCR amplicons (1), the formation of heteroduplexes or chimeras (2), or by incomplete or unspecific cleavage of the targets by the restriction enzyme (3). Error bars depict standard deviations of three replicate experiments.

References

1. **Egert, M., and M. W. Friedrich.** 2003. Formation of pseudo-terminal restriction fragments, a PCR-related bias affecting terminal restriction fragment length polymorphism analysis of microbial community structure. Appl. Environ. Microbiol. **69:**2555-2562.
2. **Hartmann, M., and F. Widmer.** 2008. Reliability for detecting composition and changes of microbial communities by T-RFLP genetic profiling. FEMS Microbiol. Ecol. **63:**249-260.
3. **Osborn, A. M., E. R. B. Moore, and K. N. Timmis.** 2000. An evaluation of terminal-restriction fragment length polymorphism (T-RFLP) analysis for the study of microbial community structure and dynamics. Environ. Microbiol. **2:**39-50.

Figure S3 A

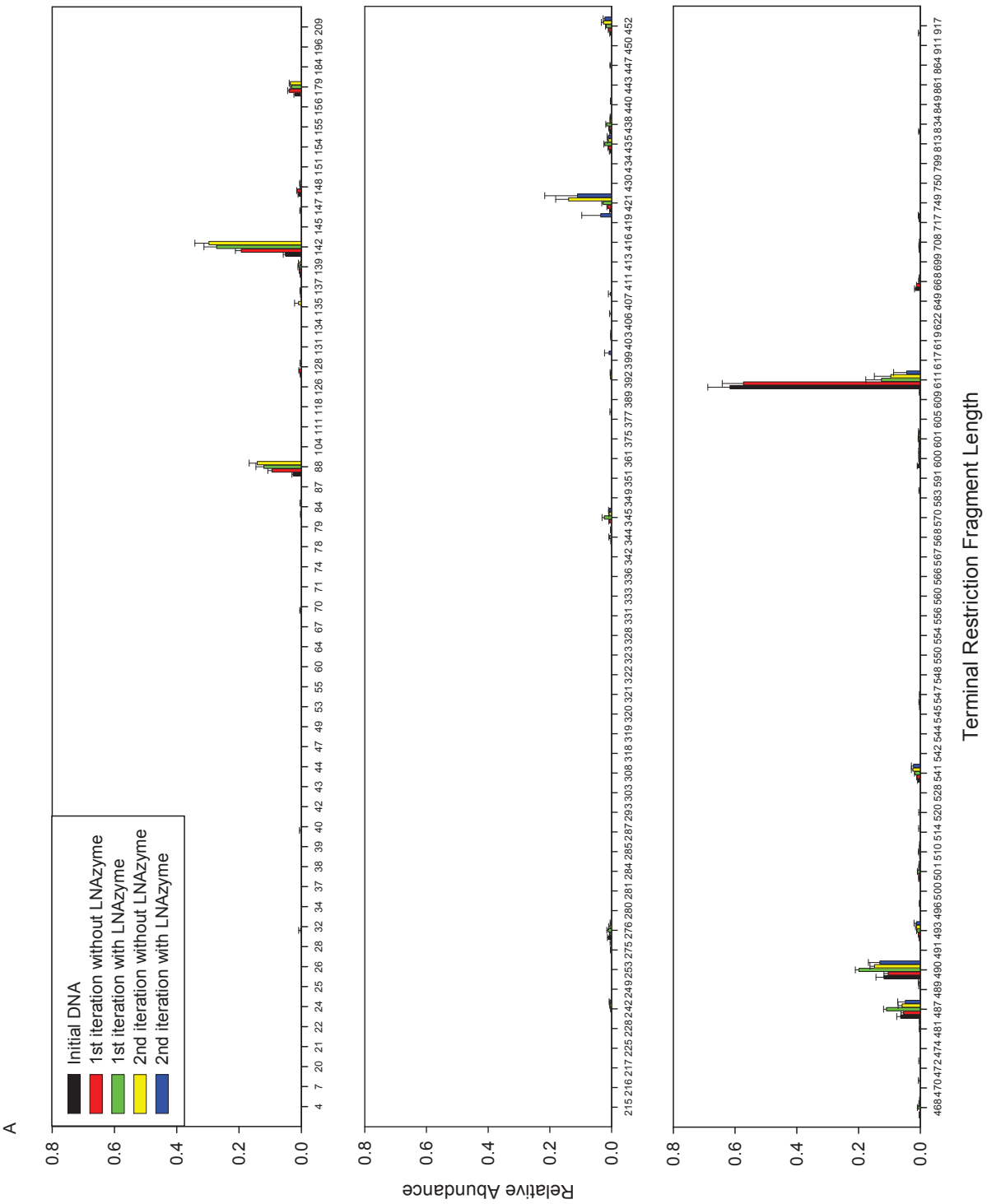
A
Initial DNA
1st iteration without LNAzyme
1st iteration with LNAzyme
2nd iteration without LNAzyme
2nd iteration with LNAzyme
Relative Abundance
Terminal Restriction Fragment Length

Figure S3 B

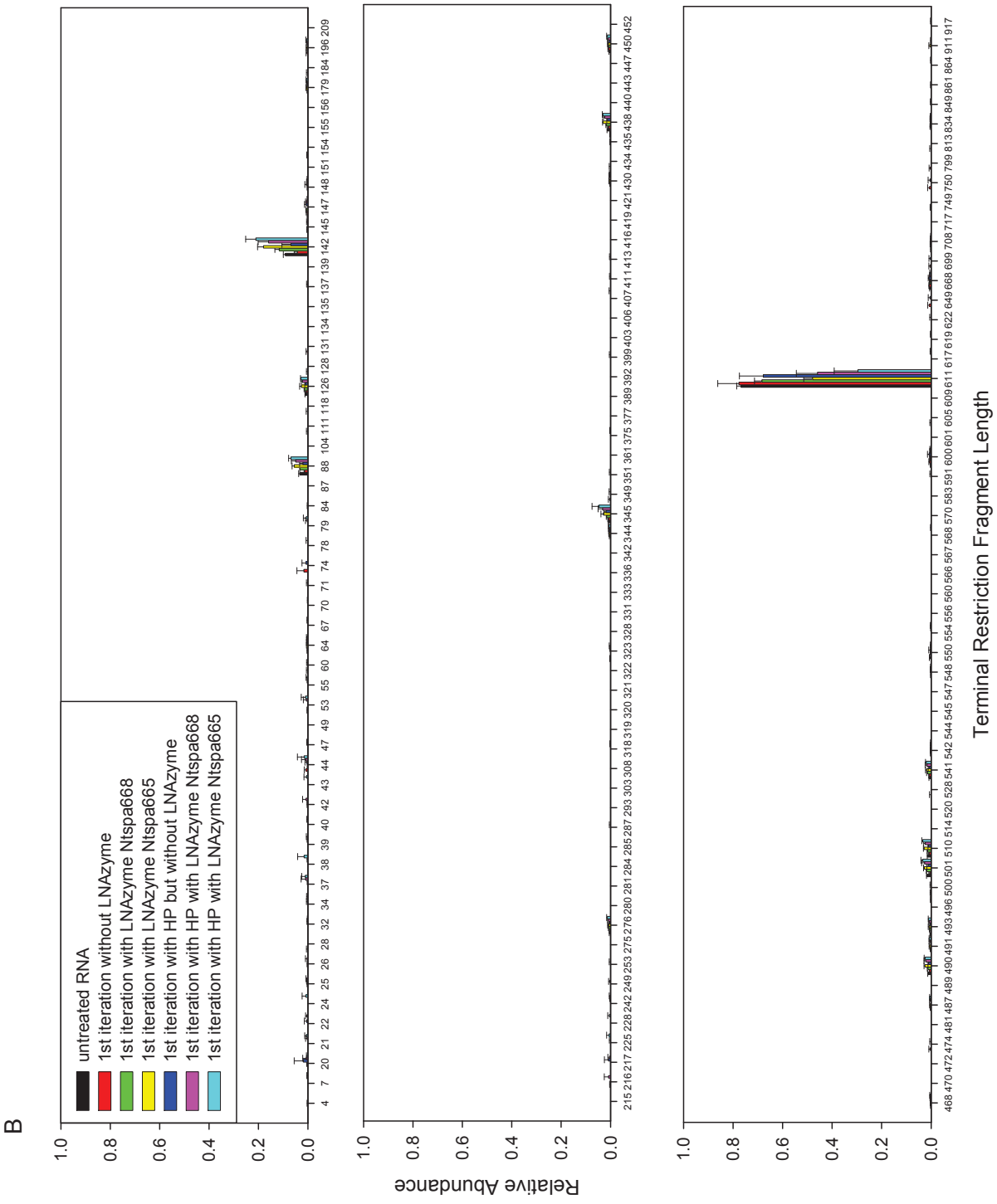
B
untreated RNA
1st iteration without LNAzyme
1st iteration with LNAzyme Ntspa668
1st iteration with LNAzyme Ntspa665
1st iteration with HP but without LNAzyme
1st iteration with HP with LNAzyme Ntspa668
1st iteration with HP with LNAzyme Ntspa665
Relative Abundance
Terminal Restriction Fragment Length

Fig. S3. Depletion of the 16S rRNA of *Ca*. N. defluvii from (A) DNA or (B) native RNA that was extracted from the *Ca*. N. defluvii enrichment culture. The bars show the relative abundances of the 16S rRNA genes of *Ca*. N. defluvii and of other bacteria before and after one or two iterations of the LNAzyme-mediated depletion. Control experiments without added LNAzymes are also shown (the second iteration without LNAzyme was performed after a first iteration with LNAzyme). The relative abundances were determined by T-RFLP analysis. This figure shows the complete T-RFLP profiles, whereas Fig. 4 (main text) contains selected peaks only. Applied LNAzymes were Ntspa668 (panel A) and Ntspa668 or Ntspa665 (panel B, which also shows the effects of additional helper probes on the efficiency of target depletion). HP = helper probes. Error bars depict standard deviations of three replicate experiments.

Figure S4

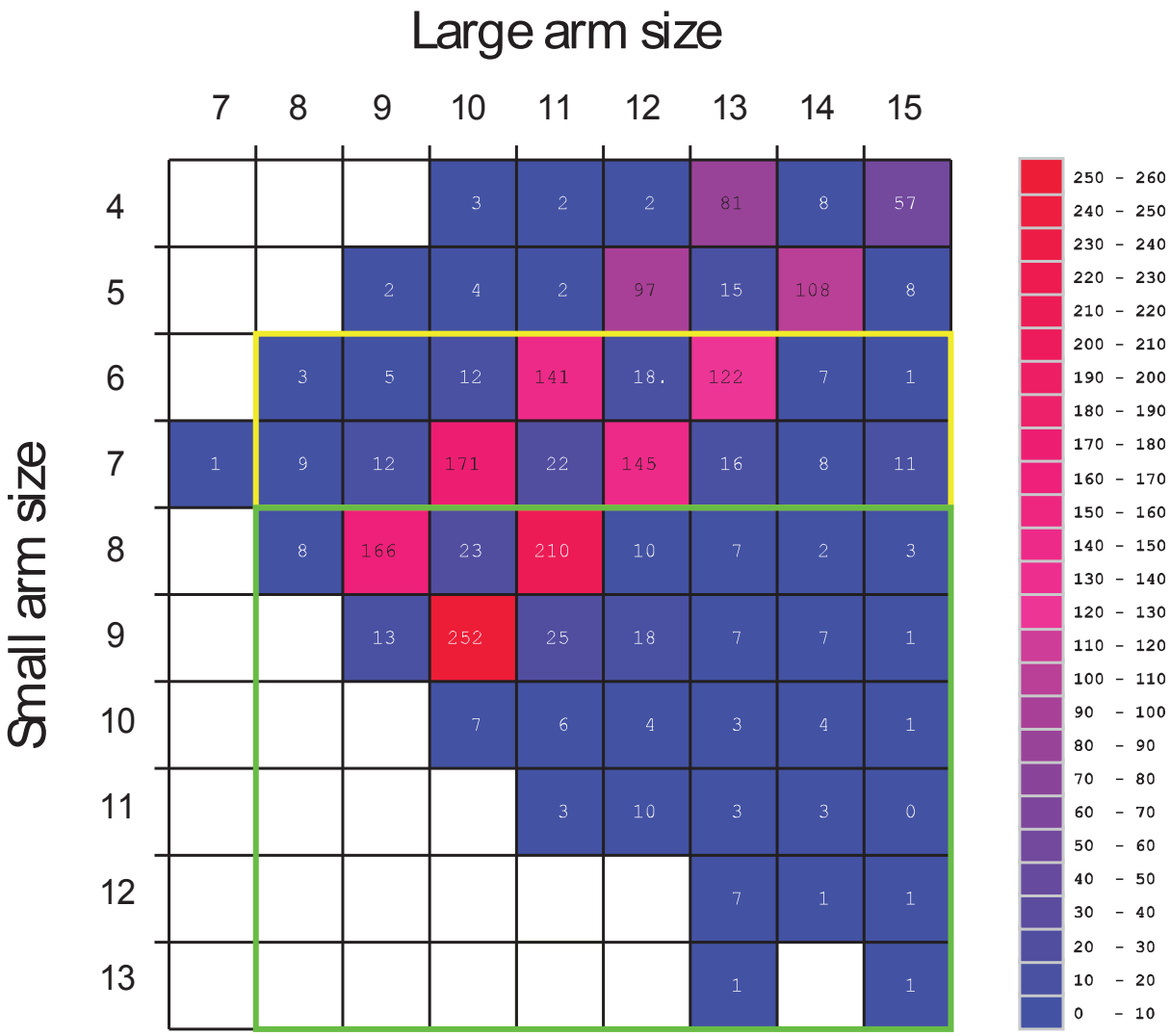

Fig. S4. Heatmap analysis of published rRNA-targeted probes (deposited in probeBase) that contain at least one RU cleavage site in their target region and thus are promising starting points for the design of specific LNAzymes. For each probe the lengths of the substrate-binding arms (in nucleotides), which would determine the suitability of the probes for use as LNAzymes, was determined and probe numbers for different arm lengths are presented. Probes that contained an RU cleavage site, but had arm lengths below or above the indicated ranges, were excluded from the analysis. The green rectangle encloses probes that may be used as efficient LNAzymes without elongation of any substrate-binding arm (i.e., the sequences upstream and downstream of the most centrally located RU cleavage site). The yellow rectangle encloses probes that might need elongation (in one direction) by a few

nucleotides to become efficient LNAzymes. The remaining probes have at least one very short substrate-binding arm, indicating that more extensive changes may be required for LNAzyme design based on these probes, which might lead to a reduced specificity and/or target group coverage. Please note that these assessments of LNAzyme efficiency are based on the results of this study and could be subject to modification when more rRNA-targeted LNAzymes have been designed and used in practice.

Chapter IV

CARD-FISH Method Exploiting Click Chemistry for *In Situ* Identification of Microbes

CARD-FISH Method Exploiting Click Chemistry for *In Situ* Identification of Microbes

Jan Dolinšek[1], Faris Behnam[1], Arno Schintlmeister[2], Andreas Anderluh[1*], Stephanie A. Eichorst[1], Alexander Galushko[1], Holger Daims[1] and Michael Wagner [1, 2]#

[1]Department of Microbiology and Ecosystem Research, Division of Microbial Ecology, University of Vienna, Vienna, Austria; [2]Large Instrument Facility for Advanced Isotope Research, University of Vienna, Vienna, Austria

Running Head: CARD-FISH Method employing Click Chemistry

*Present address: Andreas Anderluh, Institute of Applied Physics, Vienna University of Technology, Vienna, Austria

Abstract

In situ identification of microbes using catalyzed reporter deposition fluorescence *in situ* hybridization (CARD-FISH) with rRNA-targeted oligonucleotide probes is an important and widely applied tool for environmental and medical microbiologists. Here we present an easy-to-use CARD-FISH method that employs click-chemistry for the detection of rRNA-bound oligonucleotide probes within single microbial cells. Click CARD-FISH was successfully used to specifically detect bacteria and archaea in a collection of samples containing complex microbial communities, including sections embedded in three commonly used embedding media. Compared to CARD-FISH, Click CARD-FISH can improve the signal intensity of the labeled microbes. In addition, Click CARD-FISH was applied to label probe-identified bacteria with fluorine or deuterium for subsequent detection in NanoSIMS analyses. Its high signal intensity, specificity, and broad applicability should render Click-CARD-FISH an attractive method for all researchers interested in the *in situ* analyses that extend beyond fluorescence signal detection.

Introduction

Fluorescence *in situ* hybridization (FISH) with dye-labeled rRNA-targeted oligonucleotide probes is the most direct way to detect and identify microorganisms in medical or environmental samples. This technique was introduced for phylogenetic staining of microbes more than 20 years ago (1) and is considered today by many researchers as the gold standard for quantification of members of abundant microbial clades in complex communities (2-4). In contrast to the various DNA sequencing-based techniques, which are also available for studying microbial community structures, FISH results are not influenced by rRNA gene copy number variations (5, 6), polyploidy (7-9), DNA-extraction and PCR-amplification biases (10-13) as well as artifacts of cloning (14, 15) or sequencing (16). However, insufficient signal intensity of FISH-stained microbes caused by a low cellular ribosome content (2) and/or selection of probe target sites with limited accessibility (17-19) often hampers the application of this method in its conventional format. Consequently, considerable effort has been invested to develop techniques for amplification of FISH signals (20), which are often based on the use of multilabeled polynucleotide probes (21-23) and/or catalyzed reporter deposition (CARD) of dye-labeled tyramides via horseradish-peroxidase

(HRP) conjugated nucleic acid probes (24, 25). CARD-FISH with HRP-labeled oligonucleotides is about 26-41x more sensitive than conventional FISH, but still requires at least 36-54 target molecules per cell if applied in environmental samples with an average autofluorescence background (26).

The signal amplification achievable with CARD-FISH is also exploited for efficient labeling of microbes in Nano secondary ion mass spectrometry (NanoSIMS) single cell stable isotope probing experiments (27). Here, the tyramides deposited by CARD in the target cell are labeled with a halogen-containing fluorescent dye like Oregon Green® 488-X allowing the mass spectrometric detection of hybridized cells by their halogen signal (28, 29). However, FISH signal amplification is not only used for improving the identification of microbes, but it has also enabled microbial ecologists to detect specific mRNA molecules or even single genes within individual prokaryotic cells (30) though these approaches are still tedious, require special skills and need to be adapted for each sample.

Due to the importance of FISH techniques offering the straightforward deposition of various labels within the target cell, we aimed to develop a new CARD-ISH procedure that offers more labeling flexibility than conventional CARD-FISH. For this purpose we explored a combination of CARD-ISH and click chemistry (31-34) for specific labeling of microbial target cells. We focused on click reactions between (cyclo-)alkyne groups and azides, which can react with each other in a Cu(I)-catalyzed (3+2] cycloaddition (35, 36) or in a copper-free strain-promoted azide-alkyne cycloaddition (SPAAC) (37). In this approach cells can either be labeled with a compound containing an azide or an (cyclo)alkyne group (38-41). A major advantage of these click reactions is their high specificity as azides and alkynes show little side reactivity with other functional groups found in biological systems under the commonly used mild reaction conditions. Furthermore, reactive azide groups are absent in biological systems (31), but a few compounds with alkyne groups exist in cells (42).

Pioneering studies in microbiology have used azide-labeled lysostaphin for detection of *Staphylococcus aureus* via SPAAC (43) as well as an azide-labeled component of the lipopolysaccharide for activity staining of Gram-negative bacteria (44) and an alkyne-labeled modified deoxynucleoside for detection of phages within their bacterial hosts (45) via Cu(I)-catalyzed (3+2] cycloaddition. However, click-chemistry has to the best of our knowledge not yet been exploited for FISH-based detection of microbes.

In order to combine CARD-ISH with specific click labeling we modified tyramine with a bicyclo(6.1.0]nonyne (BCN) group that readily reacts with azides in SPAAC reaction (46). Using this approach, bacteria and archaea in artificial mixtures and complex natural samples

were successfully labeled with azide-bearing fluorophores. We demonstrated single-mismatch discriminating potential of this "Click-CARD-FISH" (CCF) procedure, showed that it can yield higher signal intensity than conventional CARD-FISH, and pointed on its versatility by simultaneously labeling target cells with deuterium and a fluorescence dye for combined fluorescence microscopy and NanoSIMS analyses.

Materials and Methods

Bacterial strains and environmental samples: *Escherichia coli* (DSM 498)*, Burkholderia cepacia* (DSM 7288) and *Bacillus subtilis* (DSM 10) were grown in LB medium (47) at 37°C under vigorous shaking until OD600 reached ≈ 0.8. For NanoSIMS analyses, *E. coli* and *B. subtilis* were grown in mineral medium that contained per liter 12.8 g Na_2HPO_4, 3.0 g KH_2PO_4, 0.5 g NaCl, 0.5 g $MgSO_4 \times 7H_2O$, 0.015 g $CaCl_2 \times 2H_2O$, 1.0 g NH_4Cl, 1 ml of non-chelated trace elements mixture and 1 ml of selenite-tungsten solution. Trace element solutions were prepared as described previously (48). Prior to filter-sterilization with 0.2 µm syringe filters (Asahi Glass Co. LTD, Yoshida, Japan), ^{13}C glucose was added to the medium to a final concentration of 2 g per liter. To ensure homogenous ^{13}C enrichment, cells from an overnight culture grown at 37°C under vigorous shaking were transferred twice to a new tube with the respective medium before cells were harvested by centrifugation at 14,000 × g for 5 min at 4°C and fixed using a slight modification of the procedures described previously (49). In short, bacteria were fixed by re-suspending the pellet in a 1:1 mixture (vol/vol) of 1 × phosphate-buffered saline (PBS):ethanol and stored at -20°C. Alternatively, cell pellets were resuspended in 2% formaldehyde in PBS and incubated at 4°C for 3 h. After three washes in ice-cold 1 × PBS (pH 7.5), cells were resuspended in a 1:1 mixture (vol/vol) of 1x PBS:ethanol and stored at -20°C. Environmental samples used in this study, sampling locations and enrichment conditions (if applicable) are shown in Table A1. All samples were fixed with formaldehyde prior to further analysis (49). The soil was homogenized by passage through a 2 mm sieve and fixed in 4% (v/v) formaldehyde for 1 hour at room temperature. Fixed samples were washed in 1 × PBS (pH 7.6) and stored in PBS and ethanol mixture at −20 °C until further analysis. Cells were detached from the soil using sonication and separated from soil particles using a nycodenz (Axis-Shield, Oslo, Norway) density gradient. Prior to hybridization, cells were filtered onto 0.2 µm polycarbonate filter (Millipore, Billerica, MA). Mouse gut samples were embedded in acrylic resin LR White (Ted Pella,

Redding, CA, USA), marine sponge samples in Neg-50 (Richard-Allan Scientific, Kalamazoo, MI, USA; now ThermoFischer) and biofilm from carstic cave in paraffin (Paraplast plus, Leica Microsystems, St. Louis, MO, USA). Subsequently sections with a thickness of approx. 0.5 µm (mouse gut), 4 µm (sponge samples) and 7 µm (cave biofilm) were obtained. Detailed descriptions of sample collection, embedding, and sectioning can be found elsewhere (50-52). Before hybridization, paraffin was removed from glass slides by two subsequent, 5 min washing steps in xylene (mixture of isomers; Carl Roth, Karlsruhe, Germany), followed by two 5 min washing steps in ethanol.

FISH-, CARD-FISH- and CCF-procedures: Probes labeled with fluorescent dyes or HRP were obtained from Thermo Fisher (Thermo Fisher Scientific, Ulm, Germany). The applied rRNA-targeted probes are listed in Table A2. After immobilization of fixed cells on teflon-coated 10 well glass slides (Marienfeld, Lauda-Königshofen, Germany), *in situ* hybridization was performed as described before (49) with hybridization and washing times of 1.5 h and 10 min, respectively. For FISH with 5´- and 3´-doubly labeled oligonucleotide probes (DOPE-FISH) and CARD-FISH, the procedures used by Stoecker et al. (20) and Hoshino *et al.* (26), respectively, were applied. For CARD-FISH 6-carboxyfluorescein- (6-FAM) tyramides, propargyl-dPEG®-tyramides, and BCN-tyramides (Figure A1 A-C) were used. For initial experiments these tyramides (with the exception of the 6-FAM tyramide) were synthesized in-house by using respective N-hydroxysuccinimide (NHS) esters purchased from Quanta Biodesign (Powell, OH, USA) and SynAffix B.V. (Nijmegen, Netherlands) in HPLC vials as reaction vessels as described before (53). Later on, 6-FAM- and BCN-tyramides with min. 95% purity were obtained from SynAffix. HRP-labeled probes EUB338, NON338 and Arch915 were used at a final concentration of 16 nM. During competitive hybridizations using probes GAM42a-HRP and BET42a-Cy5, the final probe concentration was 16 nM for either probe.

To allow the propargyl group of the propargyl-dPEG® tyramides after deposition in the target cells to react with 6-FAM azide (baseclick, Tutzing, Germany) (Figure A1, panel D), 20 µl of ice-cold reaction buffer (100 mM Tris-HCl pH 7, 2 mM $CuSO_4$, 25 µM 6-FAM azide, 100 mM ascorbic acid) was added to the cells and incubated on ice for 30 min. To label deposited tyramides carrying a BCN group within target cells, 20 µl of reaction buffer (identical in composition to the amplification buffer used for CARD-FISH but without tyramides and H_2O_2 but with 25 µM 6-FAM azide) was added and allowed to react for 30 min at room temperature. 6-FAM azide stock solution was prepared by resuspending the dye in a 3:1

(vol/vol) mixture of DMSO and *tert*-butanol (baseclick) to a final concentration of 1 mM. Subsequently, regardless of the click chemistry used, slides were washed three times for 5 minutes in 50 ml 1 × TTBS (50 mM Tris-base, 150 mM NaCl, 0.5% Triton X-100 (vol/vol); pH was adjusted to 7.2 with HCl] with slight shaking at room temperature. Finally, remaining salts and solutes were removed by dipping the slide in ice-cold deionized water for 10 seconds and drying it quickly with compressed air.

Fluorescent images were recorded with a Zeiss LSM 510 Meta confocal laser scanning microscope equipped with Argon (458, 477, 488, and 514 nm) and HeNe (543 and 633 nm) lasers. The *xy*-resolution of the images was 1024 × 1024 or 2048 × 2048 pixels, and at least 50 cells were analyzed for each fluorescence intensity data point. Signal intensities were analyzed by using the software package *daime* (4).

Nano-SIMS analysis: For NanoSIMS analysis, formaldehyde fixed cells or tissues were deposited onto boron-doped silicon wafers (7 × 7 × 0.7 mm) (Active Business Company GmbH, Munich, Germany) and allowed to dry. Cells were hybridized as described above, but higher grade chemicals were used (e.g. pure instead of technical ethanol) and after treatment cells were dried in a gas stream of high purity N_2 instead of compressed air. NanoSIMS measurements were carried out on a NS50L instrument from Cameca (Paris, France). Prior to data acquisition, analysis areas were pre-sputtered utilizing a high intensity, defocused Cs^+ primary ion beam. Data were acquired as multilayer image stacks obtained by sequential scanning of a finely focused Cs^+ primary ion beam over areas between 30 × 30 and 40 × 40 μm^2 with 512 × 512 pixel image resolution and approx. 80 nm physical resolution.

In the fluorine measurements, pre-sputtering was performed until a primary ion dose density of 1.4E16 ions/cm^2 was achieved. The detectors were positioned to enable parallel detection of $^{12}C^-$, $^{13}C^-$, $^{19}F^-$, $^{12}C^{14}N^-$ and $^{31}P^-$ secondary ions and the mass spectrometer was tuned to achieve a mass resolving power (MRP) of 9.100 (according to Cameca`s definition) at the mean radius of the C^- secondary ions. Images were recorded with a total dwell time of 45 msec/pixel.

In the deuterium measurements, pre-sputtering was finished at a primary ion dose density of 7.9E15 ions/cm^2 and the total dwell time for image acquisition was increased to 300 msec/pixel to improve counting statistics. The detectors were adjusted for simultaneous detection of $^{16}O^1H^-$, $^{16}O^2H^-$, $^{12}C_2^-$, $^{12}C^{13}C^-$ and $^{31}P^-$ secondary ions at a MRP of 10.200 and 13.400 for OH^- and C_2^- ions, respectively. It should be noted that $^{16}OH^-$ molecular ions were selected for determination of the hydrogen isotope composition since the limited length of the

spectrometer (viz. the magnet) impedes parallel detection of any ions > 21 amu if atomic H^- ions are detected. Nevertheless, $^{16}O^2H^-$ possesses two isobaric species, i.e. $^{17}OH^-$ and $^{16}O^1H_2^-$, which are located at the lower and higher mass end, respectively. Since the mass separation of these two isobars is too low for simultaneous blanking, the detector was positioned for selective blanking of $^{16}O^1H_2^-$ ions. The contribution of $^{17}OH^-$ ions to the signal intensity of $^{16}O^2H^-$ was estimated from the $^{16}O^1H^-$ signal intensity via multiplication by the $^{17}O/^{16}O$ isotope ratio, which, on average, amounts to 0.000380 (54) in biomass with natural oxygen isotope abundance. The applicability of this approach was evaluated by measurements of cells treated by CCF after hybridization with the negative control probe NON338. The determined $^2H / (^1H + ^2H)$ isotope fraction value of 0.022 +/- 0.016 at% was found to be in reasonable agreement with the natural abundance of deuterium, which is in the range from 0,011% to 0,016% (55-57).

Image data were evaluated using the WinImage software package provided by Cameca. Prior to stack accumulation, the individual images were aligned to compensate for positional variations arising from primary ion beam and/or sample stage drift. Secondary ion signal intensities were dead time corrected on a per-pixel basis. $^{13}C / (^{12}C + ^{13}C)$ isotope fraction distribution maps, given in at%, were plotted by calculation of the $^{13}C^-/(^{12}C^- + ^{13}C^-)$ and $^{12}C^{13}C^- / (^{12}C^{13}C^- + 2*^{12}C_2^-)$ signal intensity ratios for detection of the mono- and diatomic carbon ion species, respectively. Accordingly, $^2H / (^1H + ^2H)$ isotope fractions were obtained from calculation of $^{16}O^2H^- / (^{16}O^1H^- + ^{16}O^2H^-)$ intensity ratios after background correction of the $^{16}O^2H^-$ signal. Regions of interest (ROIs), referring to individual cells, were manually defined utilizing the nitrogen and phosphorus related secondary ion signal intensity distribution maps as indicators of biomass. These ROIs were cross-checked by the topographical/morphological appearance of the sampled areas in secondary electron intensity distribution images that were recorded simultaneously with the secondary ion images.

Results

In CARD-FISH, microbial target cells are labeled with nucleic acid probes conjugated to HRP. After hybridization, HRP-molecules immobilized within the cells catalyze the oxidation of soluble fluorescently-labeled tyramides in the presence of H_2O_2, which results in a covalent link between the phenolic group of the tyramides and tyrosine containing proteins of the cell (58). In order to develop a CARD-FISH procedure for the characterization of microbes in complex samples that exploits the advantages of click chemistry, we tested two new approaches based on Cu(I)-catalyzed (3+2] cycloaddition and SPAAC, respectively. For this purpose, tyramides carrying either a terminal alkyne (propargyl-dPEG®-tyramides; Figure A1B) or a BCN group (Figure A1C) instead of a fluorescent dye (Figure A1A) as in conventional CARD-FISH were used as substrate for HRP. Fixed *E. coli* cells were hybridized with HRP-labeled probe EUB338 and after enzyme-mediated deposition of propargyl-dPEG®-tyramides these could be detected with azide modified 6-FAM (Figure A1D and E) in a Cu-dependent click reaction. Bright fluorescence signals were observed, but the signals obtained after using BCN-tyramides and SPAAC of azide modified 6-FAM (Figure A1F) were found to be even brighter and more homogeneous (data not shown). Furthermore, Cu(I)-catalyzed (3+2] cycloaddition-based CCF resulted in contrast to SPAAC-based CCF in unspecific signals in some environmental samples (Figure A2). Consequently, the latter approach was used in all subsequent experiments.

Comparison of CCF with CARD-FISH and application of CCF. Compared to conventional CARD-FISH, BCN-based CCF resulted in brighter fluorescence signals of both Gram-negative *E. coli* and Gram-positive *B. subtilis* cells (Figure 1). In addition, for both reference species no apparent differences in the homogeneity of the obtained signals between the individual cells were observed if CARD-FISH and CCF stained cell preparations were compared. We did, however, notice a significant variation in the signal intensity of CCF (Figure 1C). On average, the signals achieved with CCF were 1.6 times brighter than those obtained with CARD-FISH staining. As expected both CARD-FISH approaches resulted in much brighter signals than FISH or DOPE-FISH, but it should be noted that these signal intensity differences were underestimated in our measurements due to the limited dynamic range of the detector of the confocal microscope. Huge differences in signal intensity between the methods led to detector saturation for CARD-FISH and CCF-labeled cells in microscope settings that allowed recording the much weaker signals from FISH or DOPE-

FISH treated cells (Figure 1). In the negative control using probe NON338-HRP no CCF signals were detectable for both reference strains even when high sensitivity settings of the detector were selected (Figure 1), demonstrating that 6-FAM azide does not react with cellular material. Regarding the specificity of CCF (mismatch discrimination at the probe target site) it is important to keep in mind that the hybridization and washing conditions that ensure stringency are the same as in the well-established CARD-FISH protocols. Consequently, no differences in specificity of CCF compared to CARD-FISH are expected and consistent with this assumption single mismatch discrimination of CCF could be demonstrated (see below).

In the next step, the suitability of CCF for detection of bacteria within different types of formaldehyde fixed samples containing complex microbial communities (activated sludge, peat soil enrichment culture, soil bacteria, fish tank filter biofilm, mouse gut, rock biofilm and several sponge samples) was evaluated by using probes EUB338-HRP and NON338-HRP, respectively. Some examples are shown in Figure 2 and A3. With all samples, no CCF related background fluorescence was observed. In addition, labeling of bacteria with CCF in LR White embedded mouse gut sections (Figure A3), paraffin-embedded cave biofilm samples grown on rock material (Figure 2) as well as Neg-50 (a cryogenic water-soluble section medium) embedded sponge sections (Figure 2 and A3, here also archaea were detected by CCF) was achieved, demonstrating compatibility of CCF with a variety of embedding media widely used in microbiology research. Except when used to stain soil bacteria, CCF yielded strong signals. Interestingly, the fluorescent signal in activated sludge was more dependent on the tyramide concentration in CCF than in CARD-FISH. Gradually increasing the tyramide concentration from 6 µM to 45 µM had no effect on the staining of *E. coli*, it did, however, had a pronounced effect on the CCF staining of bacteria in activated sludge (Figure A5).

Identification of Click CARD-FISH labeled bacteria by NanoSIMS. To test the suitability of CCF for direct identification of microbes in NanoSIMS analyses Atto514-azide (Figure A1G) was used instead of 6-FAM-azide in the labeling reaction as the former dye contains 6 fluorine atoms per molecule, which are detectable by NanoSIMS with high sensitivity and also high specificity in samples with low fluorine background. Indeed, CCF of *E. coli* and *B. cepacia* artificial mixture using probe EUB338-HRP resulted in $^{19}F^-$ / ($^{12}C^-$ + $^{13}C^-$) signal intensity ratios of cells, which were approximately 20 and 50 fold higher, respectively, than

those obtained after hybridization with the negative control probe (Figure 3A). The higher fluorine signal intensity in the *B. cepacia* cells likely reflects their much higher cellular ribosome content as this strain was grown in a full medium, while the *E. coli* cells were cultivated in a defined medium. Furthermore, single mismatch discrimination of CCF was demonstrated by hybridizing a mixture of *E. coli* and *B. cepacia* cells with probes GAM42a-HRP and probe BET42a-Cy5 as competitor probe (59). After CCF, Atto514-mediated deposition of fluorine could only be observed in *E. coli* cells, while the *B. cepacia* cells having a single mismatch in their 23S rRNA to probe GAM42a were not labeled with fluorine (Figure 3A, Figure 4). As expected CCF caused a dilution of the ^{13}C-signal of the labeled *E. coli* cells as the procedure deposits C-containing molecules (e.g. BCN tyramide, Atto514 dye) in the target cells.

In addition to strong probe-conferred halogen labeling of microbial cells for NanoSIMS analyses, CCF was also successfully applied to label probe-target cells with deuterium for subsequent NanoSIMS detection. This option will be particularly attractive for samples with a high natural halogen background. For this approach, BCN tyramides were synthesized containing four deuterium atoms (Fig. A1H). CCF was performed with *E. coli* and *B. cepacia* as described above using these tyramides and Atto514-azide (for screening of the wafers by fluorescence microscopy) leading to specific deposition of deuterium in cells after hybridization of the respective probes and subsequent signal amplification (Figure 3B, Figure 4F, Figure A4).

Discussion

CARD-FISH is very widely applied by microbiologists to detect, identify and quantify microbial populations in complex samples with rRNA-targeted oligonucleotide probes (60-64). The strong signal amplification achieved by this method renders it particularly useful in samples with high autofluorescence and/or with target microbes possessing a low cellular ribosome content. However, the signal-to-noise ratio of CARD-FISH signals in such samples is often still suboptimal. Consequently, there is a need for new methods that allow for even stronger signal amplification, but retain at the same time the simplicity and specificity of the CARD-FISH protocol. The easy-to-use CCF technique developed in this study may allow more sensitive detection of environmental microorganisms. Conveniently, for published

probes the recommended stringent hybridization and washing conditions for CARD-FISH do not have to be adapted for CCF as the latter method only differs in the way the HRP-labeled oligonucleotide probes that are bound to rRNA are detected. Nevertheless, the same rules that apply for FISH and CARD-FISH apply also for CCF. Competitor probes are commonly used in FISH (e.g. 65) and CARD-FISH (e.g. 66) to reduce unspecific probe binding. Use of competitor probes was necessary to achieve the single mismatch discrimination of CCF (Figure A4). Even when we increased the formamide concentration to 10% above the recommended concentration for the probe GAM42a, we could still observe strong unspecific staining of B. cepacia (Figure A6). In addition, we could observe staining signals even when only a fraction of available ribosome target sites were hybridized to HRP-conjugated probe (Figure A7), thus quantitative blocking with competitor probes is probably essential to prevent any undesired probe binding.

For Gram-negative as well as Gram-positive bacteria CCF yields brighter signal intensities as conventional CARD-FISH (Figure 1). On average, 1.6 times brighter signals were observed with CCF (ranging between 1.2 and 2 fold signal increase in six experiments conducted over two years with *E. coli*). Unfortunately, we did not use independent internal fluorescence intensity control (like fluorescent microspheres), thus we do not know whether the signal intensity variation stems from CARD-FISH, CCF, or both. As the *in situ* click reaction is probably not quantitative, the increase in signal intensity may reflect efficient labeling with the BCN-tyramide used for CCF. Possible reason for this is its smaller size (Figure A1) – it could be a better substrate for the HRP than the dye-coupled tyramides applied for conventional CARD-FISH. Alternatively, BCN- and 6-FAM tyramides are be deposited with similar efficiency, but as the fluorescent dye is not exposed to possible oxidation by HRP, higher fluorescence intensity can be observed in CCF. In contrast to the CCF, signal intensity of the CARD-FISH in complex samples was relatively high regardless of the tyramide concentration in the amplification buffer. This possibly stems from more favorable diffusion kinetics of 6-FAM tyramides and their better penetration through hydrated biofilm matrix (Figure A5). Indeed, such phenomenon was not observed in experiments with *E. coli* that were dispersed mostly as single cells (and thus having high effective surface/volume ratio). Similarly, when ample amounts of activated sludge biomass were applied to the well, the CCF resulted in the strong labeling of biomass on the edge, but not in the center of the well. No such bias could be observed when flocks were isolated from each other (data not shown). We speculated that the low relative signal intensity of CCF in soil samples stems from the low ribosome content of dormant bacteria. Consistently better performance of CCF (in

staining pure cultures) could also mean that high ribosome content is disadvantageous for CARD-FISH staining. By using probe competition approach as described by Hoshino and colleagues (26) we artificially decreased the number of available probe binding sites in *E. coli*. Although our results did not show a bias toward any method resulting from number of HRP-probes present in the cell (Figure A7), further physiological differences between the dormant and active cell states (67) could, however, affect the CCF performance but were not addressed by our approach. Furthermore, no false positive signals were observed with the Cu-free SPAAC-based CCF protocol in all environmental samples tested including sectioned material embedded in three commonly used embedding media (Figure 2, Figure A3), although several cyclic alkyne-containing secondary bacterial metabolites have been described that could possibly react with azides. Among those are the enediynes produced by some actinomycetes (68-70), as well as nostocyclyne A produced by the cyanobacterium *Nostoc* (71). In contrast, unspecific binding of 6-FAM azide in the presence of Cu (I) occurred in activated sludge even without added HRP-labeled probes (Figure A2), indicating that cells producing compounds with terminal alkyne groups (for a review see 42) occurred in these systems.

Besides its improved signal amplification and its specificity, an additional advantage of CCF is its flexibility regarding the choice of detector molecules that can be bound to the BCN tyramides, which are immobilized in the target cells due to the activity of the HRP. Many azide-modified fluorescent dyes with various excitation and emission maxima are commercially available. In addition, many other azide-linked detector molecules like azide-labeled oligopeptides can be easily prepared (72, 73) and can be covalently linked to the BCN tyramides within microbial cells using click chemistry with the protocol described in this study. For example, 6-FAM-azide was used for the fluorescence signal intensity measurements of CCF (Figure 1), while Atto514-azide was applied for the NanoSIMS measurements (Figure 3, Figure A4) as this dye contains six fluorine atoms per molecule. Halogen-CCF using Atto514 resulted in strong fluorine-labeling of the probe target cells and this approach might thus be particularly useful in samples containing a relatively high fluorine background like sponge tissue and mouse gut. Furthermore, in our hands storage of Oregon Green® 488-X-labeled tyramides that were used in previous halogen-CARD-ISH protocols for allowing the mass spectrometric detection of hybridized cells by NanoSIMS (28, 29) strongly reduces the halogen signal without affecting the fluorescence (data not shown), while such an effect could not be observed for Atto514-azide in CCF. Halogen-CCF is thus a promising method for direct identification of microbes in NanoSIMS analyses,

however it adds carbon, hydrogen and to a lesser extent oxygen, nitrogen and sulfur molecules to the target cells and thus dilutes the signal of stable isotopes of these atoms in target cells (Figure 3). This dilution effect, which has recently been described also for halogen CARD-ISH (D. Woebken, L. C. Burow, F. Behnam, X. Mayali, A. Schintlmeister, E. D. Fleming, L. Prufert-Bebout, S. W. Singer, A. López Cortés, T. M. Hoehler, J. Pett-Ridge, A. Spormann, M. Wagner, P. K. Weber and B. M. Bebout, Revisiting N2 fixation in Guerrero Negro intertidal microbial mats with a functional single-cell approach, in preparation) is dependent on the cellular ribosome content of the target cells and can thus not be corrected without additional experiments (see below) and must be carefully considered in quantitative single cell stable isotope experiments. In addition to halogen-CCF we also present deuterium-CCF as an alternative identification technique of microbes in NanoSIMS measurements (Figure 3, Figure A4). For this purpose, BCN tyramides labeled with four deuterium atoms were applied (Figure A1). The position of the deuterium atoms in the BCN tyramide molecule was selected in order to minimize re-exchange of D with H during storage or CCF and no indications for such a replacement were observed. While a variety of environmental samples contain large amounts of halogens, deuterium abundance in environmental samples is always low (e.g. natural deuterium abundance in seawater is 0.0156%; in biomass typical natural deuterium levels are between 0.011% and 0.016% (55-57)] and the observed deuterium content in the CCF-labeled *E. coli* and *B. cepacia* cells (typically between 1.6 and 2.8 at%) by far exceeds these numbers. Thus, this technique might become an attractive option for future NanoSIMS applications in environmental and medical microbiology. The two-step labeling protocol introduced in this study may be the key in reducing the amount of carbon deposited during tyramide labeling. Applying only a fraction of the here-used azide-fluorophore should be sufficient for successful fluorescent labeling, but would probably not result in a pronounced dye-dependent carbon addition. For example, this could be achieved by reducing dye concentration in the click reaction buffer, by using reaction buffer that contains less carbon compounds and results in lower click reaction efficiency, or by combination of both. Furthermore, such approach would increase the final $^{2}H/H$ ratio in the labeled cell and thus facilitate ^{2}H detection. In future, the use of polymeric deuterated azides may offer an excellent compromise between deuterium labeling, carbon deposition, inertness, and solubility. Finally, the deuterium-labeling might allow in future applications to quantify the amount of deposited molecules in NanoSIMS CCF-applications in order to obtain a correction factor for the above described dilution effect.

In conclusion, we have developed a modified CARD-FISH technique based on Cu-free click chemistry that offers improved signal intensity and flexibility, is not more expensive than conventional CARD-FISH, and might thus find widespread application in microbiology research. Future research efforts will focus on identifying an azide-modified dye that can also be identified by its chemical structure in Raman microspectrometric measurements. This would allow directly observing the binding of rRNA-targeted oligonucleotide probes in Raman spectra of single microbial cells (27, 74) without the need to combine this technique with fluorescence microscopy (75). In addition, the developed CCF protocol could also be useful to improve the various *in situ* hybridization techniques that exploit HRP-labeling for trapping of microbial cells (76), mRNA and gene detection in microbes (30), as well as HRP-based reporter deposition based assays in cell biology (58, 77-82).

Acknowledgements

This work was supported by the Advanced Grant Nitrification Reloaded (NITRICARE) 294343 from the European Research Council (to M.W.), by the Vienna Science and Technology Fund (WWTF) grant LS09-40 (to H.D.) and by the Graduate School "Symbiotic Interactions" of the University of Vienna (to J.D. and F.B.).

We thank David Berry, Rok Kostanjšek, Bela Hausmann, and Celine Lesaulnier for providing us with samples and to Dagmar Woebken for her valuable contribution to our discussions. We are also thankful to Sander van Berkel (SynAffix B.V.) for advice and for providing us with high-quality custom-made organic compounds.

References

1. **DeLong EF, Wickham GS, Pace NR.** 1989. Phylogenetic stains: ribosomal RNA-based probes for the identification of single cells. Science **243:**1360-1363.
2. **Wagner M, Horn M, Daims H.** 2003. Fluorescence *in situ* hybridisation for the identification and characterisation of prokaryotes. Curr. Opin. Microbiol. **6:**302-309.
3. **Teeling H, Fuchs B, Becher D, Klockow C, Gardebrecht A, Bennke C, Kassabgy M, Huang S, Mann A, Waldmann J, Weber M, Klindworth A, Otto A, Lange J, Bernhardt J, Reinsch C, Hecker M, Peplies J, Bockelmann F, Callies U, Gerdts G, Wichels A, Wiltshire K, Glöckner FO, Schweder T, Amann R.** 2012. Substrate-controlled succession of marine bacterioplankton populations induced by a phytoplankton bloom. Science **336:**608-611.
4. **Daims H, Lücker S, Wagner M.** 2006. daime, a novel image analysis program for microbial ecology and biofilm research. Environ. Microbiol. **8:**200-213.
5. **Farrelly V, Rainey FA, Stackebrandt E.** 1995. Effect of genome size and *rrn* gene copy number on PCR amplification of 16S rRNA genes from a mixture of bacterial species. Appl. Environ. Microbiol. **61:**2798-2801.
6. **Lee ZM-P, Bussema C, Schmidt T.** 2009. rrnDB: documenting the number of rRNA and tRNA genes in bacteria and archaea. Nucleic Acids Res. **37**.
7. **Angert E.** 2012. DNA replication and genomic architecture of very large bacteria. Annu. Rev. Microbiol. **66:**197-212.
8. **Hildenbrand C, Stock T, Lange C, Rother M, Soppa J.** 2011. Genome copy numbers and gene conversion in methanogenic archaea. J. Bacteriol. **193:**734-743.
9. **Breuert S, Allers T, Spohn G, Soppa J.** 2006. Regulated polyploidy in halophilic archaea. PLoS One **1:**e92.
10. **Stach EM, Bathe S, Clapp P, Burns G.** 2001. PCR-SSCP comparison of 16S rDNA sequence diversity in soil DNA obtained using different isolation and purification methods. FEMS Microbiol. Ecol. **36:**139-151.
11. **Vishnivetskaya T, Layton A, Lau M, Chauhan A, Cheng K, Meyers A, Murphy J, Rogers A, Saarunya G, Williams D, Pfiffner S, Biggerstaff J, Stackhouse B, Phelps T, Whyte L, Sayler G, Onstott T.** 2014. Commercial DNA extraction kits impact observed microbial community composition in permafrost samples. FEMS Microbiol. Ecol. **65:**217-230.
12. **Suzuki MT, Giovannoni SJ.** 1996. Bias caused by template annealing in the amplification of mixtures of 16S rRNA genes by PCR. Appl. Environ. Microbiol. **62:**625-630.
13. **Engelbrektson A, Kunin V, Wrighton K, Zvenigorodsky N, Chen F, Ochman H, Hugenholtz P.** 2010. Experimental factors affecting PCR-based estimates of microbial species richness and evenness. ISME J. **4:**642-647.
14. **Palatinszky M, Nikolausz M, Sváb D, Márialigeti K.** 2011. Preferential ligation during TA-cloning of multitemplate PCR products--a factor causing bias in microbial community structure analysis. J. Microbiol. Methods **85:**131-136.
15. **Huber J, Morrison H, Huse S, Neal P, Sogin M, Mark Welch D.** 2009. Effect of PCR amplicon size on assessments of clone library microbial diversity and community structure. Environ. Microbiol. **11:**1292-1302.
16. **Lee C, Herbold C, Polson S, Wommack E, Williamson S, McDonald I, Cary C.** 2012. Groundtruthing next-gen sequencing for microbial ecology-biases and errors in community structure estimates from PCR amplicon pyrosequencing. PLoS One **7:**e44224.
17. **Fuchs BM, Glöckner FO, Wulf J, Amann R.** 2000. Unlabeled helper oligonucleotides increase the *in situ* accessibility to 16S rRNA of fluorescently labeled oligonucleotide probes. Appl. Environ. Microbiol. **66:**3603-3607.

18. **Fuchs BM, Wallner G, Beisker W, Schwippl I, Ludwig W, Amann R.** 1998. Flow cytometric analysis of the *in situ* accessibility of *Escherichia coli* 16S rRNA for fluorescently labeled oligonucleotide probes. Appl. Environ. Microbiol. **64:**4973-4982.
19. **Behrens S, Rühland C, Inácio J, Huber H, Fonseca A, Spencer-Martins I, Fuchs B, Amann R.** 2003. *In situ* accessibility of small-subunit rRNA of members of the domains Bacteria, Archaea, and Eucarya to Cy3-labeled oligonucleotide probes. Appl. Environ. Microbiol. **69:**1748-1758.
20. **Stoecker K, Dorninger C, Daims H, Wagner M.** 2010. Double labeling of oligonucleotide probes for fluorescence *in situ* hybridization (DOPE-FISH) improves signal intensity and increases rRNA accessibility. Appl. Environ. Microbiol. **76:**922-926.
21. **Trebesius K, Amann R, Ludwig W, Mühlegger K, Schleifer KH.** 1994. Identification of whole fixed bacterial cells with nonradioactive 23S rRNA-targeted polynucleotide probes. Appl. Environ. Microbiol. **60:**3228-3235.
22. **DeLong EF, Taylor LT, Marsh TL, Preston CM.** 1999. Visualization and enumeration of marine planktonic archaea and bacteria by using polyribonucleotide probes and fluorescent *in situ* hybridization. Appl. Environ. Microbiol. **65:**5554-5563.
23. **Pernthaler A, Preston C, Pernthaler J, DeLong E, Amann R.** 2002. Comparison of fluorescently labeled oligonucleotide and polynucleotide probes for the detection of pelagic marine bacteria and archaea. Appl. Environ. Microbiol. **68:**661-667.
24. **Schönhuber W, Fuchs B, Juretschko S, Amann R.** 1997. Improved sensitivity of whole-cell hybridization by the combination of horseradish peroxidase-labeled oligonucleotides and tyramide signal amplification. Appl. Environ. Microbiol. **63:**3268-3273.
25. **Pernthaler A, Pernthaler J, Amann R.** 2002. Fluorescence *in situ* hybridization and catalyzed reporter deposition for the identification of marine bacteria. Appl. Environ. Microbiol. **68:**3094-3101.
26. **Hoshino T, Yilmaz S, Noguera D, Daims H, Wagner M.** 2008. Quantification of target molecules needed to detect microorganisms by fluorescence *in situ* hybridization (FISH) and catalyzed reporter deposition-FISH. Appl. Environ. Microbiol. **74:**5068-5077.
27. **Wagner M.** 2009. Single-cell ecophysiology of microbes as revealed by Raman microspectroscopy or secondary ion mass spectrometry imaging. Annu. Rev. Microbiol. **63:**411-429.
28. **Behrens S, Lösekann T, Pett-Ridge J, Weber P, Ng W-O, Stevenson B, Hutcheon I, Relman D, Spormann A.** 2008. Linking microbial phylogeny to metabolic activity at the single-cell level by using enhanced element labeling-catalyzed reporter deposition fluorescence *in situ* hybridization (EL-FISH) and NanoSIMS. Appl. Environ. Microbiol. **74:**3143-3150.
29. **Musat N, Halm H, Winterholler B, Hoppe P, Peduzzi S, Hillion F, Horreard F, Amann R, Jørgensen B, Kuypers M.** 2008. A single-cell view on the ecophysiology of anaerobic phototrophic bacteria. Proc. Natl. Acad. Sci. U.S.A. **105:**17861-17866.
30. **Wagner M, Haider S.** 2012. New trends in fluorescence *in situ* hybridization for identification and functional analyses of microbes. Curr. Opin. Biotechnol. **23:**96-102.
31. **Moses J, Moorhouse A.** 2007. The growing applications of click chemistry. Chem. Soc. Rev. **36:**1249-1262.
32. **Kolb H, Sharpless B.** 2003. The growing impact of click chemistry on drug discovery. Drug Discovery Today **8:**1128-1137.
33. **El-Sagheer A, Brown T.** 2010. Click chemistry with DNA. Chem. Soc. Rev. **39:**1388-1405.
34. **Jewett J, Bertozzi C.** 2010. Cu-free click cycloaddition reactions in chemical biology. Chem. Soc. Rev. **39:**1272-1279.
35. **Tornøe C, Christensen C, Meldal M.** 2002. Peptidotriazoles on solid phase: (1,2,3]-triazoles by regiospecific copper(i)-catalyzed 1,3-dipolar cycloadditions of terminal alkynes to azides. J. Org. Chem. **67:**3057-3064.

36. **Rostovtsev V, Green L, Fokin V, Sharpless B.** 2002. A stepwise huisgen cycloaddition process: copper(I)-catalyzed regioselective "ligation" of azides and terminal alkynes. Angew. Chem., Int. Ed. Engl. **41:**2596-2599.
37. **Agard N, Prescher J, Bertozzi C.** 2004. A strain-promoted (3 + 2] azide-alkyne cycloaddition for covalent modification of biomolecules in living systems. J. Am. Chem. Soc. **126:**15046-15047.
38. **Baskin J, Prescher J, Laughlin S, Agard N, Chang P, Miller I, Lo A, Codelli J, Bertozzi C.** 2007. Copper-free click chemistry for dynamic *in vivo* imaging. Proc. Natl. Acad. Sci. U.S.A. **104:**16793-16797.
39. **Sletten E, Bertozzi C.** 2011. From mechanism to mouse: a tale of two bioorthogonal reactions. Acc. Chem. Res. **44:**666-676.
40. **Salic A, Mitchison T.** 2008. A chemical method for fast and sensitive detection of DNA synthesis *in vivo*. Proc. Natl. Acad. Sci. U.S.A. **105:**2415-2420.
41. **Neef A, Luedtke N.** 2011. Dynamic metabolic labeling of DNA *in vivo* with arabinosyl nucleosides. Proc. Natl. Acad. Sci. U.S.A. **108:**20404-20409.
42. **Minto RE, Blacklock BJ.** 2008. Biosynthesis and function of polyacetylenes and allied natural products. Prog. Lipid. Res. **47:**233-306.
43. **Potapova I, Eglin D, Laschke M, Bischoff M, Richards G, Moriarty F.** 2013. Two-step labeling of *Staphylococcus aureus* with Lysostaphin-Azide and DIBO-Alexa using click chemistry. J. Microbiol. Methods **92:**90-98.
44. **Dumont A, Malleron A, Awwad M, Dukan S, Vauzeilles B.** 2012. Click-mediated labeling of bacterial membranes through metabolic modification of the lipopolysaccharide inner core. Angew. Chem., Int. Ed. Engl. **51:**3143-3146.
45. **Ohno S, Okano H, Tanji Y, Ohashi A, Watanabe K, Takai K, Imachi H.** 2012. A method for evaluating the host range of bacteriophages using phages fluorescently labeled with 5-ethynyl-2'-deoxyuridine (EdU). Appl. Microbiol. Biotechnol. **95:**777-788.
46. **Dommerholt J, Schmidt S, Temming R, Hendriks L, Rutjes F, van Hest J, Lefeber D, Friedl P, van Delft F.** 2010. Readily accessible bicyclononynes for bioorthogonal labeling and three-dimensional imaging of living cells. Angew. Chem., Int. Ed. Engl. **49:**9422-9425.
47. **Bertani G.** 1951. Studies on lysogenesis. I. The mode of phage liberation by lysogenic *Escherichia coli*. J. Bacteriol. **62:**293-300.
48. **Widdel F, Pfennig N.** 1981. Studies on dissimilatory sulfate-reducing bacteria that decompose fatty acids. I. Isolation of new sulfate-reducing bacteria enriched with acetate from saline environments. Description of *Desulfobacter postgatei* gen. nov., sp. nov. Arch. Microbiol. **129:**395-400.
49. **Daims H, Stoecker K, Wagner M.** 2005. Fluorescence *in situ* hybridization for the detection of prokaryotes, p. 213–239. *In* Osborn AM, Smith CJ (ed.), Molecular microbial ecology. Bios-Garland, Abingdon.
50. **Berry D, Stecher B, Schintlmeister A, Reichert J, Brugiroux S, Wild B, Wanek W, Richter A, Rauch I, Decker T, Loy A, Wagner M.** 2013. Host-compound foraging by intestinal microbiota revealed by single-cell stable isotope probing. Proc. Natl. Acad. Sci. U.S.A. **110:**4720-4725.
51. **Behnam F, Vilcinskas A, Wagner M, Stoecker K.** 2012. A straightforward DOPE (double labeling of oligonucleotide probes)-FISH (fluorescence *in situ* hybridization) method for simultaneous multicolor detection of six microbial populations. Appl. Environ. Microbiol. **78:**5138-5142.
52. **Kostanjšek R, Pašić L, Daims H, Sket B.** 2013. Structure and community composition of sprout-like bacterial aggregates in a Dinaric Karst subterranean stream. Microb. Ecol. **66:**5-18.
53. **Pernthaler A, Pernthaler J, Amann R.** 2004. Sensitive multi-color fluorescence *in situ* hybridization for the identification of environmental microorganisms, p. 2613-2627. *In* Kowalchuk GA, Bruijn FJ, Head IM, Akkermans AD, Elsas JD (ed.), Molecular Microbial Ecology Manual. Springer Netherlands, Houten.

54. **Gonfiantini R, Stichler W, Rozanski K.** 1993. Standards and intercomparison materials distributed by the International Atomic Energy Agency for stable isotope measurements., p. 13-29, Reference and intercomparison materials for stable isotopes of light elements, IAEA-TECDOC-825. International Atomic Energy Agency, Vienna.
55. **Doucett RR, Marks JC, Blinn DW, Caron M, Hungate BA.** 2007. Measuring terrestrial subsidies to aquatic food webs using stable isotopes of hydrogen. Ecology **88:**1587-1592.
56. **Keppler F, Harper DB, Kalin RM, Meier-Augenstein W, Farmer N, Davis S, Schmidt HL, Brown DM, Hamilton JT.** 2007. Stable hydrogen isotope ratios of lignin methoxyl groups as a paleoclimate proxy and constraint of the geographical origin of wood. New Phytol. **176:**600-609.
57. **Hagemann R, Nief G, Roth E.** 1970. Absolute isotopic scale for deuterium analysis of natural waters. Absolute D/H ratio for SMOW1. Tellus **22:**712-715.
58. **Krieg R, Halbhuber KJ.** 2010. Detection of endogenous and immuno-bound peroxidase--the status quo in histochemistry. Prog. Histochem. Cytochem. **45:**81-139.
59. **Manz W, Amann R, Ludwig W, Wagner M, Schleifer K-H.** 1992. Phylogenetic oligodeoxynucleotide probes for the major subclasses of Proteobacteria: problems and solutions. Syst. Appl. Microbiol. **15:**593-600.
60. **Auguet JC, Triado-Margarit X, Nomokonova N, Camarero L, Casamayor EO.** 2012. Vertical segregation and phylogenetic characterization of ammonia-oxidizing Archaea in a deep oligotrophic lake. ISME J. **6:**1786-1797.
61. **Krupke A, Musat N, Laroche J, Mohr W, Fuchs BM, Amann RI, Kuypers MM, Foster RA.** 2013. *In situ* identification and N(2) and C fixation rates of uncultivated cyanobacteria populations. Syst. Appl. Microbiol. **36:**259-271.
62. **Gittel A, Mussmann M, Sass H, Cypionka H, Konneke M.** 2008. Identity and abundance of active sulfate-reducing bacteria in deep tidal flat sediments determined by directed cultivation and CARD-FISH analysis. Environ. Microbiol. **10:**2645-2658.
63. **Kleindienst S, Ramette A, Amann R, Knittel K.** 2012. Distribution and *in situ* abundance of sulfate-reducing bacteria in diverse marine hydrocarbon seep sediments. Environ. Microbiol. **14:**2689-2710.
64. **Bulgarelli D, Rott M, Schlaeppi K, Ver Loren van Themaat E, Ahmadinejad N, Assenza F, Rauf P, Huettel B, Reinhardt R, Schmelzer E, Peplies J, Gloeckner FO, Amann R, Eickhorst T, Schulze-Lefert P.** 2012. Revealing structure and assembly cues for *Arabidopsis* root-inhabiting bacterial microbiota. Nature **488:**91-95.
65. **Daims H, Nielsen JL, Nielsen PH, Schleifer KH, Wagner M.** 2001. *In situ* characterization of *Nitrospira*-like nitrite-oxidizing bacteria active in wastewater treatment plants. Appl. Environ. Microbiol. **67:**5273-5284.
66. **Woebken D, Fuchs BM, Kuypers MM, Amann R.** 2007. Potential interactions of particle-associated anammox bacteria with bacterial and archaeal partners in the Namibian upwelling system. Appl. Environ. Microbiol. **73:**4648-4657.
67. **Bremer H, Dennis PP.** 1996. Modulation of chemical composition and other parameters of the cell by growth rate, p. 1553–1569. *In* Neidhardt FC, R Curtiss III, Ingraham JL, Lin ECC, Low KB, Magasanik B, Reznikoff WS, Riley M, Schaechter M, Umbarger HE (ed.), Escherichia coli and Salmonella: cellular and molecular biology, 2nd ed. ASM Press, Washington, DC.
68. **Udwary D, Zeigler L, Asolkar R, Singan V, Lapidus A, Fenical W, Jensen P, Moore B.** 2007. Genome sequencing reveals complex secondary metabolome in the marine actinomycete *Salinispora tropica*. Proc. Natl. Acad. Sci. U.S.A. **104:**10376-10381.
69. **Nicolaou KC, Smith AL, Yue EW.** 1993. Chemistry and biology of natural and designed enediynes. Proc. Natl. Acad. Sci. U.S.A. **90:**5881-5888.
70. **Van Lanen SG, Shen B.** 2008. Biosynthesis of enediyne antitumor antibiotics. Curr. Top. Med. Chem. **8:**448-459.

71. **Ploutno A, Carmeli S.** 2000. Nostocyclyne A, a novel antimicrobial cyclophane from the cyanobacterium *Nostoc* sp. J. Nat. Prod. **63:**1524-1526.
72. **Goddard-Borger ED, Stick RV.** 2007. An efficient, inexpensive, and shelf-stable diazotransfer reagent: imidazole-1-sulfonyl azide hydrochloride. Organic letters **9:**3797-3800.
73. **Hansen MB, van Gurp TH, van Hest JC, Lowik DW.** 2012. Simple and efficient solid-phase preparation of azido-peptides. Organic letters **14:**2330-2333.
74. **Milucka J, Ferdelman TG, Polerecky L, Franzke D, Wegener G, Schmid M, Lieberwirth I, Wagner M, Widdel F, Kuypers MM.** 2012. Zero-valent sulphur is a key intermediate in marine methane oxidation. Nature **491:**541-546.
75. **Huang WE, Stoecker K, Griffiths R, Newbold L, Daims H, Whiteley AS, Wagner M.** 2007. Raman-FISH: combining stable-isotope Raman spectroscopy and fluorescence *in situ* hybridization for the single cell analysis of identity and function. Environ. Microbiol. **9:**1878-1889.
76. **Pernthaler A, Dekas AE, Brown CT, Goffredi SK, Embaye T, Orphan VJ.** 2008. Diverse syntrophic partnerships from deep-sea methane vents revealed by direct cell capture and metagenomics. Proc. Natl. Acad. Sci. U.S.A. **105:**7052-7057.
77. **Chaudhuri AD, Yelamanchili SV, Fox HS.** 2013. Combined fluorescent *in situ* hybridization for detection of microRNAs and immunofluorescent labeling for cell-type markers. Front. Cell. Neurosci. **7:**160.
78. **Zhao C, Eisinger B, Gammie SC.** 2013. Characterization of GABAergic neurons in the mouse lateral septum: a double fluorescence *in situ* hybridization and immunohistochemical study using tyramide signal amplification. PLoS One **8:**e73750.
79. **Pinaud R, Mello CV, Velho TA, Wynne RD, Tremere LA.** 2008. Detection of two mRNA species at single-cell resolution by double-fluorescence *in situ* hybridization. Nat. Protoc. **3:**1370-1379.
80. **King RS, Newmark PA.** 2013. *In situ* hybridization protocol for enhanced detection of gene expression in the planarian *Schmidtea mediterranea*. BMC Dev. Biol. **13:**8.
81. **Goto S, Kawarai T, Morigaki R, Okita S, Koizumi H, Nagahiro S, Munoz EL, Lee LV, Kaji R.** 2013. Defects in the striatal neuropeptide Y system in X-linked dystonia-parkinsonism. Brain : a journal of neurology **136:**1555-1567.
82. **Colak D, Ji SJ, Porse BT, Jaffrey SR.** 2013. Regulation of axon guidance by compartmentalized nonsense-mediated mRNA decay. Cell **153:**1252-1265.
83. **Daims H, Brühl A, Amann R, Schleifer KH, Wagner M.** 1999. The domain-specific probe EUB338 is insufficient for the detection of all Bacteria: development and evaluation of a more comprehensive probe set. Syst. Appl. Microbiol. **22:**434-444.

Figures

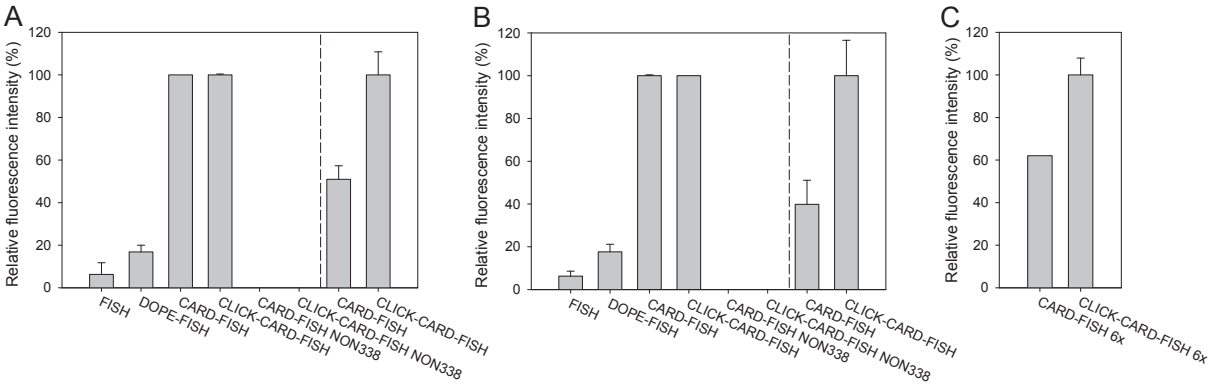

Figure 1. *E. coli* (panel A) and *B. subtilis* (panel B) were hybridized with probes EUB338-6-FAM (FISH), EUB338-2x-6-FAM (DOPE-FISH), EUB338-HRP (CARD-FISH and CCF) and NON338-HRP (CARD-FISH and CCF). For the CARD-FISH and CCF experiments amplification (using tyramides with at least 95% purity) and amplification plus labeling with 6-FAM azide was performed after hybridization, respectively. For each experiment, 6-FAM-conferred fluorescence signal intensity of at least 159 *E. coli* cells (average 504 cells) and 56 of *B. subtilis* cells (average 148 cells) was measured using CLSM. The dynamic range (8 bit) of the detector was insufficient to quantify the large difference in signal intensity between the applied methods. To accommodate for this, two image acquisition settings were applied. High sensitivity settings were used to quantify the signal intensity of FISH, DOPE-FISH and NON338 control experiments of CARD-FISH and CCF (data points on the left side of the dashed lines). Using these settings, the fluorescence signals of cells stained by CARD-FISH and CCF were in saturation leading to an underestimation of their actual signal intensity. Low sensitivity settings (data points on the right side of the dashed lines) were applied to quantify the signal intensity difference between CARD-FISH and CCF using probe EUB338-HRP. Using these settings no fluorescence signals could be recorded for the other treatments. For both panels, signal intensities were normalized to the maximum fluorescence intensity observed with the respective setting. Error bars depict one standard deviation. Panel C shows combined results of six independent CARD-FISH and CCF comparisons performed over the period of two years with *E. coli*. For each individual experiment, mean signal intensity of CCF labeled cells was normalized to mean fluorescence intensity of cells stained with CARD-FISH. Error bar shows one standard error.

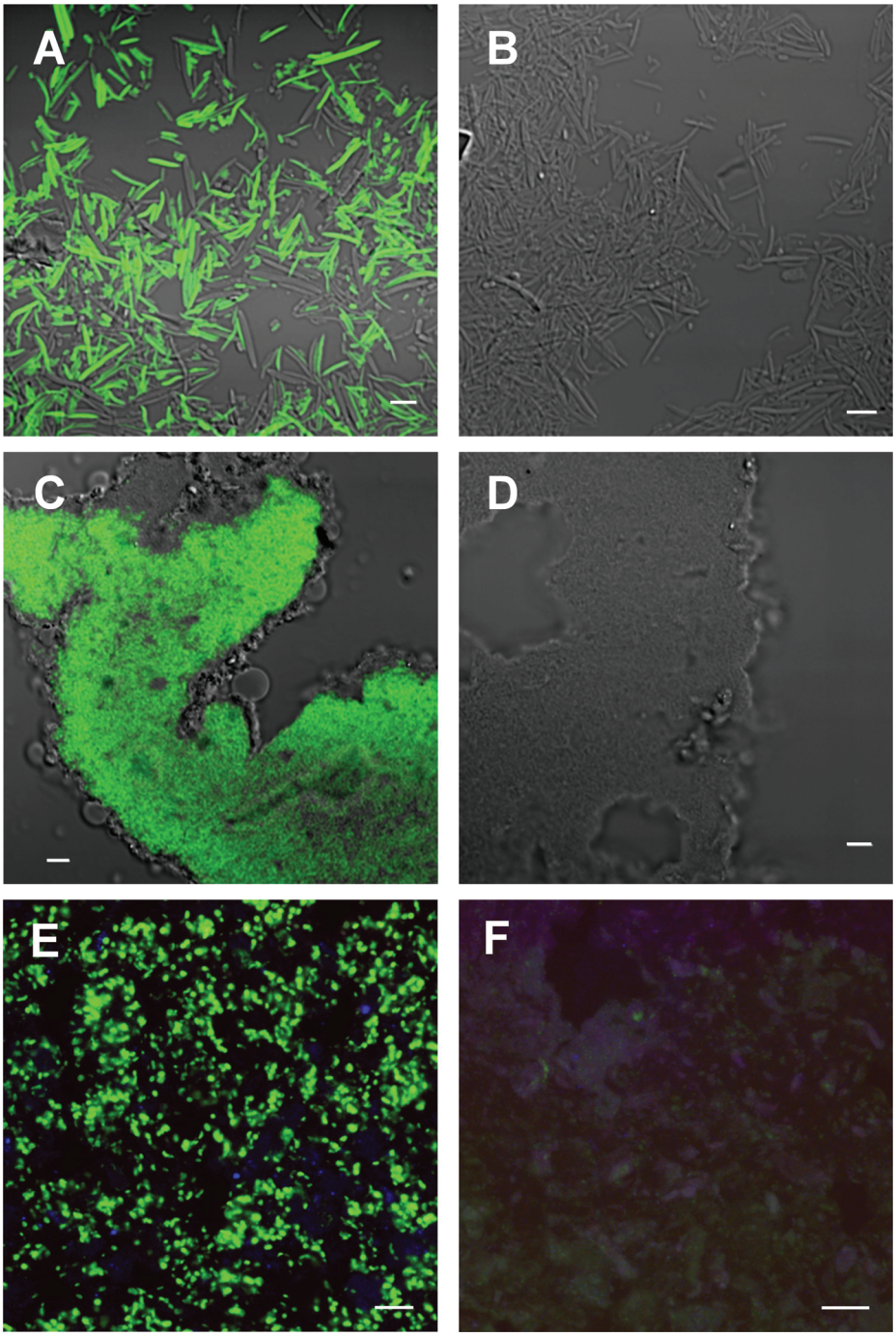

Figure 2. CCF-mediated detection of formaldehyde-fixed bacteria in selected samples. On the left side results obtained with probe EUB338 and on the right side signals observed with the negative control probe NON338 are shown. For each sample both images were recorded with the same settings. Panels A and B show CCF results obtained with mouse gut samples (with more than 10 µm long cells) and panels C and D illustrate CCF signals in paraffin-embedded cave biofilm samples. Images depicted in panels A-D are an overlay of a DIC image to visualize the biomass and a fluorescence image recorded using an excitation

wavelength of 488 nm for detecting the 6-FAM signal. Panels E and F show signals obtained with Neg-50 embedded tissue sections of the sponge *Ancorina alata*. These images were composed by overlaying images recorded in three channels of the CLSM, using excitation wavelengths of 488 (for the 6-FAM signal) and 543 and 633 nm (for autofluorescence) and appropriate filter sets. Bars in panels A-D correspond to 5 µm and in panels E and F to 10 µm. As Gram-positive cells, which are difficult to penetrate with HRP-labeled probes, were present in these samples, it is expected that some of the cells visible in the DIC images show weak or no fluorescence. In addition, we used probe EUB338-HRP for CCF (and not the mixture of probes EUB338, EUB338-II and EUB338-III) and might thus not have detected all bacteria in the samples (83).

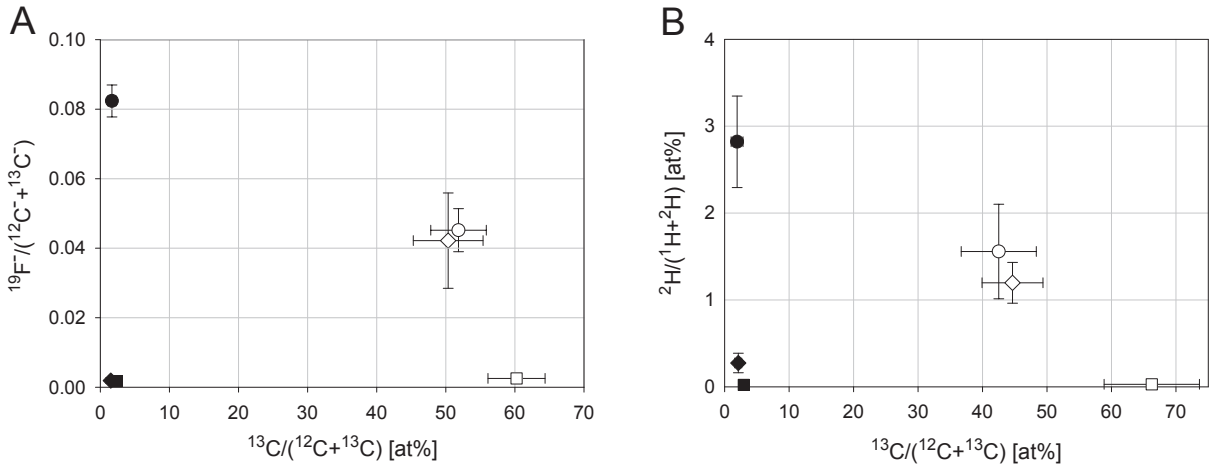

Figure 3. CCF-based detection of microbes via NanoSIMS. (A) 13C-labeled *E. coli* (empty symbols) and unlabeled *B. cepacia* (full symbols) cells were either hybridized with probe EUB338-HRP (circles) or with the negative control probe NON338 (squares). In an additional experiment an equimolar mixture of probes GAM42a-HRP and BET42a-Cy5 (diamonds) was used for hybridization. Subsequently, in all experiments CCF was performed using an azide modified Atto514 dye (containing 6 F atoms) in the labeling reaction. The 13C-label of the *E. coli* cells allowed a hybridization-independent identification of cells from both species in NanoSIMS images. After hybridization with probe EUB338-HRP both species showed strongly increased $19F^-/(12C^- + 13C^-)$ values reflecting the intracellular deposition of Atto514, while no such increase was observed with the negative control probe. The specificity of CCF is nicely demonstrated by the fact that in contrast to *E. coli* cells ($p < 0.0001$, Student's t-test) no increased $19F^-/(12C^- + 13C^-)$ ratios were observed in *B. cepacia* cells after hybridization with probe GAM42a-HRP (in the presence of BET42a-Cy5) ($p > 0.98$, Student's t-test). (B) In additional experiments D4-BCN tyramides were used for amplification and CCF was completed by using the azide-modified Atto514 dye. An artificial mixture of 13C-labeled *E. coli* (empty symbols) and *B. cepacia* cells with natural 13C abundance (full symbols) was hybridized in separate experiments with probes EUB338-HRP (circles), NON338-HRP (squares), and a mixture of probes GAM42a-HRP and BET42a-Cy5 (diamonds). Deuterium-labeling of cells worked as expected from the probe specificities, demonstrating again single-mismatch discrimination capacity of CCF as after hybridization with probe GAM42a-HRP a significantly higher deuterium content was detected in the *E. coli* than in the *B. cepacia* cells ($p < 0.0001$, Student's t-test). For each data point between 5 (negative control) and 77 cells were analyzed. Error bars depict one standard deviation.

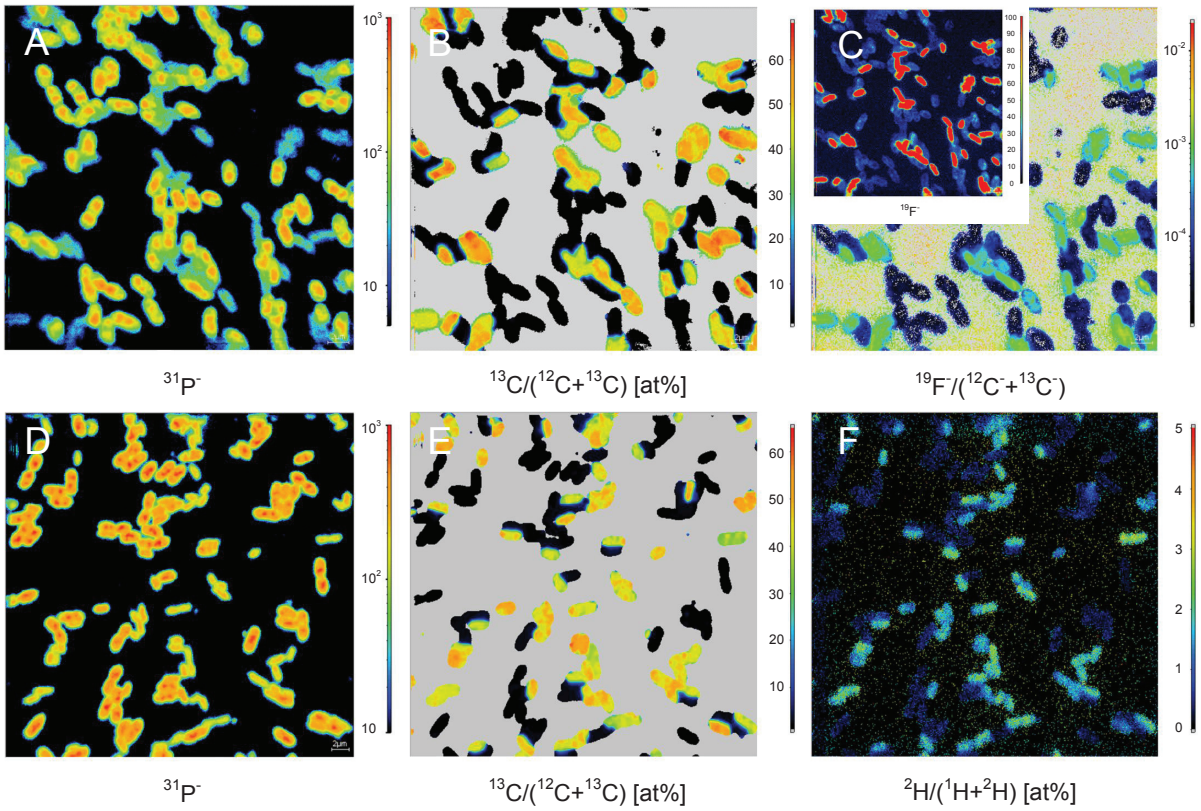

FIGURE 4. Identification of microbes by CCF and NanoSIMS. Formaldehyde fixed *E. coli* (^{13}C-labeled) and *B. cepacia* (natural ^{13}C-abundance) cells were mixed and treated by CCF using an equimolar mixture of probes GAM42a-HRP and BET42a-Cy5. In one experiment the standard BCN-tyramides and the fluorine-containing Atto514-N3 were used in the labeling reaction (panels A-C). In the other experiment, deuterium labeled BCN tyramides were applied (panels D-F). Images A-C and D-F, respectively, show the same field of view. Images A and D depict both strains as visualized by the intensity distribution of the $^{31}P^-$ secondary ion signal. Images B and E display the local carbon isotope composition that clearly discriminates *B. cepacia* (natural abundance, black color) against the *E. coli* cells (^{13}C labeled, warm colors). Images C and F demonstrate GAM42a-HRP-mediated specific labeling of *E. coli* cells with fluorine and deuterium, respectively. It should be noticed that the $^{19}F^-$ signal intensity was normalized to the total intensity of C^- secondary ions (i.e. $^{12}C^- + ^{13}C^-$), which is well suited for intercomparison of intensity data acquired in separate measurement runs. However, utilizing the C^- intensity as reference signal brings about a high level of scattering in the areas which contain only traces of carbon, which is evidently the case for the bare surface of the silicon wafer on which the cells were deposited. For the sake of comparison the absolute $^{19}F^-$ signal intensity is shown in the inset of panel C. Image size is 30 x 30 µm^2 for panel A-C and 35 x 35 µm^2 for panel D-F.

Appendix

CARD-FISH Method Exploiting Click Chemistry for *In Situ* Identification of Microbes

Jan Dolinšek[1], Faris Behnam[1], Arno Schintlmeister[2], Andreas Anderluh[1*], Stephanie A. Eichorst[1], Alexander Galushko[1], Holger Daims[1] and Michael Wagner [1, 2]#

[1]Department of Microbiology and Ecosystem Research, Division of Microbial Ecology, University of Vienna, Vienna, Austria; [2]Large Instrument Facility for Advanced Isotope Research, University of Vienna, Vienna, Austria

Running Head: CARD-FISH Method employing Click Chemistry

*Present address: Andreas Anderluh, Institute of Applied Physics, Vienna University of Technology, Vienna, Austria

A1 Supplementary tables

TABLE A1. Samples containing complex microbial communities used in this study. All samples were successfully analyzed by CCF, but not for all samples pictures are shown in Figure 2 and Figure A3.

Sample type	Origin	Sampling	Reference
Mouse gut	specific pathogen-free C57BL/6 mice	/	(1)
Peatland soil enrichment[a]	Schlöppnerbrunnen, Germany	9/2010	Unpublished
Soil	Lainzer Tiergarten, Vienna, Austria	11/2013	Unpublished
Nitrifying activated sludge	wastewater treatment plant, Bad Salzuflen, Germany	3/2011	Unpublished
Nitrifying activated sludge	wastewater treatment plant, Ingolstadt, Germany	3/2011	(2)
Bacterial biofilm	Vjetrenica cave, Bosnia and Herzegovina	9/2010	(3)
Sponge *Ancorina alata*	Jones Bay, New Zealand	4/2010	(4)
Sponge *Rhopaloides odorabile*	nearby Townsville, Australia	10/2010	Unpublished
Sponge *Ianthella basta*	nearby Townsville, Australia	10/2010	Unpublished

[a] Enrichment was maintained in mineral medium (5) with addition of 5 mM SO_4^{2-} and 3,3 mM lactate for approx. 6 months at 14 °C.

TABLE A2. Probes used in this study.

Probe	Sequence (5´- 3´)	Target groups	Formamide (%)	Reference
EUB338	GCT GCC TCC CGT AGG AGT	most *Bacteria*	35[a]	(6)
BET42a	GCC TTC CCA CTT CGT TT	*Betaproteobacteria*	35	(7)
GAM42a	GCC TTC CCA CAT CGT TT	*Gammaproteobacteria*	35	(7)
NON338	ACT CCT ACG GGA GGC AGC	negative control probe	35	(8)
Arch915	GTG CTC CCC CGC CAA TTC CT	most *Archaea*	35	(9)

[a] As described in study by Hoshino et al. (10), HRP-labeled probes form less stable duplex with RNA than probes labeled with cyanine-dyes. To compare signal intensities obtained with CARD-FISH and Click-CARD-FISH it was critical to ensure complete and reproducible hybridization of EUB338-HRP, and for this purpose we used 20% formamide in hybridization buffer. To assess compatibility of CCF with various environmental samples, 35% formamide was used in hybridization buffer when using probe EUB338-HRP.

A2 Supplementary figures

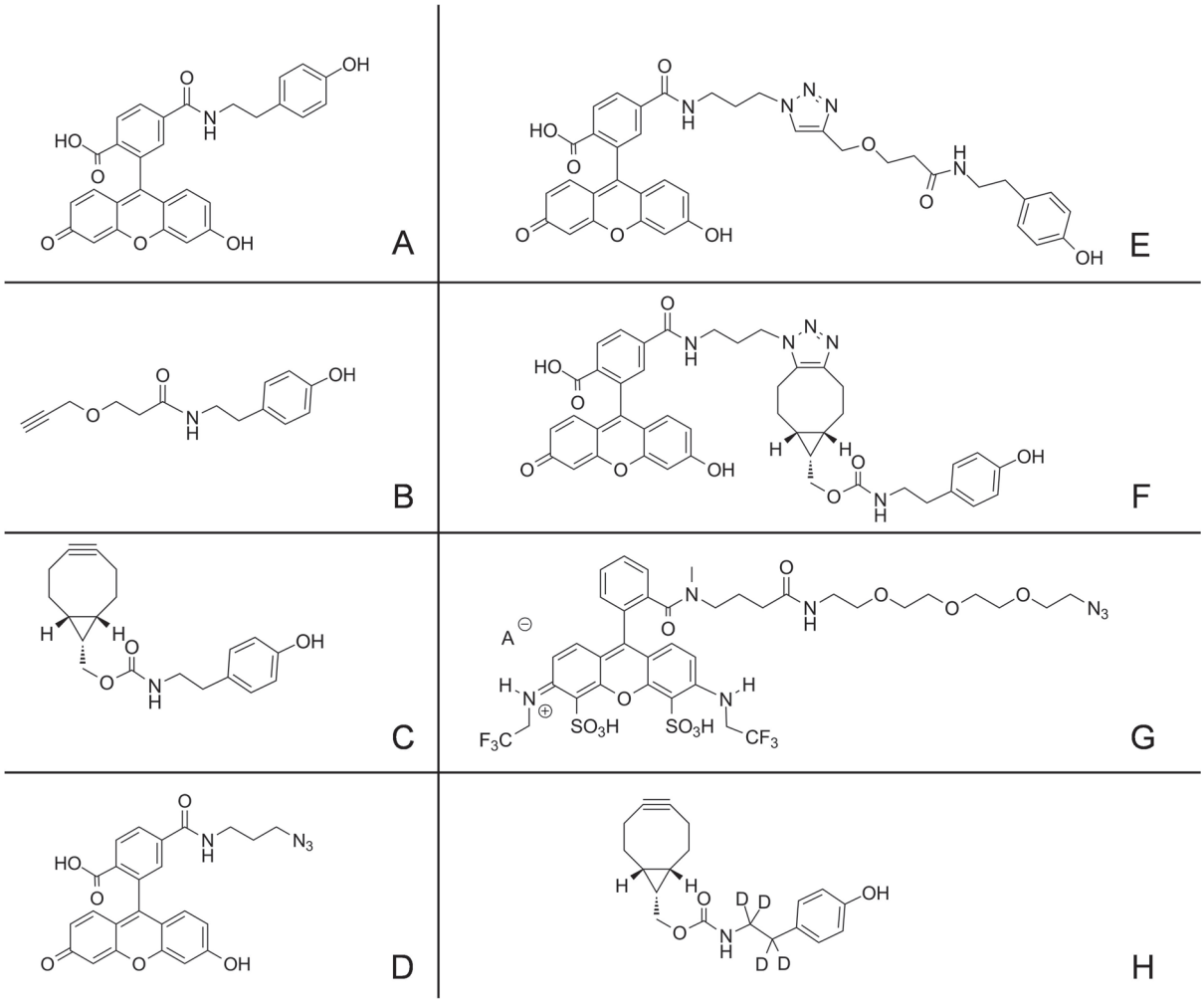

FIGURE A1. Structural formulae of tyramides and dyes used in this study. (A) 6-FAM tyramide, (B) propargyl-dPEG®-tyramide, (C) BCN tyramide, (D) 6-FAM azide, (E), Cu(I)-catalyzed (3+2] cycloaddition product of propargyl-dPEG®-tyramide and 6-FAM azide, (F) product of SPAAC between BCN tyramide and 6-FAM azide, (G) Atto514 azide, and (H) D_4-BCN tyramide.

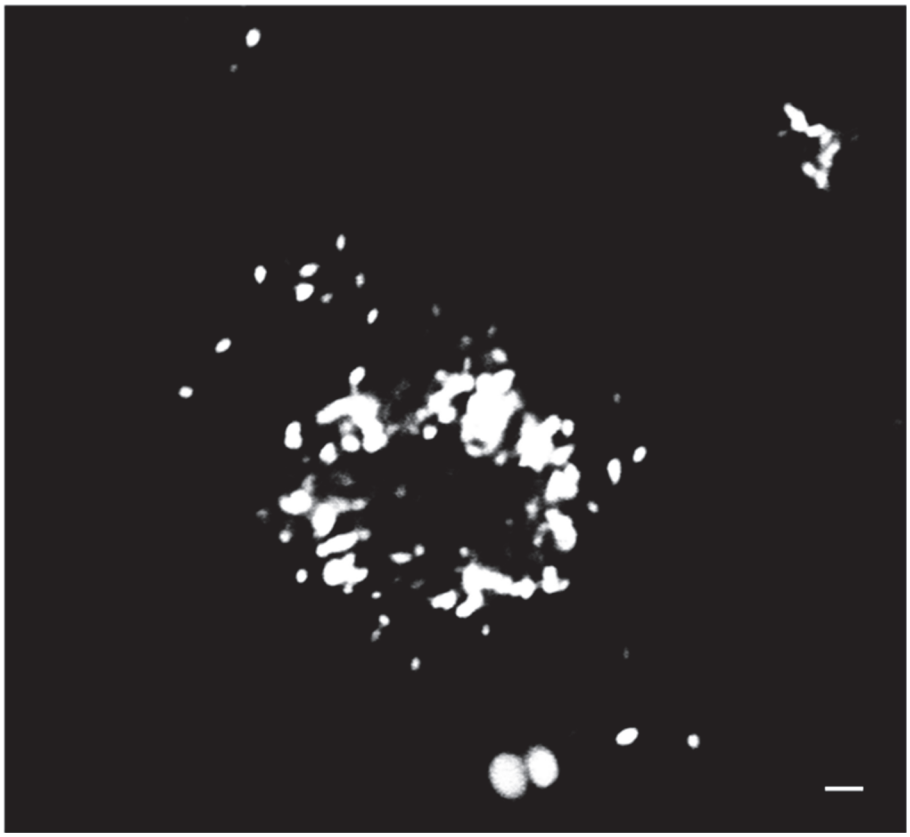

FIGURE A2. Unspecific binding of 6-FAM azide to cell-like particles in a paraformaldehyde-fixed activated sludge sample (Ingolstadt, Germany, see Table A1) after incubation in the click buffer in the presence of Cu(I). When Cu was omitted from the click buffer no signal was observed, demonstrating that the unspecific signals did not reflect autofluorescence or unspecific binding of the dye (data not shown). Scale bar corresponds to 2 μm.

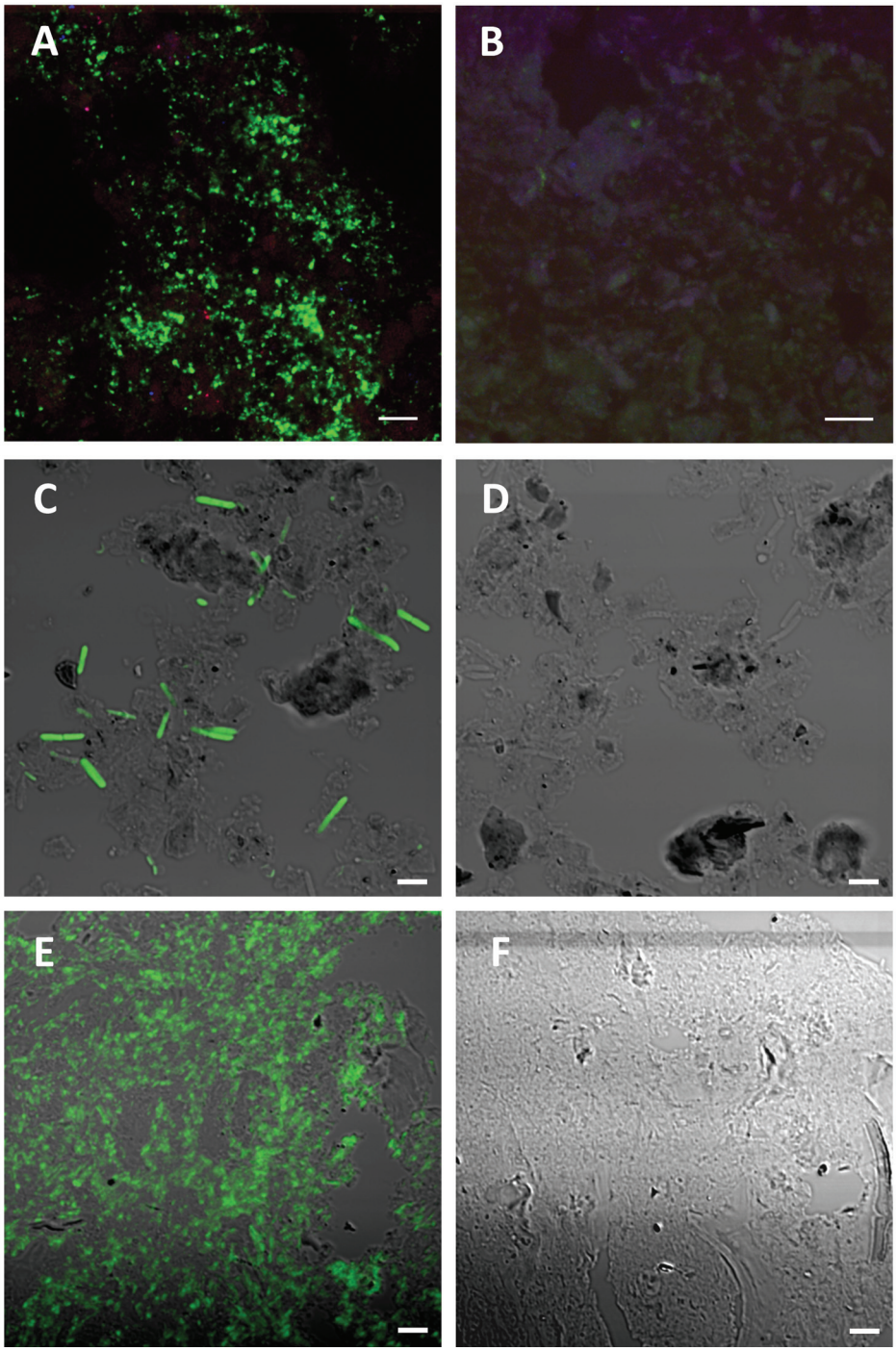

FIGURE A3. Examples for the application of CCF in complex samples containing formaldehyde-fixed microbes. Neg-50 embedded tissue sections of the sponge *Ancorina alata* hybridized with probe Arch915 targeting most archaea (panel A) and the negative control probe NON338 (panel B, same image as in Fig. 2 F). These images were composed by overlaying images recorded in three channels of the CLSM, using excitation wavelengths of 488 (for the 6-FAM signal) and 543 and 633 nm (for autofluorescence) and appropriate filter sets. CCF with probe EUB338 (panel C) and NON338 (panel D) in an anaerobic sulfate

reducing enrichment culture from a peatland soil. CCF in LR-white resin embedded mouse gut sections hybridized with probes EUB338 (panel E) and NON338 (panel F). For each sample both images were recorded with the same settings. Images depicted in panels C-F are an overlay of a DIC image to visualize the biomass and a fluorescence image recorded using an excitation wavelength of 488 nm for detecting the 6-FAM signal. Bars in panels A and B correspond to 10 µm. Bars in panels C-F correspond to 5 µm. It should be noted that we did not optimize permeabilization treatments for CCF for the samples shown in this figure, as we were only interested whether bright and specific signals could be obtained. As many Gram-positive cells, which are difficult to penetrate with HRP-labeled probes, were present in these samples, it is expected that some of the cells visible in the DIC images show weak or no fluorescence. In addition, we used probe EUB338-HRP for CCF (and not the mixture of probes EUB338, EUB338-II and EUB338-III) and might thus not have detected all bacteria in the samples (11).

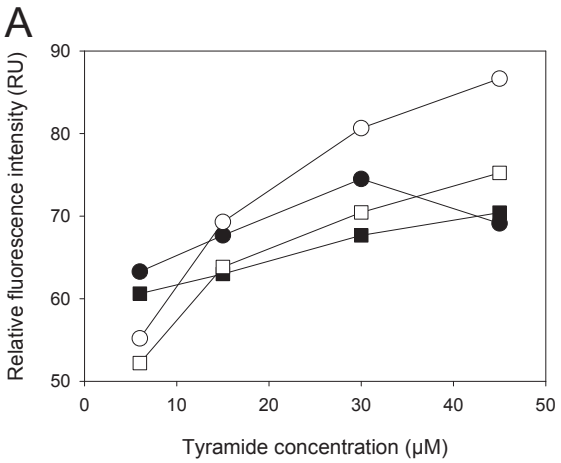
A
Relative fluorescence intensity (RU)
90
80
70
60
50
0
10
20
30
40
50
Tyramide concentration (µM)

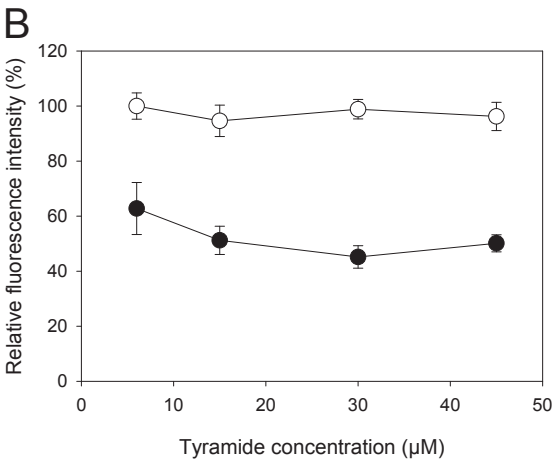
B
Relative fluorescence intensity (%)
120
100
80
60
40
20
0
0
10
20
30
40
50
Tyramide concentration (µM)

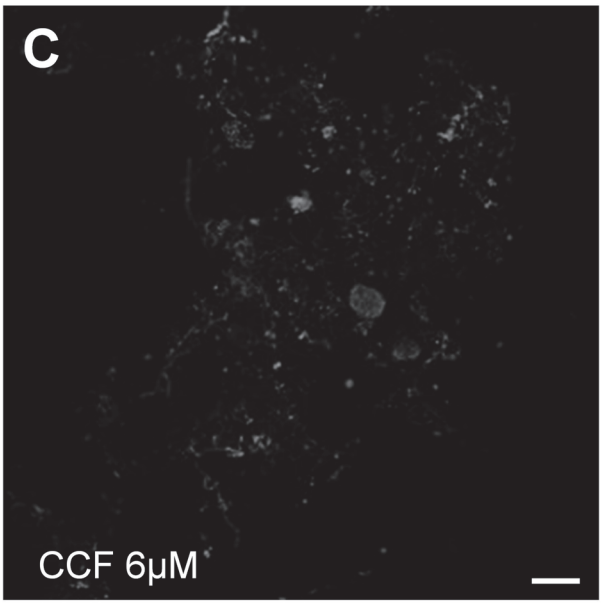
C
CCF 6µM

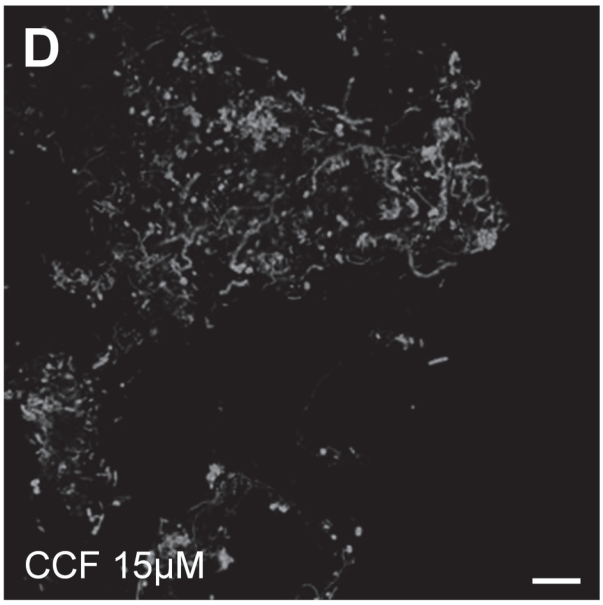
D
CCF 15µM

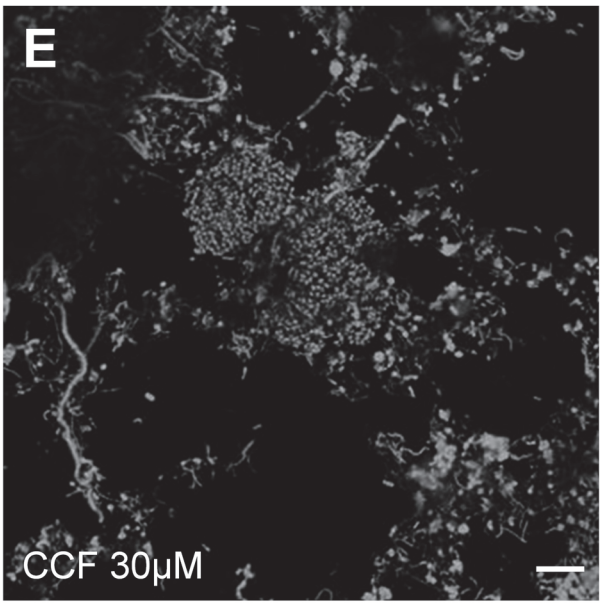
E
CCF 30µM

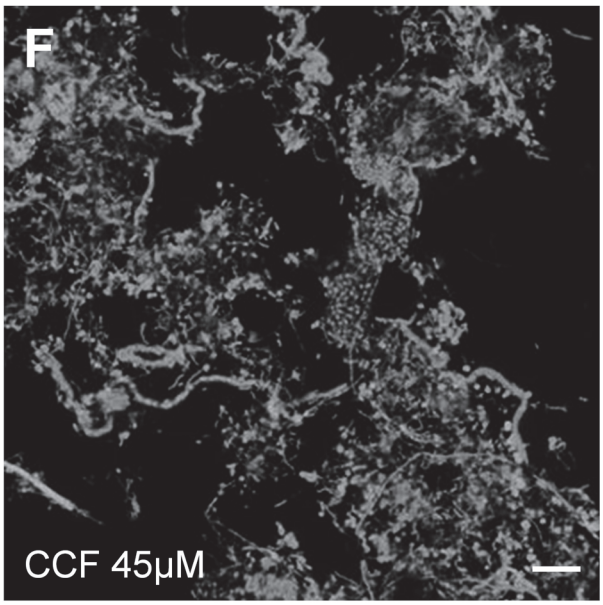
F
CCF 45µM

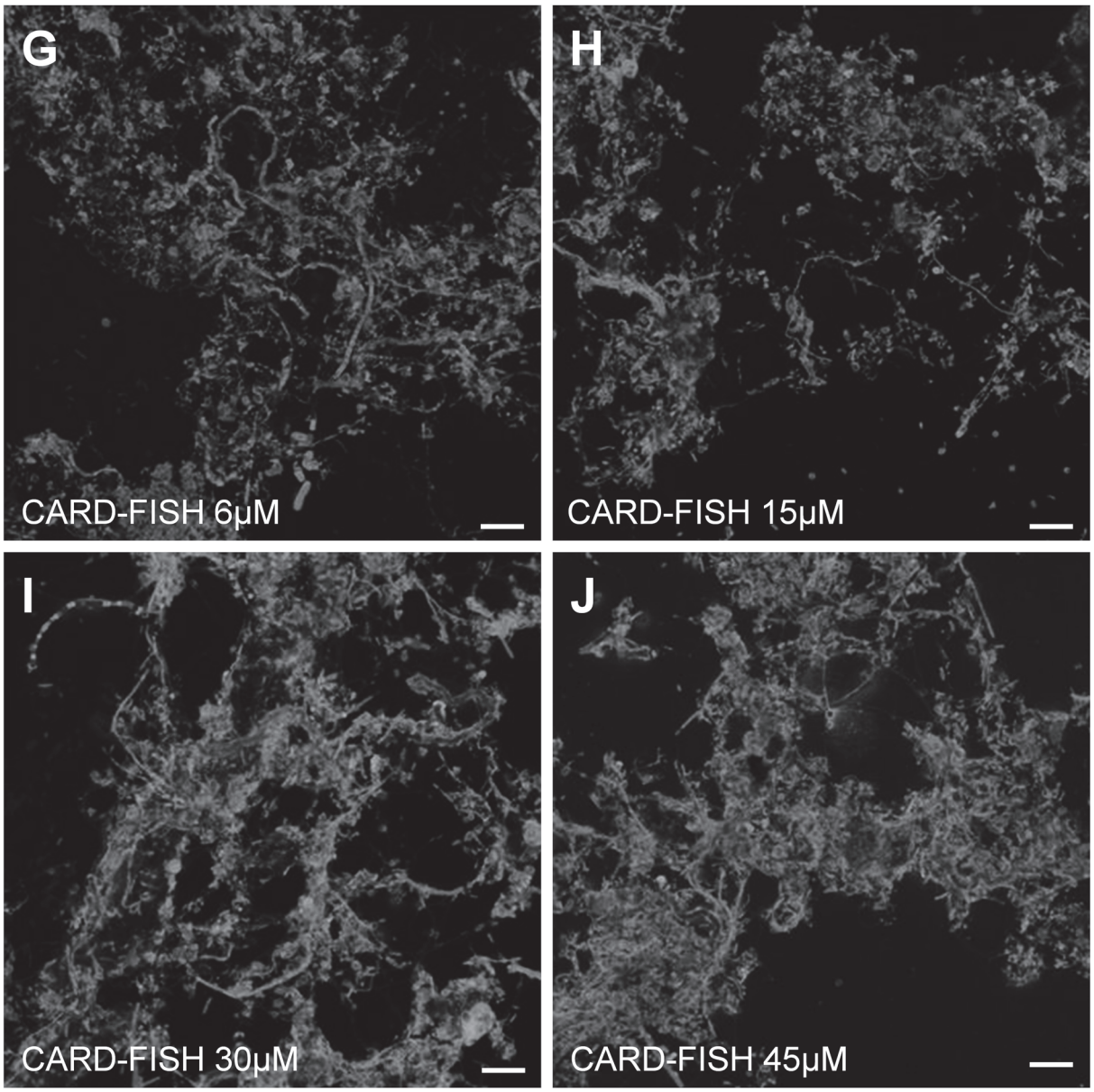

FIGURE A4. Effect of tyramide concentration on CARD-FISH and CCF staining efficiency. The concentration of BCN- (white symbols) and 6-FAM (black symbols) tyramides was stepwise increased from 6 µM to 45 µM. (A) EUB338-HRP probe was hybridized to formaldehyde-fixed activated sludge collected at the Bad Salzuflen municipal waste water treatment plant (see above). Fixed flocs were applied either at high density (circles) or as individual flocs (squares). Data points represent average pixel intensity in fluorescent objects from approx. 10 images (in relative units; RU). As the cutoff of 30 units was used to reproducibly reduce the background and to facilitate object detection, the fluorescence intensities describing low BCN tyramide concentrations (6 µM and possibly 15 µM) do not reflect realistic intensity values and are an overestimation. (B) Signal intensity is independent

of tyramide concentration when staining single *E. coli* cells. (C-F) Effect of BCN-tyramide concentration on CCF efficiency when staining bacteria (probe EUB338) in activated sludge is shown as fluorescence images. (G-J) CARD-FISH signal intensity varies less with increasing 6-FAM tyramide concentration. Bars correspond to 10 µm.

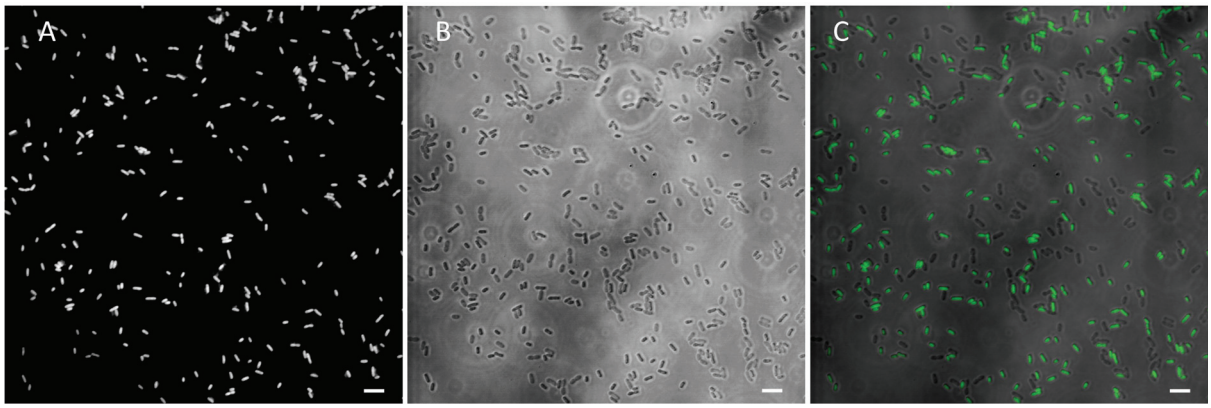

FIGURE A5. Specificity of CCF. Formaldehyde fixed *E. coli* (labeled with ^{13}C) and *B. cepacia* were mixed, hybridized with an equimolar mixture of probes GAM42a-HRP and BET42a-Cy5, and CCF with D-4-BCN tyramides and Atto514 azide was performed. As expected only *E. coli* cells showed the green Atto514 fluorescence (panel A), demonstrating single mismatch discrimination of CCF. Panel B depicts a DIC image to show all cells and panel C shows an overlay of panels A and B. Cells without fluorescence in panel C are *B. cepacia*. Scale bars correspond to 5 µm.

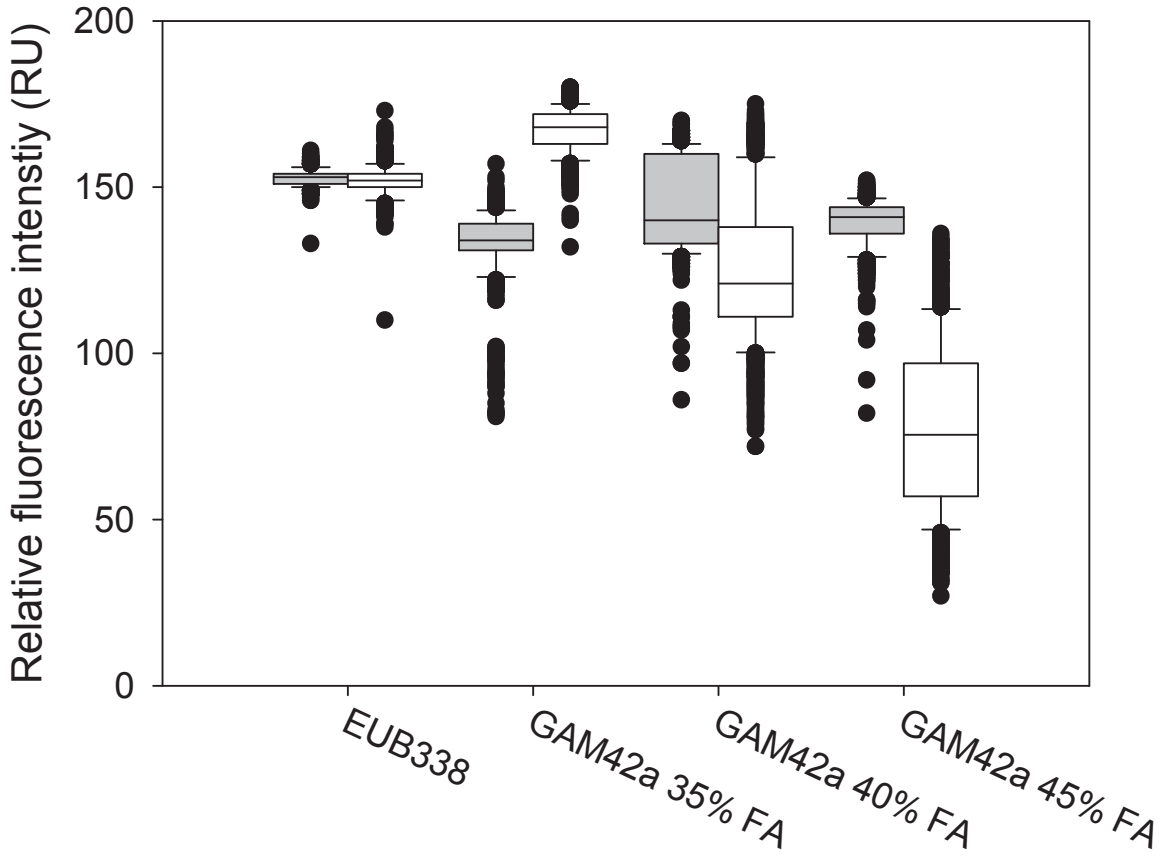

FIGURE A6. Specificity of GAM42a-HRP used in CCF in the absence of competitor probe. Formaldehyde fixed *E. coli* and *B. cepacia* were hybridized either with probe EUB338-HRP (as positive control) or with GAM42a-HRP only but with increasing formamide (FA) concentration in hybridization buffer. Afterwards, the CCF with BCN tyramides and 6-FAM azide was performed as described before. Grey plots show the "formamide series" of the probe GAM42a-HRP when hybridized to *E. coli* (perfect match). When GAM42a-HRP was hybridized to *B. cepacia*, the signal did decrease with increasing formamide concentration, but was nevertheless clearly detectable (white plots). Black circles show outliers. RU stands for relative units.

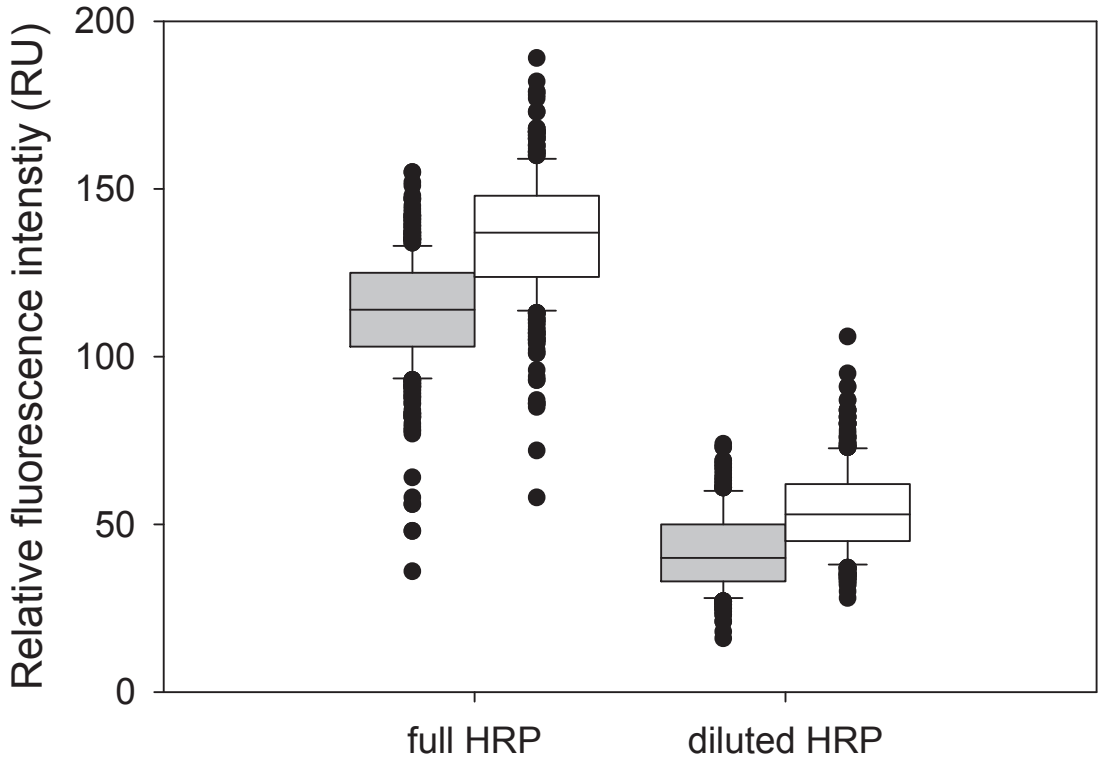

FIGURE A7. Mean signal intensities (in relative units) of CARD-FISH (grey plots) and CCF (white plots) stained cells after reduction of effective HRP molecules in target cells. The approach developed by Hoshino et al. (12) was used to simulate the low-ribosome cells. HRP-conjugated EUB338 probes were used either alone or in combination with EUB338-Cy5 probes that competed for available target sites on the 16S rRNA. Signals observed after further dilution of HRP-conjugated probes with Cy5-EUB338 probes were too weak to measure with the applied microscope settings (data not shown).

References

1. **Berry D, Stecher B, Schintlmeister A, Reichert J, Brugiroux S, Wild B, Wanek W, Richter A, Rauch I, Decker T, Loy A, Wagner M.** 2013. Host-compound foraging by intestinal microbiota revealed by single-cell stable isotope probing. Proc. Natl. Acad. Sci. U.S.A. **110:**4720-4725.
2. **Dolinšek J, Lagkouvardos I, Wanek W, Wagner M, Daims H.** 2013. Interactions of nitrifying bacteria and heterotrophs: identification of a *Micavibrio*-like putative predator of *Nitrospira* spp. Appl. Environ. Microbiol. **79:**2027-2037.
3. **Kostanjšek R, Pašić L, Daims H, Sket B.** 2013. Structure and community composition of sprout-like bacterial aggregates in a Dinaric Karst subterranean stream. Microb. Ecol. **66:**5-18.
4. **Behnam F, Vilcinskas A, Wagner M, Stoecker K.** 2012. A straightforward DOPE (double labeling of oligonucleotide probes)-FISH (fluorescence *in situ* hybridization) method for simultaneous multicolor detection of six microbial populations. Appl. Environ. Microbiol. **78:**5138-5142.
5. **Widdel F, Pfennig N.** 1981. Studies on dissimilatory sulfate-reducing bacteria that decompose fatty acids. I. Isolation of new sulfate-reducing bacteria enriched with acetate from saline environments. Description of *Desulfobacter postgatei* gen. nov., sp. nov. Arch. Microbiol. **129:**395-400.
6. **Amann RI, Binder BJ, Olson RJ, Chisholm SW, Devereux R, Stahl DA.** 1990. Combination of 16S rRNA-targeted oligonucleotide probes with flow cytometry for analyzing mixed microbial populations. Appl. Environ. Microbiol. **56:**1919-1925.
7. **Manz W, Amann R, Ludwig W, Wagner M, Schleifer K-H.** 1992. Phylogenetic oligodeoxynucleotide probes for the major subclasses of Proteobacteria: problems and solutions. Syst. Appl. Microbiol. **15:**593-600.
8. **Wallner G, Amann R, Beisker W.** 1993. Optimizing fluorescent *in situ* hybridization with rRNA-targeted oligonucleotide probes for flow cytometric identification of microorganisms. Cytometry **14:**136-143.
9. **Stahl DA, Amann R.** 1991. Development and application of nucleic acid probes, p. 205-248. *In* Stackebrandt E, Goodfellow M (ed.), Nucleic Acid Techniques in Bacterial Systematics. John Wiley & Sons Ltd., Chichester, England.
10. **Hoshino T, Yilmaz S, Noguera D, Daims H, Wagner M.** 2008. Quantification of target molecules needed to detect microorganisms by fluorescence *in situ* hybridization (FISH) and catalyzed reporter deposition-FISH. Appl. Environ. Microbiol. **74:**5068-5077.
11. **Daims H, Brühl A, Amann R, Schleifer KH, Wagner M.** 1999. The domain-specific probe EUB338 is insufficient for the detection of all Bacteria: development and evaluation of a more comprehensive probe set. Syst. Appl. Microbiol. **22:**434-444.
12. **Hoshino T, Yilmaz S, Noguera D, Daims H, Wagner M.** 2008. Quantification of target molecules needed to detect microorganisms by fluorescence *in situ* hybridization (FISH) and catalyzed reporter deposition-FISH. Appl. Environ. Microbiol. **74:**5068-5077.

Chapter V

Discussion

Discussion

Chemolithoautotrophic nitrifiers direct the energy gained during the oxidation of ammonia or nitrite into CO_2 fixation and downstream biosynthesis of cellular compounds. It is well established that nitrification can support a diverse and abundant microbial community in laboratory settings (1, 2) and was recently proposed to be the main source of organic carbon in the extensive Nullarbor cave system in southern Australia (3). By using SIP, Moreno et al. found that the ciliate *Epistylis galea* benefited from autotrophic nitrification in activated sludge (4). However, as the sewage water contains a rich cocktail of diverse organic substances, the extent to which nitrification may support heterotrophic bacteria in WWTPs is difficult to determine. Why nitrifying bacteria secrete (actively or passively) soluble microbial products and thus support the cohabitation of diverse heterotrophic microbial community (see Chapter I) is largely unknown. Considering the relatively low energy efficacy of nitrifying lifestyle (especially nitrite oxidation), it is seemingly unfavorable for AOB or NOB to excrete fixed organic carbon to their surroundings. Nevertheless, nitrifiers might be doing it for a good reason. For example, it is unclear how *Candidatus* Nitrospira defluvii deals with oxidative stress (5). It is conceivable that *ca*. N. defluvii partly relies on cohabiting microbes to detoxify the produced H_2O_2 (H_2O_2 is membrane permeable). Hitchhiking on this function (among others) is proposed to lead to genome reduction in abundant marine cyanobacteria (*Prochlorococcus*), thereby reducing the cost of the DNA synthesis and increasing overall species fitness (6). Such or similar dependency would be a good reason for *Nitrospira* to support the growth of symbiotic heterotrophs by diverting a proportion of fixed carbon into the surrounding medium. In the study presented in Chapter II, we aimed to clarify the ecology (who is involved and why) of such interactions in nitrifying activated sludge from a municipal WWTP. Similar to nitrifiers, a *Micavibrio*-like bacterium showed ^{13}C labeling pattern in RNA-SIP. The phylogenetic analysis of the retrieved 16S rRNA sequences suggested that the *Micavibrio*-related alphaproteobacterium (*Micavibrio aeruginosavorus* is a well-studied predatory bacterium) is a likely predator of lineage I *Nitrospira*. While the exact nature of the interaction could not be determined in our study, its specificity was clearly shown. For example, 3D colocalization analysis showed that the majority of detected *Micavibrio*-like bacterium is found in close proximity to the lineage I *Nitrospira*. Additional work in our laboratory showed that the association is well established

in that particular ecosystem (WWTP in Ingolstadt). Detection of this bacterium in close proximity of lineage I *Nitrospira* in samples from different WWTPs suggests that this association may be widespread in engineered systems (data not shown). Future efforts, possibly involving modern single-cell (or rather single-cluster) isolation techniques (like laser microdissection or cell identification/ isolation by Raman microspectroscopy and optical tweezers), combined with (meta)genome amplification and sequencing, may reveal more about the exact nature of this association. It would also be interesting to analyze the response of *Nitrospira* to predation. For example, transcriptome analysis might point on the possible phenotypic plasticity of the *Nitrospira* (see 7). Also, controlled experiments by applying synthetic microbial ecology principles might allow researchers to test some lessons from macro-scale predator-prey observations in the microbial world (8, 9).

Partly, the associations between uncultured nitrifiers and heterotrophs might be poorly characterized due to a lack of suitable tools. Although molecular methods (especially PCR) have been pivotal for advances in microbial ecology, they are not without flaws or drawbacks. Primers used to discriminate between domains of life, i.e. bacteria, archaea, and eukaryotes are well evaluated, have high specificity, and allow, due to their high coverage, discovery-oriented experimental approaches. The simultaneous characterization of bacterial, archaeal, and eukaryotic communities in almost any given sample is now regarded as routine task (e.g. presence of bacteria in a sample will have little influence on the description of the archaeal community and vice versa). For example, it was fairly straightforward to distinguish between nitrifiers and their eukaryotic partners in described marine symbioses (10, 11). More challenging is to follow populations within a bacterial community by 16S amplicon analysis. For in-depth analysis it is possible to employ group specific primers, but tremendous bacterial diversity and poor primer coverage for some phylogenetic groups limit such approaches. Similar limitations are encountered in rRNA targeted FISH studies. Although invaluable informations on nitrifier ecology have been obtained by FISH and colocalization studies (12, 13), detailed characterization of the complete nitrifying community (and interactions within it) would require extensive rRNA sequencing, probe design, probe synthesis, and finally numerous hybridization experiments. For most studies, such an approach is too time- and cost-intensive (see discussion in Chapter II). Many of the aforementioned problems have been alleviated by recent developments in high-throughput sequencing. The almost complete diversity (retrievable with available primers) description of a microbial community has become a standard, and the resulting massive database buildup allows to look for organisms

of interest in "sequenced life" with a high chance of success (Chapter II and \ Lagkouvardos et al). However, such an approach has not yet been used to analyze nitrification-driven communities from WWTPs.

Still, organisms with a high rRNA sequence similarity can have a dissimilar metabolic potential, therefore the function of a microbe should not be inferred based on its rRNA sequence alone. DNA- and RNA-SIP are thus seen as a filter that distinguishes process relevant microbes from other organisms abundant in a sample. An additional advantage of DNA- and RNA-SIP is that they are discovery methods, i.e. no prior information on the sample is necessary (like microbial composition, PFLA composition or genomic data). This does not, however, apply to incubation conditions. Careful selection of relevant incubation parameters (pH, temperature, substrate concentrations, etc.) is essential for a successful labeling experiment. In the ideal case, the physical and chemical parameters should closely resemble environmental conditions. Otherwise it is possible that the microbial activity will be either attributed to present, but less relevant microbes, or the isotope labeling will be too low for efficient separation of labeled nucleic acids (the isotope fraction of 13C in nucleic acids, necessary for successful RNA SIP, has been estimated to be approx. 10 at%, see 14). Just as important is a selection of the suitable incubation time. To improve the chance of finding a good compromise between labeling intensity and incubation duration, several time-points are usually collected during labeling experiments. With prolonged incubation times, the likelihood of cross-feeding between active microbes and microbes that feed on released SMP increases, which in turn can lead to false-positive results (15). The study presented in Chapter II, aiming to characterize ^{13}C labeled microbes beyond primary producers, was based on the detection of such cross-feeding. We incubated activated sludge with ^{13}C bicarbonate (at near neutral pH, bicarbonate ion is in equilibrium with CO_2, the carbon source for nitrifiers) and at the same time supplied the microcosms with NH_4^+ or NO_2^-. We postulated that when given enough time, active AOB and NOB in activated sludge will secrete or leak fixed carbon, which will in turn serve as the substrate for any associated bacteria. Finally, the predominant rRNA in heavy fraction of SIP gradient originated from AOB and NOB. After the isolation of the ^{13}C labeled RNA we constructed a 16S rRNA library by cloning RT-PCR products. To our disappointment, only nitrifier 16S rRNA sequences were obtained. Obviously, we could have analyzed the representative sample of rare non-nitrifiers only by collecting and screening (e.g. by RFLP or high-throughput membrane hybridization) very large number of clones. Alternatively, we could have bypassed the problem of low heterotroph abundances in

the labeled gradient fractions by high throughput 16S amplicon sequencing (like 454 pyrosequencing), however, at the time of the study, its use was not yet feasible for "routine" sequencing projects. To retain full discovery potential in our study, we were also reluctant to use primers with more narrow specificity (and thereby screening only a fraction of detectable bacterial diversity). Considering bacterial diversity in WWTPs, the use of group specific primers would require extensive oligonucleotide design and synthesis, and substantial effort would be required to analyze obtained PCR products. We circumvented redundant sequencing of RT-PCR amplified rRNA from autotrophic AOB and NOB by cleaving their (native) 16S rRNA with specific LNAzymes (for further detail on LNAzymes, their characteristics, and potential use see Chapter III). LNAzymes are catalytic, locked nucleic acids (LNA) containing DNA oligonucleotides that can bind to RNA in a sequence specific manner and cleave it at a predicted site. The sequence of the target recognition domain of LNAzymes (it can be any sequence) must be reverse complementary to the targeted RNA sequence. We designed several LNAzymes so that they could bind to, and specifically cleave the 16S rRNA of abundant nitrifiers. Such rRNA was not amplified by RT-PCR, and the remaining rRNA (from heterotrophs) could be detected without difficulty. As the proportion of clones with non-nitrifier 16S rRNA inserts constituted approximately 50% of the resulting library, more iterations of the LNAzyme cleavage procedure (see Chapter III) were not necessary. Nonetheless, the final number of analyzed sequences was very small according to today´s standards. Although we complemented 16 rRNA sequencing with T-RFLP, the phylogenetic resolution of such fingerprinting might not be sufficient to reveal further details on the nitrification powered food-web. Future application of high-throughput sequencing in similar experiments (or even by using samples collected in the course of our work) may reveal further heterotrophs possibly involved in symbioses with nitrifiers.

Despite many (and continuous) attempts to purify it, at the time of our study, the long-term enrichment culture of *Candidatus* Nitrospira defluvii contained a diverse heterotrophic population. Total relative abundance of heterotrophs was varying between 15% and 50% (C. Dorninger, personal communication). Possibly, some of those heterotrophs had or evolved an intricate relationship with *Ca.* Nitrospira defluvii, and their role could be more complex than being recalcitrant contaminants (see above). To learn more about nitrifier symbioses, we analyzed the enrichment maintained in our laboratory by LNAzyme mediated cleavage and subsequent rRNA analysis. The LNAzyme treatment reduced the relative abundance of *Nitrospira* sequences in the clone library from the initial 78% down to 20% (or even 7%,

depending on the protocol modification) and thus allowed a detailed community description. Possible consequences of cohabitation of lineage I *Nitrospira* with heterotrophic bacteria are described in detail in the discussion sections of Chapters II and III. In conclusion, the presented studies shed light on the ecology of lineage I *Nitrospira*, and expanded our understanding of biological controls that can have an effect on nitrification.

As mentioned in the Chapter I, it is critical to confirm RNA-SIP results by additional (independent) experiments. A small amount of unlabeled RNA is distributed also to the heavy fractions of the density gradient (14), and the mere detection of a specific phylotype does not guarantee its labeling. Shifts in relative abundance of candidate rRNA toward the heavier fractions (compared to negative control) are a good indication of actual labeling. However, independent detection of isotope incorporation (NanoSIMS, Raman microspectroscopy, FISH-MAR, magnetic bead capture combined with IRMS etc.) can provide even stronger support to the data obtained by SIP. NanoSIMS is a powerful tool that allows precise determination of the isotopic composition with a superb spatial resolution. However, such analysis alone gives little information on the identity of microbes in complex samples (shape and size alone are notoriously poor designators of microbial identity), and must be combined with *in situ* hybridization (ISH) to unambiguously link detected activties with identities. To that end, some studies successfully used the superimposition of images obtained by FISH with reconstructed isotopic images (16). Nevertheless, much effort has been invested into the direct identification of labeled cells during NanoSIMS measurements by introducing a heterotracer element via the *in situ* hybridization (ISH). So far, such heterotracers were halogens otherwise not present in the sample (see Chapter I). As it offers easy-to-use and flexible protocols, biologists started to rely on click chemistry for the detection of biomolecule synthesis (for more detail see Chapter IV and the Appendix 1). We realized that click chemistry could complement existing ISH strategies, especially when fluorescent labeling of microbes is not the primary goal (e.g. for the NanoSIMS studies). With an aim to facilitate future SIP studies, Click-FISH and Click CARD-FISH (CCF) were developed (presented in Appendix 1 and Chapter IV).

Two properties of these methods emerged as their major strengths. One asset of Click-FISH is that the presented framework will allow the specific labeling of microbes with “speciality” compounds without the need to reevaluate oligonucleotide specificity. The specificity of ISH is determined by hybridization and washing conditions. Regardless of the final labeling, in

Click-FISH, these two steps are always the same for a given oligonucleotide (Appenidix 1). Analogously, in CCF the hybridization and washing are identical as in the well-established CARD-FISH (Chapter IV). By using newly developed protocols, we have successfully and specifically labeled biomass with two different fluorescent dyes, without having to synthesize additional tyramides or reevaluate hybridization conditions of oligonucleotides used. Neither of the methods resulted in pronounced increase of the signal intensity compared to standard FISH or CARD-FISH. In addition, the signal intensity was more dependent on tyramide concentration in CCF than in CARD-FISH. In contrast to the pure cultures, more than double amount of tyramides was necessary for comparable labeling with CCF when applied to activated sludge. We could not explain this concentration dependence, and future experiments would benefit from a very precise tyramide concentration control (as BCN tyramides are liquid in pure form and were delivered in mg aliquots, we relied on the assumed amounts rather than determine them by weighing). One should keep in mind that a certain amount of care is necessary when using click chemistry. Despite specific oligonucleotide hybridization and tyramide deposition and inertness of azides or alkynes in biological systems, compounds can bind to biomass unspecifically. For example, we intended to label “clickable” oligonucleotides after ISH with the azide modified fluorous tag, an amphiphilic molecule with azide head and fluorinated aliphatic tail. The large nonpolar tag likely left most of the unwashed molecule (4,4,5,5,6,6,7,7,8,8,9,9,9-tridecafluorononyl azide) bound to the membranes rather than dissolving into an aqueous washing buffer. To remove the unspecifically bound florous tag, washing in organic solvent would be required, which would most likely dissolve cellular membranes and possibly lyse the cells. Indeed, our experiments showed that addition of 20% (v/v) of organic compounds like chloroform or tetrahydrofuran to a reaction buffer results in extensive cell lysis (data not shown). Probably unsuitable for identification of microbes, such tags could be used as membrane marker that would make cell contours clearly visible in a NanoSIMS image. In addition, we noticed that presence of Cu(I) in the reaction buffer can lead to unspecific labeling when used in certain environmental samples. It is therefore necessary to prescreen the targeted sample by exposing it to the azide-modified dye alone under the conditions used in the click reaction. It would be interesting to isolate (by laser microdissection) the labeled biomass and identify the substances (for example by combination of genome sequencing and metagenomic library screening) that reacted with azides in presence of Cu(I). This could lead to the isolation of new compounds suitable for the click chemisty.

Introduction of isotope labeling as the identity marker in CCF approaches is another important improvement that may aid the NanoSIMS research community. A major drawback of existing halogen labeling is a high halogen content and patchy (halogen) distribution within certain samples that can make links between halogen concentration and microbial identity unreliable. For example, marine sponges can have a high content of diverse halogens. Similarly, fluorine is commonly added to mice food, and is therefore present in high amounts in mouse gut and feces (F. Behnam and D. Berry, personal communication). Labeling with isotopes will not suffer from environment-specific issues, as we expect that the isotopic composition is largely uniform in natural samples. Given that the difference between the marker isotopic fraction before (in non control) and after labeling is well above the natural isotopic variation, microbial identity can be established with a high degree of confidence. Typically, the relative isotopic abundances in natural samples are between 0.0026 - 0.0184 at% for deuterium, 0.963 - 1.147 at% for ^{13}C and 0.346 - 0.421 at% for ^{15}N (for example, relative abundance of deuterium after isotopic labeling was between 1.6 - 2.8 at%). As they are commonly used for metabolic labeling, ^{13}C or ^{15}N will not be main identity markers, although their use for this purpose is not excluded. Due to the availability of reagents, we used deuterium in our experiments. The detection of deuterium by NanoSIMS is not straightforward, as direct $H^-/^2H^-$ ion measurements would prevent the simultaneous detection of standard tracers (^{13}C, ^{15}N) and other secondary ions relevant for biomass detection. To avoid this drawback, we used $^{16}OH^-$ and $^{16}O^2H^-$ ions to detect deuterium labeling. Technically more straightforward would be the detection of ^{18}O as isotope marker, but the low number of available chemicals labeled with this isotope and their high price limit its current use.

Besides low natural background and variation, the known ratio of marker isotopes in the sample prior to labeling (i.e. its natural isotopic composition) allows one to calculate the addition (at least partially) of other elements during ISH. As discussed in Chapter IV and Appendix 2, significant amounts of unlabeled carbon, nitrogen, hydrogen and oxygen are deposited to the biomass during CARD-FISH and CCF. This leads to an underestimation of metabolic labeling and can prevent its quantitative determination. By applying calculations described in Appendix 2, we could correct for 16% of such undesired carbon addition via measuring the $H/^2H$ ratio. This correction factor will likely improve with further refinements of CARD-FISH or CCF. During labeling with these methods, much of the carbon is deposited unspecifically (i.e. deposited also in negative control). Therefore, the improved protocol will likely omit or polymers like dextran sulphate and undefined “blocking reagent”, or replace them with more soluble and inert polymers used for macromolecular crowding, like low-

molecular weight polyethylene glycol, Ficoll, or polyvinyl pyrrolidone. In summary, our contributions to the microbial ecologist´s toolbox presented in Chapters III and IV will facilitate future studies using isotope tracers, particularly those studies focusing on microbial food webs.

References

1. **Rittmann BE, Regan JM, Stahl DA.** 1994. Nitrification as a source of soluble organic substrate in biological treatment. Water Sci. Technol. **30:**1-6.
2. **Kindaichi T, Ito T, Okabe S.** 2004. Ecophysiological interaction between nitrifying bacteria and heterotrophic bacteria in autotrophic nitrifying biofilms as determined by microautoradiography-fluorescence *in situ* hybridization. Appl. Environ. Microbiol. **70:**1641-1650.
3. **Tetu SG, Breakwell K, Elbourne LD, Holmes AJ, Gillings MR, Paulsen IT.** 2013. Life in the dark: metagenomic evidence that a microbial slime community is driven by inorganic nitrogen metabolism. ISME J. **7:**1227-1236.
4. **Moreno AM, Matz C, Kjelleberg S, Manefield M.** 2010. Identification of ciliate grazers of autotrophic bacteria in ammonia-oxidizing activated sludge by RNA stable isotope probing. Appl. Environ. Microbiol. **76:**2203-2211.
5. **Lucker S, Wagner M, Maixner F, Pelletier E, Koch H, Vacherie B, Rattei T, Damste JS, Spieck E, Le Paslier D, Daims H.** 2010. A Nitrospira metagenome illuminates the physiology and evolution of globally important nitrite-oxidizing bacteria. Proc. Natl. Acad. Sci. U. S. A. **107:**13479-13484.
6. **Morris JJ, Lenski RE, Zinser ER.** 2012. The Black Queen Hypothesis: evolution of dependencies through adaptive gene loss. mBio **3**.
7. **Shemesh Y, Jurkevitch E.** 2004. Plastic phenotypic resistance to predation by Bdellovibrio and like organisms in bacterial prey. Environ. Microbiol. **6:**12-18.
8. **De Roy K, Marzorati M, Van den Abbeele P, Van de Wiele T, Boon N.** 2013. Synthetic microbial ecosystems: an exciting tool to understand and apply microbial communities. Environ Microbiol.
9. **Hector A, Schmid B, Beierkuhnlein C, Caldeira MC, Diemer M, Dimitrakopoulos PG, Finn JA, Freitas H, Giller PS, Good J, Harris R, Hogberg P, Huss-Danell K, Joshi J, Jumpponen A, Korner C, Leadley PW, Loreau M, Minns A, Mulder CP, O'Donovan G, Otway SJ, Pereira JS, Prinz A, Read DJ, et al.** 1999. Plant diversity and productivity experiments in european grasslands. Science **286:**1123-1127.
10. **Fiore CL, Jarett JK, Olson ND, Lesser MP.** 2010. Nitrogen fixation and nitrogen transformations in marine symbioses. Trends. Microbiol. **18:**455-463.
11. **Webster NS, Taylor MW.** 2012. Marine sponges and their microbial symbionts: love and other relationships. Environ. Microbiol. **14:**335-346.
12. **Schramm A, De Beer D, Wagner M, Amann R.** 1998. Identification and activities *in situ* of Nitrosospira and Nitrospira spp. as dominant populations in a nitrifying fluidized bed reactor. Appl Environ. Microbiol. **64:**3480-3485.
13. **Maixner F, Noguera DR, Anneser B, Stoecker K, Wegl G, Wagner M, Daims H.** 2006. Nitrite concentration influences the population structure of Nitrospira-like bacteria. Environ. Microbiol. **8:**1487-1495.
14. **Manefield M, Whiteley AS, Ostle N, Ineson P, Bailey MJ.** 2002. Technical considerations for RNA-based stable isotope probing: an approach to associating microbial diversity with microbial community function. Rapid Commun. Mass Spectrom. **16:**2179-2183.
15. **Neufeld JD, Dumont MG, Vohra J, Murrell JC.** 2007. Methodological considerations for the use of stable isotope probing in microbial ecology. Microb. Ecol. **53:**435-442.
16. **Berry D, Stecher B, Schintlmeister A, Reichert J, Brugiroux S, Wild B, Wanek W, Richter A, Rauch I, Decker T, Loy A, Wagner M.** 2013. Host-compound foraging by intestinal microbiota revealed by single-cell stable isotope probing. Proc. Natl. Acad. Sci. U.S.A. **110:**4720-4725.

Appendix I

Abstract

Abstract

Efficient nitrogen removal is one of the central processes in modern waste-water treatment plants (WWTPs). It relies heavily on the oxidation of ammonia to nitrite and further to nitrate, catalyzed by diverse chemolithoautotrophic bacteria that harness the released energy to fix CO_2 and for concomitant growth. Although it might play an important part in ecology of nitrifying microbes, nitrifier-dependent heterotrophy is arguably among the least researched of all chemolithoautotrophically fuelled food-webs. To identify organisms that receive fixed carbon from nitrifiers in WWTPs, RNA stable isotope probing was combined with newly developed LNAzymes digestion of target rRNA molecules, T-RFLP analysis, and 16S rRNA sequencing. In addition to known nitrifiers, ^{13}C labeled rRNA was affiliated with obligatory predatory bacterium *Micavibrio aeruginosavorus*. Further activated sludge examination with fluorescence *in situ* hybridization (FISH) and 3D colocalization analysis confirmed the specific and close cohabitation of lineage I *Nitrospira* with the *Micavibrio*-related alphaproteobacterium, most likely an obligatory predatory bacterium. LNAzymes-mediated digestion of rRNA was employed to analyze a long-term enrichment of *Ca.* Nitrospira defluvii containing a diverse nitrification-dependent heterotrophic community. These results provide new insights into the ecology of nitrite oxidizing bacteria and associated bacteria and extend our notion of factors that can control *Nitrospira* populations. To assist future stable isotope studies, two widely used methods for microbial community analysis, FISH and CARD-FISH (Catalyzed Reporter Deposition FISH) were modified and made compatible with click-chemistry labeling. The additional labeling flexibility of Click CARD-FISH was demonstrated by specifically and simultaneously labeling cells in an artificial community with deuterium and fluorine, which are useful identity markers in NanoSIMS studies. Furthermore, the newly introduced phylogenetic labeling of cells with deuterium holds high promise for its universal applicability and possibility of correcting biases inherent to phylogenetic staining by CARD-FISH.

Zussamenfassung

Eine Hauptaufgabe von modernen Kläranlagen besteht in der Entfernung von Stickstoffverbindungen. Ein wichtiger Schritt der Stickstoffentfernung ist die Nitrifikation, die Oxidation von Ammoniak zu Nitrat und weiter zu Nitrit. Diese wird von verschiedenen chemolithoautotrophen Bakterien katalysiert, die mit der daraus gewonnenen Energie Kohlenstoff fixieren und in ihre Biomasse einbauen. Derzeit gibt es wenige Untersuchungen zu heterotrophen Organismen, die direkt von der Nitrifikation abhängig sind, obwohl diese eine wichtige Rolle in der Ökologie von Nitrifizierern spielen könnten. Für die Identifizierung von jenen Organismen, die über eine Nahrungskette mit Nitrifizierern verbunden sind, wurde Belebtschlamm einer Kläranlage untersucht. RNA stable isotope probing wurde mit einem in dieser Studie entwickelten LNAzym-Verdau von rRNA sowie T-RFLP Analyse und 16S rRNA Sequenzierung kombiniert. Die ^{13}C markierte rRNA kodiert neben den bekannten Nitrifizierern auch das obilgat räuberische Bakterium *Micavibrio aeruginosavorus*. Weiters wurde der Belebtschlamm mittels Fluoreszenz in situ Hybridisierung (FISH) analysiert und mit 3D Kolokalisierungs-Analysen genauer betrachtet. Die Untersuchungen bestätigten, dass lineage I *Nitrospira* eng und spezifisch mit einem *Micavibrio*-ähnlichem Alphaproteobakterium zusammen lebt, und ergaben, dass jenes Alphaproteobakterium als obligater Räuber lebt. Weiters wurde, wieder mit Hilfe von rRNA Verdau mittels LNAzymen, eine Analyse einer Langzeit-Anreicherung von *Ca*. Nitrospira defluvii durchgeführt, die auch aus einer diversen, heterotrophen und von Nitrifikation abhängigen mikrobiellen Gemeinschaft bestand. Die Ergebnisse lieferten neue Einblicke in die Ökologie von Nitrit oxidierenden Bakterien und ihren assoziierten Mikroben und darüber, wie Gemeinschaften von *Nitrospira* beeinflusst werden können. Um zukünftige Analysen mit NanoSIMS zu unterstützen, wurden zwei weit verbreitete Methoden in der Analyse von mikrobiellen Gemeinschaften, FISH und CARD-FISH (Catalyzed Reporter Deposition FISH) modifiziert, indem sie mit der sogenannten Click-Chemie kombiniert wurden. Die dadurch gewonnene zusätzliche Flexibilität von Click CARD-FISH wurde gezeigt, indem spezifisch und simultan Zellen einer künstlichen Gemeinschaft mit Deuterium und Fluor markiert wurden, welche nützliche Marker in NanoSIMS Studien darstellen. Ausserdem verspricht das Markieren von Zellen mit Deuterium universale Anwendbarkeit und umgeht die Nachteile, die beim phylogenetischen Labeling mit CARD-FISH präsent sind.

Appendix II

Click-FISH; a Tool for Post-Hybridization Staining

Click-FISH; a Tool for Post-Hybridization Staining

Introduction

To many biologists, the term "click chemistry" was introduced in 2008, when Salic and Mitchinson published a method for efficient and straightforward monitoring of DNA synthesis in cells, tissues, or even whole organisms (1). Until then, DNA synthesis (and with it cell activity), cell division, or tissue growth, was typically followed by allowing cells to incorporate the uracil analogue BrdU (bromodeoxy uracil) into DNA during synthesis. Incorporated BrdU can be detected with antibodies, the whole procedure involves, however, extensive permeabilization, DNA denaturation, and is in general tedious. That changed by using EdU (ethynil deoxyuracil), an uracil analogue that can be detected by the "click" reaction with an azide-conjugated dye (N3-dye). The azide group reacts readily with the terminal alkyne group in a stereospecific Cu(I) catalyzed (3 + 2] cycloaddition (CuAAC) reaction (2, 3). Such azide-conjugated dyes are significantly smaller than the antibodies used for BrdU detection, thus no cell permeabilization is necessary. Furthermore, the entire hands-on time for sample processing is significantly reduced. Soon after being published, the method was commercialized by Invitrogen/Life Technologies, and became widely available to the scientific community. More information on click chemistry, its potential benefits and caveats can be found in Chapter 4 and references therein.

Fluorescence *in situ* hybridization (FISH) has been a central tool in modern microbial ecology, indispensable for the direct visual examination of microbes in their natural environments. In FISH, oligonucleotides covalently linked to a fluorescent dye penetrate into the cell and, under appropriate conditions, hybridize to RNA in a sequence-specific manner. In most cases, 16S rRNA is the targeted molecule, as it is a well-characterized phylogenetic marker and extensive sequence databases cover most environments. It is usually present in several thousand copies per cell, which warrants its detection already with low-cost microscopy equipment. In FISH, the conditions under which probes are used allow most of the targeted sites being hybridized to a probe, while at the same time unspecific binding, which gives false-positive results, is minimized. This is commonly achieved by varying the formamide (destabilizes probe-target duplex) concentration in the hybridization buffer, while

keeping the hybridization temperature constant (4). For a given probe, the optimal formamide concentration must be determined experimentally from probe dissociation profiles or "formamide series" (FA series). Indeed, only recent refinements of hybridization models provide researchers with an "educated guess" of the oligonucleotide hybridization properties (5), but their reliability is yet to be tested.

In situ hybridization is not only useful for direct fluorescent staining, it can also be used to deliver other "functionalities" into targeted cells, like enzyme horseradish-peroxidase (HRP) or iodine in the case of SIMS *in situ* hybridization (6, 7). However, as already the change of a fluorescence dye can influence the hybridization properties of a given oligonucleotide (8-10), it is conceivable that the conjugation of almost any functional group will result in an altered probe-target duplex stability. While the effects of changing the fluorescent dye can be readily identified by performing FA series and subsequent microscopy analysis, *in situ* hybridization characteristics of non-fluorescent oligonucleotides can be much more challenging to determine. To expand detection possibilities without the need to reevaluate the hybridization conditions, we used CuAAC as the means of detecting oligonucleotides in cells after *in situ* hybridization (Click-FISH). With the promise of simpler and more reliable labeling, we extended our investigation by including copper-free, strain promoted alkyne-azide cycloaddition (SPAAC) compatible probes in our experiments (bicyclononyne or BCN-conjugated probes). We successfully used both approaches to discriminate between bacteria in an artificial mixture with high specificity. This section details the labeling protocol and the hybridization properties of probes suitable for the specific labeling of microbes by click chemistry.

Materials and Methods

Environmental samples, *Escherichia coli* (strain K12), *Bulkhorderia cepacia* (strain DSM 7288), and *Bacillus subtilis* (strain DSM 10) cells used in this study were grown/incubated, fixed and stored as described in chapter 4. All *in situ* hybridization experiments were conducted as described elsewhere (Chapter II, see also 11). Oligonucleotides carrying terminal alkyne groups were purchased from baseclick (Tutzing, Germany), while 5´ and 3´ BCN labeled oligonucleotides were kindly provided by Biomers (Ulm, Germany). The structural chemical formulas of modified nucleosides, a canonical BCN group, 6-FAM azide,

and the respective products of click reactions between them are shown in Figure 1. All oligonucleotides used in this study are listed in Table 1. The click reaction conditions and the microscopic analysis procedure are delineated in detail in chapter 4.

Results and Discussion

Initial experiments with oligonucleotides carrying terminal alkyne groups resulted in poor performance of "Click-FISH" and compelled us to optimize the conditions of the *in situ* CuAAC reaction. Parallel tests with fluorescently labeled oligonucleotide probes showed that oligonucleotide dissociation from its target site during the click reaction can have a major effect on the final labeling efficiency. Finally, better results were obtained when probe-target duplexes were stabilized by low temperature (the CuAAC reaction was performed on ice) rather than by increasing the ionic strength of the buffer (data not shown). Similarly to the labeling of deposited BCN-tyramides, click reaction conditions used in Click CARD-FISH (CCF; chapter 4) were proven to provide the best results (in terms of final labeling intensity) also in SPAAC based FISH. Despite a significant progress, the optimal conditions for post-hybridization oligonucleotide labeling are yet to be found. When assuming similar RNA binding affinity of the alkyne-, BCN-, and 6-FAM- modified probes (at 20% formamide (v/v) in the hybridization buffer), the efficiency of the click reaction can be calculated from the obtained fluorescence intensities (shown in figure 2D). Compared to standard FISH, the fluorescence signal intensity obtained by click FISH was 1.4 fold higher in *E. coli*, 1.2 fold higher in *B. cepacia*, and 1.6 fold higher in *B. subtilis*. The increase was even less pronounced in BCN FISH, being (on average) between 1 and 1.1 fold. Considering the number of "clickable" sites on an oligonucleotide (Table 1), this signal intensities translate into reaction efficiency between 25 and 31% for CuAAC and 49 to 56% for SPAAC. One reason for a low reaction efficiency could be the inaccessibility of the reactive groups bound to the hybridized probes. The slight variation between the efficiency of the click reaction when used in different organisms could result from the variation in the ribosomal structure at the binding position and therefore different steric hindrances for the click reaction. Alternatively, it is possible that the overall binding affinity is much lower for the probes internally labeled with terminal alkyne groups. To examine this possibility, one would have to label such probes on the 5´end with standard fluorescent dye, and compare its hybridization properties with the commonly used FISH probes.

Hybridization properties of click chemistry compatible oligonucleotides were determined from FA series shown in figures 2A-2C. The major concern in using alkyne modified oligonucleotides was possibility that the alkyne group linked to thymidine or cytidine bases via the 8-C linker (figures 1A and 1B) could affect base pairing strength and thus significantly change stability of the probe-RNA duplex. In turn, weak target affinity or/and reduced specificity of such probe could be observed. It should be noted that in contrast to the alkyne containing oligonucleotides, the BCN- groups were conjugated to oligonucleotides similarly to fluorescent dyes used in DOPE FISH, i.e. via the linker at the 3´and 5´ends of the probe, and were not expected to directly interfere with base pairing between the probe and its target. Compared to standard FISH, the BCN- or alkyne- modifications did not result in large shifts in the probe-RNA duplex stability. When hybridized to the target organism, the observed dissociation profiles of the probes EUB338 and Bet42a were similar, regardless of the probe modification. Where standard and click chemistry-compatible probes differ is the stability of the duplex when it contains one mismatch (hybridization to non-target organism). As single mismatch might not be sufficient to discriminate between target and non-target organism, it is common to add competitor probes to hybridization buffer in order to prevent fluorescent probe binding to non-target organisms (Figure 1A, see also 11). Competitor probes have, due to their perfectly matching sequence, higher affinity to non-target organisms than labeled probe, and when used simultaneously, block the available non-target binding sites. As evident from figures 1B and 1C, BCN or alkyne modified probes have lower affinity for the non-target site and therefore greater discriminating power. Beside probe-RNA duplex association/dissociation dynamics, the ribosomal fold stability and therefore site accessibility (12, 13) vary in FA series. The high fluorescence intensity of click FISH at 60% FA might be explained by a better site accessibility for the fluorescent azide after ribosome denaturation by high FA concentration. It is conceivable that a higher formamide concentration leads to partly irreversible ribosome conformation changes, allowing better access of 6-FAM-N3 to the probe during CuAAC. Furthermore, the limited site accessibility could be the reason for the much lower apparent amount of the hybridized alkyne-modified EUB338 probe (labeled with several alkyne groups) at 20% formamide (v/v) compared to when 30% FA was used in the hybridization buffer (Figure 2C). Such effect would, however, have a strong effect on the efficiency estimates of CuAAC reaction and result in an efficiency underestimation (see above).

Click-FISH with post-hybridization offers an alternative labeling strategy, where labeling specificity of the oligonucleotide probes is not altered with the change of conjugated functional group. It probably won´t find widespread use in microbial ecology, it might however, serve as a niche method when specific labeling of microbes with non-fluorescent tags is required. According to our data, one can use already evaluated probes without changing the hybridization conditions. We do nevertheless recommend that a potential unspecific azide binding to biomass during CuAAC is tested beforehand with a fluorescent azide.

Figures and Tables

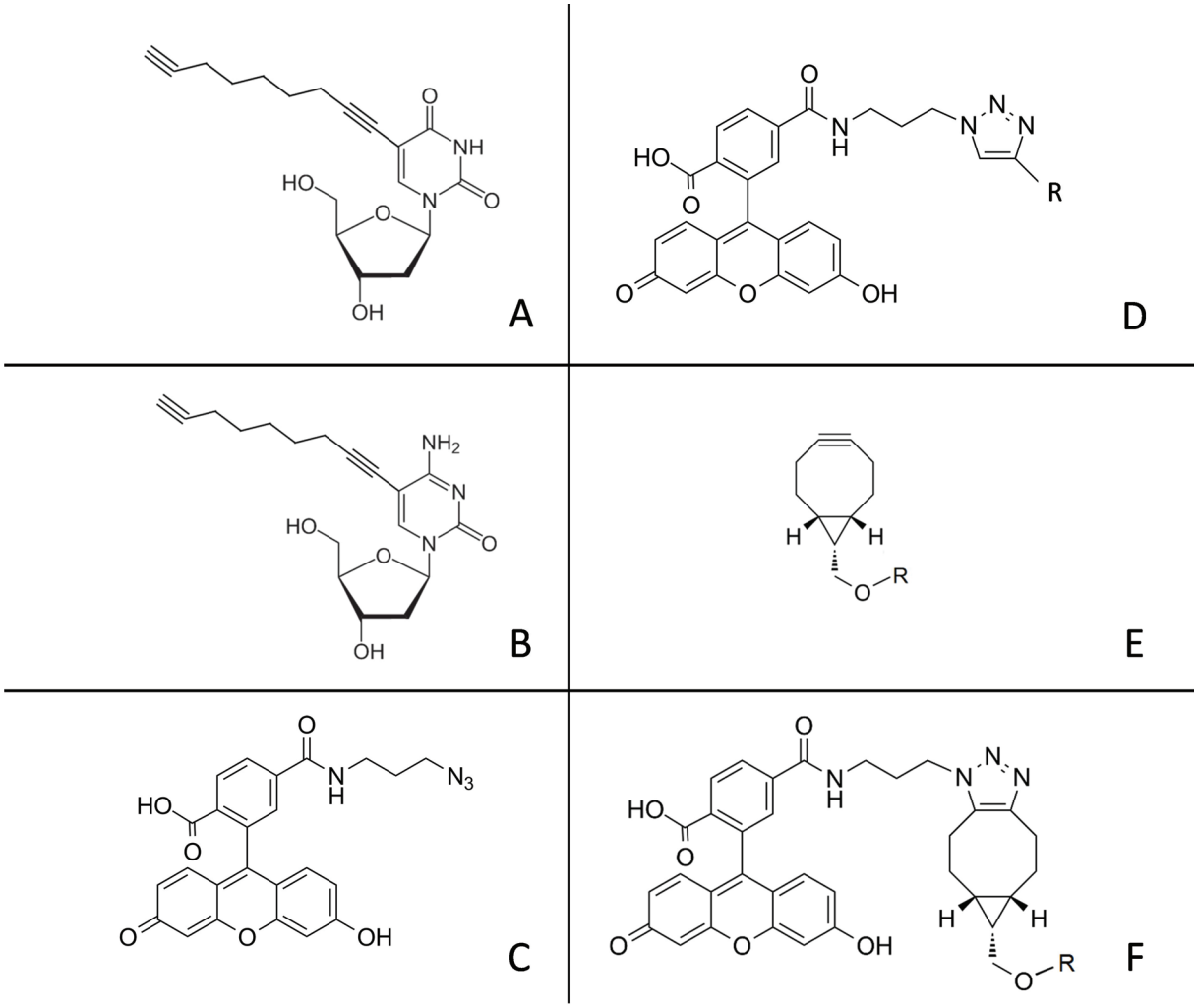

Figure 1: Structural formulas of compounds used in this study. (A) 5-Octa-1,7-diynyl-2\'-deoxyuridine, (B) 5-Octa-1,7-diynyl-2\'-deoxycytidine, (C) 6-FAM azide, (D) product of CUAAC of 6-FAM azide and terminal alkyne, (E) (1R,8S,9s)-bicyclo(6.1.0]non-4-yn-9-ylmethane ether modification and (F) product of SPAAC of 6-FAM azide and BCN group.

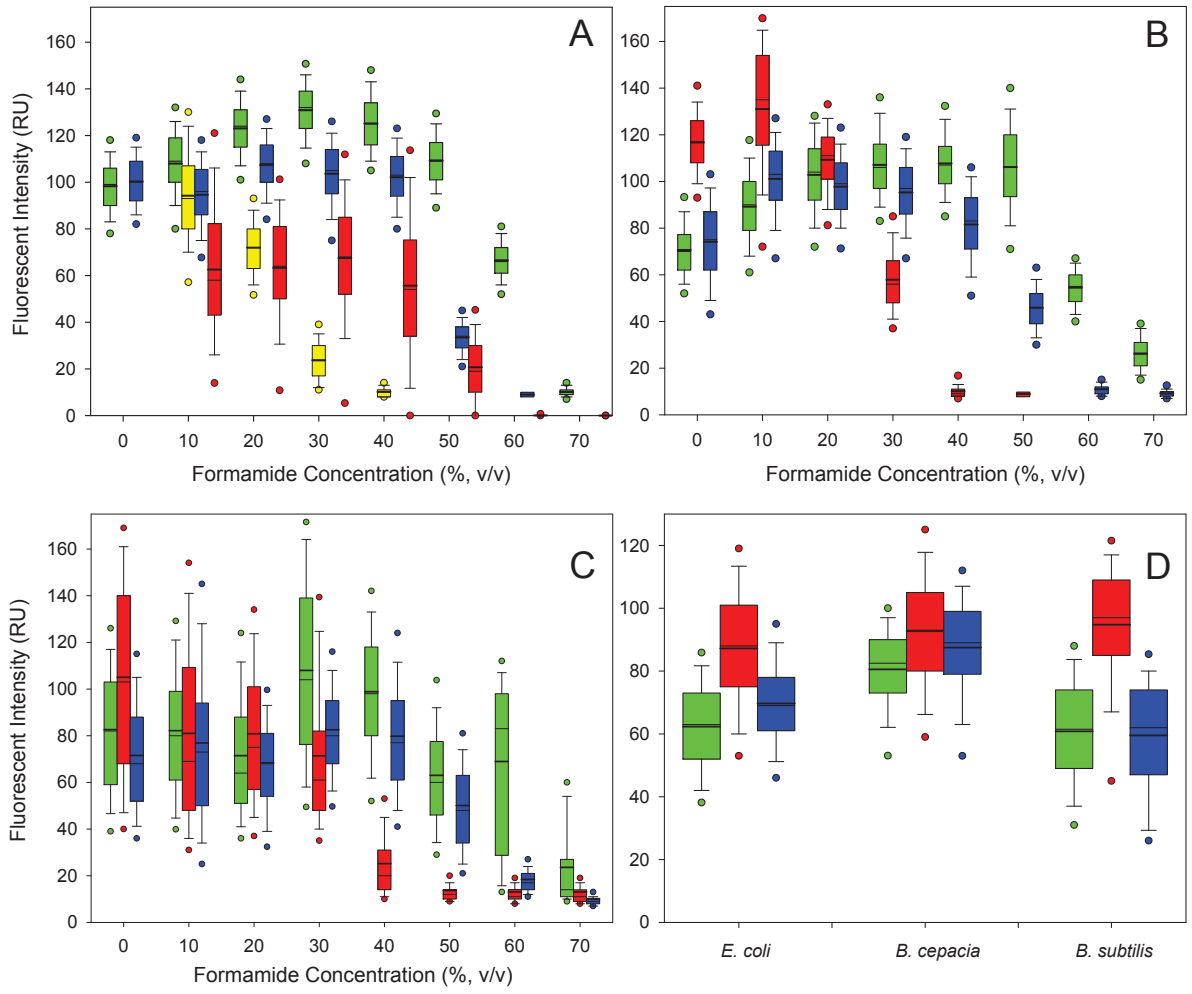

Figure 2: Probe-RNA duplex stability of click chemistry compatible oligonucleotide probes was assessed by varying FA concentrations in the hybridization buffer and compared with 6-FAM monolabeled probes. Dissociation profiles of EUB338 probe were determined with the *E. coli* as target organism (green). Probe Bet42a was hybridized to *B. cepacia* (blue) as target organism and to *E. coli* (red) as non-target organism having one mismatch in the target RNA region. FA concentrations used in all experiments (unless data point is omitted) were 0%, 10%, 20%, 30%, 40%, 50%, 60%, and 70%. For each data point, average fluorescence intensities of at least 200 single cells were determined. The thick line in the box plot shows the average fluorescence intensity of measured cells, error bars show 10th and 90th percentile, and circles represent 5th and 95th percentile. (A) Hybridization of singly 6-FAM labeled probes, the yellow color shows hybridization of Bet42a probe to *E. coli* in the presence of an unlabeled Gam42a competitor probe. (B) Hybridization of doubly BCN labeled probes and (C) hybridization of probes carrying terminal alkyne groups. (D) Signal intensity obtained after hybridization of 6-FAM (green), alkyne modified (red) and BCN conjugated (blue)

EUB338 probes to PFA-fixed *E. coli*, *B. cepacia* or *B. subtilis* cells and subsequent click reaction with 6-FAM azide (where applicable). The hybridization buffer contained 20% (v/v) formamide. RU stands for relative units.

Table 1: Probes used in this study.

Probe Name	Sequence (5´- 3´)	Target groups	Formamide (%)	Reference
EUB338	GCT GCC TCC CGT AGG AGT	most *Bacteria*	35	(14)
BET42a	GCC TTC CCA CTT CGT TT	*Betaproteobacteria*	35	(4)
GAM42a	GCC TTC CCA CAT CGT TT	*Gammaproteobacteria*	35	(4)
NON338	ACT CCT ACG GGA GGC AGC	negative control probe	35	(15)
EUB338-click	GC**Y** GCC **Y**CC **X**G**Y** AGG AG**Y***	most *Bacteria*	35	this study
NON338-click	A**X**T C**X**T A**X**G GGA GG**X** AG**X***	negative control probe	35	this study
BET42a-click	G**X**C T**Y**C C**X**A CT**Y** CGT **Y**T*	*Betaproteobacteria*	35	this study

* Terminal alkyne modification (**X** = C8-Alkyne-dC; **Y** = C8-Alkyne-dU)

References

1. **Salic A, Mitchison T.** 2008. A chemical method for fast and sensitive detection of DNA synthesis *in vivo*. Proc. Natl. Acad. Sci. U.S.A. **105:**2415-2420.
2. **Rostovtsev V, Green L, Fokin V, Sharpless B.** 2002. A stepwise huisgen cycloaddition process: copper(I)-catalyzed regioselective "ligation" of azides and terminal alkynes. Angew. Chem., Int. Ed. Engl. **41:**2596-2599.
3. **Tornøe C, Christensen C, Meldal M.** 2002. Peptidotriazoles on solid phase: (1,2,3]-triazoles by regiospecific copper(i)-catalyzed 1,3-dipolar cycloadditions of terminal alkynes to azides. J. Org. Chem. **67:**3057-3064.
4. **Manz W, Amann R, Ludwig W, Wagner M, Schleifer K-H.** 1992. Phylogenetic oligodeoxynucleotide probes for the major subclasses of Proteobacteria: problems and solutions. Syst. Appl. Microbiol. **15:**593-600.
5. **Yilmaz LS, Parnerkar S, Noguera DR.** 2011. mathFISH, a web tool that uses thermodynamics-based mathematical models for in silico evaluation of oligonucleotide probes for fluorescence *in situ* hybridization. Appl. Environ. Microbiol. **77:**1118-1122.
6. **Schönhuber W, Fuchs B, Juretschko S, Amann R.** 1997. Improved sensitivity of whole-cell hybridization by the combination of horseradish peroxidase-labeled oligonucleotides and tyramide signal amplification. Appl. Environ. Microbiol. **63:**3268-3273.
7. **Li T, Wu TD, Mazeas L, Toffin L, Guerquin-Kern JL, Leblon G, Bouchez T.** 2008. Simultaneous analysis of microbial identity and function using NanoSIMS. Environ. Microbiol. **10:**580-588.
8. **Moreira BG, You Y, Behlke MA, Owczarzy R.** 2005. Effects of fluorescent dyes, quenchers, and dangling ends on DNA duplex stability. Biochem. Biophys. Res. Commun. **327:**473-484.
9. **Stoecker K, Dorninger C, Daims H, Wagner M.** 2010. Double labeling of oligonucleotide probes for fluorescence *in situ* hybridization (DOPE-FISH) improves signal intensity and increases rRNA accessibility. Appl. Environ. Microbiol. **76:**922-926.
10. **Hoshino T, Yilmaz S, Noguera D, Daims H, Wagner M.** 2008. Quantification of target molecules needed to detect microorganisms by fluorescence *in situ* hybridization (FISH) and catalyzed reporter deposition-FISH. Appl. Environ. Microbiol. **74:**5068-5077.
11. **Daims H, Stoecker K, Wagner M.** 2005. Fluorescence *in situ* hybridization for the detection of prokaryotes, p. 213–239. *In* Osborn AM, Smith CJ (ed.), Molecular microbial ecology. Bios-Garland, Abingdon, United Kingdom.
12. **Yilmaz LS, Okten HE, Noguera DR.** 2006. Making all parts of the 16S rRNA of *Escherichia coli* accessible *in situ* to single DNA oligonucleotides. Appl. Environ. Microbiol. **72:**733-744.
13. **Okten HE, Yilmaz LS, Noguera DR.** 2012. Exploring the *in situ* accessibility of small subunit ribosomal RNA of members of the domains Bacteria and Eukarya to oligonucleotide probes. Syst. Appl. Microbiol. **35:**485-495.
14. **Amann RI, Binder BJ, Olson RJ, Chisholm SW, Devereux R, Stahl DA.** 1990. Combination of 16S rRNA-targeted oligonucleotide probes with flow cytometry for analyzing mixed microbial populations. Appl. Environ. Microbiol. **56:**1919-1925.
15. **Wallner G, Amann R, Beisker W.** 1993. Optimizing fluorescent *in situ* hybridization with rRNA-targeted oligonucleotide probes for flow cytometric identification of microorganisms. Cytometry **14:**136-143.

Appendix III

Isotope Quantification Error in NanoSIMS Studies can be Estimated by Introducing Deuterium as Phylogenetic Identifier

Isotope Quantification Error in NanoSIMS Studies can be Estimated by Introducing Deuterium as Phylogenetic Identifier

As discussed in the manuscript "*Improved CARD-FISH Method Exploiting Click Chemistry for In Situ Identification of Microbes*", Click CARD-FISH (CCF; see chapter IV) can cause the dilution of the tracer isotope atoms (the tracer isotopes enriched during incubation are "diluted") in examined cells and complicate the analysis and interpretation of NanoSIMS results. This phenomenon and its implications are discussed in detail in Woebken et al., 2013 (the exact formula derivations and an extended discussion are presented in Supplementary Information) and Chapleur et al. (1, 2). Tracer dilution cannot be estimated when phylogenetic information is obtained with halogen labeling (3-5), as the halogen content of the targeted cells is unknown and can vary within an examined population. In Chapter V, I argue that the main advantage of ^{2}H (D in the rest of this chapter) over halogen labeling is that the extent of metabolic tracer dilution during CCF can be estimated by quantifying the D addition. To confirm this assumption, I derived a framework that allowes us to identify the tracer composition skew resulting from CCF. As shown below, all necessary informations for such correction are either determined during the NanoSIMS analysis, are known (natural isotopic ratios of relevant elements), or can be safely assumed (H/C ratio of the investigated cell).

Formulations by Woebken and coauthors were the starting point for the following derivation. According to the *equation 1* in Woebken et al., the fraction of tracer element atoms added by the treatment ($F_{X,\ add}$) can be calculated from isotopic composition of cells before (a_i) and after (a_f) the treatment, and isotopic composition of added material (a_{add}), for which they assume that it equals natural relative isotopic abundance (e.g. ^{13}C at% is approximately 1.1%).

$$F_{X,add} = \frac{a_{X,f} - a_{X,i}}{a_{X,add} - a_{X,i}} \quad (1)$$

Importantly, authors do not neglect carbon removed by treatment. However, they do note that it is virtually impossible to track carbon losses caused by the treatment, in our case CCF. They derive following equation (*equation S12*), pointing on the potential effect of tracer removal during the treatment:

$$\frac{n_{X,add}}{n_{X,i}} = \frac{a_{X,i} - a_{X,f}}{a_{X,f} - a_{X,add}} \left(1 - \frac{n_{X,rem}}{n_{X,i}}\right) \quad (2)$$

In equation 2, $n_{X,i}$, $n_{X,add}$ and $n_{X,rem}$ stand for the number of tracer atoms present in a cell before the treatment, added by the treatment and removed during the treatment. Although one cannot estimate the amount of carbon removed by the treatment, the $n_{X,rem}$ in equation 2 can be neglected, if $a_{X,i}$ and $n_{X,i}$ are replaced by $a_{X,non}$ and $n_{X,non}$, respectively. Suffix *X,non* refers to the tracer atoms in cells that went through entire CCF procedure but were hybridized with probe NON338-HRP (non control). In such control, amount of carbon removed during the treatment will be similar to the amount of carbon removed when using targeted probes (e.g. EUB338). Similarly, the tracer atoms added unspecifically during CCF are also comparable in such control, and can be disregarded. As the part $n_{X,rem}$ approaches zero, equation 2 simplifies to:

$$\frac{n_{X,add}}{n_{X,non}} = \frac{a_{X,non} - a_{X,f}}{a_{X,f} - a_{X,add}} \quad (3)$$

The number of atoms added during the treatment (e.g. number of C atoms in added tyramides) can be expressed as:

$$n_{X,add} = n_{X,f} F_{X,add} \quad (4)$$

where $n_{X,\ add}$ is the number of tracer atoms added during the treatment, $n_{X,f}$ is the number of tracer atoms present after the treatment and $F_{X,\ add}$ is the fraction of added tracer atoms (see also equation S1 in Woebken et al.). By using NON338 control as initial cell state, we can separate specific or "desired" tracer atoms addition (tyramides) from unspecific one (any other buffer components). In turn, this allows us to express the number of added molecules (n_{add}) by dividing both sides of equation 4 by the number of carbon atoms in added molecule $N_{X,add}$ (e.g. number of C atoms in BCN tyramide is 19):

$$n_{add} = \frac{n_{X,\ add}}{N_{X,\ add}} = \frac{n_{X,\ f}}{N_{X,\ add}} F_{X,\ add} \tag{5}$$

A certain amount of tracer atoms will be added specifically via HRP-conjugated probes. However, if only one probe is hybridized to the ribosome, and if one considers the molecular mass of ribosome alone (approx. 2.3 MDa) (6) compared to the molecular mass of HRP-conjugated oligonucleotide probe (approx, 50kDa), the hybridized probes represent minor portion (approx. 2% or less of $n_{X,non}$, depending on the cell ribosome content) of added tracer atoms.

For the sake of simplicity and clarity, I will only focus on carbon (C) and deuterium (D) from now on. If necessary, carbon and deuterium can be replaced by any other suitable element (X). When tyramides used during CCF contain deuterium (each D_4-BCN-tyramide contained four D atoms), we can express the expected D/H ratio after labeling as:

$$\frac{n_{D,\ non} + n_{D,\ add}}{n_{H,\ non} + n_{H,\ add}} = \frac{n_{C,\ non} \left(\frac{H}{C}\right)_{non} a_{D,\ non} + n_{add} N_{D,\ add}}{n_{C,\ non} \left(\frac{H}{C}\right)_{non} a_{H,\ non} + n_{add} N_{H,\ add}} \tag{6}$$

where $n_{C,non}$ stands for total number of carbons inside a cell prior to labeling (nonEUB control), $(\frac{H}{C})_{non}$ is the ratio of hydrogen to carbon atoms in cell before labeling (or nonEUB control), $N_{H,add}$ is the number of hydrogen atoms in added molecule (e.g. D_4-BCN tyramide), $N_{D,add}$ is the number of deuterium atoms in the added molecule (e.g. D_4-BCN tyramide) and n_{add} is the total number of molecules (e.g. D_4-BCN tyramide) added. To simplify the equation, we did not correct for the natural abundance of hydrogen (or deuterium) in added compounds.

By substituting n_{added} in equation 6 by equation 5 adapted for carbon, we obtain equation 7.

$$\frac{n_{D,non}+n_{D,add}}{n_{H,non}+n_{H,add}}=\frac{n_{C,non}(\frac{H}{C})_{non}a_{D,non}+(\frac{n_{C,f}}{N_{C,add}}F_{C,add})N_{D,add}}{n_{C,non}(\frac{H}{C})_{non}a_{H,non}+(\frac{n_{C,f}}{N_{C,add}}F_{C,add})N_{H,add}} \quad (7)$$

According to equation S1 (1), we can write:

$$F_{X,i}=1-F_{X,add} \quad (8)$$

Similarly to equation 4, the number of tracer atoms before the treatment can be expressed as:

$$n_{X,i}=n_{X,f}F_{X,i} \quad (9)$$

Equations 8 and 9 can be combined into:

$$n_{X,i}=n_{X,f}(1-F_{X,add}) \quad (10)$$

When we arrange equation 10 so that it refers to carbon and exchange subscript *i* (before treatment) with subscript *non* (non EUB338 control), we get:

$$n_{C,non} = n_{C,f}(1 - F_{C,add}) \tag{10a}$$

We can replace the term $n_{C,non}$ in equation 7 to yield:

$$\frac{n_{D,non} + n_{D,add}}{n_{H,non} + n_{H,add}} = \frac{n_{C,f}(1 - F_{C,add})\left(\frac{H}{C}\right)_{non} a_{D,non} + \left(\frac{n_{C,f}}{N_{C,add}} F_{C,add}\right) N_{D,add}}{n_{C,f}(1 - F_{C,add})\left(\frac{H}{C}\right)_{non} a_{H,non} + \left(\frac{n_{C,f}}{N_{C,add}} F_{C,add}\right) N_{H,add}} \tag{11}$$

When dividing both numerator and denominator on the right side of equation 11 by $n_{C,f}$, we obtain (after a few minor rearrangements):

$$\frac{n_{D,non} + n_{D,add}}{n_{H,non} + n_{H,add}} = \frac{\left(\frac{H}{C}\right)_{non} a_{D,non} - F_{C,add}\left(\frac{H}{C}\right)_{non} a_{D,non} + F_{C,add}\left(\frac{N_{D,add}}{N_{C,add}}\right)}{\left(\frac{H}{C}\right)_{non} a_{H,non} - F_{C,add}\left(\frac{H}{C}\right)_{non} a_{H,non} + F_{C,add}\left(\frac{N_{H,add}}{N_{C,add}}\right)} \tag{12}$$

For the sake of further simplification we can write:

$$\frac{n_{D,non} + n_{D,add}}{n_{H,non} + n_{H,add}} = \left(\frac{n_{D,f}}{n_{H,f}}\right) \tag{13}$$

By substituting the left side of equation 12 by equation 13, multiplication of both sides of the obtained equation by the denominator (of the right side of the eq. 12) and some further rearrangements (e.g. multiplication of the numerator and denominator of subsequent equation by *-1*) we get:

$$F_{C,add} = \frac{\left(\frac{H}{C}\right)_{non}\left(\left(\frac{n_{D,f}}{n_{H,f}}\right)a_{H,non} - a_{D,non}\right)}{\left(\frac{H}{C}\right)_{non}\left(\left(\frac{n_{D,f}}{n_{H,f}}\right)a_{H,non} - a_{D,non}\right) + \left(\frac{N_{D,add}}{N_{C,add}}\right) - \left(\frac{n_{D,f}}{n_{H,f}}\right)\left(\frac{N_{H,add}}{N_{C,add}}\right)} \quad (14)$$

Finally, the calculated $F_{C,add}$ can be inserted into the rearranged equation 1 (equation 2 in Woebken et al.) (1):

$$a_{C,non} = \frac{a_{C,f} - a_{C,add}F_{C,add}}{1 - F_{C,add}} \quad (15)$$

Such an $a_{C,non}$ can be regarded as a better approximation of the isotopic ratios in the cell before the CCF.

However, when using the current CCF protocol, only a portion of tracer dilution can be corrected for. BCN-tyramides were the sole component that was labeled with D, therefore only their contribution to label dilution can be directly corrected for. Additionally, one could correct for tracer originating from fluorescent dyes added by the click reaction by assuming click reaction efficiency. This can be achieved by simply adding the number of atoms in the dye multiplied by the click reaction efficiency factor E (e.g. $N_{C,add} = N_{C,BCN\ tyramide} + (E \times N_{C,azide\ dye})$). As described in the appendix part "Click-FISH Method Development", this factor is estimated to be approximately 0,5 for SPAAC. There is, however, a large proportion of added carbon (mainly from buffer components that are also present in the NON338 control) that cannot be corrected for by using the calculations described above.

References

1. **Woebken D, Burow LC, Behnam F, Mayali X, Schintlmeister A, Fleming ED, Prufert-Bebout L, Singer SW, López Cortés A, Hoehler TM, Pett-Ridge J, Spormann A, Wagner M, Weber PK, Bebout BM.** 2013. Revisiting N_2 fixation in Guerrero Negro intertidal microbial mats with a functional single-cell approach. ISME J., under review.
2. **Chapleur O, Wu TD, Guerquin-Kern JL, Mazeas L, Bouchez T.** 2013. SIMSISH technique does not alter the apparent isotopic composition of bacterial cells. PLoS One **8:**e77522.
3. **Musat N, Halm H, Winterholler B, Hoppe P, Peduzzi S, Hillion F, Horreard F, Amann R, Jørgensen B, Kuypers M.** 2008. A single-cell view on the ecophysiology of anaerobic phototrophic bacteria. Proc. Natl. Acad. Sci. U.S.A. **105:**17861-17866.
4. **Behrens S, Lösekann T, Pett-Ridge J, Weber P, Ng W-O, Stevenson B, Hutcheon I, Relman D, Spormann A.** 2008. Linking microbial phylogeny to metabolic activity at the single-cell level by using enhanced element labeling-catalyzed reporter deposition fluorescence *in situ* hybridization (EL-FISH) and NanoSIMS. Appl. Environ. Microbiol. **74:**3143-3150.
5. **Li T, Wu TD, Mazeas L, Toffin L, Guerquin-Kern JL, Leblon G, Bouchez T.** 2008. Simultaneous analysis of microbial identity and function using NanoSIMS. Environ. Microbiol. **10:**580-588.
6. **Melnikov S, Ben-Shem A, Garreau de Loubresse N, Jenner L, Yusupova G, Yusupov M.** 2012. One core, two shells: bacterial and eukaryotic ribosomes. Nat. Struct. Mol. Biol. **19:**560-567.

Appendix IV

Publications

Acknowledgements

Curriculum Vitae

Publication list

1.) E. Tsoukala, G. Agelis, **J. Dolinšek**, T. Botić, A. Cenčič and D. Komiotis. An efficient synthesis of 3-fluoro-5-thio-xylofuranosyl nucleosides of thymine, uracil, and 5-fluorouracil as potential antitumor or/and antiviral agents. Bioorganic and Medicinal Chemistry, 15(9):3241-3247, May 2007.

2.) M. Gračner, T. Avšič-Županc, V. Punda-Polić, **J. Dolinšek**, D. Bouyer, D. H. Walker, J. E. Zavala-Castro, N. Bradarič, P. A. Crocquet-Valdes and D. Duh. Comparative ompA gene sequence analysis of Rickettsia felis-like bacteria detected in Haemaphysalis sulcata ticks and isolated in the mosquito c6/36 cell line. Clinical Microbiology and Infection: the official publication of the European Society of Clinical Microbiology and Infectious Diseases, 15 Suppl 2:265–266, December 2009.

3.) **J. Dolinšek**, C. Dorninger, I. Lagkouvardos, M. Wagner and H. Daims. Depletion of Unwanted nucleic acid templates by selective cleavage: LNAzymes, catalytically active oligonucleotides containing locked nucleic acids, open a new window for detecting rare microbial community members. Applied and Environmental Microbiology, 79(5):1534–1544, March 2013.

4.) **J. Dolinšek**, I. Lagkouvardos, W. Wanek, M. Wagner and H. Daims. Interactions of nitrifying bacteria and heterotrophs: Identification of a *Micavibrio*-like putative predator of Nitrospira spp. Applied and Environmental Microbiology, 79(6):2027–2037, March 2013.

5.) **J. Dolinšek**, F. Behnam, A. Schintlmeister, A. Anderluh, Stephanie A. Eichorst, A. Galushko, H. Daims and M. Wagner. CARD-FISH method exploiting click chemistry for *in situ* identification of microbes. *Manuscript in preparation*

Oral Presentations

Jan Dolinšek and Holger Daims (2009) *Use of DNAzymes in Microbial Ecology*, oral presentation at INTIME 07 conference In Lackenhof, Austria

Trophic interactions of nitrifying and heterotrophic bacteria in activated sludge, talk was held at Science Day on the 14.03.2011, organized by Faculty of Life Sciences (University of Vienna) and at "Initiativekolleg" *Symbiotic Interactions* symposium, on the 26.11.2011 organized by University of Vienna.

Jan Dolinšek, Faris Behnam, Andreas Anderluh, Holger Daims and Michael Wagner (2011) *The Use of Click Reaction(s) in Microbial Ecology*, oral presentation at INTIME 08 conference in Slettestrand, Denmark

Jan Dolinšek, Faris Behnam, Arno Schintlmeister, Andreas Anderluh, Holger Daims* and Michael Wagner (2012) *Click chemistry: a new approach for single cell microbial ecology*, invited oral presentation at ISME 14 in Copenhagen, Denmark (*presenting author)

Poster Presentations

Jan Dolinšek, Christiane Dorninger, Ilias Lagkouvardos, and Holger Daims (2010) *A novel approach using DNAzymes to remove selected PCR templates from complex mixtures greatly facilitates the molecular detection of rare organisms*, ISME 13, Seattle, USA

Jan Dolinšek, Michael Wagner and Holger Daims (2009) *Trophic interactions of nitrifying and heterotrophic bacteria in activated sludge identified by molecular approaches*, SAME 11, Piran, Slovenia

Acknowledgements

More than six years that have passed between the start of my doctoral work and the dissertation were filled with ups, downs and occasional periods of horizontal transitions. Hardly being a rock that can withstand any storm, turbulences and swirls at work most often found their way to occupy me at home. Therefore I must firstly express my deepest gratitude to Nathalie, who was always there for me, soothingly keeping my head up, steering my look forward.

Than to Holger Daims, who offered me the position, guided me through my research, and at the same time largely ignored my whims and other shortcomings. His contribution to the publications is very much acknowledged.

I am indebted to Michael Wagner for his support, his example and inspiration.

Very special thanks go to Ilias and Faris, for adding the fun component into work (and beyond). It would be so different without you. And to Uli, for making this difference even greater.

I also am thankful to:

Micha Pester, who gave me a timely example of how to plan and execute experiments.

Andi Anderluh, for his sense of duty, good spirits and regular lab journal updates.

Arno Schintlmeister, who has patiently answered all my possible and impossible questions.

Sander van Berkel (from Synaffix), for his help.

Ex-DOMEies (Frank Maixner, Kilian Stöcker & Doris Steger) for being experienced. And being there when needed. All other DOMEies, you were great colleagues.

Faculty members that helped me during my time at university of Vienna, one way or another.

I am really grateful to Angela Sessitsch and Günter Brader who allowed me to finish my first postdoc before completion of doctoral thesis. And to Milica, for taking the concept of patience to another level.

To Relica, who would love to see me graduate.

And finally to my family, for their unlimited, life-long support.

Curriculum Vitae – Jan Dolinšek

Date of Birth: 16.02.1982
Birthplace: Slovenj Gradec
Citizenship: Slovenian

Education

since 2007	PhD at the Department of Microbial Ecology, University of Vienna Focus on trophic interactions of nitrifying and heterotrophic bacteria and development of new molecular tools useful in microbiology under the mentorship of Prof. Michael Wagner and Dr. Holger Daims.
2011-2013	**"**Postdoc" position at the Health & Environment Department, Austrian Institute of Technology Member of interdisciplinary team, focusing on fungal toxin degradation, and led by Dr. Angela Sessitsch.
2001-2006	Diploma (Master) study of Biochemistry, University of Ljubljana Graduated with the work entitled "Determination of the *ompA* gene sequence of the uncharacterized bacterium of the genus *Rickettsiae*" under the tutorship of Prof. Tatjana Avšič-Županc
1999-2001	International Baccalaureate Diploma Programme in Maribor
1997-1999	Gymnasium (high school) in Slovenj Gradec